DAM FILTERS: PHYSICAL BEHAVIOR, PROBABILITY OF MALFUNCTIONING, AND DESIGN CRITERIA

by

YUSUKE HONJO

Ko-Gaku-Shi, Nagoya Institute of Technology
(1973)

Ko-Gaku-Shu-Shi, Kyoto University Graduate School
(1975)

S.M., Massachusetts Institute of Technology
(1983)

SUBMITTED IN PARTIAL FULFILLMENT

OF THE REQUIREMENTS FOR THE

DEGREE OF

DOCTOR OF PHILOSOPHY

at the

MASSACHUSETTS INSTITUTE OF TECHNOLOGY

January, 1985

Signature of Author _____
Department of Civil Engineering, January 31, 1985

Certified by _____
Thesis Supervisor

Accepted by _____
Chairman, Departmental Committee on Graduate Students

DAM FILTERS: PHYSICAL BEHAVIOR, PROBABILITY OF MALFUNCTIONING, AND DESIGN CRITERIA

by

YUSUKE HONJO

Submitted to the Department of Civil Engineering on January 29, 1985 in partial fulfillment of the requirements for the Degree of Doctor of Philosophy.

ABSTRACT

Dam filters are studied first through a physical model of soil particle transport, and then through statistical analysis of laboratory data. The former model is useful in understanding physical factors involved in the soil particle transport phenomenon. However, the very complex nature of the phenomenon prevents one from reliably evaluating the parameters of physical models. The latter method identifies soil parameters that are statistically significant in explaining the behavior of filters. Its main drawback is that it is sometimes difficult to give a physical interpretation to the obtained parameters. In this study, the two methods are used interactively by using the understanding from the physical model to evaluate and to interpret the results of statistical analysis.

It is found that DF15/DB85, which is the parameter used in the conventional Terzaghi's criteria, is the single most significant parameter in predicting filter performance. A secondary parameter, DB95/DB75, is found to be also significant. This parameter is linked to the capability of the base soil's intrinsic stability property (i.e., the self-healing capability.

The implication of the present findings is that the conventional design criteria (DF15/DB85 < 5) is conservative for the case of base soils with low DB95/DB75, but unconservative for soils with high DB95/DB75 (for base soils with widely graded coarser portions).

The proposed filter design criterion is calibrated so that the probability of filter malfunctioning is the same as that provided by the conventional criteria in the case of uniformly graded base soils. The proposed criterion has some spread in the higher DB95/DB75 range due to the scarceness of the data (see Fig. 3.29); its average is given as

$$\frac{DF15}{DB85} < 5.6 - 0.6\,\frac{DB95}{DB75} \quad \left(\text{for } \frac{DB95}{DB75} \leq 5\right)$$

A method is also proposed to evaluate the probability of filter malfunctioning for an entire dam. The method is based on a generalization of the weakest link model to a two-dimensional continuum. A case study using construction records of Carter's Dame, Georgea, is used to illustrate this method.

Thesis Supervisor: Dr. Daniele Veneziano
Title: Professor of Civil Engineering

TABLE OF CONTENTS

Table of Contents (cont'd)

Table of Contents (cont'd)

ACKNOWLEDGEMENT

The author would very much like to acknowledge his thesis Supervisor, Professor Daniele Veneziano, whose contributions to this research are too many to point out. Without his critical advice, this study would not have been completed.

He also gratefully appreciates the interested members of his thesis committee, Professor Robert V. Whitman, Erik H. Vanmarcke and Gregory B. Baecher, all of whom have contributed to this research.

His stay at M.I.T. for three and a half years has been supported by Takenaka Doboku Co., Ltd., Tokyo. This support is gratefully acknowledged.

The author is indebted to many people in the course of this achievement. Among them he would like to express his heartfelt thanks to Mr. M. Endo and Mr. T. Kawasaki who strongly helped him in obtaining the scholarship, and to Professor M. Matsuo for his arrangement for the author's enrollment at M.I.T.

In the statistical analysis done in this thesis, obtaining the literature was one of the critical issues. The author acknowledges the help provided by Dr. Y. Esashi and Mr. A. Whittle in this respect.

A special appreciation goes to Ms. Cathy Lydon for her quick and accurate typing of this manuscript under a

very tight schedule. Mr. A. Doteuchi helped the author by drafting many of the figures in Chapter II with his excellent skill. This help is acknowleged.

The friendships he has obtained during his stay at M.I.T. are one of the most fruitful outcomes that he will enjoy for the remainder of his life. K. Ayan, L. Chouinard, M. Heidari, S. Liao, S.Paikowsky and M. Suzuki are some of the people has has shared more things than his office with.

The author acknowledges the morale support of his parents towards this goal.

Finally, he would like to give his heartfelt acknowledgement to Yurie, his wife, and Kota and Michiko, his children. The pain and frustration (and also joys) we have experienced these three and one half years were not easy ones. I would not have been able to achieve this goal without their help. I know the endurance, encouragement and love of Yurie was essential and I would like to dedicate this thesis to her.

LIST OF TABLES

List of Tables (cont'd)

LIST OF FIGURES

List of Figures (cont'd)

List of Figures (cont'd)

List of Figures (cont'd)

List of Figures (cont'd)

List of Figures (cont'd)

List of Figures (cont'd)

List of Figures (cont'd)

CHAPTER I. INTRODUCTION

In the first part of this chapter, current design criteria for dam filters are reviewed. Issues in the filter design and research needs are then identified in Section 1.2. Finally, the objectives of the present study are presented in Section 1.3.

1.1 Current Practice

The first rational approach to filter design was proposed by Terzaghi in the 1920's. Most of the experimental work that leads to now so called conventional filter criteria was done in the 1940's and 1950's by Bertram (1940), Hurley & Newton (1940), USCE (1941, 1948 and 1953), Karpoff (1955). The filter criteria used in practice today have been developed mainly by U.S.C.E. and U.S.B.R. on the bases of these experiments.

The following is a summary from U.S.C.E. Engineering Manuals EM1110-2-1901 (1952), EM 1110-2-2300 (1982) and Sherard, et al (1963):

A filter material must meet two basic requirements:

(1) The filter material must be fine enough to prevent particles of the base soil from washing into its voids.

(2) The filter must be more pervious than the base soil so that the head dissipated by flow of water through it, and therefore

the seepage forces developed within it, are relatively small.

These requirements are referred to as the "stability" and "permeability" criteria respectively.

Two most widely accepted filter criteria for stability and permeability are:

(1) Stability: DF15 / DB85 < 5

(2) Permeability: DF15 / DB15 > 5

In addition, the following rules are sometimes followed:

(3) DF50 / DB50 < 25

(4) The grain size curve of the filter material should roughly parallel that of the base material,

(5) The filter should not contain more than 5% of fines passing through the No. 200 sieve, and the fines should be cohesionless.

The conventional filter criteria, although sometimes considered to be too conservative, are accepted widely among practical engineers. Most of dam filters are designed based on this criteria, and their performances are considered to be satisfactory. However, in recent years, there has been a trend towards using wider variety of soils as base soils and filters and some problems have been found with the above criteria. Furthermore, people are more interested in understanding the basic mechanism

of filtering and the migration of soil particles within soil media. These problems will be discussed in more detail in the next section.

1.2 Current Issues in Filter Design

Present research in soil particle transport is given from two different viewpoints: In Section 1.2.1, the studies are grouped according to the problem they focus on; for example, use of special types of soil used as the core material. In Section 1.2.2,the problems are classified according to a scenario of a failure event of an earth dam on which a lot of current research is based. The information concerning the laboratory experiments on filters are summarized in Appendix A.

1.2.1 Studies on the Mechanism of Filtering and Related Problems

An active area of research concerning the physical mechanism of filtering is to study it in a context of mroe general problems of particle transport within soil media. The practical motivation for the work are: (i) the tendency of using wider variety of soils as base soils and filters (e.g., broadly graded soils such as glicial tills, and geotextile filters); (ii) attempts to establish more economical design criteria, based on a better undering of the physical phenomenon (e.g., for the design of

filters to protect the seabed from wave action); and (iii) need for a rational quality control method during the construction of filters and cores of dams.

In reviewing the literature on filter design criteria and soil particle transport the following problems are considered separately:

(1) Internal stability of widely graded and gap graded soils,

(2) Experiments on soil against screen to understand self-healing process,

(3) Void phase description based on microscopic and geometric considerations,

(4) Design criteria for filters to protect the seabed from wave action,

(5) Design criteria for geotextile filters,

(6) Influence of spatial variability of soil parameters and Quality Control.

(1) Internal Stability of Widely Graded and Gap Graded Soils

Sherard (1979) pointed out that there have been a number of incidents in which sinkholes have appeared on crests and slopes of embankment dams that are comprised of coarse, broadly graded soils, frequently of glaicial origin. He attributed this fact to the internal unstability of these soils, in the sense that the fine portion

is not compatible with coarser particles.

The migration of finer particles in the coarser portion of the soils is sometimes called "suffusion", and is important not only in embankment dam design but also in studying the properties of certain natural deposit. Study of this phenomenon is also important to understand the mechanism of soil particles transport problem in general.

In a chapter of a book by Kovacs (1981) gives a good review of this topic especially within the Eastern Europe literature. It is estimated that:

no suffusion	if D60/D10 < 10
transition condition	if 10 < D60/D10 < 20
suffusion probable	if D60/D10 > 20

These results are said to be based on experiments and on theoretical considerations based on a capillary tube model. The same author mentioned that the shape of distribution curves is a dominant factor; he introduces two methods to check suffusion based on the shape of the grain size distribution curves:

(i) Lubotchkov's Method: Soil is not susceptible to suffusion if the distribution curve lies between a given band with the notation of Fig. 1.1(a); a simplified mathematical formula is

$$\Delta S_1/\Delta S_2 \leq 4.0; \quad \text{if} \quad \frac{D_{n-1}}{D_n} = \frac{D_n}{D_{n+1}} = 10$$

The method is said to be based on the characteristic grain size distribution curves which gives upper and lower bound for suffusion. However, the logic is hard to understand from the brief summary given by Kovacs.

ii) Kezdi's Method: This method checks suffusion based on Terzaghi's filter criteria by separating the grain size distribution into two portions.

With the notation of Fig. 1.1(b), suffusion is avoided if:

$$\frac{D^F_{15}}{D^B_{85}} < 4 < \frac{D^F_{15}}{D^B_{15}} \quad \text{for any } D_n$$

A similar method is also proposed by DeMello (1975) and applied by Sherard (1979). Kezdi's method assumes that soil particles larger than D_n compose the skeleton and those smaller than D_n are moving in this skeleton. Unfortunately, the reality is that the same size of particles can contribute to both skeleton or moving soil. For this reason, the method seems applicable only to special cases such as gap-graded soils.

Wittman (1977, 1978) has carried out some experiments on a gap graded sand and gravel mixture which is typical of alluvial sediments of the Rhine, Rhone and Danube rivers.

Based on the experiments, he proposed a chart to classify the dominant failure phenomena as a function of sand/gravel mixing ratio and dry density (see Fig. 2.12 in Chapter II). If the gravel content is high (more than 75%), the sand particles wash through gravel skeleton (i.e., suffusion or colmatation); whereas if the sand content is high (more than 30%(%)), piping by heave (i.e., zero effective stress condition) is the dominant mode of failure. He also found that suffusion and colmatation can occur under lower hydraulic gradient than the critical gradient which is accepted as a good criterion to judge safety against piping by the heave phenomenon. Some of his findings will be applied to the soil particle transport model developed in the next chapter. Some additional considerations about gap graded soils will be made in the next section.

(2) Experiments with Soil Against Screen to Understand the Self-Healing Process of Base Soil

In the filtering process, the behavior of the base soil is a very important factor: DB85 of Therzaghi's criteria (DF-15/DB85<4-5) can be interpreted as meaning that, for stability, it is sufficient to prevent the coarse 15% of base soil from penetrating the filter. For the purpose of investigating the behavior of base soil, soil-against-screen type experiments have been carried out by several researchers.

The idea is to replace the filter by a screen so

that the behavior of the base soil can be more easily observed. The main advantage of replacing the filter by a screen is that for the latter there is no uncertainty on the size of the openings.

Soares (1980) carried out a series of experiments of this type under supervision of Dr. P. Vaughan at Imperial College. The objective of the study was to find a grain size of base soil such that if that soil particle size is retained by the filter, the base soil is stable without significant loss of material. This particle size could depend on the grading and the uniformity coefficient (D60/D10) of the base soil.

The aim of the first group of tests (series 1S & 2S in the original text) was to see the influence of the uniformity coefficient of the soil on the effectiveness of the filter; in this series, the size of the screen opening was set to the 85% size of the base soil. The uniformity coefficient varied from 1.86 to 13.30. The loss of base soil increased gradually with the increase of the uniformity coefficient, but even for D60/D10=13.30 case, the loss was not large enough for one to convince the non-stability of filter.

The second group of experiments (Series 3S) aimed at finding which particle size controls filtration. Four different sieves with opening sizes agree to D50, D68, D83 and D97 of the base soil were used. The uniformity co-

efficient of the base soil was set to 2.86 in all cases (see Fig. 1.2). The greater loss of soil was observed for D97 case (see Fig. 1.3), and the author concluded that particles between D80 and D90 control the filtering process.

In a third group of test (series 4S), Soares used gap graded base soils. These soils were prepared in such a way that two particle size ranges (0.600 - 0.850mm and 0.075-0.150mm) were mixed in different proportions. The grain size distributions are shown in Fig. 1.4. The mesh opening size was 0.85mm which agreed to the particle sizes between D92 and D72. The results presented in Fig. 1.5 show that there is significant decrease of internal soil stability when the amount of the finer portion increases from 30% to 40%. Furthermore, the author observed that the major loss of particle for samples with less than 30% of the finer portion occurred during placement and saturation of the samples, and the loss of soil through sieve during flow took place at the very beginning of the test. On the other hand, the samples with more than 40% of the finer portion lost their material mostly during flow, and the loss did not stop even when the test was stopped. Based on these observations, Soares suggested that there might exist a critical mixing ratio beyond which the coarser sand cannot produce, at least immediately, the self-healing filter at the sieve

interface.

Soares emphasizes the fact that, throughout all the experiments, the stability is controlled by the coarser particles: In the very early stage of the experiments, a layer consists of coarser particles formed at the soil-screen interface, and except for gap graded soils this layer can protect the rest of the soil from washing through. Therefore, the fraction of soil particles that compose this layer is a key factor in this filtration process. As mentioned before, Soares' conclusion was that a size between D80 and D90 of the base soil can be used as the controlling particle size.

Mendez (1981) continued Soares's work by carring out two series of experiments. In the first series, Mendez used a mixture of graded sand and London clay with proportions of 60% sand and 40% clay. Downward flow was applied to this soil placed against a screen whose opening could retain 85% finer fraction of this mixed soil. It was observed that the soil formed a self-healing layer of sand against the screen surface.

The second series of experiments aimed at forwarding the study by Soares on the gapgraded sand. Mendez mixed two particle size ranges of sands (0.600-0.850mm and 0.075-0.150mm) in the proportion of 50% to 50%; these sands used were the same as the ones Soares had used in her gapgraded soil tests. Mendez also prepared the sand

with intermediate size distribution as shown in Fig. 1.6. Results for sands with intermediate size content showed the effectiveness of using DB85 as the controlling grain size (see Fig. 1.7(a)). However, the result of the completely gap graded soil showed bigger loss as presented in Fig. 1.7(b). This result did not agree with Soares' results where Soares found proportional loss of base soil as the ratio of finer portion increase in her gapgraded soil experiment. Based on the result, Mendez speculated that if the sand is gapgraded, the coarser portion cannot act as an effective self-healing filter to the finer portion; therefore, the soil is internally non-stable.

Southworth (1980) also carried out a series of experiments with soil against screen. He used three cohesionless soils whose D60/D10 rates between 3 to 10. He plotted the mass of soil washed out from the screen against percent of the soil finer than the screen opening size as shown in Fig. 1.8 (cf.Fig. 1.3 of Soares' results). The loss increases rapidly between 80% and 90%, which present essentially the same behavior as those obtained at Imperial College. Southworth's results will be used later (Chapter II).

(3) Void Phase Description Based on Microscopic and Geometric Considerations

Some studies have been attempted to provide a better description of the voids in filters based on microscopic

and geometric considerations on the granular medium.

Tayler (1948) is probably the first to have discussed the void size of filters in this way. He considered a packing of spheres with the same diamter, and speculated that the maximum size of particles which can pass through this medium might be 1/6.5 of the size of the spheres. The result is based on the size of the opening created by three tightly touching spheres.

Silveira (1965, 1975) made a probabilistic extention of this idea. He showed a procedure to obtain the void size distribution from a given grain size distribution based on the following assumptions: (i) all particles are spherical, (ii) voids are created only from 3 (his later paper (1975) extended it to 4) particles, (iii) the radis of the particles defining the void are random. The void size can be calculated based on the multinominal distribution of sphere sizes. Wittman (1979) measured the void size of gravel and compared it to Silveira's theory. He found that the theory is nearly correct but gives somewhat smaller void sizes.

Vanmarcke & Honjo (1985) considered randomly drawn lines in space where spheres of given grain size distribution are randomly located. They defined "distance between particles" as the length of line between two adjacent particles which the line intersects. The first order solution to calculate the expected distance between part-

icles was obtained. They also showed that this expected distance is highly correlated to D15 based on the calculation done for many grain size distributions. The result is considered to give a good explanation for using DF15 as the representative void size of the filter.

This idea was extended later by Honjo (1983) to the soil particle transport problem. He assumed: (i) all the particles are spherical, (ii) location of the particles are random in space, and (iii) distance between particles, if randomly measured, follows an exponential distribution. Based on these assumptions, Honjo developed a procedure to calculate expected length of a pipe of given diameter in the void phase of soil. This length can be related to the probability of a particle passing through a filter.

A more detailed survey of this topic can be found in Honjo (1983).

It is the opinion of the writer that there are two main drawbacks in this geometric approach:

(i) The problem is very complex and interactive due to the fact that once a particle which was moving is caught, it clogs a path and becomes a barrier to the incoming particles. This interaction is very difficult to describe by the available models,

(ii) If the final goal is to assess the safety of an earth structure, it is very difficult if not impossible to relate this microscopic model to the behavior of entire structure.

In this study, a geometric approach is not attempted. Rather, focus is on a scale somewhat larger than that of individual particles.

(4) Criteria for Filter to Protect Seabed from Wave Action

DeGraauw, et al (1984) have published an intermediate report on the study of filter criteria to protect the seabed from wave action in the Oosterschelde in the Netherlands. Their investigation has focused on measuring critical hydraulic gradient with various filter constructions; for example, influences of cyclic flow vs. steady flow, and parallel flow vs. perpendicular flow to the base soil-filter interface plane. The critical gradient is gradient at which the flow occurs that is responsible for the base soil transport. This is because more economical filters can be designed if one takes the flow situation into account compared to the classic geometrically sandtight filters.

Because of this difference in focus, a direct comparison of the result with other experiments is difficult; however, the study points out some important facts:

(i) For the cases when flow is perpendicular to the interface, it was found for the wide variety of the materials that base soil particles migrate into filter much easily under the cyclic flow cases than under the steady flow cases. This can be attributed to the arching of the base soil particles between the grains of the filter (arches cannot be stable under reversed flow).

(ii) Internal stability of the filter was tested by applying cyclic flow to a specimen consisting of the same soil but with 2 differently colored layers. After exposed to the cyclic flow for 6 hours, samples were taken from the interface and sieved. It was found that material is internally stable with Dmax/Dmin=30 and unstable with Dmax/Dmin=100, where Dmax and Dmin are the maximum and the minimum grain size respectively. The interesting point about this result is that the uniformity coefficient differs only 4.2 to 5.3 in these soils.

The authors also identified some future research needs, and states "the machanism are better understood, thus enhancing the economy of design. After the era of

geometrically sand tight filters, which is almost over, after the current era of filters with critical hydraulic gradients that are not to be exceeded, the era will come of filters in which some material transport will be allowed. However, very little information on the latter is now available."

(5) Design Criteria for Geotextile Filters

In the last ten years, geotextile filters have gradually gained application in important civil structures. The papers by Hoare (1982) and Lawson (1982) reviewed the state of the art in this area. Design criteria are based on the same principle as for soil filters. What is interesting is the generally agreed mechanism by which geotextile filters retain soils from washing through.

Figure 1.9 illustrates the mechanism (Lawson (1982)): very close to the geotextile, a highly permeable zone of large soil particles forms a bridging network. The finer particles in this zone have been washed away in the early stage of the installation of the geotextile filter. Right behind the bridging zone, there exists a so called "soil filter" whose permeability decreases as the distance from the geotextile increase. This layer is actually retaining the rest of the soil from washing through. The soil behind this layer is essentially undisturbed.

Although geotextiles do not directly retain in situ soil, their choice is very important for the formation of

the "soil filter". The ideal "soil filter" should meet two criteria: (i) the permeability of the system should remain relatively constant with time; and (ii) no further in situ soil should be piped out after the formation of the "soil filter".

As one can see from the above description, the mechanism is essentially the same as the "self-healing process" of the base soil. As a result, the criteria established for geotextile filters are very similar to conventional filter criteria:

Piping requirement: O_I < D85 soil

Permeability requirement: O_I > D15 soil

where O_I is an indicative pore size of the geotextile.

Because of this similarity, results obtained in this study should be applicable also to geotextile filters.

(6) Influence of Spatial Variation of Soil Parameters and Quality Control

To the writer's knowledge, Witt & Brauns (1984)'s recent study is the first attempt to investigate the influence of parameter variation on the reliability of filters. They looked for the minimum dimensions of a sample which can represent the grain size distribution of an homogeneous soil mass. In this context, they took 128 adjacent samples from a 16 x 18 grid elements from their test embankment. Both D15 and D85 were found to follow

lognormal distributions; however, the coefficient of variation for D85 was one third that of D15 (Fig. 1.10(b)). They also provided a figure which shows the spatial correlation of D15 and D85 (Fig. 1.10(c)). They combined their findings with Freudenthal's classic reliability model to show the influence of parameter variation on the failure probability.

1.2.2 Cracking, Leakage, Erosion and Filters

One of the main lines of current research on dam filters is based on the following failure scenario (Vaughan & Soares (1982), Sheard, et al(1984(b)). Even in dams designed and constructed according to good modern practice, the risk of developing concentrated leaks through the impervious core is relatively high. The leaks may be caused by: (i) development of cracks by differential settlement; (ii) cracks due to hydraulic fracturing; (iii) construction deficiencies; (iv) high concentration of flowlines from soil into fractured rock and, (v) cracks due to drying especially in arid areas. The consequences of these concentrated leaks can be either: (i) gradual clogging of the leaks by particles migrating from upstream or closure of cracks by upper soil collapsing; or (ii) development of larger erosion channels which finally result in piping failure.

This scenario is based on the failure (or near fail-

ure) of dams, some of which were designed and constructed in accordance with state of the art. In the case of Balderhead Dam in England, leaks were induced by hydraulic fracturing and the filter failed to retain fines migrated from crack walls (Vaughan, et al (1970), Sherard (1973)). Hyttejuvet Dam in Norway suffered concentrated leak during the first filling of the reservoir, which is supposed to have resulted from hydraulic fracturing of the core (Wood, et al (1976)), Sherard (1973)). Differential settlement due to irregular shape of the rock foundation is considered to be responsible for the serious damages by erosion in Stockton Dam in California as well as Matahina Dam in New Zealand (Sherard (1973)). Failure of the secondary Dam of Wadi Qattarah in Libya was induced by drying shrinkage cracks through the core (Khan (1983)). As to the failure of Teaton dam in Idaho in June 1976, it is generally agreed that the internal erosion initiated due to the high concentration of flowlines from the impervious core into the joints of rock at the site (Chadwick (1981), Seed & Duncan (1981)). Seed and Duncan (1981) stated in conclusion: "If the contact surfaces between the impervious core and the jointed rock at the Teaton site had been appropriately sealed and a filter layer had been provided to prevent movement of core material into any voids that may have inadvertently remained unsealed, the piping which lead to failure of dam could not have occurred."

This scenario identifies some important aspects of dam design and construction allowing to which we can systematically classify some current research efforts:

(i) Prevention of Embankment Cracking

This is a classic problem in dam design and construction. Many provisions during design and construction to prevent cracking can be found in standard reference books such as Sherard, et al (1963) and Wilson, et al (1979). However, recent research work has been based on the fact that it is impossible to totally eliminate the probability of cracking of the core nil, and has attempted to investigate countermeasures which can protect embankment dams from erosion even if some cracks develop.

(2) Erodibility of Base Soils and Dispersive Clay

Once a crack has developed and has been filled with flowing water, it is important to evaluate erodibility of the base soil. For this purpose, Arulanandan & Perry (1983) have proposed a parameter called "critical shear stress", which is the stress required to initiate erosion during hydraulic flow. The parameter was found to be a function of clay type, composition of pore, property of eroding fluid and structure of soil. They also pointed out that even if the clay is erodible, it is possible to prevent dam failure if adequate protective filters are provided. Hjeldnes & Lavania (1980) investigated a similar problem for two particulr soils.

The related problem of "dispersible clay" has attracted attention of dam engineers since the early 1970's. It was first mentioned by Australian engineers after studying the failure of small uniform dams by piping (Aitchison & Wood (1965)). It is believed that certain clays, presence of certain types of water, erode rapidly by individual colloidal clay particles going into suspension. Tests to identify dispersive clays have been proposed by Sherard, et al (1972), (1976a), (1976b), and Sherard and Decker (1976). It is gradually becoming a concensus that even for dispersive clay particles migrated from crack walls can be retained by properly designed filters (Sherard 1979, Sherard, et al, 1976, 1984b).

(3) Filters to Retain Fines Migrated from Crack Walls

In this dam failure scenario, filters should be designed to retain fines migrated from crack walls. This idea was originally proposed by Vaughan and applied to the design of Cow Green dam (Vaughan, et al (1975)). He states: "The investigation of the damage to the Balderhead dam showed that the filter downstream of the core had failed to prevent loss of material from the core due to internal erosion. The investigation indicated that, if crack forms in a clay core and the water velocity through it is slow, segregation of eroded material may

occur, with only finer particles reaching the filter. ... To be fully effective, a filter must prevent the passage of these finest particles and this approach was adopted for the design of the Cow Green filter."

Vaughan and Soares have more systematically studied the problem in Soares (1980) and Vaughan & Soares (1982). To summarize their main conclusions:

(i) The finest particle size that a filter should retain can be determined from clay flock size. This depends on the clay-water chemistry at each site.

(ii) A relationship can be determined experimentally between the size of particles retained by a filter and its permeability. This relationship seems suitable for the preliminary design of a filter.

The proposal of using permeability as a filter criterion seems reasonable since permeability is closely related to size and structure of the void phase of a soil. Furthermore, such a criterion is in accordance with the use of the finer portion of a filter grain size distribution such as DF15, because of widely accepted relationships between permeability and the finer grain size (e.g., Hazen's formula).

Sherard and coworkers recently published a paper

on the designing of filters for silts and clays (Sherard, et al, 1984b). Two different types of laboratory tests have been developed by the authors, namely slot test and slurry test. In the former test, a slot is made in base material, and then a relatively high hydraulic gradient (e.g., 1000) is applied. In the slurry test, the base soil is prepared in slurry form (water content about 2.5 times the liquid limit), and also the high gradient was applied. It is reported that the two types of tests gave comparable results.

The materials used by the authors for the base soils include a wide variety of clays and silts of different geological and geographical origin, including highly dispersive clays. All the filters consist of clean, fine sands of different gradation. For each of 36 different base soils, they determined the value of DF15 of filters which correspond to transition between stable and non-stable conditions.

The boundary DF15/DB85 ratios were found to range between 9 to 57, and not to depend significantly on Atterberg's limits. Furthermore, no significant difference was found between ordinary nondispersive clays and highly dispersive clays having similar particle size distribution.

Based on this series of experiments, one may con-

clude that the conventional filter criterion is valid, although sometimes too conservative, to design filters against cracked clay or slit core. However, it is the writer's opinion that they are too quick in justifying conventional filter criterion, DF15/DB85. Since the experiment is comprehensive, more discussions on physical mechanisms of filtering may bring deeper insight to the phenomenon.

One of the aims of the present study is to give a deepen understanding in the soil particle transport within soil mediam. There is a strong, physical similarity between the ordinary base soil-filter problem and the problem of filters retaining the fines migrated from crack walls: for example, Vaughan and Soares (1982) claim that their permeability cirterion is valid for both clay particles and usual cohensionless uniform base soils if DB85 is used as the minimum particle size to be retained, and Sherard, et al (1984b) has reported Terzaghi's criteria works well for clay particles, also. The writer believes that, although most of the experimental data this thesis is based on is on cohesionless base soils, the results should shed some light also on filtering against clay particles migrated from the crack walls.

1.3 Purpose of the Present Study

In the dam filter design, one faces a problem similar to those of many other geotechnical engineering problems: conventional design criteria has been derived mainly by empirical means, and it is the consensus of the profession that the criteria, although sometimes conservative, work well on most of the cases. However, because of the broadening of the applications and the requirement for more economical design, there is a necessity to understand the phenomenon in greater detail. In addition, there are a few incidents reported that the conventional criteria did not work satisfactorily.

The objectives of the present study are as follows:

(i) To improve understanding of the mechanism of soil particle transport, especially in the context of filtering through physical modeling and statistical analysis of existing experimental data.

(ii) To search for improved filter criteria as well as to assess uncertainty involved in them.

(iii) To propose a method to calculate the probability of malfunctioning of a filter for an entire earth structure. The model should help in evaluating the degree of uncertainty

one can tolerate in design and in the quality control during construction.

This thesis is organized as shown in Fig. 1.11. First, in Chapter II, a soil particle transport model is developed. Although the transport model is fundamental and popular in many other fields, it has never been applied to the soil particle transport problem. The model is capable of accounting for special features of the soil particle transport phenomenon, particularly the release and absorption of soil particles. The model is verified by using experimental data by Southworth (1980) on soil against sereen. Many numerical simulations of soil particle transport at base soil-filter interface are also presented; these results are helpful in understanding the mechanisms involved in filtering. It is emphasized that the self-healing mechanism of base soil plays a major role in the filtering process; the properties of base soil that are desirable for this process are discussed.

In light of the physical insights obtained in Chapter II, a statistical anaysis of existing laboratory data on filter performance is carried out in Chapter III. It is believed to be the first attempt to analyze the filter performance data by a statistical method. The conventional criteria are analyzed first to evaluate their perform-

ance. Then the analysis is extended to searching for improved design criteria. This analysis confirmed the primal role of DF15/DB85 (the parameter used in the conventional Terzaghi's criteria), however, a secondary parameter (DB95/DB75) is found, which is considered to give information on the self-healing properties of the base soil. The implication is that even if the conventional filter criteria (i.e., DF15/DB85 < 4-5) is on the average conservative, the same criteria becomes unconservative if the base soil has broadly distributed coarser portions. The uncertainty involved in the proposed criteria is also analyzed.

In Chapters II and III, the particle transport problem is restricted only at the specimen scale. The problem is extended to the scale of the whole structure in Chapter IV, where a model to account for the spatial variability of soil properties is developed. The model is a generalization of the well known weakest link concept to a two dimensional continuum. Through this model, one can calculate the failure probability of the entire structure by knowing the failure probability at each individual point of the base soil-filter interface plane, and a parameter that has the measure of correlation distance.

The construction record of Carters Dam, Geogea is used for a case study in Appendix C. Based on the grain size data, the average failure probability function is ob-

tained using the results of Chapter III. The correlation structure is estimated from the construction control density tests data because the grain size data are too few to estimate the spatial correlation. The calculated failure probability appears to be reasonable.

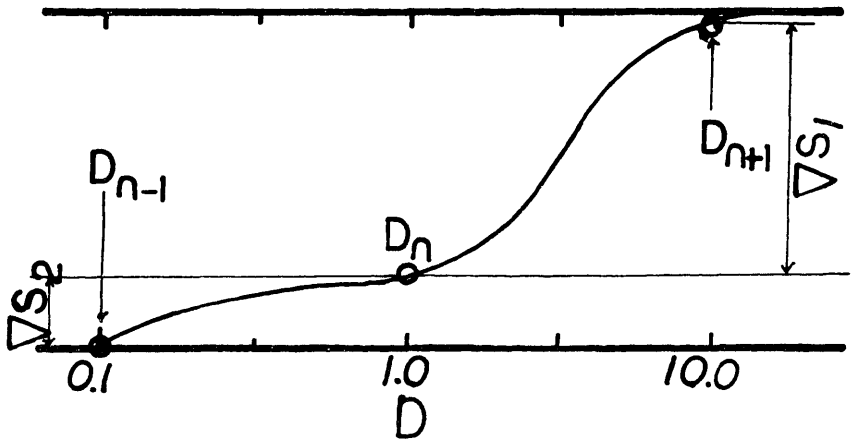

(a) Lubotkov's Method

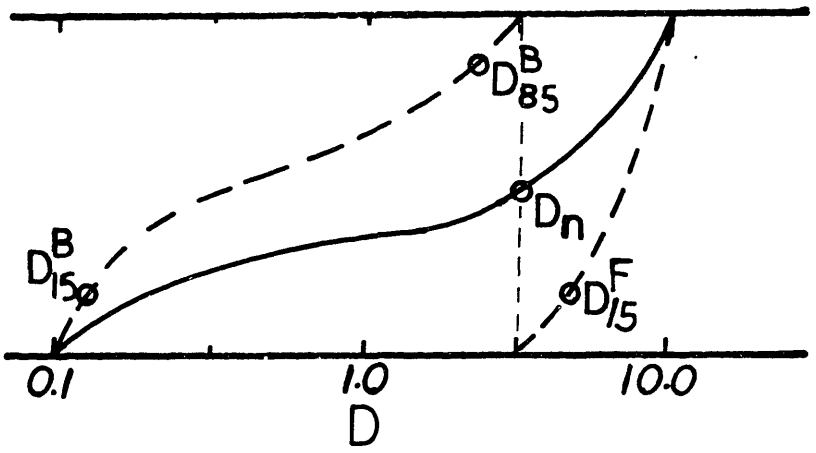

(b) Kezdi's Method

Fig. 1.1 Methods to Judge Internal Stability of Soils

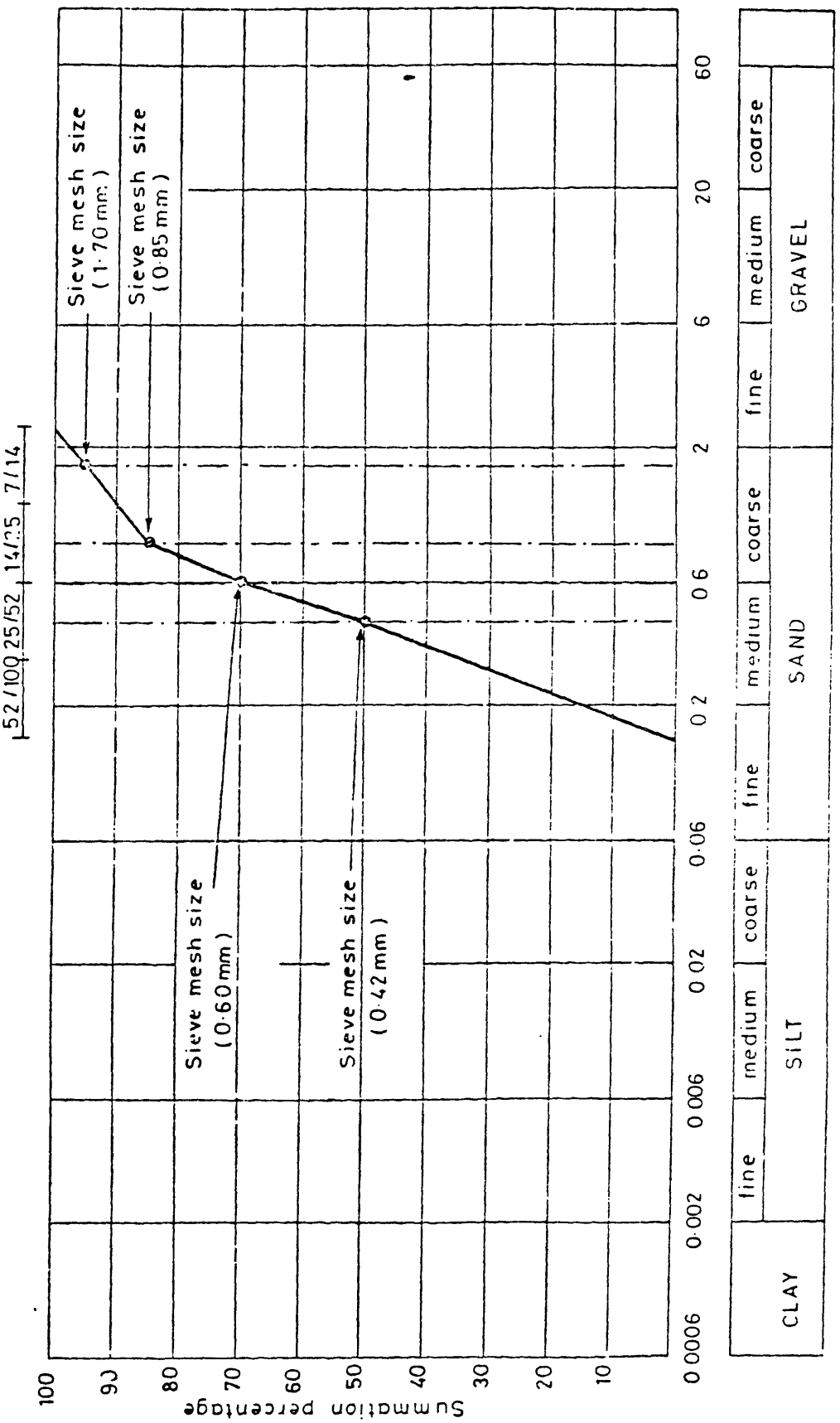

Fig. 1.2 Sieve and Sand Combination - Series 3S Tests (after Soares, 1980)

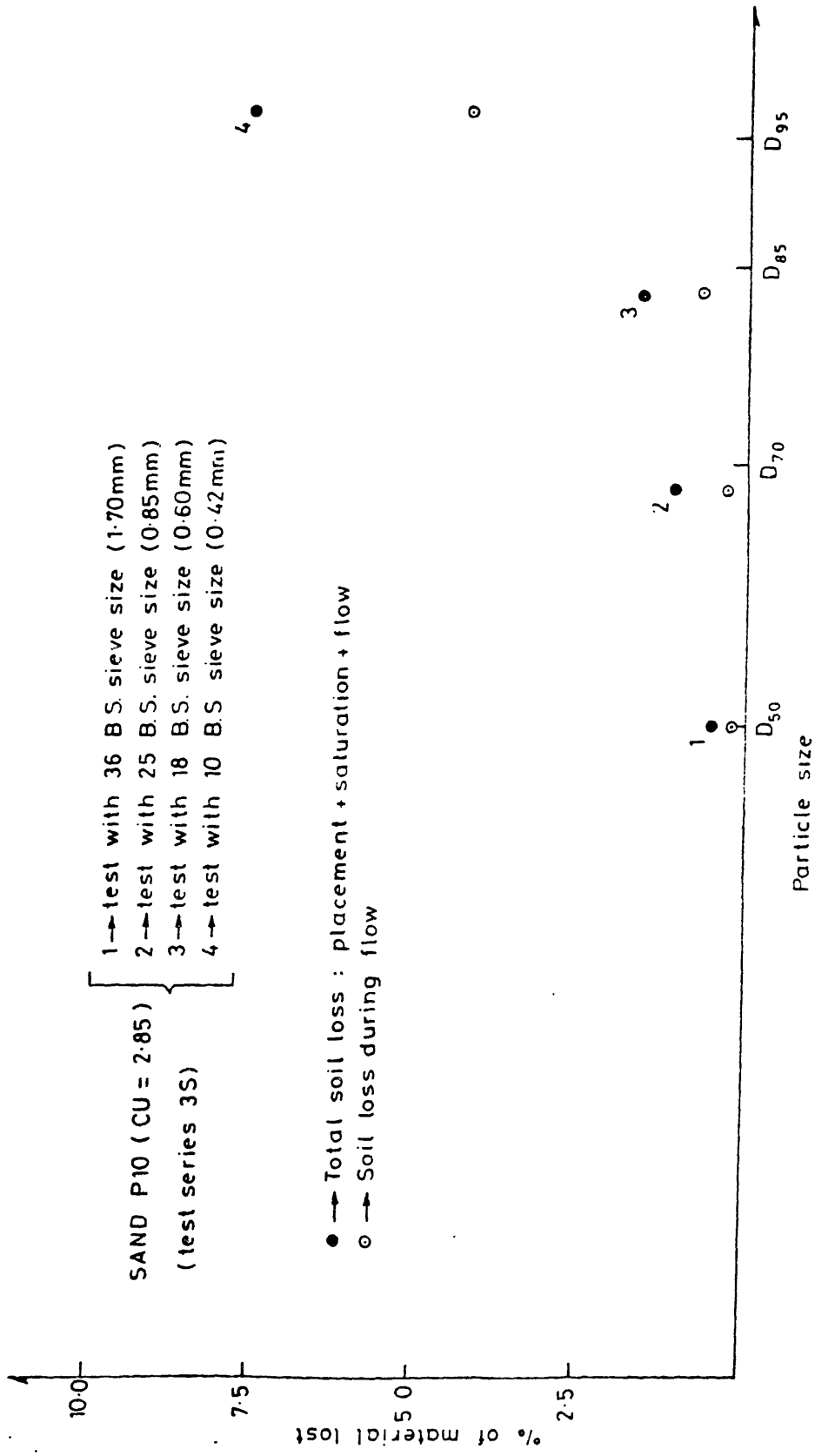

Fig. 1.3 Test Results - Series 3S (after Soares, 1980)

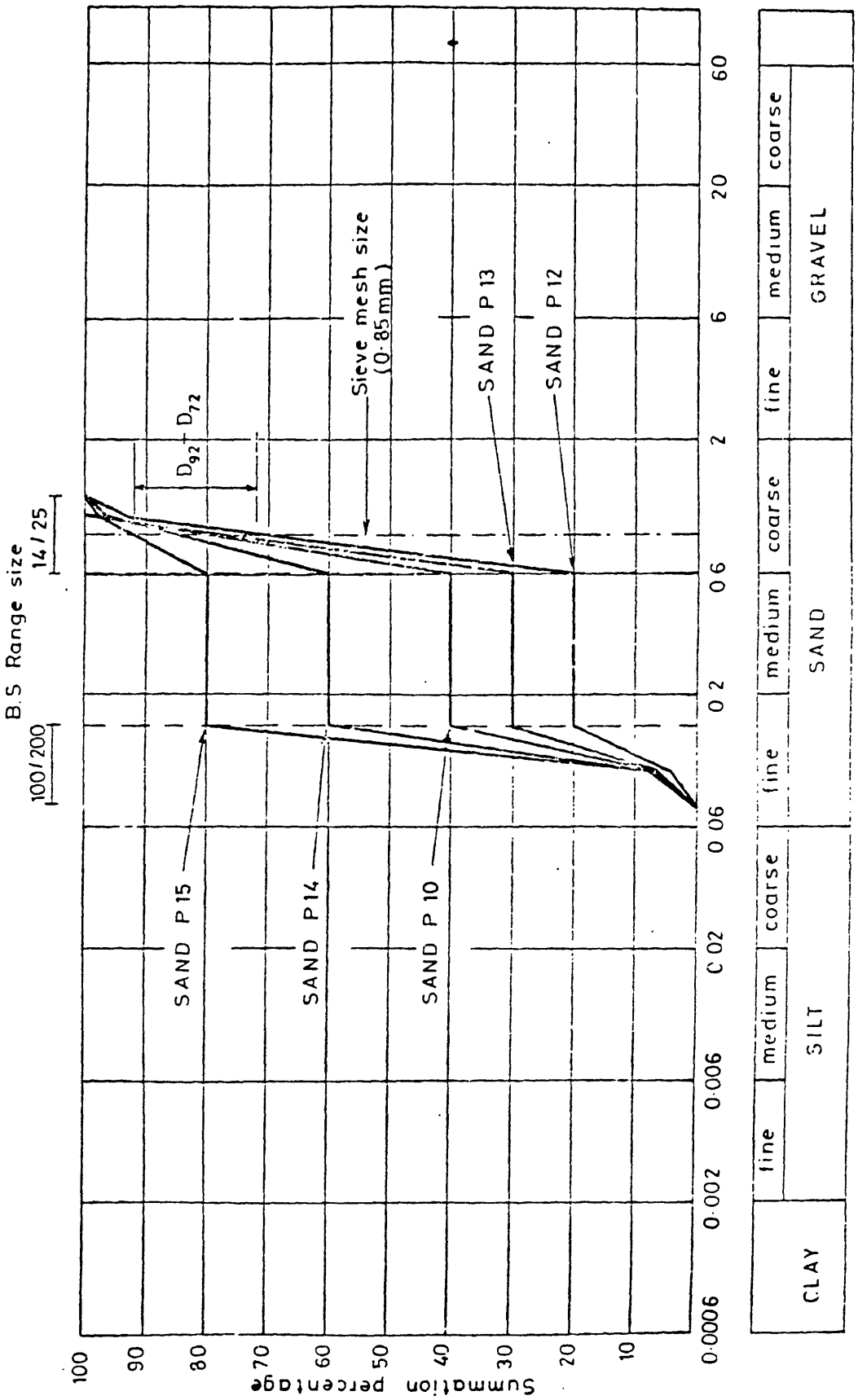

Fig. 1.4 Sieve and Gap Graded Sands Combination - Series 4S Tests (after Soares, 1980)

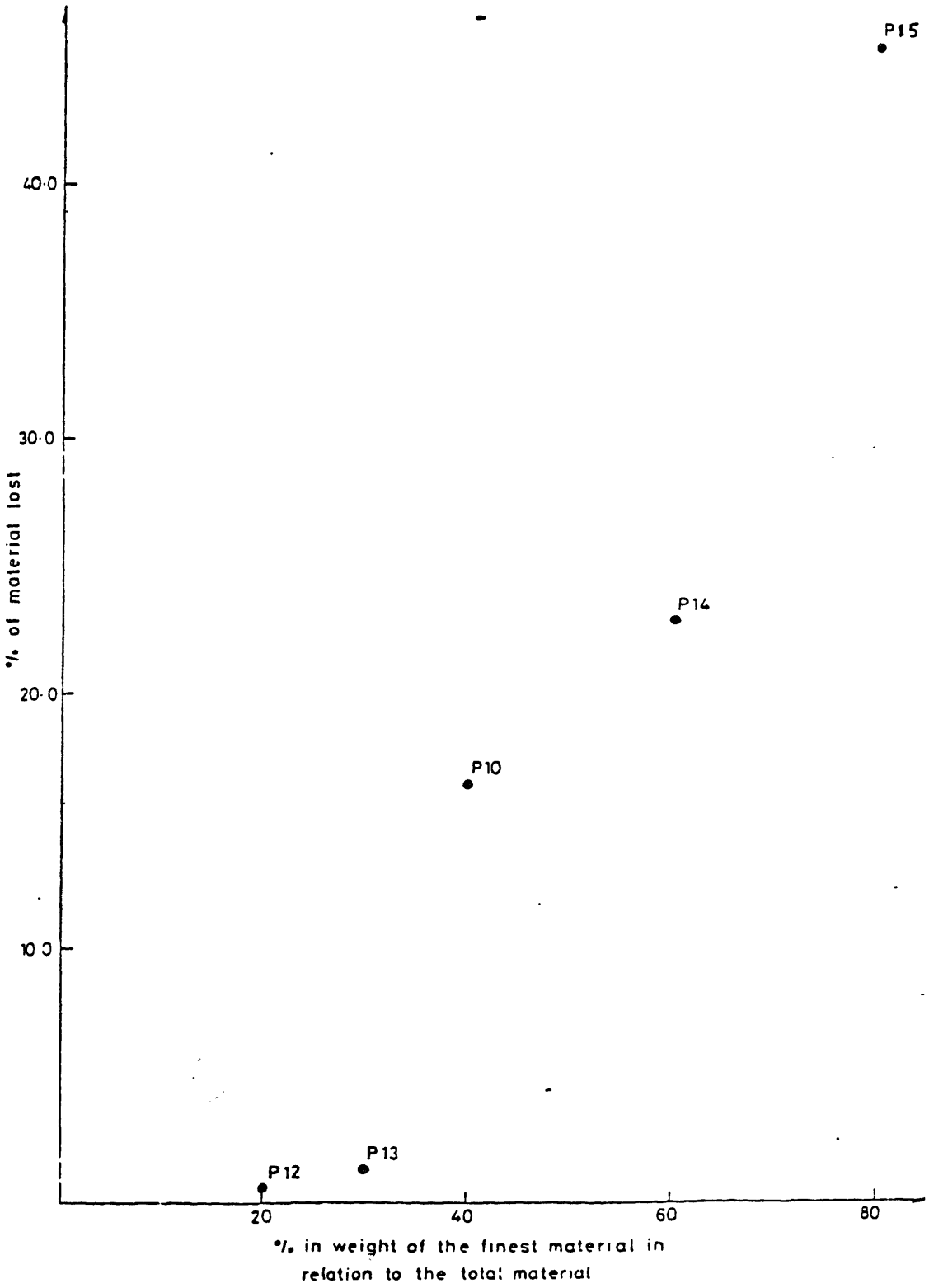

Fig. 1.5 Test Results - Series 4S (after Soares, 1980)

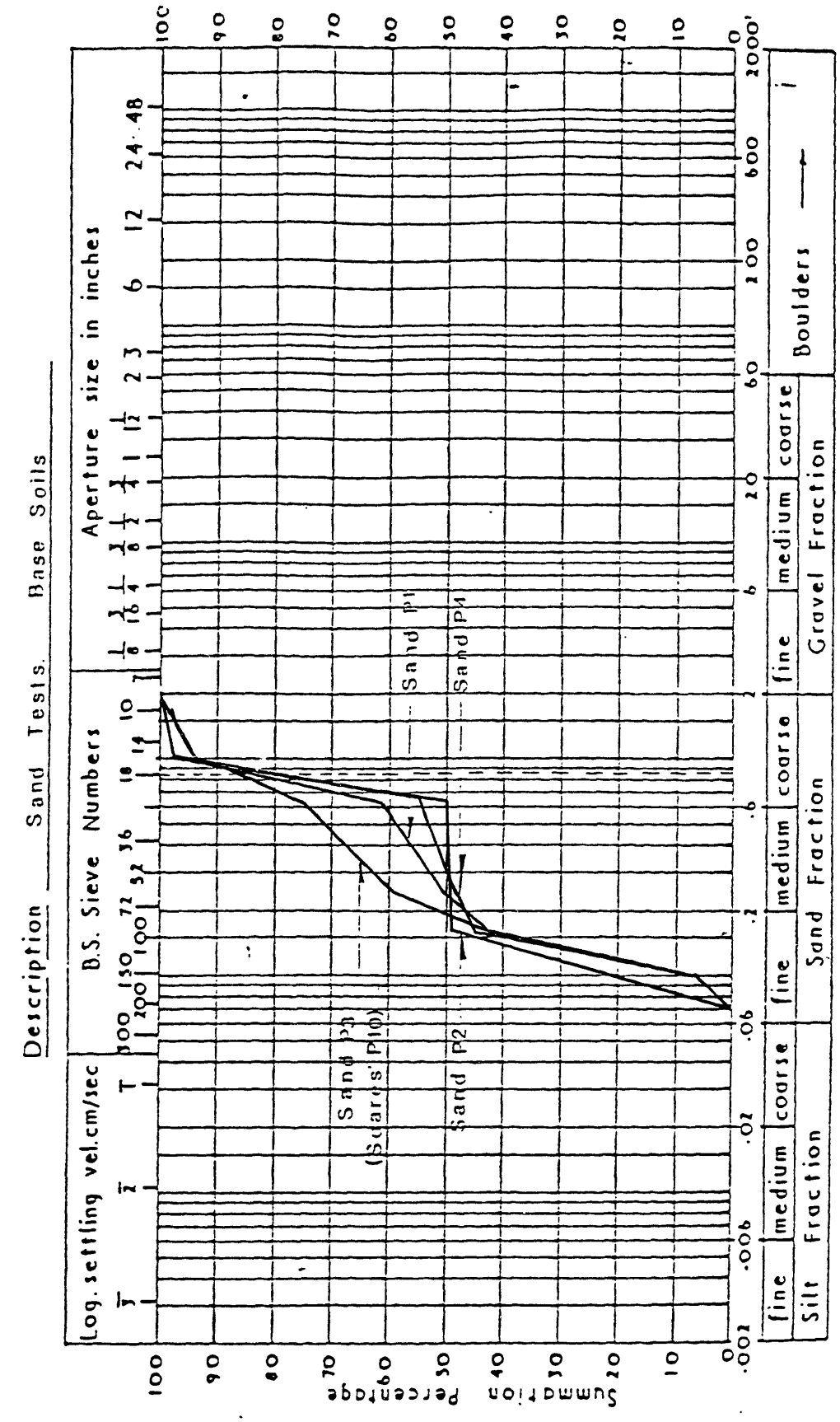

Fig. 1.6 Sieve and Sands Combination (after Mendez 1982)

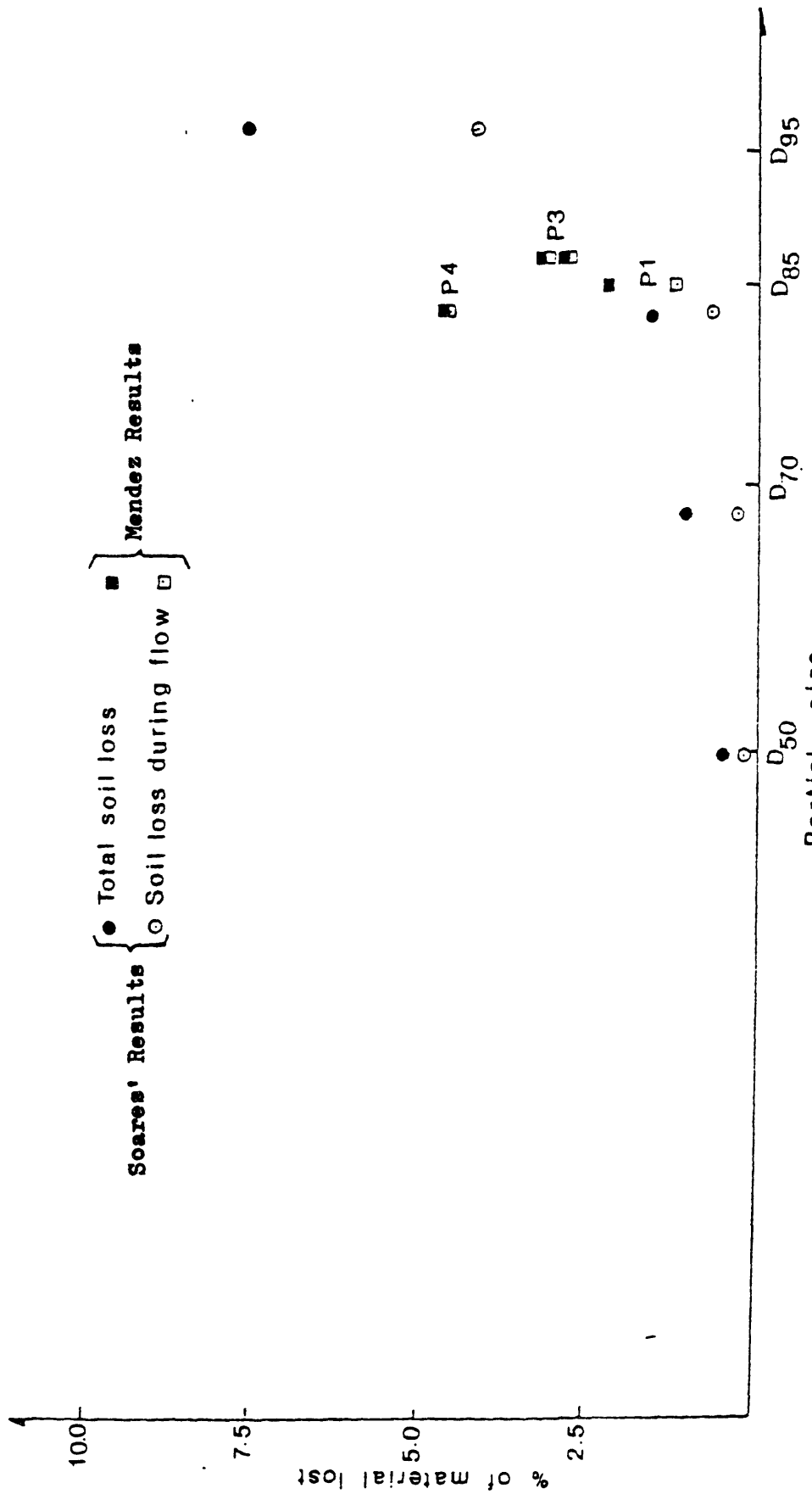

Fig. 1.7(a) Test Results for Sieve and Sands Combination (after Mendez 1982)

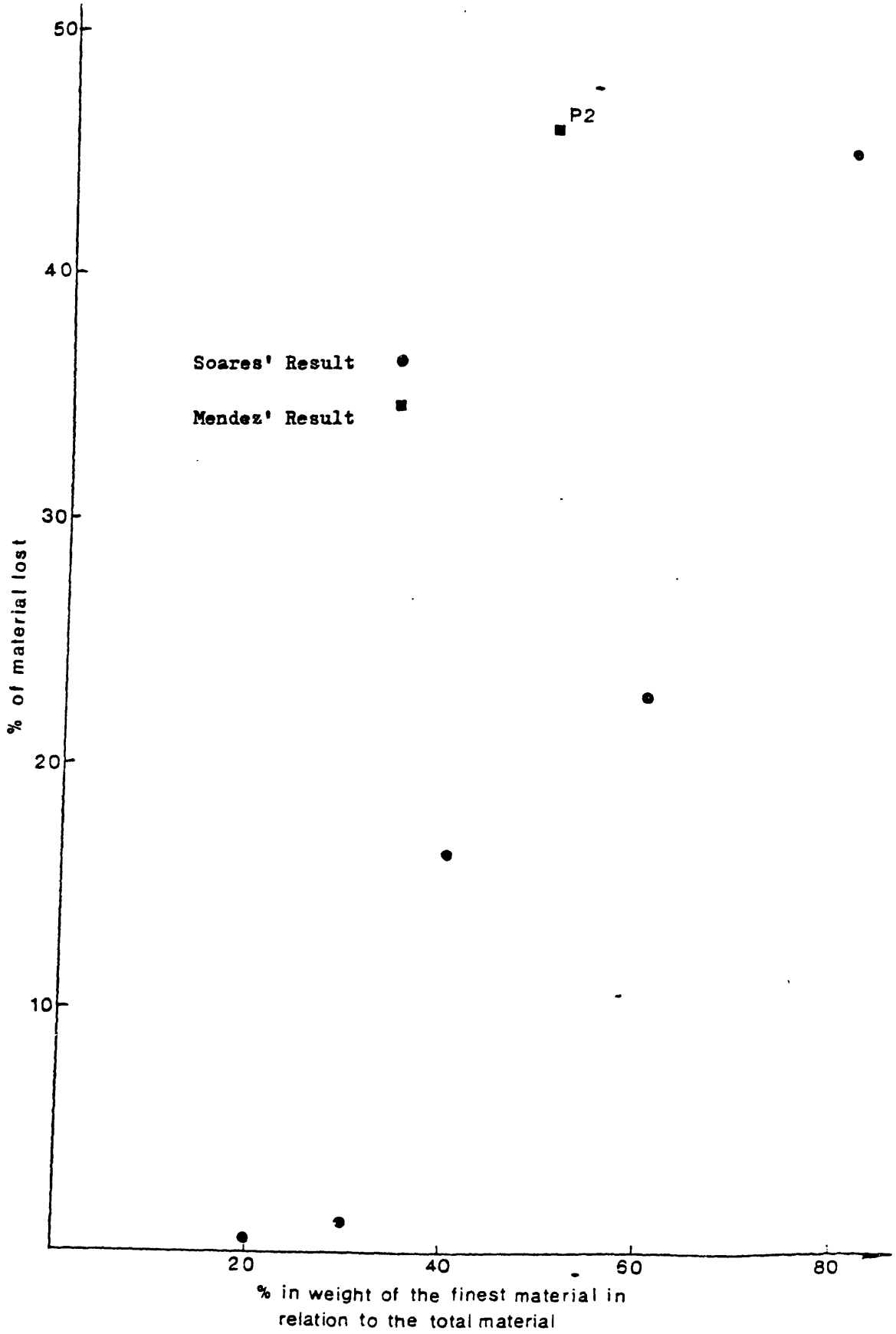

Fig. 1.7(b) Test Results for Gap-Graded Sands (after Mendez 1982)

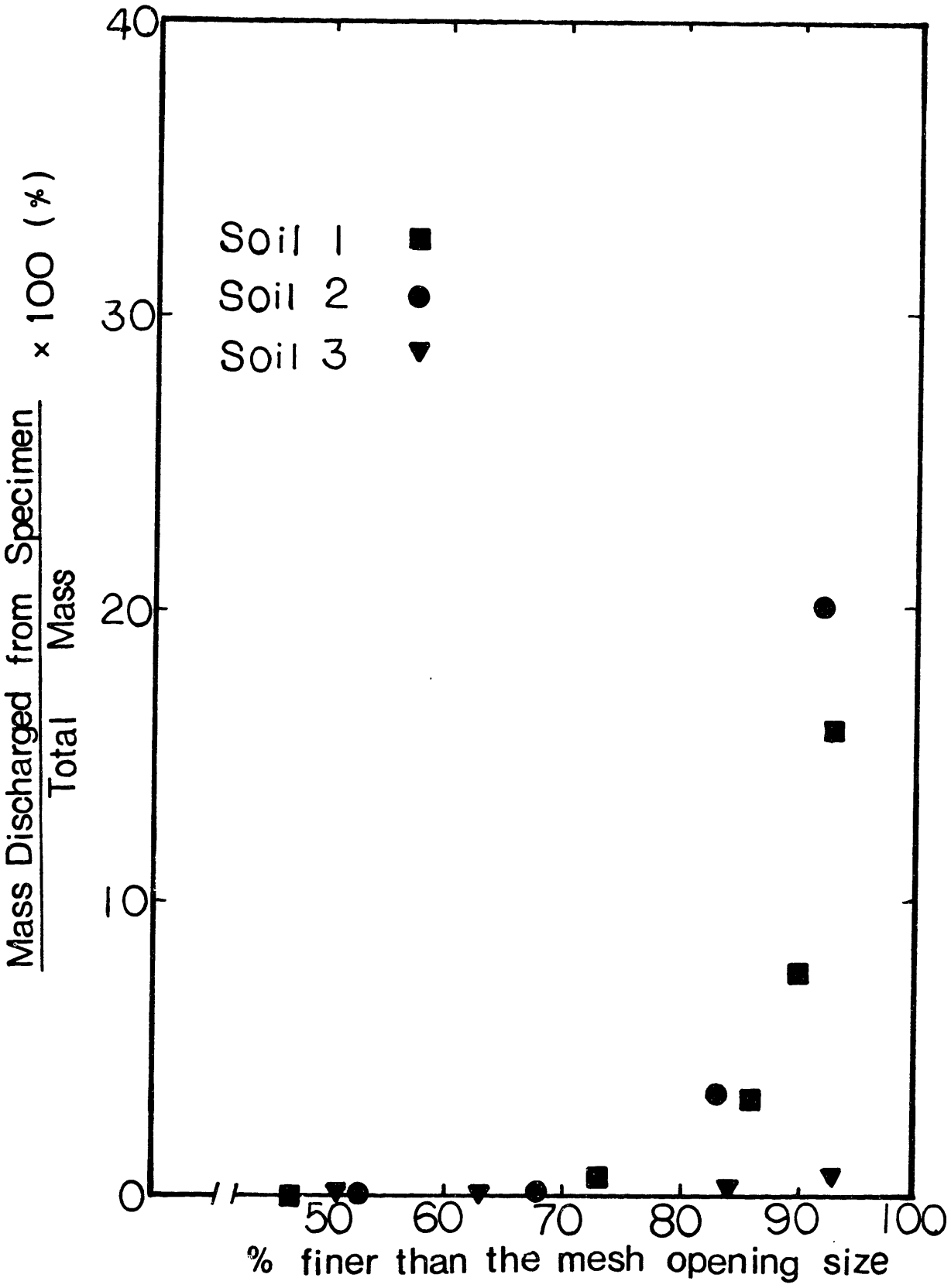

Fig. 1.8 Results of Southworth's Tests of Soil against Screen

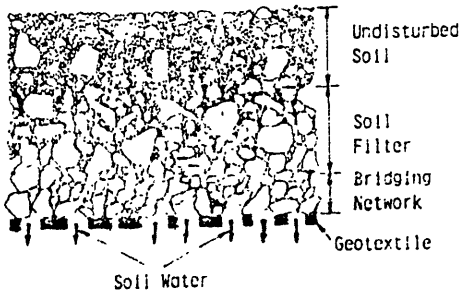

Fig. 1.9 Formation of Soil Filter behind the Geotextile Filter (after Lawson)

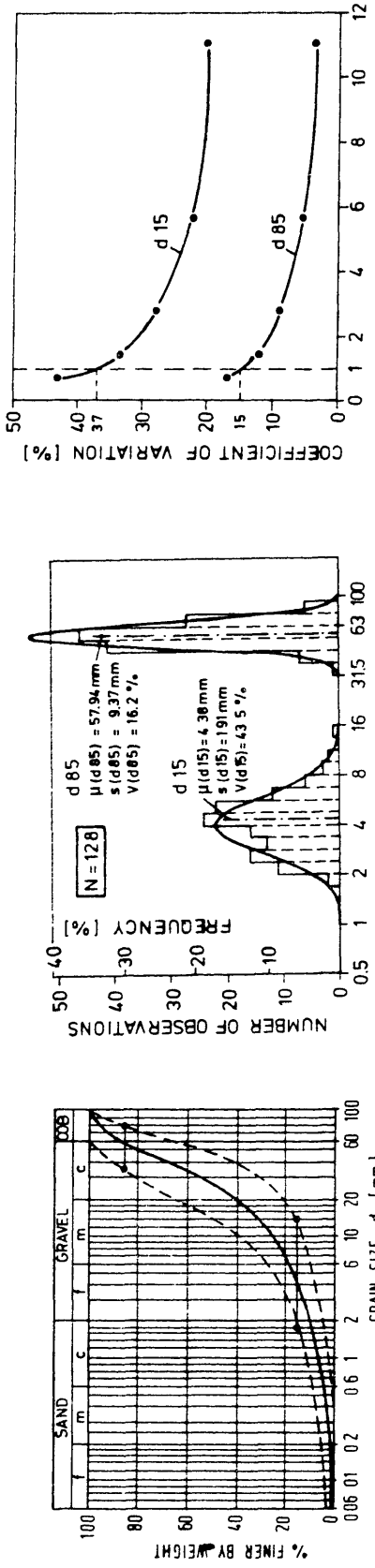

(a) Average grain size distribution in the test fill

(b) Histograms and frequency distributions of d15 and d85 for 128 unit samples

(c) Coefficients of variation for d15 and d85 in dependence on sample mass

Fig. 1.10 Spatial Variation of Grain Sizes (after Witt and Brown, 1984)

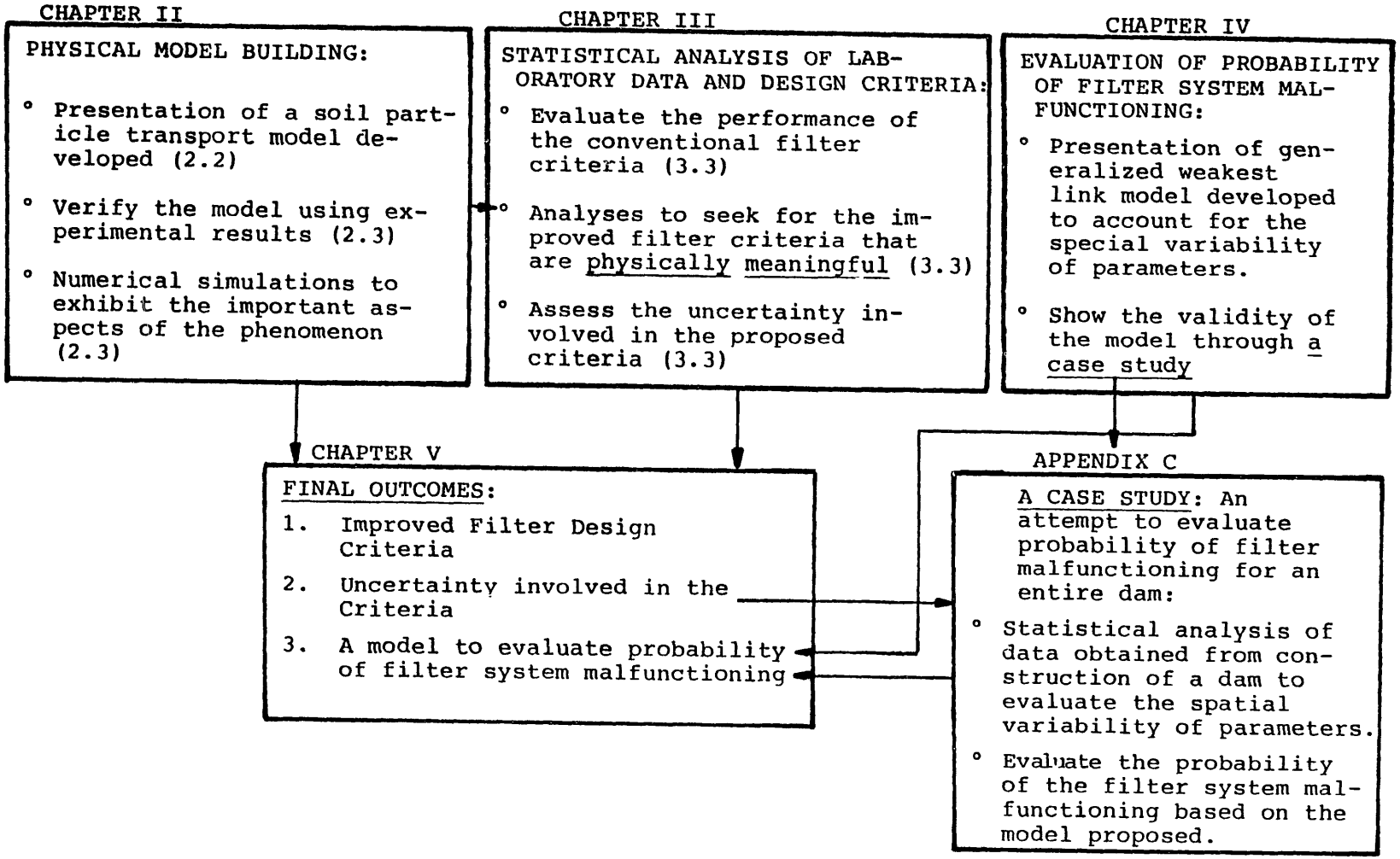

FIGURE 1.11 THE ORGANIZATION OF THE THESIS

CHAPTER II. PHYSICAL ASPECTS OF SOIL PARTICLE TRANSPORT

In this chapter, a simple one dimensional model is introduced to describe the movement of soil particles within a soil medium. The presentation is somewhat qualitative due to the difficulties of obtaining model parameters. Still, the model provides useful physical insight into the soil transport phenomenon, and helps to interpret the results of the statistical analysis in the next chapter.

2.1 Introduction

Not many theoretical studies exist regarding the soil particle transport. Among those are Silveira (1965, 1975), Wittman (1978) and Honjo (1983). All of these studies attempt to model the movement of soil particles within a soil medium by considering the void phase geometry of granular soil. This approach faces two main difficulties:

(i) The main practical concern is to predict the behavior of whole earth structures, or of smaller soil volume (e.g., a specimen). It is unfortunately very difficult, if not impossible, to deduce the behavior of a soil mass from void or granular characteristics.

(ii) The soil transport phenomenon is largely determined by very complex interactions between moving soil particles and stable particles which work as barriers; at different time and space locations, the same particle may change from one type to the other.

Instead of looking at the problem at the scale of individual particles, we will develop a model in terms of absorption and release of various size particles. The model is of a type which is commonly used in many transport problems, (e.g., chemical solute transport in porous media, contaminant transport in ground water), satisfies the conservation of mass and is capable to model convection, absorption, release (generation) and dispersion of solute or, for us, particles.

Before developing the model, some useful terminology should be established. Free Particles are those particles that are in a state of moving. The remainder of particles act as barriers and are called Stable Particles. The notion from free or stable conditions is not associated with a particular particle size; rather, particles change from one type to the other depending on the change of state of the medium in time and in space.

The phenomenon by which a particle changes from free

to stable is called absorption. The reverse phenomenon is called release.

Only a one dimensional deterministic formulation of the problem is presented in this chapter. This is because the model purpose is to understand the physics of the phenomenon. Detailed experimental results are essential to the estimation of model parameters, and to the extension to 2 or 3 dimensions.

2.2 Modeling of Soil Particle Transport

The main factors that influence soil particle transport are discussed first in Sections 2.2.1-5. A model is then developed in Section 2.2.6 and methods for its numerical implementation are described in Section 2.2.7.

2.2.1 Conservation of Mass

Conservation of Mass is a fundamental principle of all transport phenomena. It is the basis of the continuity equation in fluid mechanics; for soil particle transport, it can be expressed as follows.

Consider the small one dimensional element (x,x+dx) illustrated in Fig. 2.1. The inflow into and the outflow from the element of free particles with grain size in the interval (w,w,+dw) during the time interval (t,t,+dt) are written as $Q(x-dx,t,w)v(x-dx,t,w)dtdw$ and $Q(x,t,w)v(x,t,w)dtdw$, respectively; where $Q(x,t,w)$ denotes the dry

density of free particles at x,t and w and v(x,t,w) is their velocity. (Throughout this chapter, the specific gravity of soil is assumed to be the same for all particle size.) Let $\varepsilon(x,t,w)dxdwdt$ be the net amount of particles added to the free particles from the stable particles in time (t,t+dt) and space (x,x+dx), for size (w,w+dw). Conservation of mass in the element (x,x+dx) implies

$$\{Q(x,t+dt,w) - Q(x,t,w)\}dxdw$$

$$= Q(x-dx,t,w)v(x-dx,t,w)dtdw - Q(x,t,w)v(x,t,w)dtdw + \varepsilon(x,t,w)dxdtdw$$

or

$$\frac{\partial}{\partial t} Q(x,t,w) = -\frac{\partial}{\partial x}\{Q(x,t,w)v(x,t,w)\} + \varepsilon(x,t,w) \qquad (2.2.1)$$

Since there is no flow of stable particles, the only change that these particles experience in time (t,t+dt) is due to absorption and release. Therefore,

$$\{S(x,t+dt,w) - S(x,t,w)\}\, dxdw = -\varepsilon(x,t,w)dxdwdt$$

or

$$\frac{\partial}{\partial t} S(x,t,w) = -\varepsilon(x,t,w) \qquad (2.2.2)$$

where S(x,t,w) is the dry density of stable particles at x,t and w.

Equations (2.2.1) and (2.2.2) express conservation

of mass, respectively for the free and stable particles.

2.2.2 Momentum Equation

Fluid mechanics problems are usually governed by two basic equations: one is conservation of mass (continuity equation), the other is the momentum equation (Navier-Stocks equation for Newtonian fluids). Also for particle transport problems, it is desirable to have a momentum equation.

It is well known that Darcy's law, which is the basic equation for slow steady flow through porous media, can be derived from Navier-Stocks' equation (see for example, Bear 1972). Therefore, if it is reasonable to assume that free particles move with the fluid, as is usually the case for chemical suspensions, one can obtain the velocity of flow from Darcy's law (or more fundamentally, from Navier-Stocks' equation). This assumption corresponds to "simple convection" cases, and is usually considered as a first approximation to reality in chemical solute transport problems.

In soil particle transport, the same assumption is unrealistic due to the much larger resistance that free particles experience in their motion. Therefore, particle velocity may be much slower than the fluid velocity.

Unfortunately, there is no general framework which can treat our problem and we shall be forced to introduce somewhat artificial assumptions on the velocity of free particles. A mitigating factor is that if one is not interested in the change of soil conditions with absolute time, but only intend to predict relative changes of conditions, then all one needs to specify is relative easiness with which particles move according to their size.

2.2.3 Absorption and Release

In the soil particle transport problem, absorption and release are the central issues. The amount of research on these problems in geotechnical engineering is very limited, we cannot expect to obtain much information from this area, but abundant literature is available on similar problems from other disciplines, e.g., the transport of chemical solute through soil. (Lapidus & Amundson (1952), Lindstrm & Bcersma (1970), Boast (1973), Hendricks (1978), Murali & Aylmre (1983)). Many terminologies and ideas will be borrowed from this area.

Mathematical models for chemical solute transport are very similar to that for soil particles introduced in previous sections. The dry density of free particles $Q(x,w,t)$ is replaced by the concentration of chemical solute in fluids, and the dry density of stable particles, $S(x,w,t)$, is analogous to concentration of chemical ab-

sorbed on solid surfaces. Using previous notations, the net absorption/desorption (release) of chemicals is generally expressed through the equation.

$$\varepsilon(x,t,w) = \varepsilon[\, S(x,t,\cdot),\ Q(x,t,\cdot),w] \qquad (2.2.3)$$

Notice that $Q(x,t,\cdot)$ and $S(x,t,\cdot)$ are functions containing information of $Q(x,w,t)$ and $S(x,w,t)$ for all w, and $\varepsilon(x,t,w)dxdtdw$ is the net abosrption/release at x,t and w.

If there is only one type of chemical solute (this is equivalent to the case of one grain size in the soil particle transport), the model is called single species model. On the other hand, if several chemicals are involved, the model is called multi-species model. Naturally mathematical models for the latter are more complicated and involve a larger number of parameters, which may be difficult to estimate.

The relationships that govern the adsorption and desorption (release) of chemical solute are called isothermals. There are mainly two types of isothermal models. One is called the equilibrium absorption model and applied when the absorption and desorption of chemicals occur very fast compared to convection and dispersion; as a result, one can assume that a certain chemical equilibrium condition is satisfied at all points of space

and time. A general form of the equilibrium absorption model is

$$S(x,t,w) = \nu[\, S(x,t,\cdot),\ Q(x,t,\cdot),w] \qquad (2.2.4)$$

By substituing Eq. (2.2.4) to Eq. (2.2.2), we obtain

$$\varepsilon(x,t,w) = -\frac{\partial}{\partial t} S(x,t,w)$$

$$= -\frac{\partial}{\partial t} \nu[\, S(x,t,\cdot),\ Q(x,t,\cdot),w] \qquad (2.2.5)$$

See Eq. (2.2.3) for the notations. Some of typical models of this category are shown in Table 2.1. In the linear model, the ratio between $S(x,t,w)$ and $Q(x,t,w)$ is constant for all x,t and w; thus, $S = a\ (Q_{max} - Q)$ condition is always satisfied (see the table for notations). By Eq. (2.2.5), we obtain

$$\varepsilon(x,t,w) = -\frac{\partial}{\partial t} S(x,t,w) = a\frac{\partial}{\partial t} Q(x,t,w)$$

This is also shown in Table 2.1. This is the simplest assumption one can make, and the advantage is that the differential equation (d.e.) obtained only includes constant coefficient terms. Freudlick model assumes a log-linear relationship between Q and S. Since, in most of the chemical problems, the absorption and desorption rates are functions of Q and S, the model is physically more realistic than the linear model. The obtained d.e.

has coefficients which explicitly includes function Q. The Longmuir Model is another popular model in the chemical transport; it assumes a linear relationship between 1/S and 1/Q. Since this mdoel allows Q to be infinite, application to particle transport problem is not appropriate.

The other model, called dynamic absorption/desorption model is more realistic in a sense that it takes the time needed in the chemical actions that result in absorption and desorption explicitly into account. A general form of this model can be written as follows:

$$\varepsilon(x,t,w) = - \nu^{+} [S(x,t,\cdot),Q(x,t,\cdot),w]\ Q(x,t,w) + \nu^{-} [S(x,t,\cdot),Q(x,t,\cdot),w]\ S(x,t,w) \qquad (2.2.6)$$

where ν^{+}: absorption rate

ν^{-}: desorption rate .

Some models of this type are shown in Table 2.2. The linear model assumes constant absorption rate and desorption rate. The log-linear model assumes the power functions for these rates, which are physically more realistic.

Although the equilibrium absorption model is only an approximation, it is usually mathematically more

tractable. The equilibrium absorption model has been extended to multi-species problems, see for example Murail & Alymore (1983).

In soil particle transport, one must use multi-species model because the very essence of the problem resides in the different behavior of different grain sizes. On the other hand, the absorption and release of soil particles are more mechanical than chemical phenomena at least for cohesionless soils. Therefore, time needed for the actions may not be an important factor. This fact allows us to introduce the equilibrium absorption model to our problem. In fact, we will introduce a parameter which has clear physical interpretation, and whose mathematical form is the same as that of the equilibrium absorption model in Section 2.2.6.

2.2.4 Distance Lag Effect

In the soil particle transport, the factor that controls particle velocity, absorption and release should be the state of the soil a little distance downstream of the particles under consideration. The distant lag effect is one of the distinguished features of the problem. The way it operates is illustrated in Fig. 2.2.

One way to introduce distance lag effect into the model is to rewrite Eq. (2.2.1) as

$$\frac{\partial}{\partial t} Q(x,t,w) = -\frac{\partial}{\partial x} \{Q(x,t,w) v [S(x+\Delta x,t,\cdot), Q(x+\Delta x,t,\cdot), w]\}$$

$$+ \varepsilon [S(x+\Delta x,t,\cdot)\ Q(x+\Delta x,t,\cdot), S(x,t,\cdot), Q(x,t,\cdot) w] \quad (2.2.7)$$

where Δx: the distance lag, a quantity with values of the order of particle size.

$Q(x,t,w)$: the dry density of free particles at space x, time t and size w.

$S(x,t,w)$: the dry density of stable particles at x, t and w.

$Q(x,t,\cdot)$: a function containing information of $Q(x,t,w)$ for all w.

$S(x,t,\cdot)$: a function containing information of $S(x,t,w)$ for all w.

The left side of Eq. (2.2.7) presents the change of dry density of free particles with time t. This should be equal to the net in flow of particles at x,t and w (the first term) and the net amount of release of free particles (the second term) in order to satisfy the mass conservation. The velocity is function of $S(x+\Delta x,t,\cdot)$, $Q(x+\Delta x,t,\cdot)$ and w, where Δx is showing distance lag. The net release of free particles, $\varepsilon dxdwdt$, is a principle function of all $S(x+\Delta x,t,\cdot)$, $Q(x+\Delta x,t,\cdot)$, $S(x,t,\cdot)$, $Q(x,t,\cdot)$ and w. By comparing Eq. (2.2.7) to Eq. (2.2.1), one can

understand how the equation has been modified for the log distance lag effect.

For stable particles, Eq. (2.2.2) is modified as

$$\frac{\partial}{\partial t} S(x,t,w) = - \varepsilon[S(x+\Delta t,t,\cdot), Q(x+\Delta x,t,\cdot), S(x,t,\cdot), Q(x,t,\cdot), w] \qquad (2.2.8)$$

See Eq. (2.2.7) for the notations. Equations (2.2.7) and (2.2.8) should be solved simultaneously.

2.2.5 Dispersion

Equation (2.2.1) assumes that the velocity of all particles of the same size w is the same at any given locations x and time t. However, for reasons given below, the velocity of particles is actually different for different particles. As a result, particles tend to disperse as they travel through the porous medium. In order to describe this process, it is usually assumed that the flux Qv is given by

$$Qv = Q\bar{v} + q$$

where $Q\bar{v}$ is the mean flux and q is dispersive flux. The most common assumption for q is

$$q = - D \frac{\partial Q}{\partial x}$$

where D is a constant. In this case

$$Qv = Q\bar{v} - D \frac{\partial Q}{\partial x} \qquad (2.2.9)$$

It is widely recognized that dispersion depends mainly on two mechanisms

(i) Molecular diffusion. This is the process observed in chemical suspension. Particles tend to move in the direction of their concentration gradient under the influence of their kinetic activity (known as Fick's law). Molecular diffusion is usually a micro phenomenon which is a function of time and is independent of the velocity of particles.

(ii) Mechanical dispersion. Because of irregularities of the porous medium, the velocity and direction of flow vary from point to point. Specifically,
   (a) within a given pore, the flow rate is slower near the wall than in the middle,
   (b) the flow is faster in larger pores than in smaller ones, and
   (c) the direction of flow at each point differs from the average flow direction.

These velocity variations result on a dispersion of particles as they travel in the medium. Mechanical dispersion is a micro phenomenon and is usually a function of velocity. In general, the second mechanism plays the main role in engineering problems such as chemicals in ground water flow (Bear [1972]).

Substitution of Eq. (2.2.9) to Eq. (2.2.1), we obtain

$$\frac{\partial Q}{\partial t} + \frac{\partial}{\partial x}\{Q\bar{v} - D\frac{\partial Q}{\partial x}\} = \varepsilon$$

$$\frac{\partial Q}{\partial t} + \frac{\partial}{\partial x}(Q\bar{v}) = D\frac{\partial^2 Q}{\partial x^2} + \varepsilon \qquad (2.2.10)$$

Equation (2.2.10) is called the convection-dispersion equation.

2.2.6 Proposed Model

Through Sections 2.2.1-5, we have considered various aspects of soil particle transport. In this section, this information is put together to propose a final model.

The conservation of mass equation for free and stable particles forms the basis of our formulation. In this equation, multi-species release and absorption and distance lag effects are taken into account. In spite of the fact that, in numerical calculations, we need to introduce some artificial velocity functions, the model gives a good physical picture of the phenomenon.

The effect of dispersion is not included in our present study because (a) this is probably a secondary effect, and (b) there are practical difficulties in evaluating the dispersion coefficient.

The isothermals introduced in Section 2.2.3 are not directly applicable to our problem; we need to describe particles release and absorption. One may assume that the following relationship holds at all points of soil medium at time t

$$\nu[\, S(x+\Delta x,t,\cdot),Q(x+\Delta x,t,\cdot),w] = \frac{S(x,t,w)\,dxdw}{Q(x,t,w)\,dxdw} \qquad (2.2.11)$$

where the notations are given in Eq. (2.2.7). Equation (2.2.11) states that the ratio of the dry density of stable and free particles of size w at (x,t) is a function, $\nu(\cdot)$, of dry density of stable and free particles of all sizes at $(x+\Delta x,t)$ and of size w. We shall call this ν <u>the retention ratio</u>.

Another convenient way to look at the retention ratio is to transform it to a quantity given by

$$\lambda\,[S(x+\Delta x,t,\cdot),Q(x+\Delta x,t,\cdot),w] = \frac{S(x,t,w)}{S(x,t,w)+Q(x,t,w)}$$

$$= \frac{\nu\,[\,S(x+\Delta x,t,w),Q(x+\Delta x,t,w),w]}{1+\nu\,[S(x+\Delta x,t,w),Q(x+\Delta x,t,w),w]} \qquad (2.2.12)$$

λ gives the fraction of particles of size w at (x,t) that are mechanically blocked by particles at $(x+\Delta x,t)$. λ is termed here <u>retention proportion</u>.

It should be pointed out that Eq. (2.2.11) has a form similar to that of the equilibrium absorption isothermals introduced in Section 2.2.3 and is, therefore, mathematically very tractable because ν is not an explicit function of t. According to Eq. (2.2.2), the net rate of release is

$$\varepsilon(x,t,w) = -\frac{\partial}{\partial t} S(x,t,w) = -\nu[S(x,+\Delta x,t,\cdot),Q(x+\Delta x,t,\cdot),w] \frac{\partial}{\partial t} Q(x,t,w) \qquad (2.2.13)$$

By substitute (Eq. 2.2.13) to Eqs. (2.2.7) and (2.2.8), one obtains the final equations:

$$\{1 + \nu [S(x+\Delta x,t,\cdot),Q(x+\Delta x,t,\cdot),w]\}\frac{\partial}{\partial t} Q(x,w,t) + \frac{\partial}{\partial x} \{Q(x,w,t)\nu [S(x+\Delta x,t,\cdot),Q(x+\Delta x,t,\cdot),w]\} = 0 \qquad (2.2.14)$$

and

$$\frac{\partial}{\partial t} S(x,t,w) = \nu[S(x+\Delta x,t,\cdot),Q(x+\Delta x,t,\cdot),w] \frac{\partial}{\partial t} Q(x,t,w) \qquad (2.2.15)$$

Given appropriate boundary conditions, these equations can be solved for S(x,t,w) and Q(x,t,w).

It is worthwhile to point out the possible extension of the model. In Section 2.1, we have pointed out that most of the available soil transport models try to describe the void phase of the soil and, therefore,

encounter some difficulty in extensioning results to a larger scale; moreover, the complex interaction between particles is almost hopeless to describe. The model proposed here can describe these aspects, although the parameter used in the model (the retention ratio, ν,) may be difficult to evaluate from experimental results. These two models, opposite may be seen as, is complementary, and if one could obtain the retention ratio as a function of soil parameters such as porosity and grain size distribution, then one would be able to establish a link between the two models.

2.2.7 Method for Solving Eqs. (2.2.14) and (2.2.15)

Equations (2.2.14) and (2.2.15) are linear partial differential equations of the first order. A useful method to obtain analytical solutions for this type of equation is the method of characteristics. The method not only gives an answer to the problem but also frequently provides insight into the physical problem. An application of the method to a groundwater contaminant transport problem can be found in Charbeneau (1981).

Another possibility is to use numerical procedures. The latter procedure can easily incorporate the lag distance effect and are more practical to produce the results under a variety of initial and boundary conditions,

as well as for different ν functions. The most convenient numerical scheme works backwards, i.e., the solution is formed starting from downstream and moving against the direction of flow.

The procedure for backward calculation is shown in Fig. 2.3. After setting the initial condition (Step 1), time, size of particles, and space are varied incrementally in a do loop fashion (Steps 2 through 7). The retention ratio for (x,t,w) is obtained based on the solution Δx downstream (Step 8). The velocity is also obtained in the same way (Step 9). Then the inflow to and outflow from the element is calculated based on the information obtained in the previous steps (Step 10). Finally, the density of free particles and stable particles are found for the next time. Calculation is made very simply by the equilibrium absorption assumption (Step 11). The location (x), size (w) and time (t) are checked to see whether calculation has been completed (Steps 12 - 15).

In order to ensure accuracy of the computation, the ratio between the minimum element thickness (Δx_{min}) and the velocity, v, times time interval, Δt, is kept larger than five. Furthermore, a check is made by calculating the total mass in the system, and then comparing it to the initial value.

2.3 Numerical Examples and Their Physical Interpretations

We are going to investigate some aspects of soil particle transport by using the model proposed in the previous section. Experiments with soil against a screen have been carried out by several investigators to study the "self-healing process" of base soils at the filter interface. The advantage of using a screen in place of a soil filter is that in the former, there is no uncertainty in the opening size and, therefore, the action of base soil particles can be observed under simplified but clearer boundary conditions. Because of this simplified boundary condition, this model is used in the numerical simulations calculated in Sections 2.3.1 and 2.3.2. In Section 2.3.1, "self-healing process of base soil" is investigated (see Section 1.2.1(2)). We first try to reproduce the result of soil against a screen experiment done by Southworth (1980). Then some quantitative discussions are made on this process. In Section 2.3.2, the other important aspect of base soil action during the filtering process, "the internal stability of base soil", is investigated. The action is illustrated by the numerical simulation results obtained by the proposed model. Finally, in Section 2.3.3, the clogging process of filters is simulated.

2.3.1 Self-Healing Process of Base Soils

In his study, Southworth (1980) used four different soils to experimentally investigate the self-healing process. Since his fourth soil contains more than 85% of fines (i.e., particles smaller than 0.074 mm) and is considered to be cohesive, only first three soils are included in the analysis. These three soils are termed Soils 1, 2 and 3 respectively. The grain size distribution and the compaction condition of the soils are shown in Fig. 2.4 and Table 2.3 respectively. These soils are fairly well to well graded (D60/D10=10, 3 and 6 respectively) and contain some silt. The dry densities at the beginning ($\gamma_{d\ initial}$) and at the end ($\gamma_{d\ final}$) of the experiment are given in Table 2.3, whereas $\gamma_{d\ initial}$ can be obtained from measurement of the initial void ratio, whereas γ_{d} final is estimated from the settlement for the case when there is no discharge observed from the screen. The difference between $\gamma_{d\ initial}$ and $\gamma_{d\ final}$ is a result of densification due to the applied flow.

In order to simulate the experiment using the proposed model, each soil is separated into two portions: one coarser and the other finer than the screen opening. Two functions must then be assumed for the free particles of each of these portions: velocity v and the retention proportion λ. Unfortuantely, not much information is

available on setting these functions; for simplicity, it is assumed here that velocity and retention proportion are assumed to be the same for the two portions of soil. Furthermore, both quantities are assumed to vary linearly from 1.0 to 0.0 and from 0.0 to 1.0 between $\gamma_{d\ min}$ and $\gamma_{d\ final}$ as shown in the Fig. 2.5. In the figure, $\gamma_{d\ final}$ is the final density the specimen reaches by flow-induced densification. These imply that v is 0.0 and λ is 1.0 when γ_d equals $\gamma_{d\ final}$ (all particles are stable), and that v is 1.0 and λ is 0.0 when γ_d is less or equal to $\gamma_{d\ min}$ (all particles are free). Note in Fig. 2.5 that the distance lag effect is included in these functions.

Another important parameter in the numerical implementation of the model is the size of the spatial discretization interval, especially near the screen. This size also fixes the distance lag effect scale, Δx; for, in calculation, conditions of downstream neighboring element are used to calculate v and λ. It is chosen that the thickness of the ten nearest elements to the screen are always set equal to the opening size of the screen.

Results for Soil 1 against #30 sieve (0.51 mm opening) are shown in Fig. 2.6 together with the space discritization scheme used to produced them (Fig. 2.6(a)).

In Fig. 2.6(b) and (c), the behaviors of the finer and coarser portion of soil are illustrated, where the solid lines indicate γ_d of the stable particles, whereas the dotted lines that of the free particles. As one can see from the figure, both portions of soil become free in the initial stage of the experiment (t=2); as time goes on, the soil stabilizes gradually from the elements closer to the screen (t=8). At t=64, most of the portions of the soil are stable and about 6 mm of settlement has taken place.

Most interestingly, the element closest to the screen is fully occupied by the coarser particles, and hinders the rest of the finer particles to be washed through. Southworth observed the phenomenon in the course of his experiment (see Fig. 2.7). He termed it formation of a self-healing filter.

The result of present calculations is displayed in a different form in Fig. 2.8. In this figure, the dry density of the soil, γ_d, is plotted against the ratio r between γ_d of finer soil to the total γ_d. Since we know the initial values of γ_d and r (e.g., r = 86% for soil 1 against the #30 seive), we can show the initial condition as a point on the plane (point C for the present case). We assume $\gamma_{d\ initial}$ and $\gamma_{d\ final}$ are constant for all ranges of r. Later, we will see r changes only

in the element closest to a screen; therefore, the assumption made should not have much influence on the calculated results. Based on the calculated results, we can trace the path followed by each element on the γ_d-r plane. Element 40, which is the element very next to the screen progressively looses finer particles and trankates at point $(0, \gamma_{d\ final})$. Element 39, which is adjacent to Element 40, changes its density with time but r remains the same; it stabilizes when it reaches the point $(0.86, \gamma_{d\ final})$.

Because plots of the type in Fig. 2.8 gives insight into the physical process, many results will be presented later in the same form. We call it a <u>state diagram</u>. In Fig. 2.8, other calculated results for Soil 1 is also presented which exhibit similar behavior.

A state diagram of the calculated results of Soil 3 are presented in Fig. 2.9. The main diffence between Soil 3 and the other two soils is that in the former case γd is already densified to $\gamma_{d\ final}$ at the beginning of the test. The peak of paths shows that soils loosen somewhat at first, but they redensify to $\gamma_{d\ final}$. Except for the element very next to the screen (element A), r remains the same.

The fraction of specimen mass discharged from the screen and the amount of settlement of the specimen are

shown for the three soils in Figs. 2.10 and 2.11. The experimental results are compared with results from the present model. One may observe that they agree rather well, except for the case of large fractions of fines. This is especially true for Soil 3.

The main difference between Soil 1,2 on one side and Soil 3 on the other is that Soil 3 is in a rather dense condition from the beginning of the experiment. This is why for Soil 1 and 2 some settlement occurred also when there is no particle discharge from the screen (see Fig. 2.11); whereas no settlement of Soil 3 is found in the case. The high density of Soil 3 may also be responsible for discrepancies between the calculated and experimental results under denser conditions, where the particles are more interlocked and tend to form arches over the screen openings. This arching action is not introduced in the present model.

A most interesting point in these figures is that both the discharge and the settlement increase dramatically as r increases between 80 and 90%. This can be explained by considering the filtering mechanism: the base soil is retained by a layer which is formed next to the screen, and which consists of only particles coarser than the opening size. Therefore, the amount of particles lost from the specimen depends on how

quickly this layer is formed. There are at least two factors controlling the phenomenon: One is the percentage of particles retained by the screen. The other is the thickness of the layer to be formed. The finer the screen opening size, the larger percentage of retained particles, and the smaller the particles that form the layer, the thinner the layer can be. This multiplicative effect seems to explain why a very small amount of soil is lost when the percentage of fines is below 80%. On the other hand, the ability to retain base soil is quickly reduced as this percentage increases above 90%. This gives a rational basis for using DB85 in filter design criteria: if DB85 is retained by the base soil-filter interface, then a self-healing process takes place without significant loss of the base soil (see also 1.2.1(2)).

2.3.2 Internal Stability of Base Soil

Wittman (1978) have conducted an interesting experiment on gravel sand mixtures (see 1.2.1(1)). Figure 2.12 summarizes the conclusion he obtained for particle transport phenomena through his study. The abscissa indicates the percentage of sand by weight, r, whereas the ordinate gives the dry density, γ_d. A maximum of γ_d is reached when sand and gravel are mixed in a given

proportion. For the same mixing ratio, γ_d varies depending on the compaction effort and on the water content. When γ_d is too low, the particles cannot form a skeleton; this is called the impossible region.

Performing many permeability tests at different mixing ratios, Wittman found that the particle transport phenomenon is different depending on r and γ_d. When the gravel content is high, the skeleton tends to be composed only of gravel; as a result, the sand particles can move freely in this skeleton. If sand particles are washed out from the skeleton, the phenomenon is called <u>suffusion</u>; if they are accumulated, it is called <u>colmatation</u>. In the region where sand content is higher, the skeleton consists of both sand and gravel; in this case there is no internal particle movement and the only possible pattern of failure by flow is piping by heave (i.e., zero effective stress condition).

A diagram similar to that of Wittman is introduced next as a useful representation of soil particle transport. The soil is first divided into two portions: one, grain sizes smaller than a certain value, is called finer soil. The rest of the soil is called coarser soil. We can combine these two portions in any arbitrary mixing ratio, r, and measure $\gamma_{d\ min}$ and $\gamma_{d\ max}$ in some specified way. The associated r-γ_d plane (see Fig. 2.13 (c)) was

termed earlier the state diagram. Now, a third axis is introduced which indicates the retention proportion of finer soil, λ (i.e., the ratio between γ_d of free portion of finer soil and γ_d of total finer soil). λ should be 0.0 for the region where γ_d does not exceed $\gamma_{d\ min}$, which implies that all the finer soil particles are free. On the other hand, λ is 1 where the dry density $\gamma_{d\ final}$ (where all the finer soil particles are stable). A linear increase of γ is assumed between $\gamma_{d\ min}$ and $\gamma_{d\ final}$ as shown in Fig. 2.13(b). Figure 2.13(a) combines Fig. 2.13(b) and Fig. 2.13(c).

If λ can be 1.0 for any mixing ratio of coarser soil and finer soil, then the soil is said to be internally stable soil. This is the case shown in Fig. 2.13. This implies that a layer which consists of any mixing ratio of coarser soil and finer soil (this includes the case of pure coarser soil layer) can retain finer soil particles perfectly if the layer is sufficiently dense (if γ_d is high enough).

However, there are soils that are internally unstable: for them λ cannot be 1.0 for some mixing ratio, r. Figure 2.14 illustrates one such case. The property is most clearly shown in Fig. 2.14(b). Section A-A' where λ is less than 1.0 even when $\gamma_d=\gamma_{d\ max}$. That is to say, a layer with some r cannot retain finer soil

particles even if they are compacted to $\gamma_{d\ max}$. The soil Wittman used in his experiment is an example of such soil.

In order to study the self-healing process based on the concepts introduced in this section, two kinds of hypothetical soils are considered; Demo-soil 1 and Demo-soil 2. As shown in Fig. 2.15, Demo-soil 1 is internally stable soil, and its $\gamma_{d\ min}$ and $\gamma_{d\ final}$ vary according to the percentage of soil finer than the screen opening. On the other hand, Demo-soil 2 is internally unstable soil as shown in Fig. 2.16. Specifically, regions with more than 80% of coarser soil cannot retain the finer soil.

Of course, classification of soil into only two portions is a drastic simplification, but some important aspects of the self-healing process can be analyzed. Cases when soil is divided into three portions will be considered later.

Points A, B and C in Figs. 2.15 and 2.16 indicate the initial conditions assumed in the following numerical experiments.

The first numerical experiment is presented in Fig. 2.17. The initial state of the soil corresponds to point A with 90% of the coarser soil and 10% of finer soil. For internally stable Demo-soil 1 (Fig.

2.17(a)), Element 20, which is closest to the scree, quickly loses its finer particles. The rest of the element just densifies to $\gamma_{d\ final}$ while for them r remained constant. This indicates that a filering layer which consists only of the coarser soil successfully retains the finer soil. On the other hand, Demo-soil 2 (Fig. 2.17(b)) cannot form such a layer, and gradually loses the finer soil from all the elements. This soil stabilized only after all the finer soil has been lost and all the elements have finally reaches (r=0.0, γ_d = 18.0).

The behavior is exactly the same if one starts from point B (80% finer soil) as shown in Fig. 2.18. The only difference is that the path is longer because it contains more finer soil. The behavior is again the same if one begins from some point on $\gamma_{d\ final}$ line as shown in Fig. 2.19.

As mentioned earlier, just dividing soil into two portions may be an over simplification of the problem. In order to investigate the effect of a more refined classification Demo-soil 3 is introduced. This soil consists of 3 portions, namely the coarser portion, the middle portion and the finer portion. We consider this soil as being partially internally unstable soil, meaning that a layer consisting of only coarser portions

can retain the middle portion but cannot retain the finer portion, whereas a layer consisting of mixture of the coarser and the middle soil can retain the finer portion.

Numerical results are shown in Fig. 2.20 for a case in which the screen can retain only the coarser portion of the soil. Demo-soils 1 and 2 are shown in Fig. 2.20(a) and (b) for comparison. For Demo-soil 3 (Fig. 2.20(c)), a first filtering layer is formed in element 20, which is the closest element to the screen; this layer consists only of the coarser portion. Interestingly, the second filtering layer is formed in element 19, which is the second closest element to the screen; this layer consists of a mixture of the coarser and middle portions. It is clear from the figure that this second filtering layer is retaining the rest of the soil. Since there must be two filtering layers formed to retain the soil, the time needed for the formation of these layers is longer and the amount of soil lost is larger.

What was learned from the last two sections about the self-healing process can be summarized as follows: In the successful formation of a <u>self-healing filters</u> at the base soil-filter interface, the size of soil particles that is retained by the interface is the key factor. Both

the experimental and numerical results indicate that the critical size of base soil particle to be retained is between DB80 and DB90. (Section 2.3.1). Internal stability of a base soil is another important factor in the filtering process. For some soils, the self-healing filtering layer at the interface fails to hinder the finer portion of the soil. This is a case of internally unstable soil of which retention proportion λ is smaller than 1 even after the densification by flow (Section 2.3.2). This can be a problem, for example, when a widely graded soil is used as a base soil; because of the large gap in grain size between the filtering layer formed and the soil to be retained, a large fraction of the fines may be lost before an adequate filtering layer is formed.

2.3.3 Clogging of Filters

In this section, the clogging process of a filter is studied and simulated numerically. Figure 2.21 illustrates the space discretization scheme and initial conditions used for this purpose. The system consists of 40 elements, of which 20 are of base soil and 20 of filter soil. Each element has unit thickness. Two analyses (A and B) have been made, using different initial conditions of the base soil: In Case A, the ratio between the finer and coarser portions of base soil is 50/50;

in Case B, this ratio is 85/15; see Fig.2.21(b) and (c).

The properties assumed for the base soil are as shown in Fig. 2.22. This is an internally stable soil, whose retention proportion changes linearly from 0.0 to 1.0 between $\gamma_{d\ min}$ and $\gamma_{d\ final}$. This retention proportion is assumed to be the same for the finer and the coarser portions. The initial conditions are shown in Fig. 2.22(a).

The property assumed for the base soil-filter mixture is somewhat complicated. It has a different retention rate for the finer and coarser portions of the base soil. The state diagram for this soil is presented in Fig. 2.23(a): the abscissa gives the fraction r between the base soil and the total mixture by weight. The ordinate is the dry density, γ_d. The mixture soil is internally unstable for both portions of the base soil. However, for the finer portion, there is a wide range of r for which the retention rate cannot reach 1.0. The variation of the retention rate with γ_d are shown in Fig. 2.23(b) for different r. For the smaller values of the retention proportion of the finer portion is much smaller than that of the coarser portion. It is also assumed that there is no movement of filter soil particles; in other words, filter material is always stable.

Numerical results for Case A are shown in Fig. 2.24. We can observe that the coarser portion of the

base soil is accumulated in elements on both sides of the interface, and this layer is blocking the finer portion of the base soil from washing through: In other words, the accumulation of the finer portion mainly takes place from the second element from the interface. If one looks at the two elements of both sides of the interface, one realizes that accumulation of the coarser portion is initially pronounced on the base soil side; however, penetration and accumulation of the coarser portion into the filter gradually increases and seems to form a stable blocking layer inside the filter.

The results for Case B, which are shown in Fig. 2.25, are similar. However, accumulation of the coarser portion in the elements, adjacent to the interface on the base soil side is smaller than in the previous case. Also, accumulation in this element only occurs in the initial stage (i.e., t=6) and the main blocking layer gradually moves inside the filter (i.e., t=25,100). Finally, a stable blocking layer is formed in the first element of the filter. In this case, accumulation of the finer soil starts from the element right next to the interface.

The state diagram for the elements near the interface are presented in Fig. 2.26 for both Case A and Case B. From the path of Element 20, which is the element right inside the base soil from the interface, one can observe the early accumulation of coarser particles, which are

then gradually lost. This is because the rate of coarser particles entering the element is smaller than that of particles leaving the element. On the other hand, Element 21, which is the first element of the filter, gradually absorbs the coarser particles and stabilizers. The behavior of Elements 22 and 23 is very unstable, i.e., the paths oscillate in the state diagram. This behavior is explained by the fact that there is no filtering layer to retain particles in these elements.

The above may not constitute a general explanation of the filter clogging process. The examples presented here are just demonstrations of how complex the particle transport problem can be even under relatively simple conditions.

2.4 Summary and Conclusions

In order to study the physical mechanism of soil particle transport, a mathematical model has been introduced.

The model is based on the principle of conservation of mass for free and stable particles. Absorption and release of these particles are described by the retention ratio, i.e., by the ratio between the dry density of stable and free particles for each particle size. By introducing this parameter, the equations have the same

form as to equilibrium absorption isothermals in chemical solute transport; these equations are mathematically very tractable.

Another special feature of the proposed model is the distance lag effect for the velocity, absorption and release of free particles. This assumption implies that the state of particles at a given location is controlled by the state of the medium a little distance Δx downstream. Under this assumption, the retention ratio has a clear physical interpretation: it is the rate of particles mechanically blocked by the particles located ∇x downstream.

Unfortunately, we have not successfully obtained momentum equations for the particles. Rather, we are forced to make some assumptions about the velocity of particles. However, if one is not concerned about the change of conditions with absolute time and is rather concerned with the relative change of conditions of the soil, then the present model is a reasonable one. In fact, numerical results from the model are quite helpful in understanding the mechanism involved in soil particle transport.

It is also possible to consider particle dispersion. However, this phenomenon has not been considered in the numerical calculations because (a) it is of

secondary importance and (b) it is almost impossible to estimate the dispersion coefficient.

A numerical procedure is used to solve the equations. In particular, a backward formulation is found to be very convenient for taking the distance lag effect into consideration.

The case of soil against a screen has been considered to study the self-healing process of base soils. Experimental results by Southworth (1980) are reproduced rather accurately by the proposed model. It appears from these results as well as experiments performed by other investigators (see Section 1.2.1(2)) that the self-healing process of the base soil results from the formation of a filtering layer of large particles next to the screen. This layer retains the rest of the soil from washing through. The two main factors influecning the formation of this self-healing filter are (a) the percentage of particles retained by the screen, and (b) the thickness of the layer to be formed. Thus, the more particles are retained, the faster the filtering layer develops. Also the smaller the particles retained, the thinner the layer can be. This multiplicative effect results in very small amount of base soil loss when the retained particle size is smaller than 80% finer by weight. However, if the size is more than 90% finer by

weight, the loss of base soil is significant. This result supports the use of DB85 in filter design criteria.

The internal stability of base soil is considered to be another importnat factor in the self-healing process. Following suggestions in Wittman (1978), base soil is classified as internally stable or internally unstable. In the context of self-healing, internally stable soils are soils whose filtering layer formed behind the screen is capable of retaining the rest of the soil from washing through. On the other hand, internally unstable soils cannot form retaining filtering layer. By using the model, it is shown that internally unstable soils cannot retain their finer portion irrespective of the initial conditions. In reality, the self-healing mechanism can be much more complicated than explained here because soil does not consist of only two portions. A numerical example with a soil that consists of three portions is presented. It is shown that, if the filter formed next to the screen can retain an intermediate part of the base soil, another filter is formed behind the first filter to retain the rest of the soil; naturally, the amount of soil lost during the filter formation is larger.

Several numerical examples demonstrating the clogging of filters by base soil particles are presnted. Although, the assumption introduced in the calculation was

rather simple, the obtained results exibit very complex interaction of soil particles at the base soil-filter interface, which indicates the complexity of phenomenon.

It appears that the proposed model is capable of simulating many aspects of soil particle transport problem. As mentiond in Sectin 2.2.6, one of the most interesting extensions of the present model is to combine this model and the particle/void geometrical models (see Section 1.2.1(3)) so that the parameters introduced in this model, such as retention ratio, ν, can be determined based on the more physical consideration.

TABLE 2.1 EQUILIBRIUM ABSORPTION MODELS WITH SINGLE SPECIES

Name	Equilibrium Condition	Graphic Representation	Comments
Linear Model	$S = a\ (Q_{max} - Q)$ therefore (Eq. (2.2.8)), $\varepsilon = -\frac{\partial s}{\partial t} = a\frac{\partial Q}{\partial t}$ If $Q_{max} = S_{max}$ $a = 1.0$	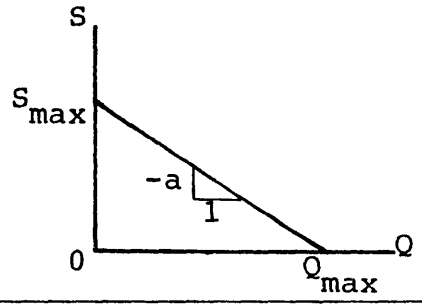	° The simplest assumption. ° The differential equations (d.e.) obtained only have constant coefficients.
Freudlick Model (Log-linear model)	$S = a\ (Q_{max} - Q)^b$ that is: $\varepsilon = -\frac{\partial s}{\partial t} =$ $ab(Q_{max}-Q)^{b-}\frac{\partial Q}{\partial t}$	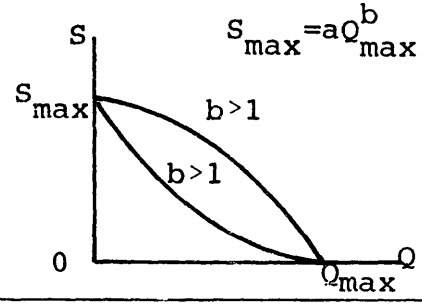	° The d.e. are linear, but the coefficients explicitely include Q.
Langmuir Model ($\frac{1}{Q}$~$\frac{1}{s}$ Linear Model	$S_{max} - S = aQ/(1-aQ)$ that is $\frac{\partial s}{\partial t} = -\frac{a}{(1-aQ)^2}\frac{\partial Q}{\partial t}$	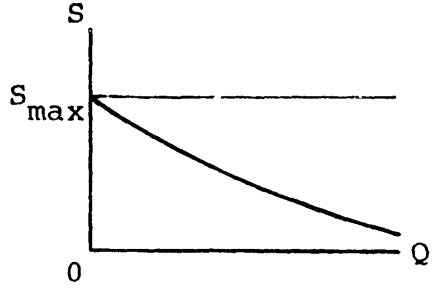	The model seems not appropriate for the soil particle transport problem, since Q cannot be infinite in any case.

TABLE 2.2 DYNAMIC ABSORPTION/RELEASE MODEL WITH SINGLE SPECIES

Name	Equilibrium Conditions	Graphic Representation	Comments
Linear Model	$\frac{\partial s}{\partial t} = k_1 Q - k_2 S$ This is a special case of Eq. (2.2.6): $\nu^+ = k_1 = \text{const.}$ $\nu^- = k_2 = \text{const.}$	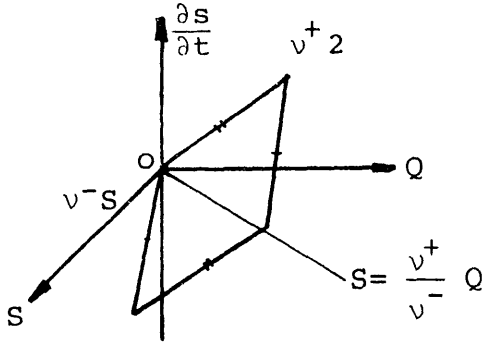	° Simplest dynamic model
Log-Linear Model	$\frac{\partial s}{\partial t} = (\frac{S}{S_{max}})^{k_1} Q$ $- (\frac{S_{max}-S}{S_{max}})^{k_2} S$ This is another case of Eq. (2.2.6): $\nu^+ = (S/S_{max})^{k_1}$ $\nu^- = \{(S_{max}-S)/S_{max}\}^{k_2}$	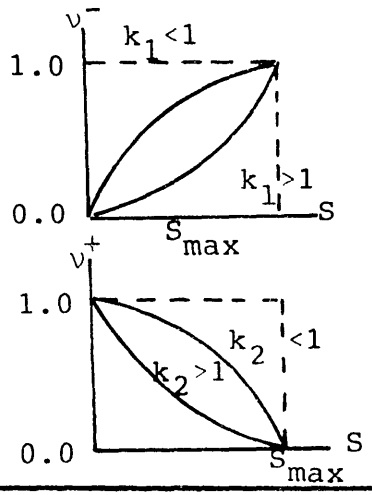	° An extension of Freudlick model to dynamic case.

TABLE 2.3 SUMMARY OF COMPACTION CONDITIONS

(KN/m^3)

Soil	Spec. Grav.	$\gamma_{d\ max}$	$\gamma_{d\ min}$	γ_d at the start of the experiment	γ_d at the end of the experiment
1	2.68	19.2	16.8	17.9	18.7
2	2.70	___	___	17.8	18.3
3	2.55	17.3	13.7	16.8	16.8

TABLE 2.4 SUMMARY OF THE RESULTS OF SOUTHWORTH'S EXPERIMENT

Soil	Screen	Opening Size (mm)	% Soil from the Screen	Mass Discharge (% to whole specimen)	Settlement of the sample (mm)
1	# 14	1.3	93	15.7	12.5
	# 24	0.80	90	7.5	8.3
	# 30	0.51	86	3.3	5
	# 60	0.23	73	0.5	4
	#200	0.074	47	0	4
2	# 10	1.9	92	20	15
	# 24	0.8	83	3.4	7
	# 40	0.38	68	0.1	4
	# 60	0.23	53	0	3
3	# 30	0.51	93	0.2	0.5
	# 40	0.38	84	0.1	0
	# 50	0.28	63	0.1	0
	# 60	0.23	51	0	0

TABLE 2.5 CHARACTERISTICS OF SOILS USED IN THE NUMERICAL EXPERIMENT

Soil	Component			Stable/Nonstable Conditions
	Coarser Portion (C)	Middle Portion (M)	Finer Portion (F)	
Demo Soil 1	15(%)	15(%)	70(%)	Internally stable soil, i.e., C can retain both M and F.
Demo Soil 3	15(%)	15(%)	70(%)	Partially Internally Nonstable soil, i.e., C can retain M but not F. M can retain F.
Demo Soil 2	15(%)	15(%)	70(%)	Internally nonstable soil, i.e., C can retain neither M nor F.

Note: Screen can only retain coarser portion (C).

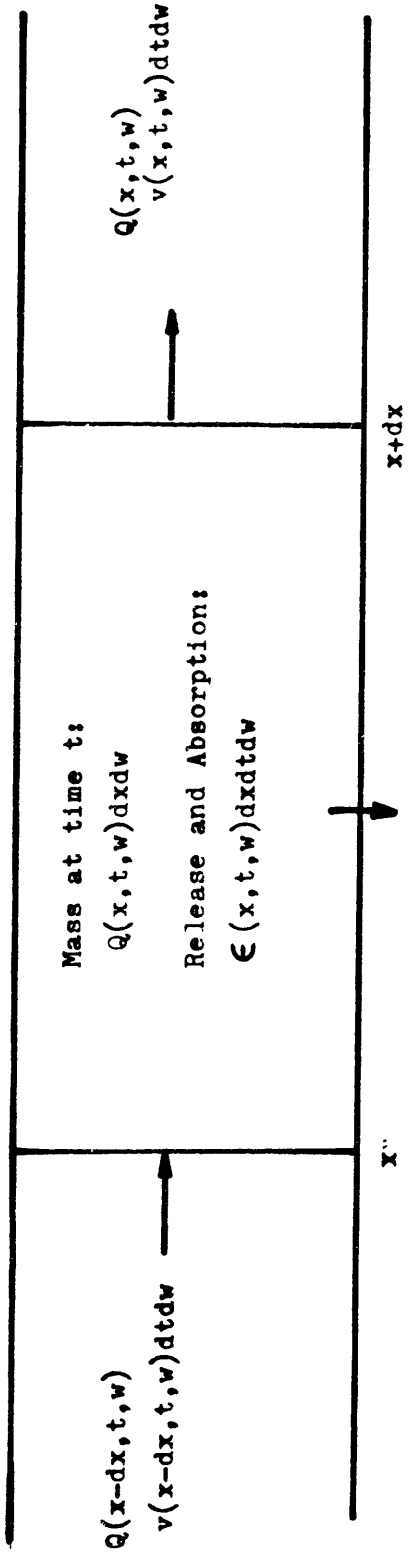

Fig. 2.1 Conservation of Mass of Free Particles in Element (x,x+dx)

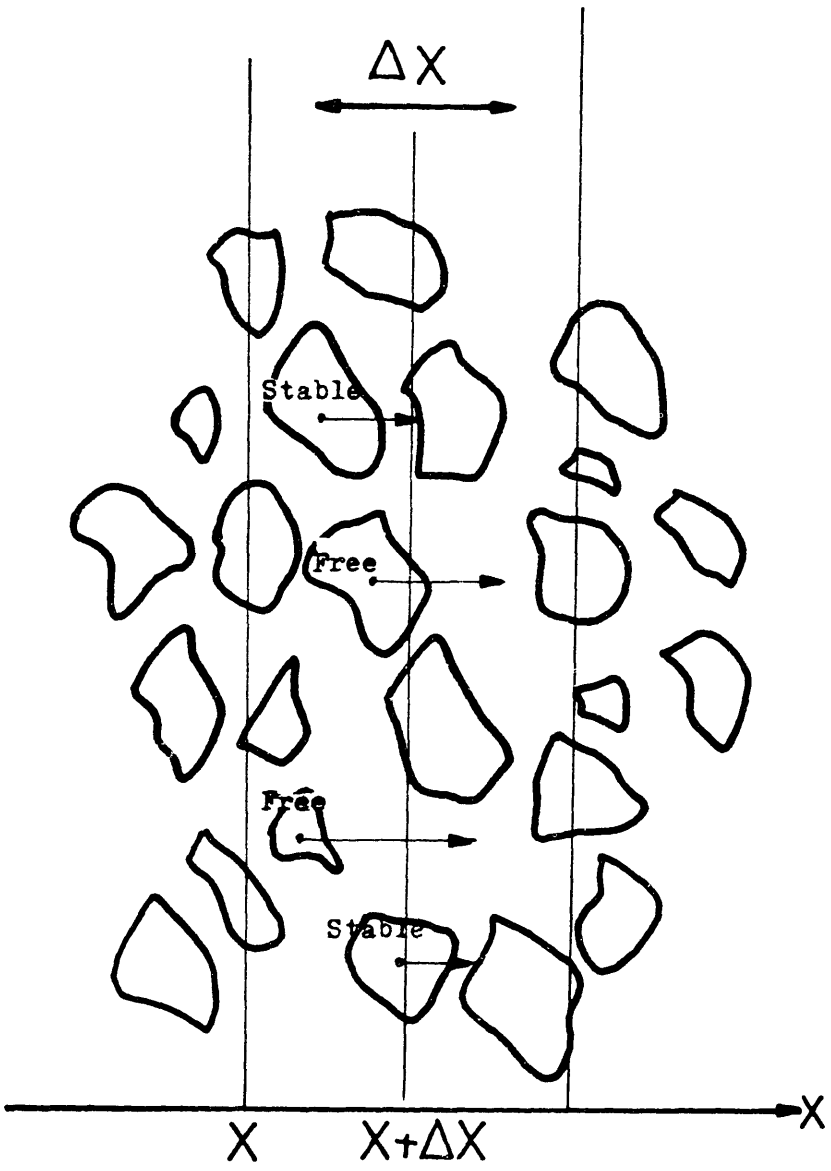

Fig. 2.2 A Conceptual View of the Distance Lag Effect: The Condition of Particles at x are Controlled by the Condition of the Medium at x+Δx.

Step 1. Set Initial Conditions: $Q(x,t,w)$, $S(x,t,w)$ at $t=0$

Step 2. Set $t = t_o$

Step 3. $t = t + \Delta t$

Step 4. Set $w = w_o$

Step 5. $w = w + \Delta w$

Step 6. Set $x = x_1$ (Backward computation)

Step 7. $x = x - \Delta x$

Step 8. Retention Ratio (Distance lag effect):

$$\nu(x,t,w)=\nu\,[\,Q(x+\Delta x,t,w),\ S(x+\Delta x,t,w),\ \text{for all } w;w]$$

Step 9. Velocity (Distance lag effect):

$$v(x,t,w)=v\,[\,Q(x+\Delta x,t,w),\ S(x+\Delta x,t,w),\ \text{for all } w;w]$$

$$v(x-\Delta x,t,w)=v\,[\,Q(x,t,w),\ S(x,t,w)\ \text{for all } w;w]$$

Step 10. Inflow and Outflow:

$$\Delta Q^{+} = Q(x-\Delta x,t,w)\cdot v(x-\Delta x,t,w)\cdot\Delta t$$

$$\Delta Q^{-} = Q(x,t,w)\cdot v(x,t,w)\cdot\Delta t$$

Step 11. Results of absorption/release:

$$Q(x,t,+\Delta t,w)=\{\nu/(1+\nu)\}\{Q(x,t,w)+S(x,t,w)+\Delta Q^{+}-\Delta Q^{-}\}$$

$$S(x,t,+\Delta t,w) = \nu\cdot Q(x,t,+\Delta t,w)$$

Step 12. If $x > x_o$, go to 7

Step 13. If $w < w_1$, go to 5

Step 14. If $t < t_1$, go to 3

Step 15. Stop

FIGURE 2.3 FLOW CHART FOR THE BACKWARD CALCULATION OF THE PROPOSED SOIL PARTICLE TRANSPORT MODEL.

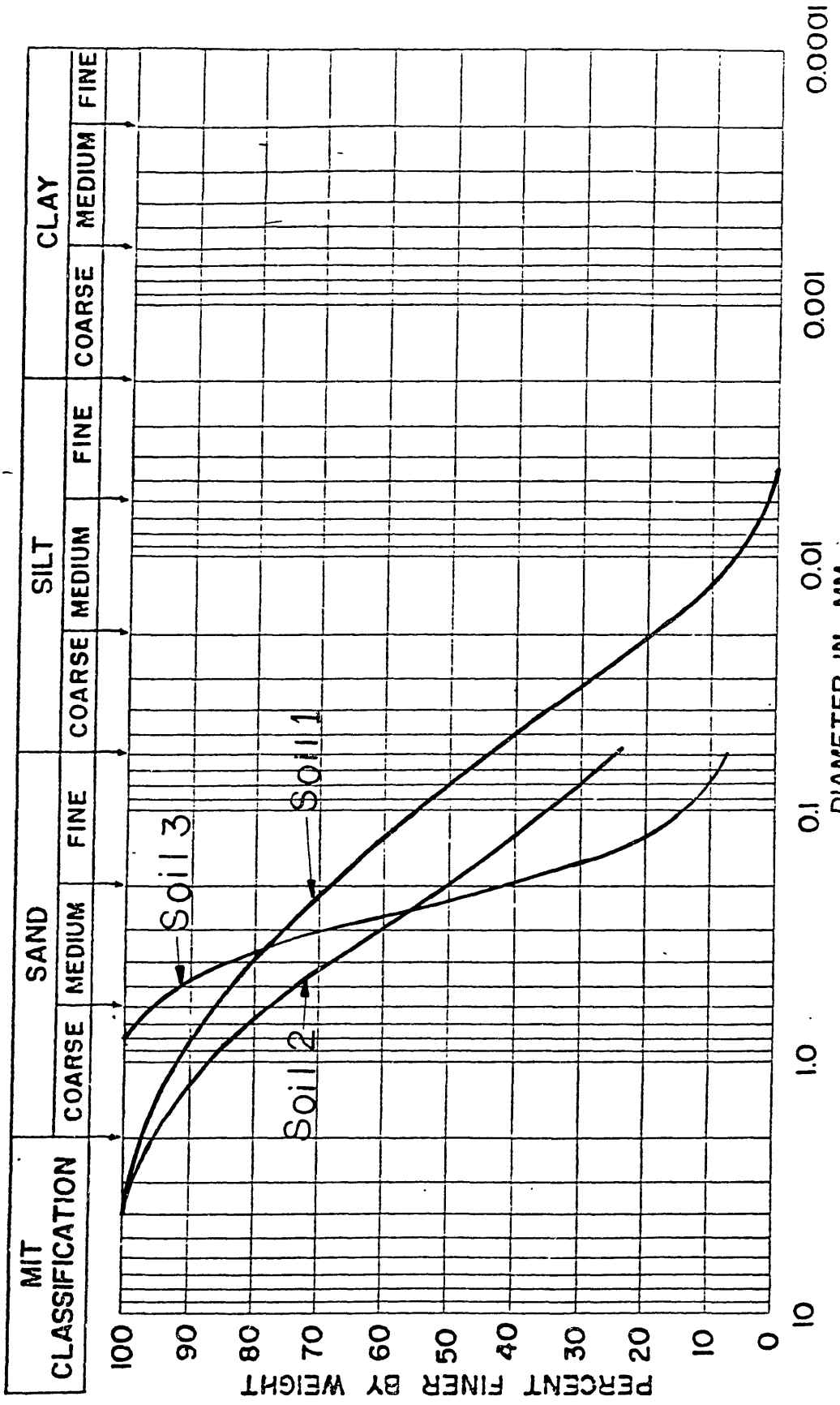

Fig. 2.4 Grain size distribution of soil used in Southworth(1980)'s experiment

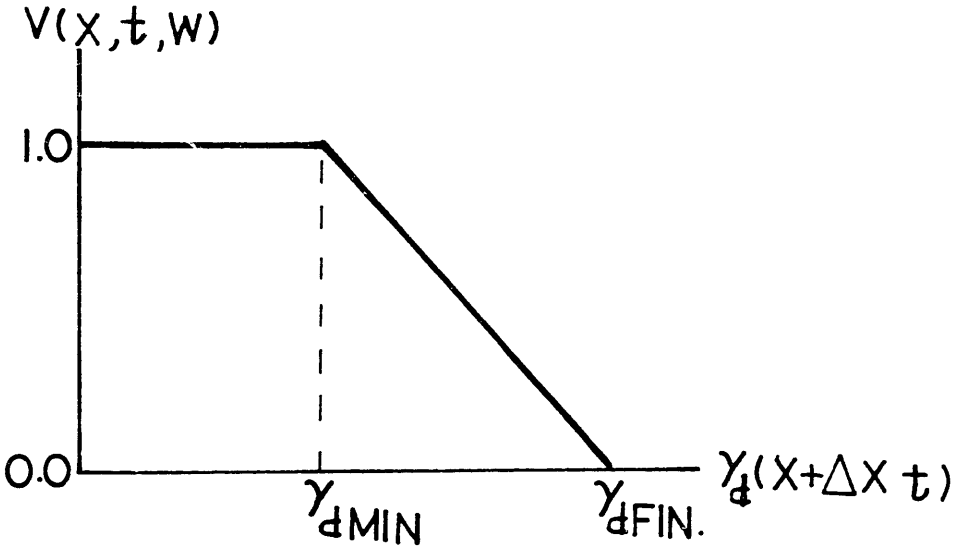

(a) Velocity

$$\lambda(x,t,w) = \frac{\text{Dry Density of Stable Particles}}{\text{Total Dry Density}}$$

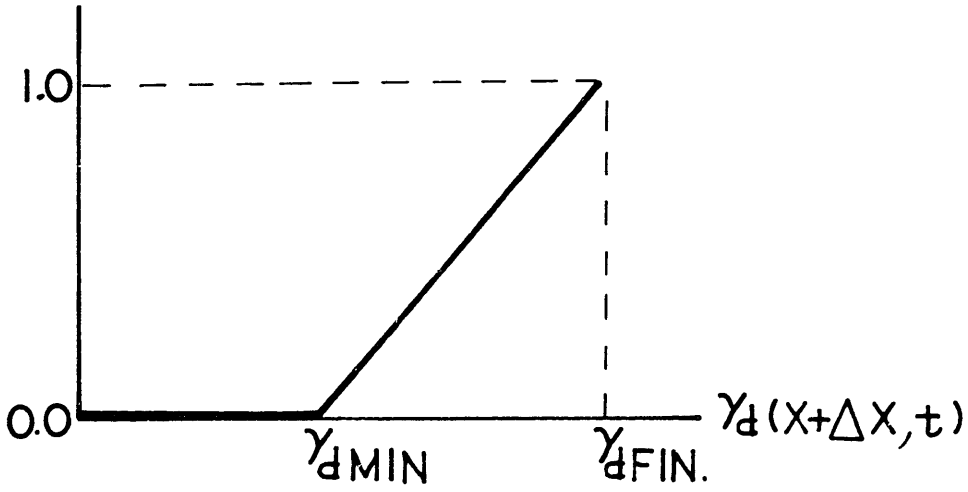

(b) Retention Proportion

Fig. 2.5 Assumptions Employed in the Calculation

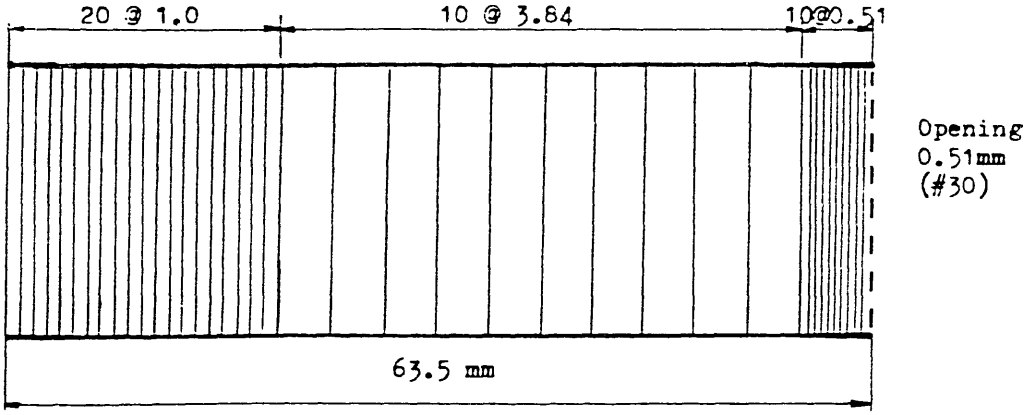

(a) Space Discritization

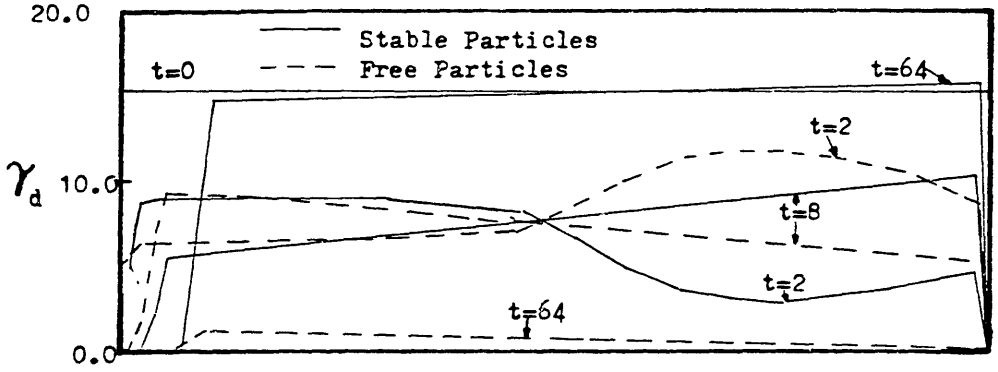

(b) Behavior of Particles Finer than the Opening

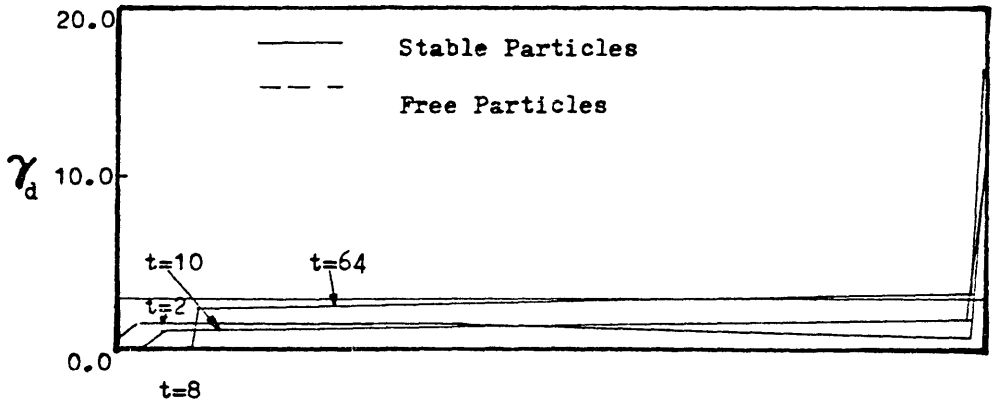

(c) Behavior of Particles Coarser than the Opening

Fig. 2.6 Calculated Result for Soil 1 Screen #30.
(86% of Soil Finer than the Opening Size)

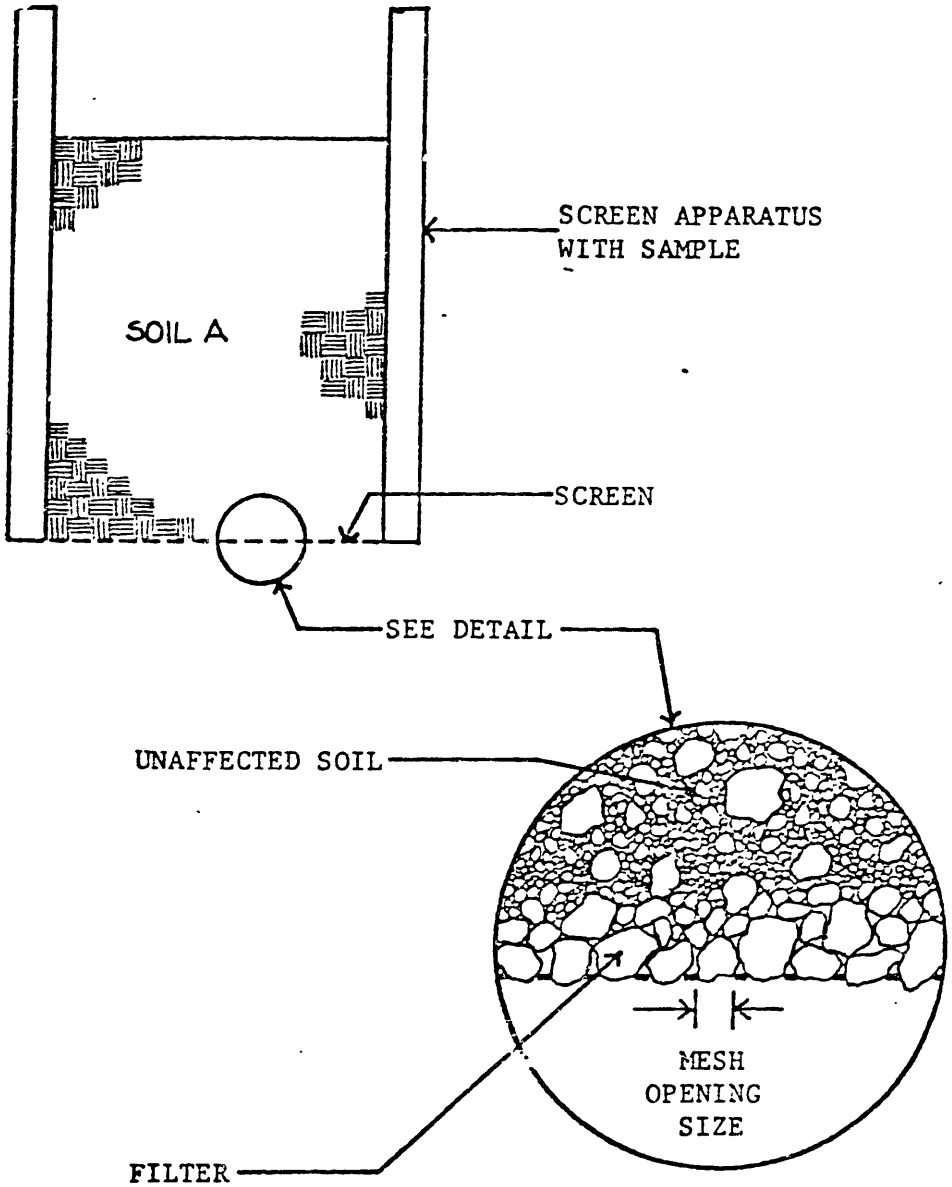

Fig. 2.7 Conceptual Diagram of Self-healing Filter Formed in Cohesionless Soil (after Southworth, 1980)

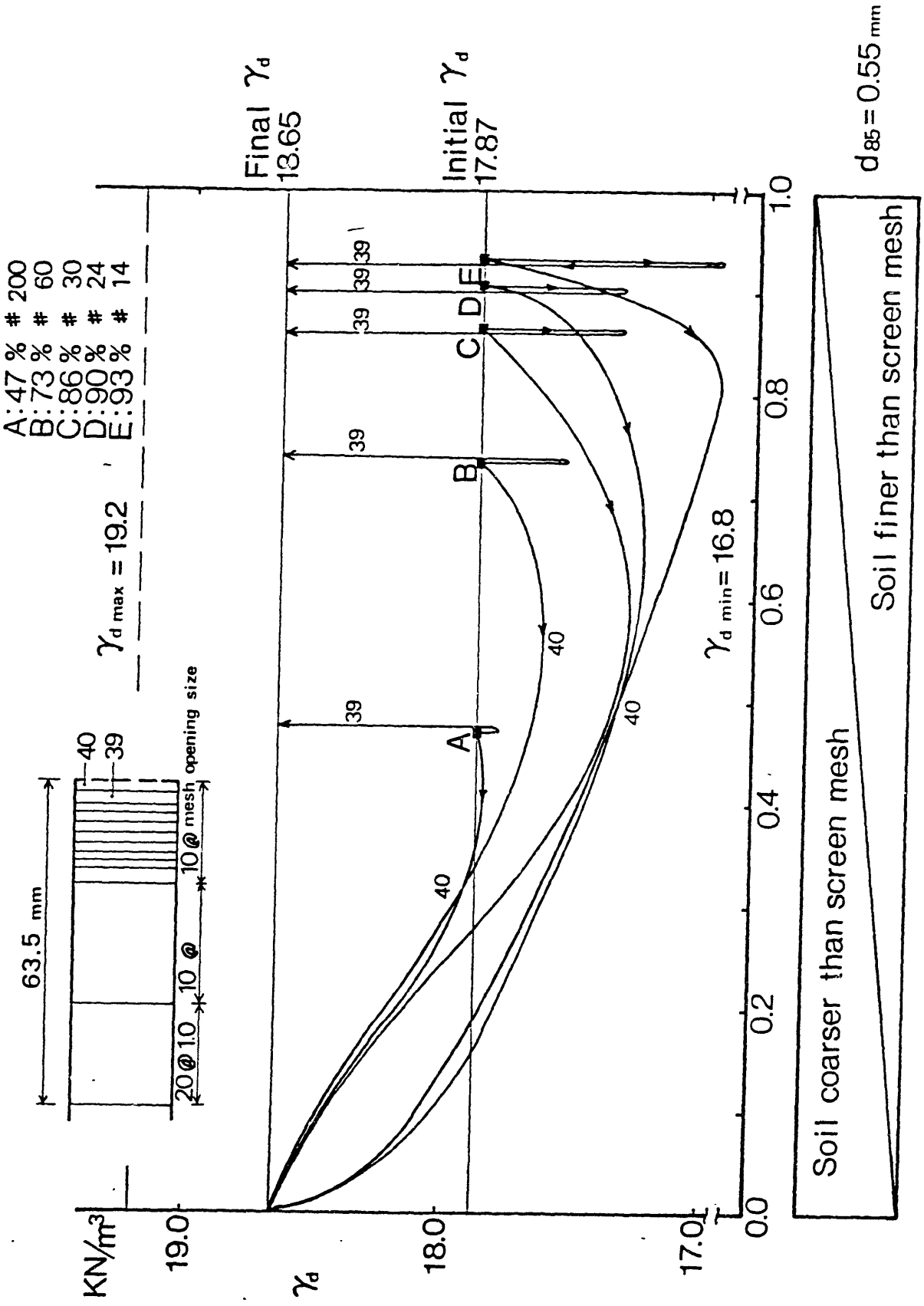

Fig. 2.8 State Diagram of the Calculated Results of Soil 1

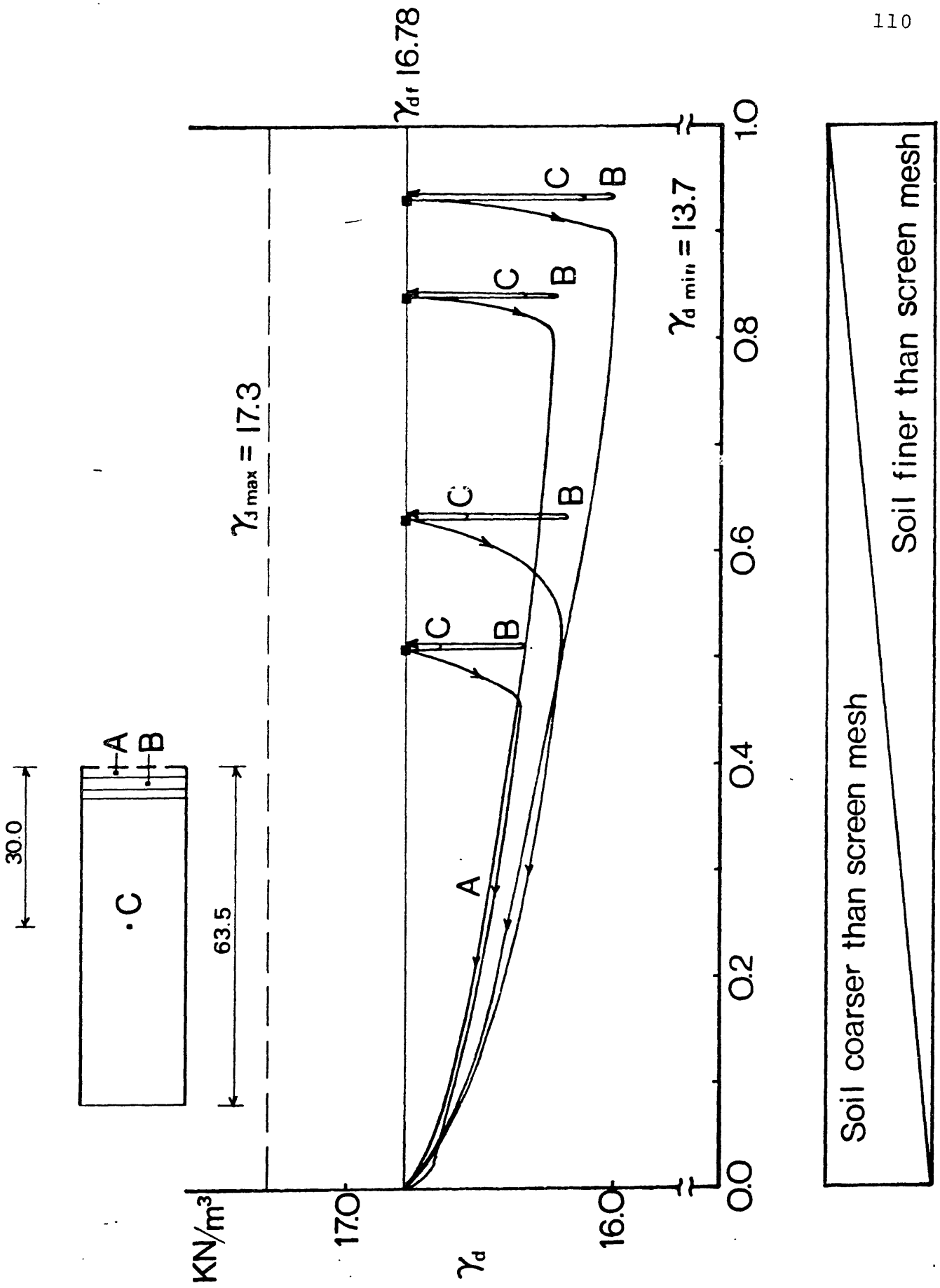

Fig. 2.9 State Diagram of the Calculated Results of Soil 3

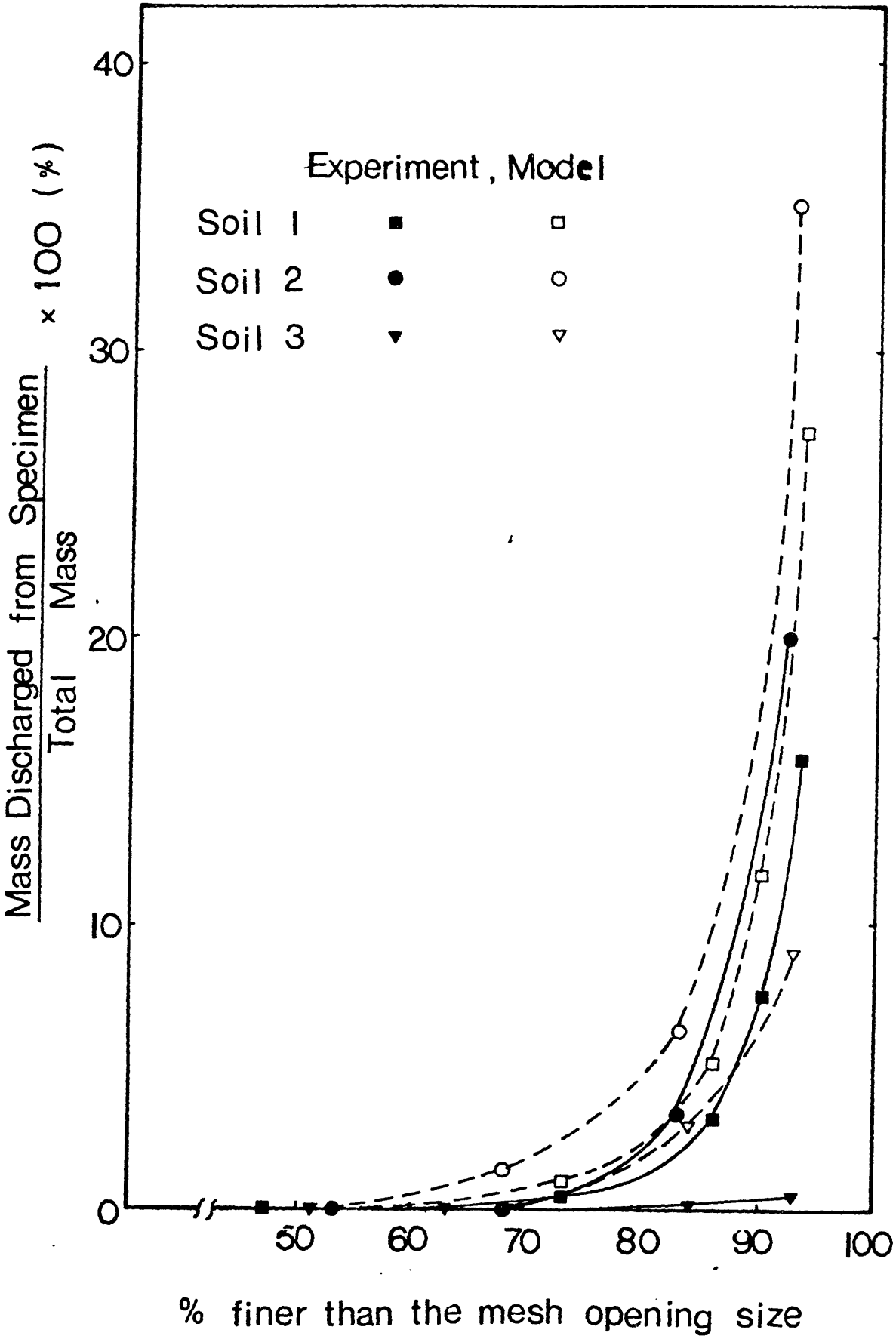

Fig. 2.10 Mass Discharged from the Screen in Southworth's Experiment: Experimental vs. Calculated Results

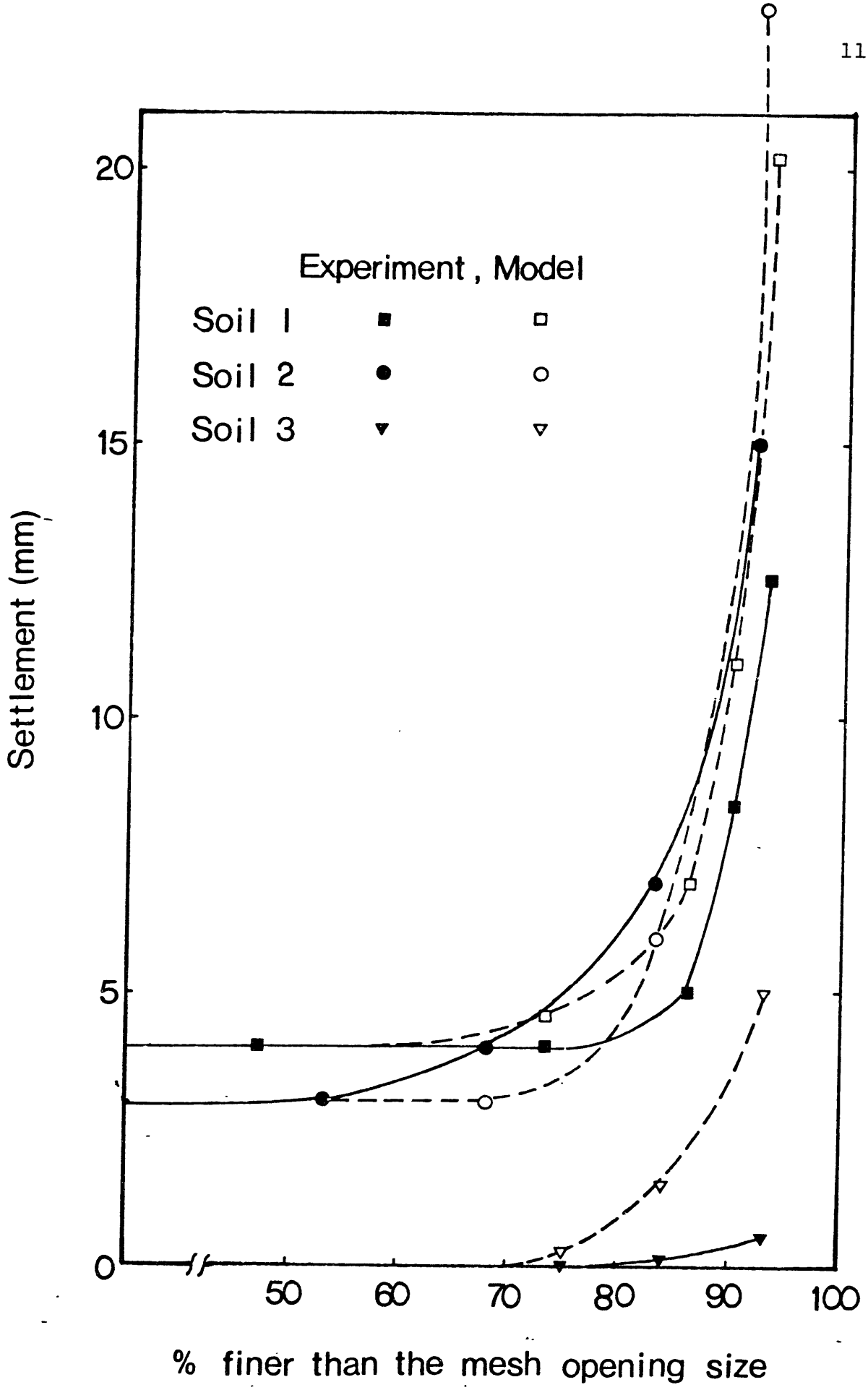

Fig. 2.11 Settlement of Specimens in Southworth's Experiment: Experimental vs. Calculated Results

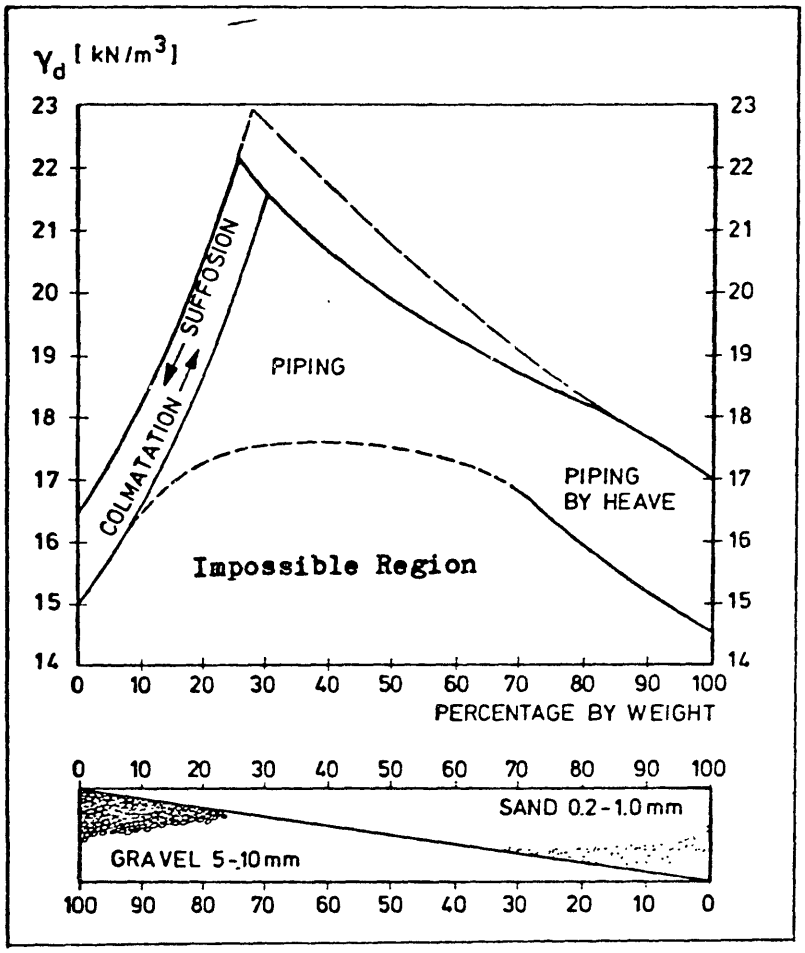

Fig. 2.12 Particle Transport Phenomena in Sand and Gravel Subsoil (after Wittman, 1978)

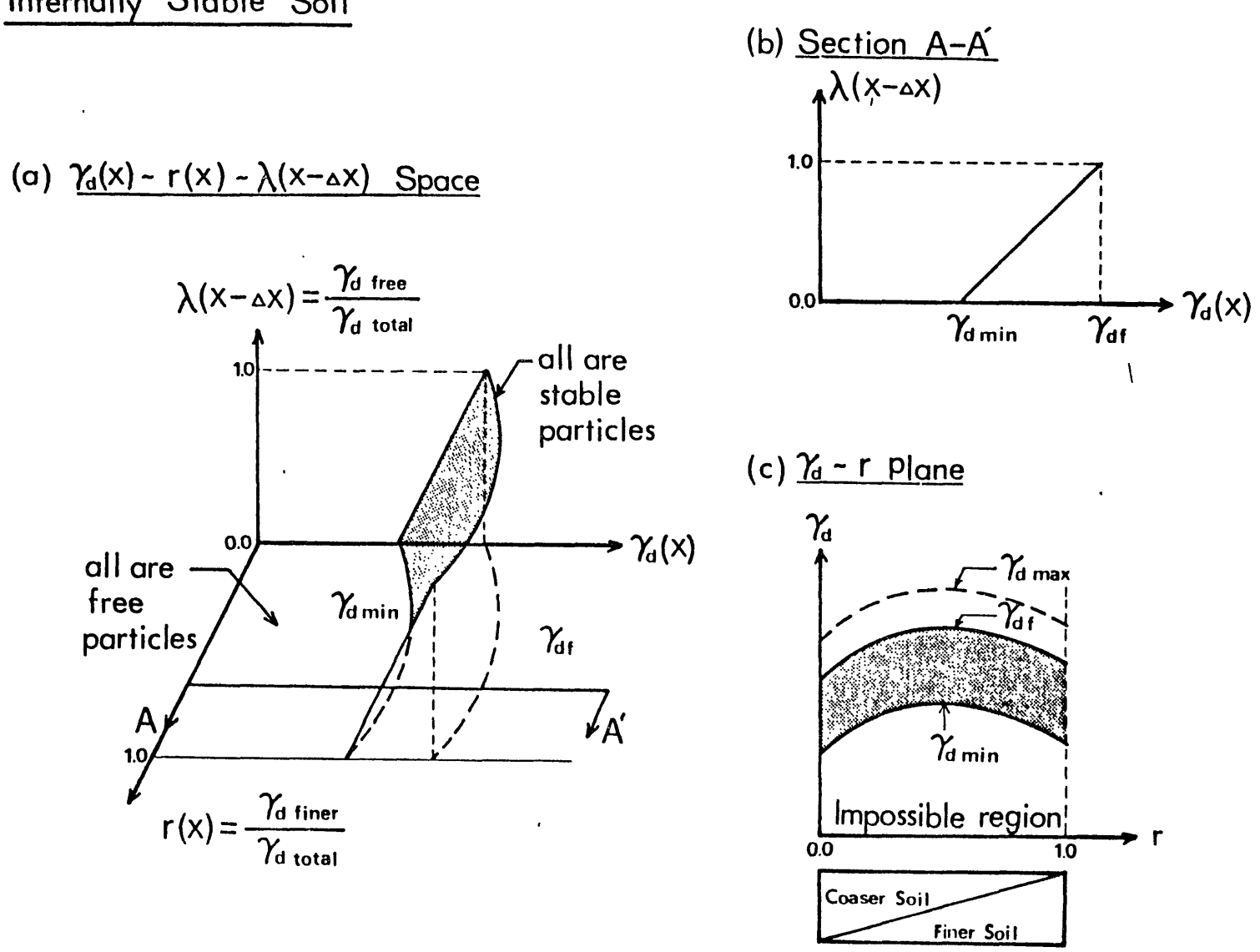

Fig. 2.13 Conceptual View of Internally Stable Soil

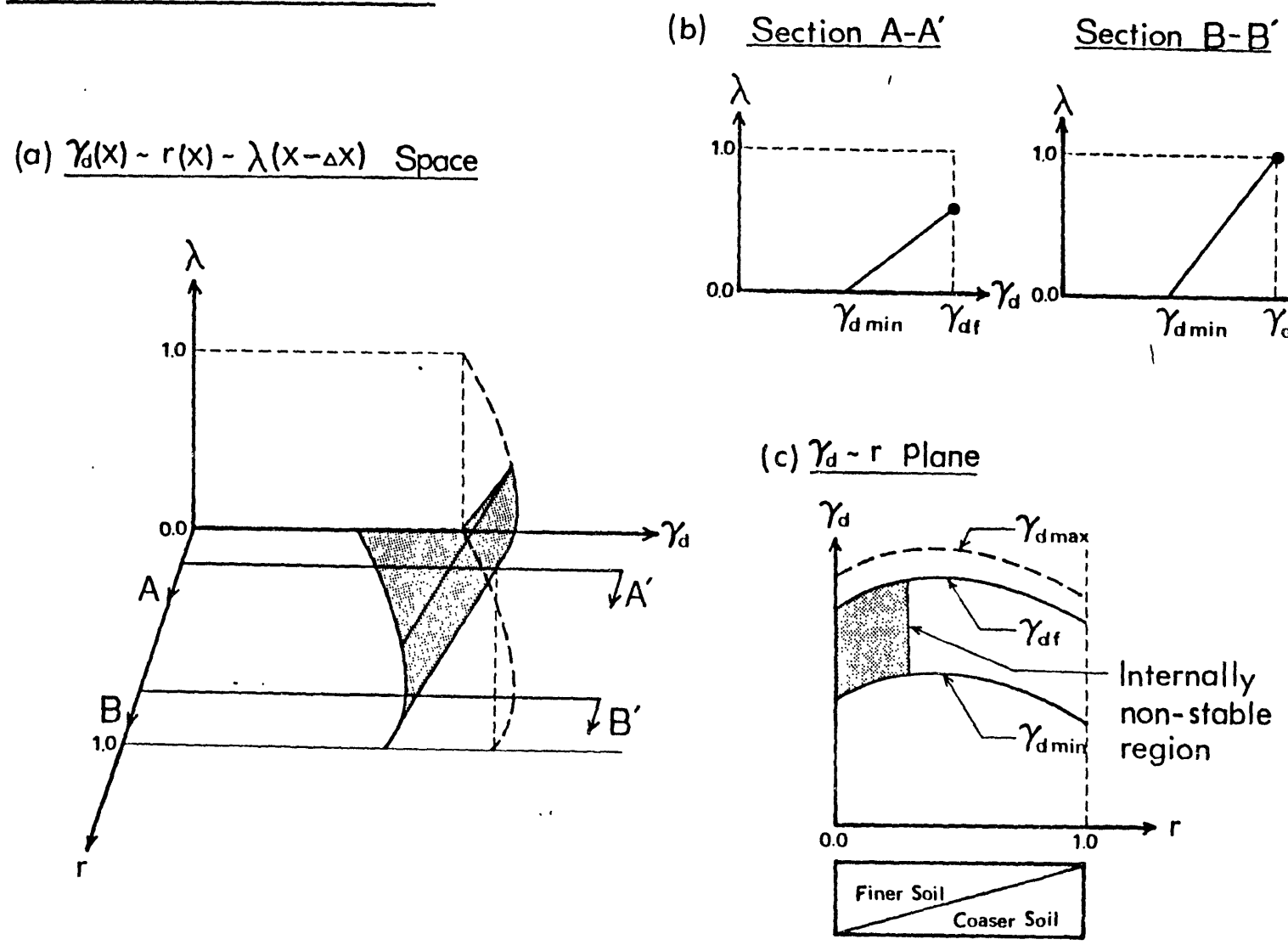

Fig. 2.14 Conceptual View of Internally Non-Stable Soil

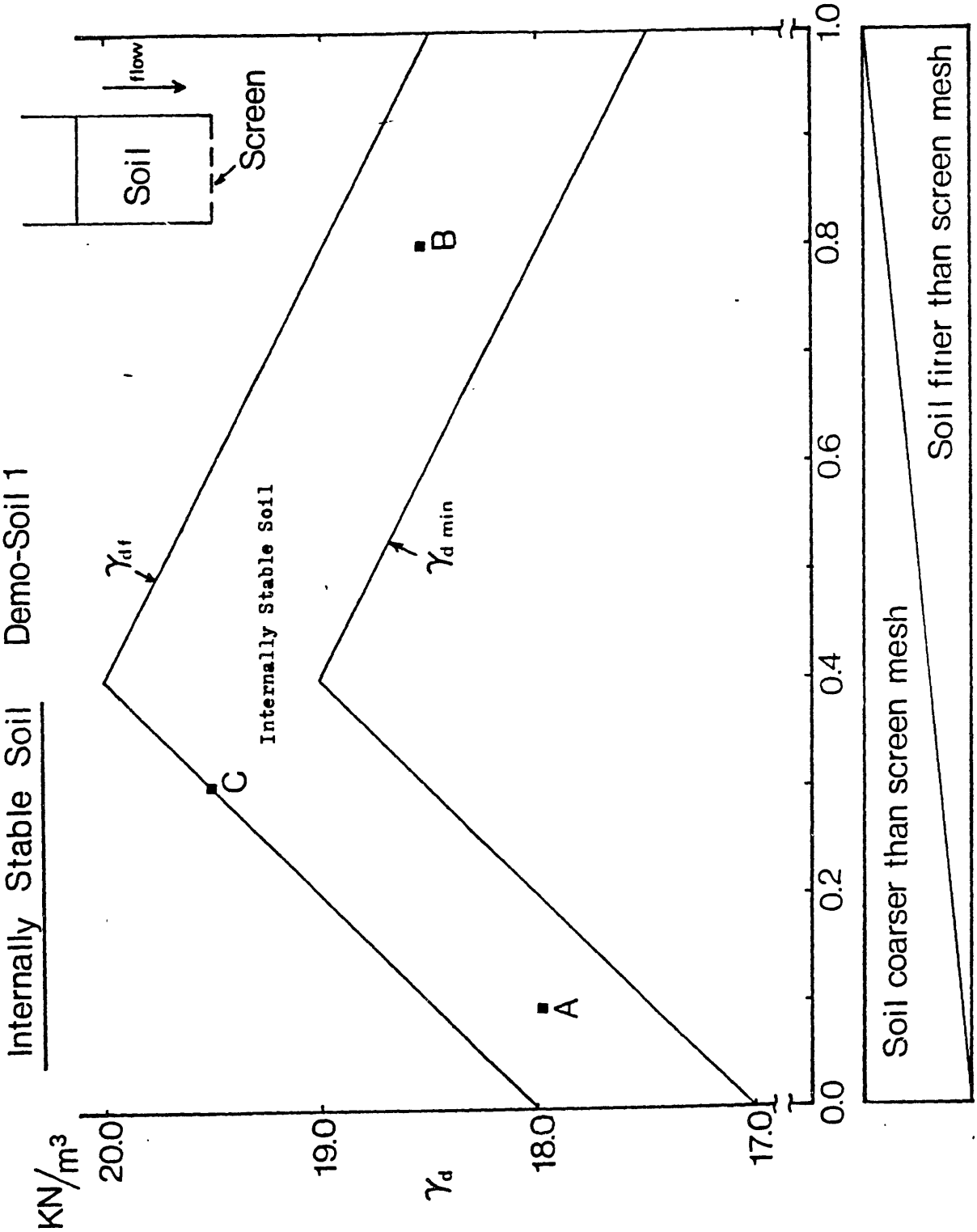

Fig. 2.15 The State Diagram for Demo-Soil 1: Internally Stable Soil

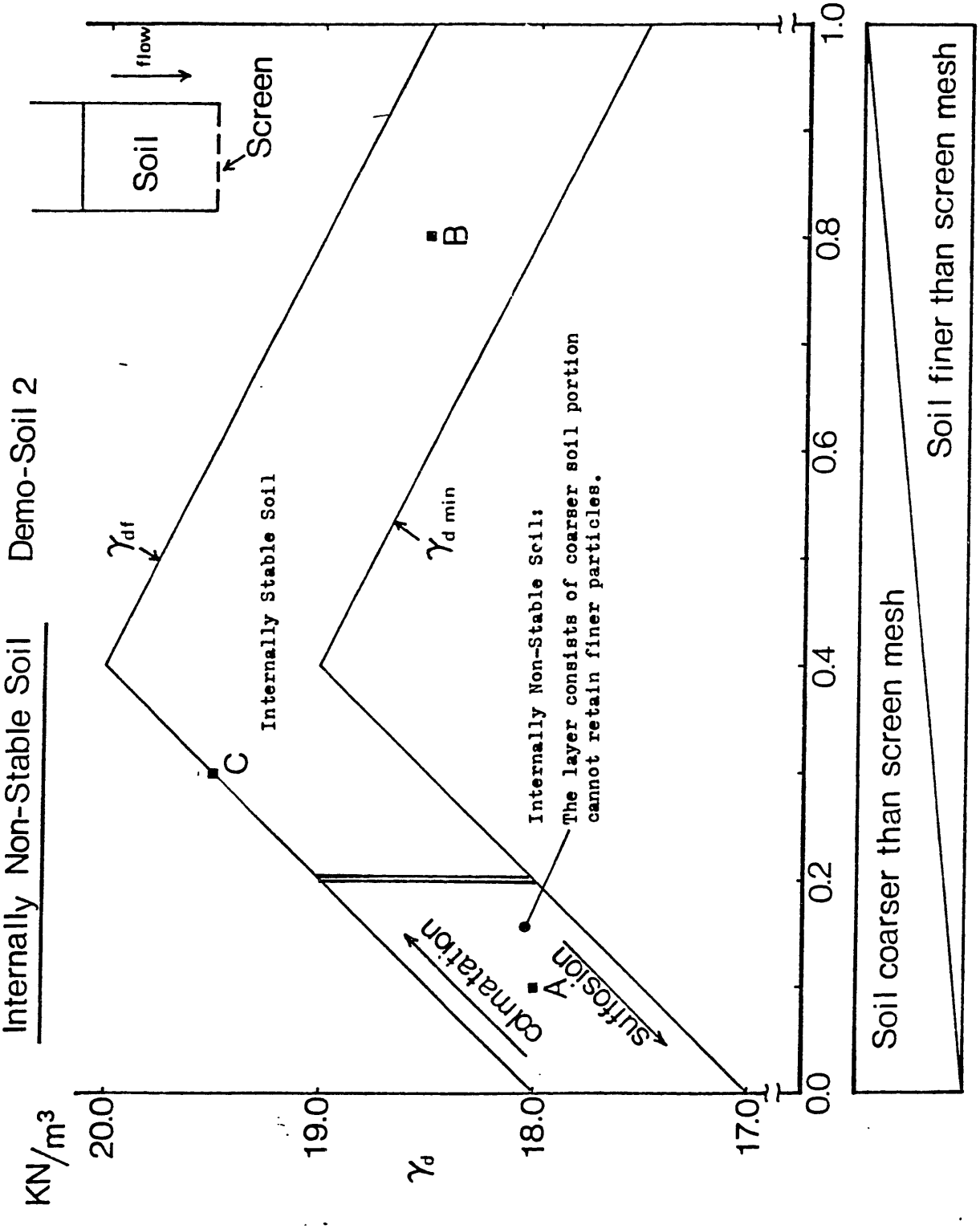

Fig. 2.16 The State Diagram for Demo-Soil 2: Internally Non-Stable Soil

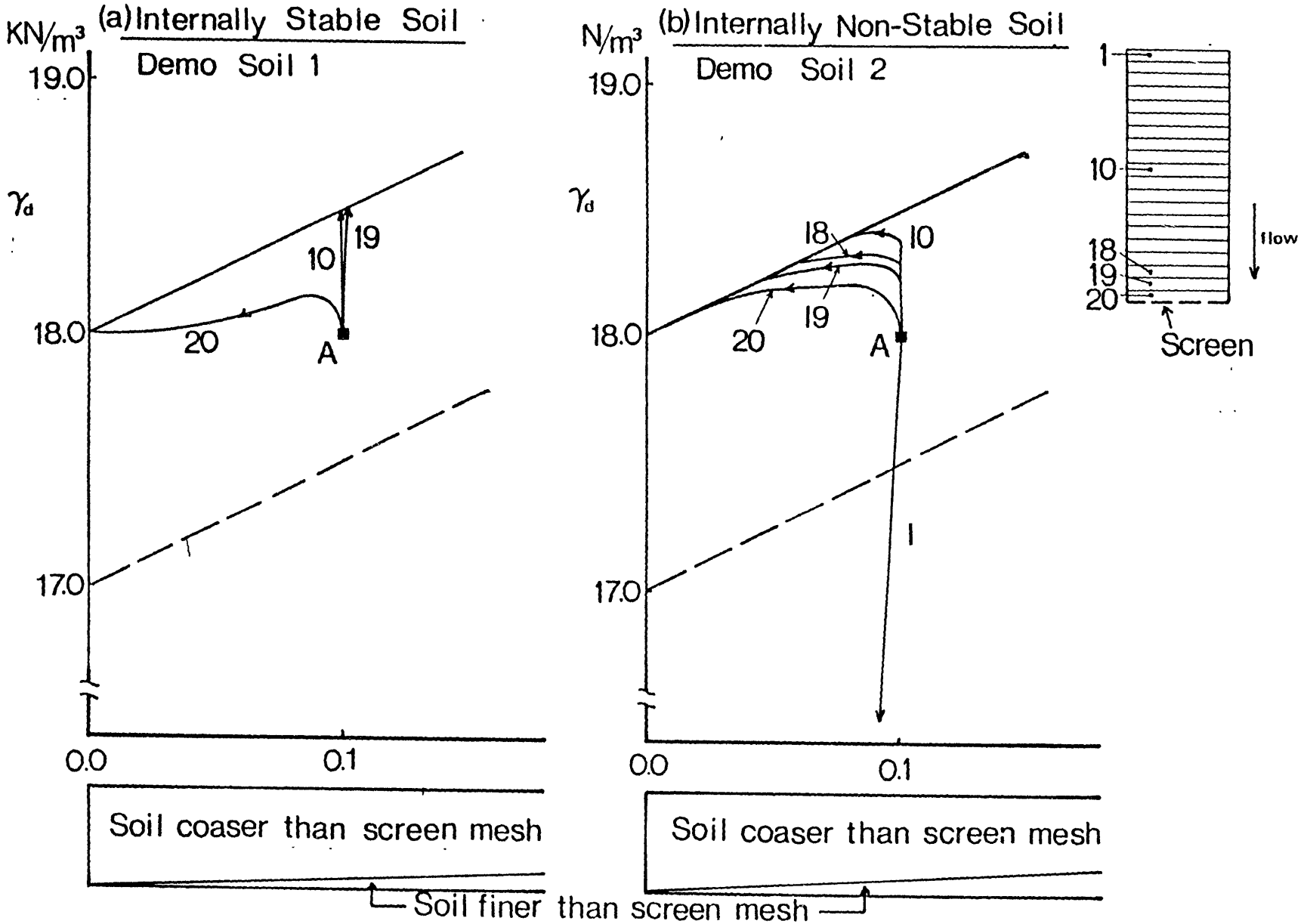

Fig. 2.17 Results of Calculation (A): Demo-Soils 1 & 2

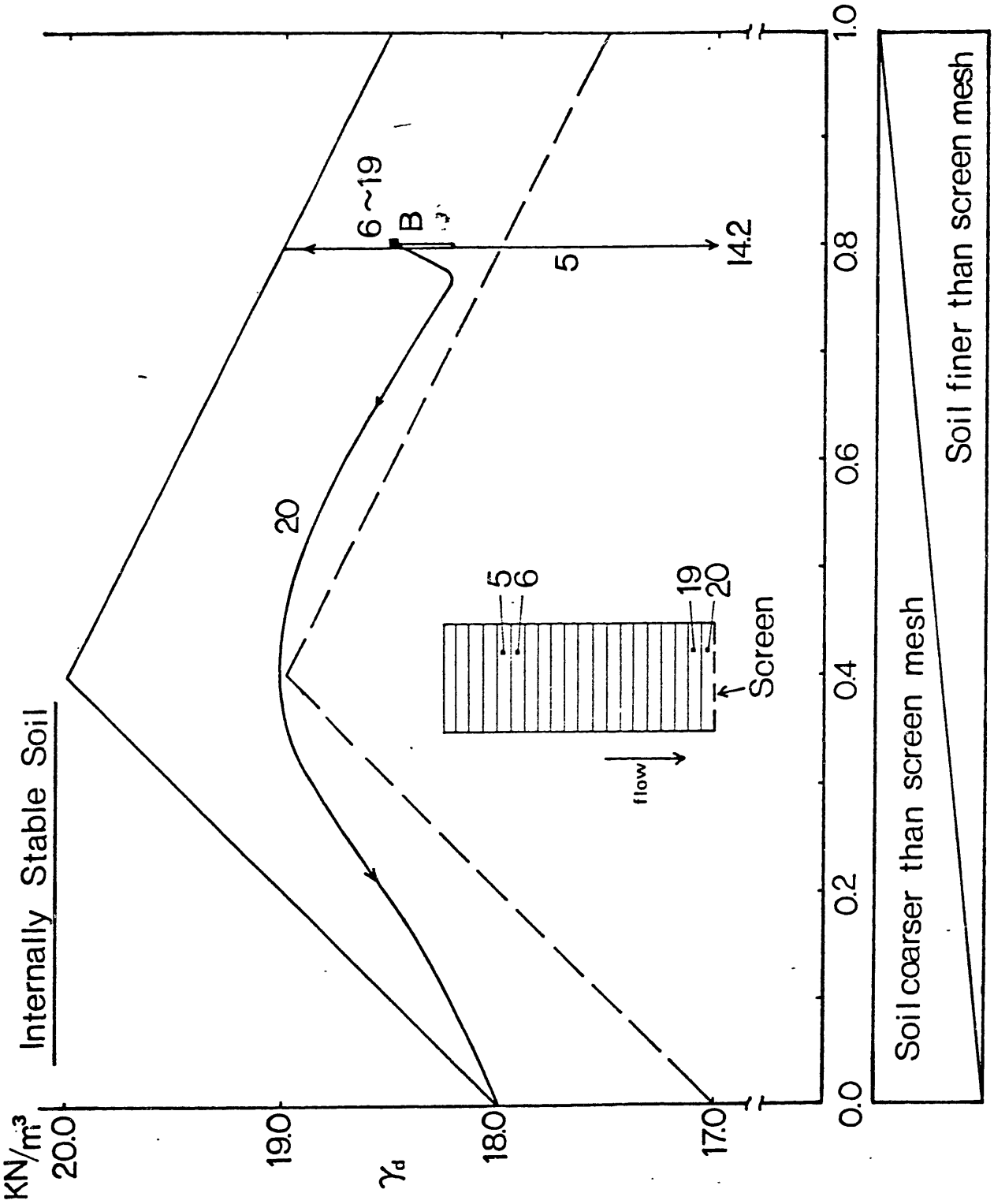

Fig. 2.18(a) Results of Calculation (B): Demo-Soil 1

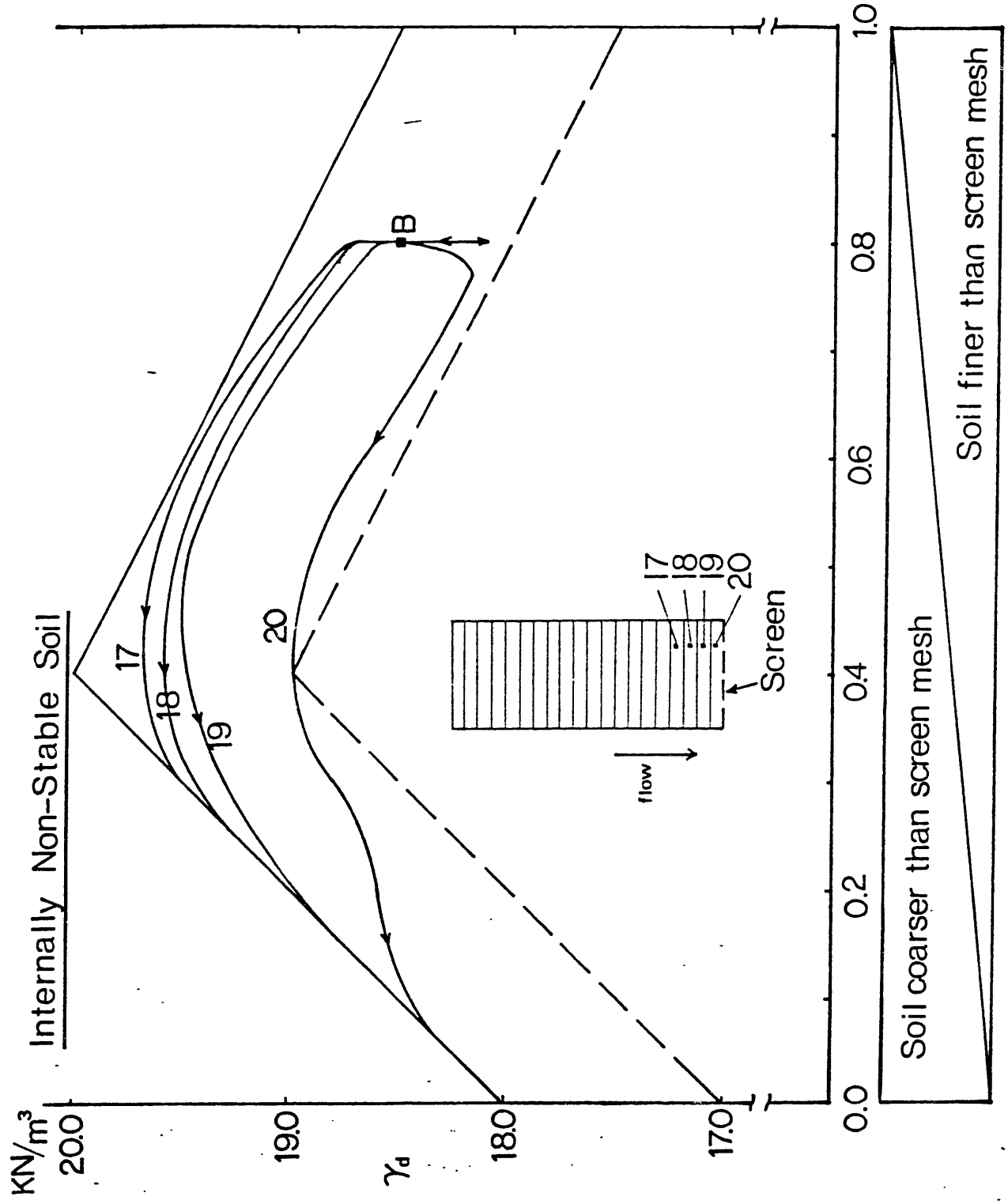

Fig. 2.18(b) Results of Calculation (B): Demo-Soil 2

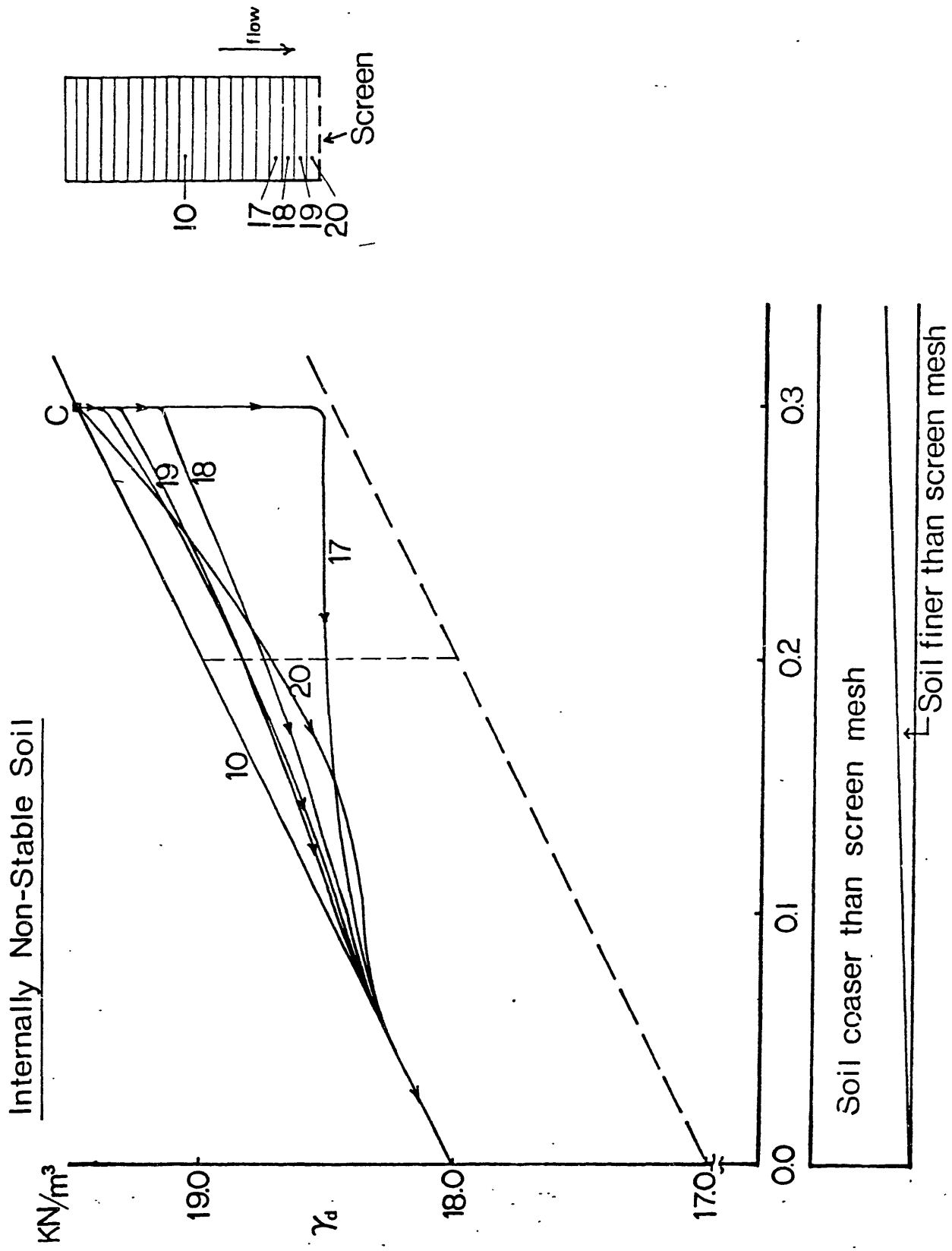

Fig. 2.19 Results of Calculation (C); Demo-Soil 2

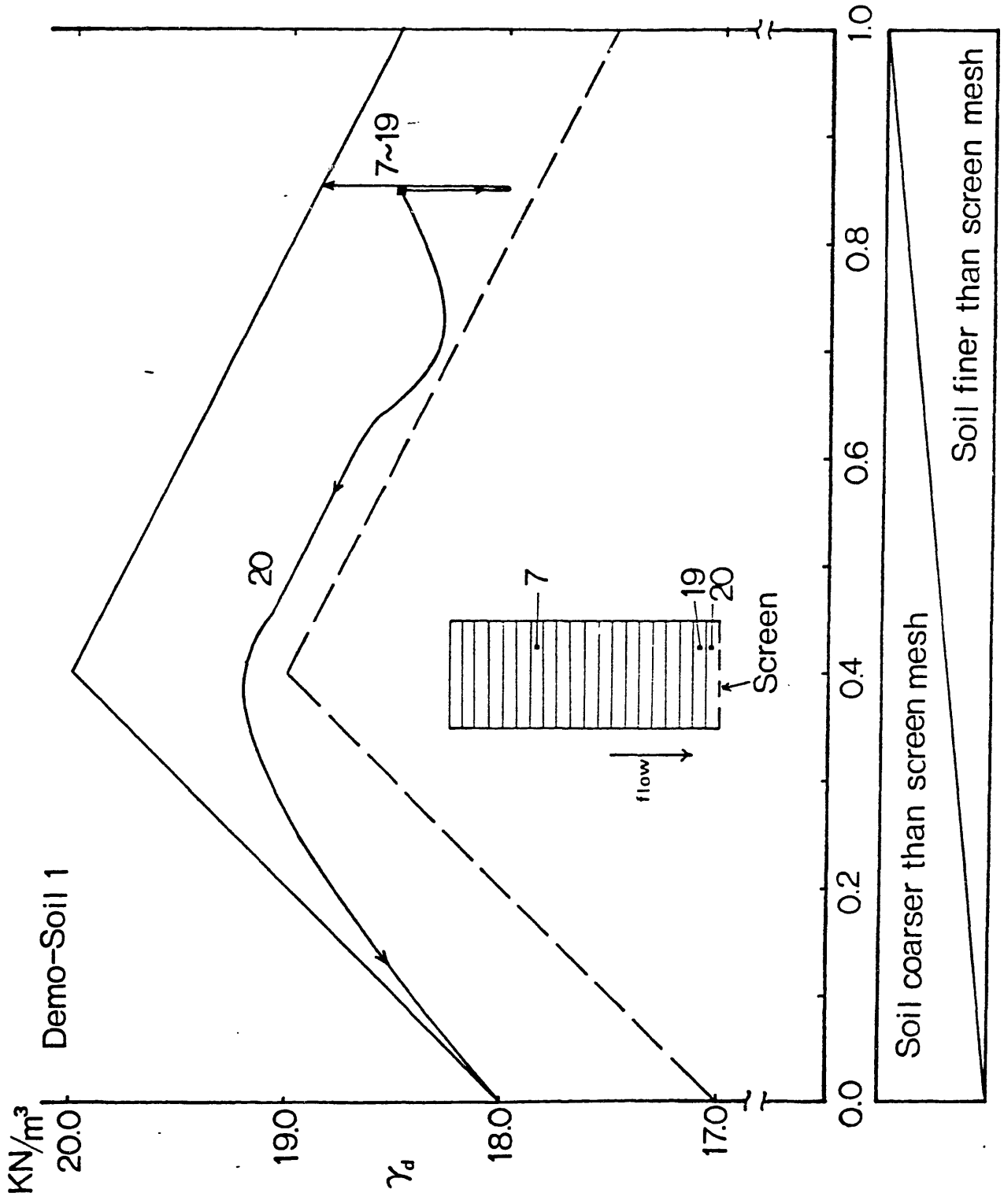

Fig. 2.20(a) Results of Calculation for Demo-Soil 1: Internally Stable Soil

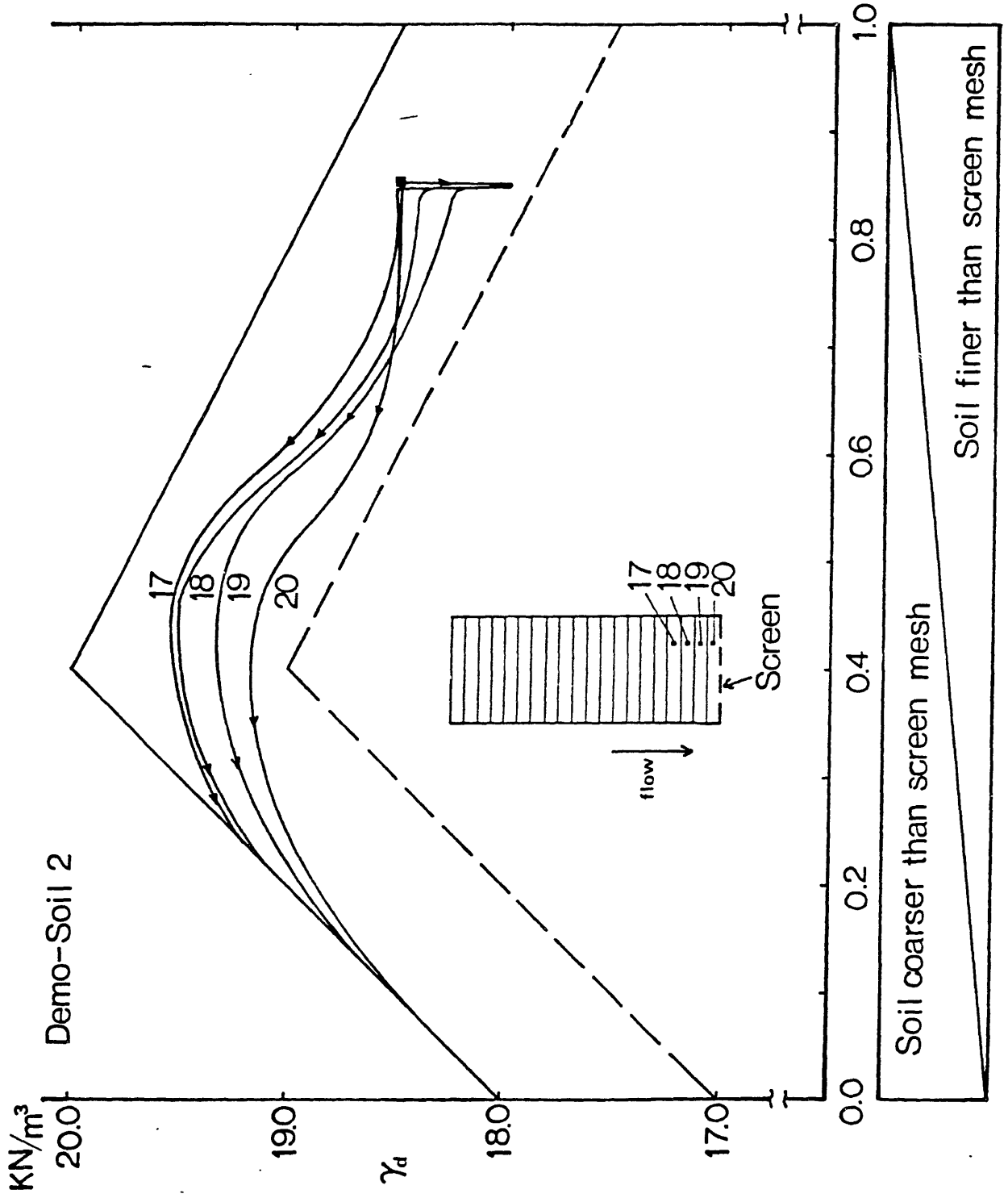

Fig. 2.20(b) Results of Calculation for Demo-Soil 2: Internally Nonstable Soil

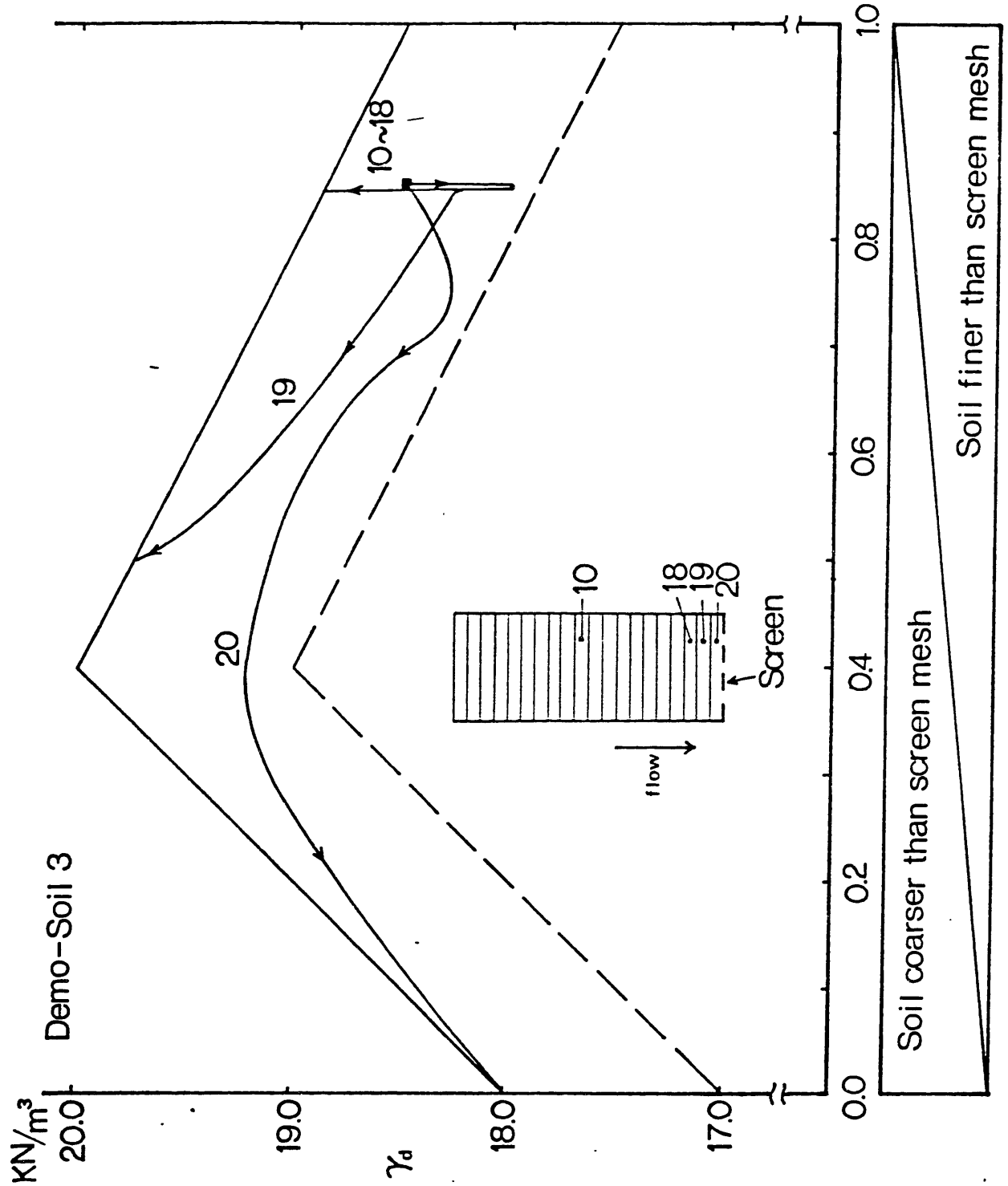

Fig. 2.20(c) Results of Calculation for Demo-Soil 3: Partially Internally Stable Soil

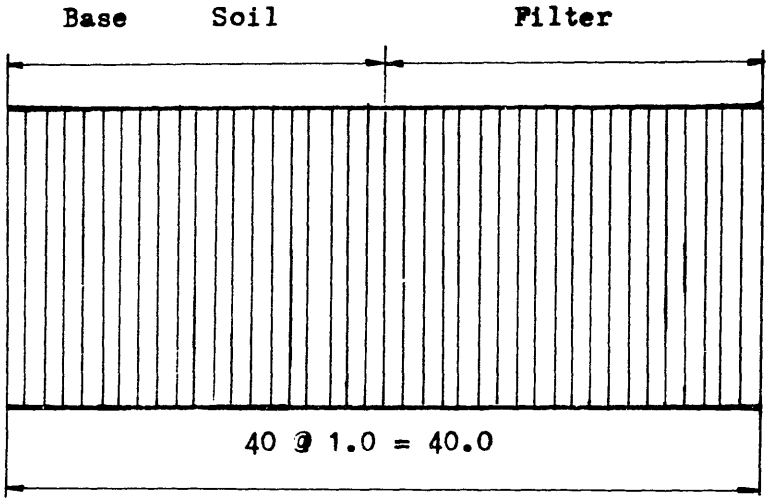

(a) Space Discretization Schema

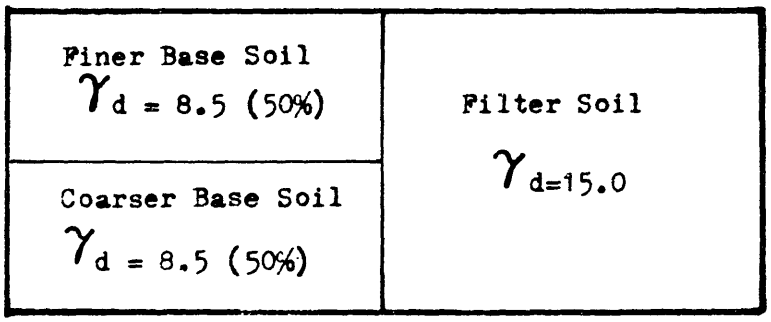

(b) Initial Condition for Case A

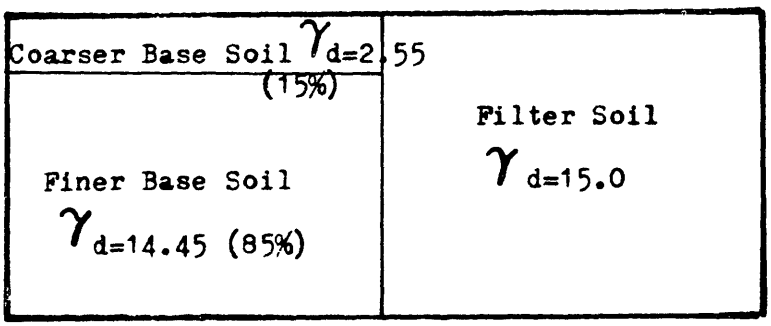

(c) Initial Condition for Case B

Fig. 2.21 Space Discretization Scheme and Initial Conditions for Filter Clogging Calculation

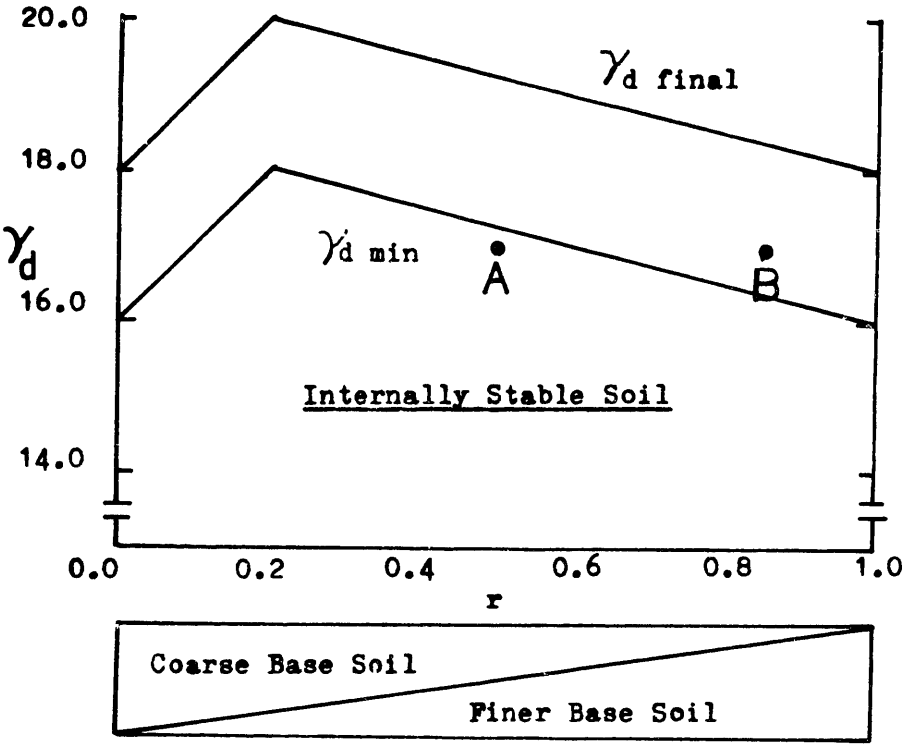

(a) The state diagram for Base Soil: Points A and B indicate the initial conditions of calculations.

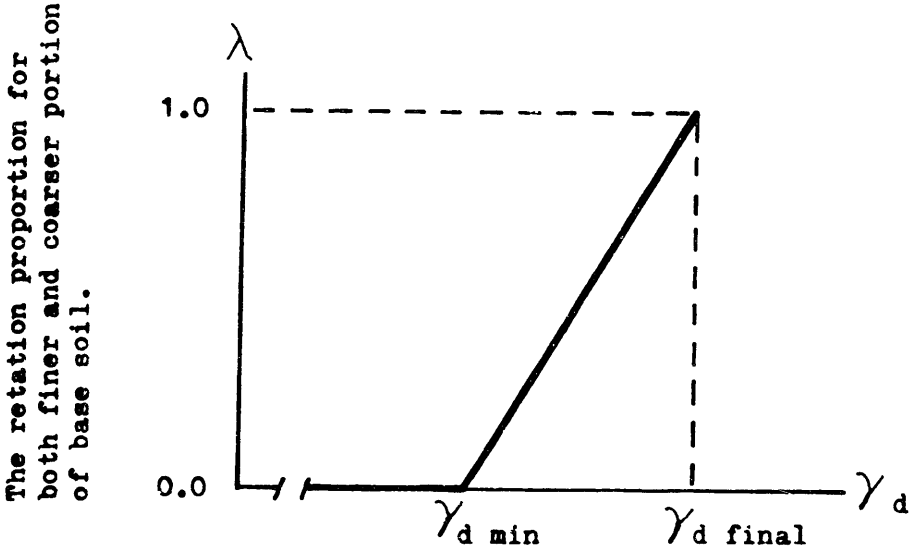

(b) The retention proportion of Base Soil for both the finer and the coarser portion of the Base Soil. It is Internally Stable Soil (i.e. =1.0 at d= d final)

Fig. 2.22 Property of the Base Soil

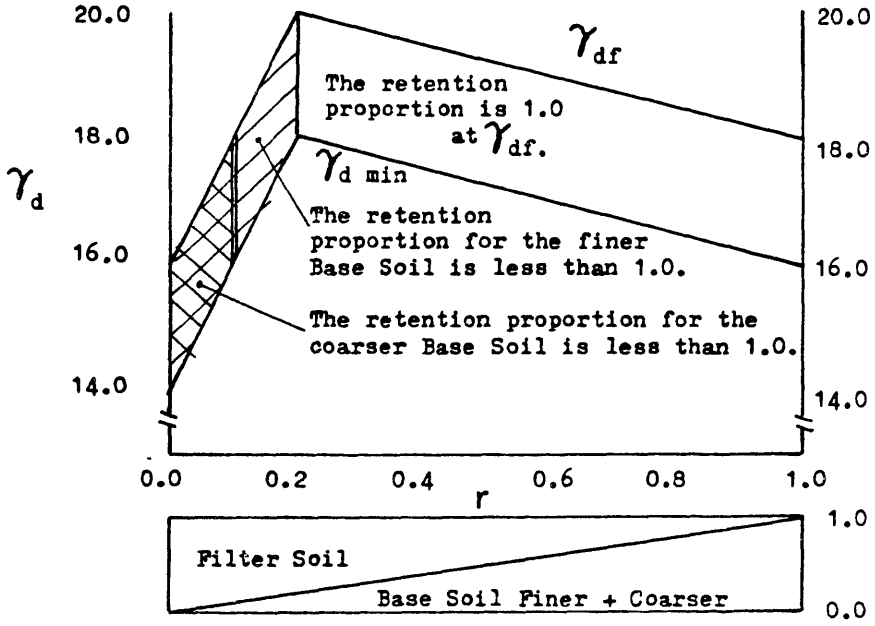

(a) The state diagram for Filter and Base Soil Mixture: The retention proportion of Filter Soil and Base Soil mixture.

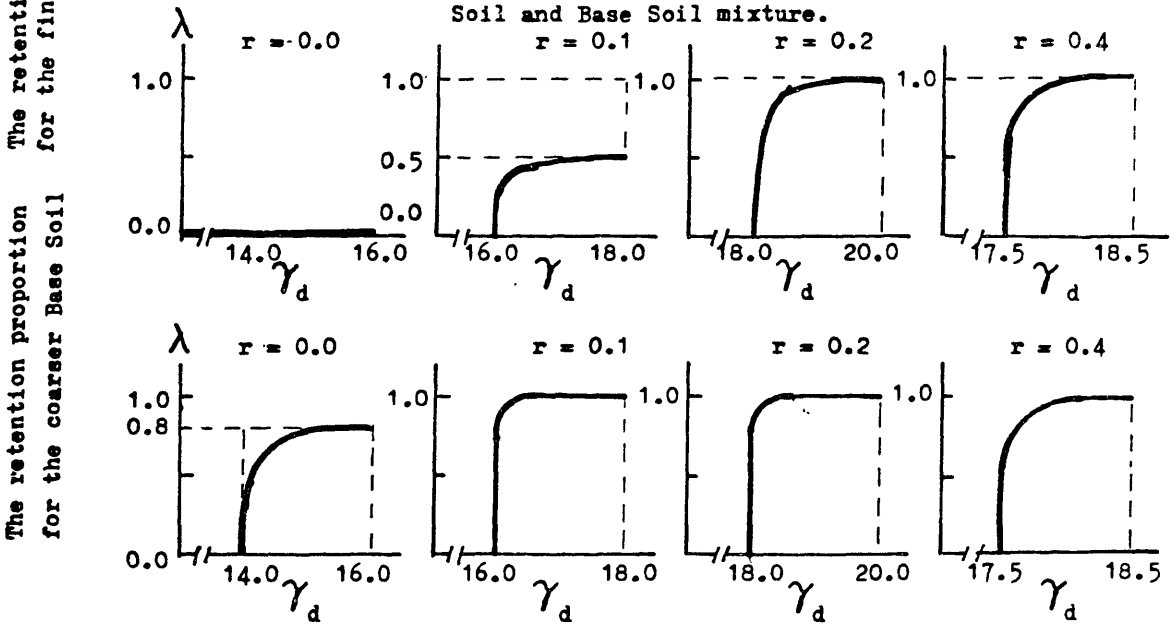

(b) The retention proportion of filter - Base Soil Mixture for the finer base soil (upper row) and the coarser base soil (lower row) for r=0.0, 0.1, 0.2 and 0.4.

Fig. 2.23 Property of the Base soil - Filter Mixture Soil

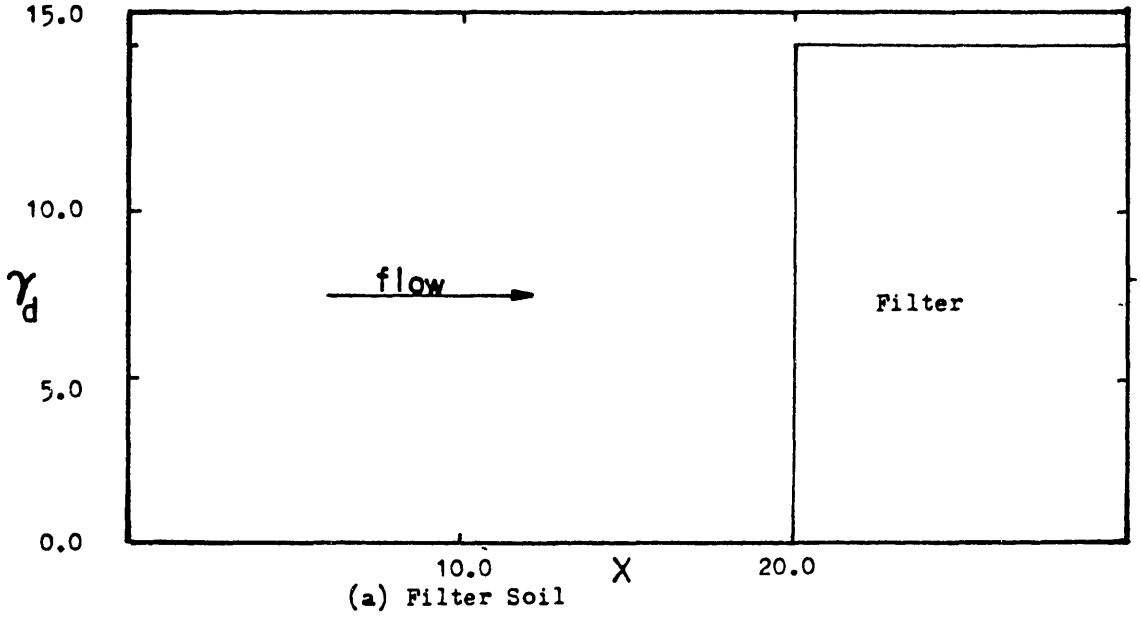

(a) Filter Soil

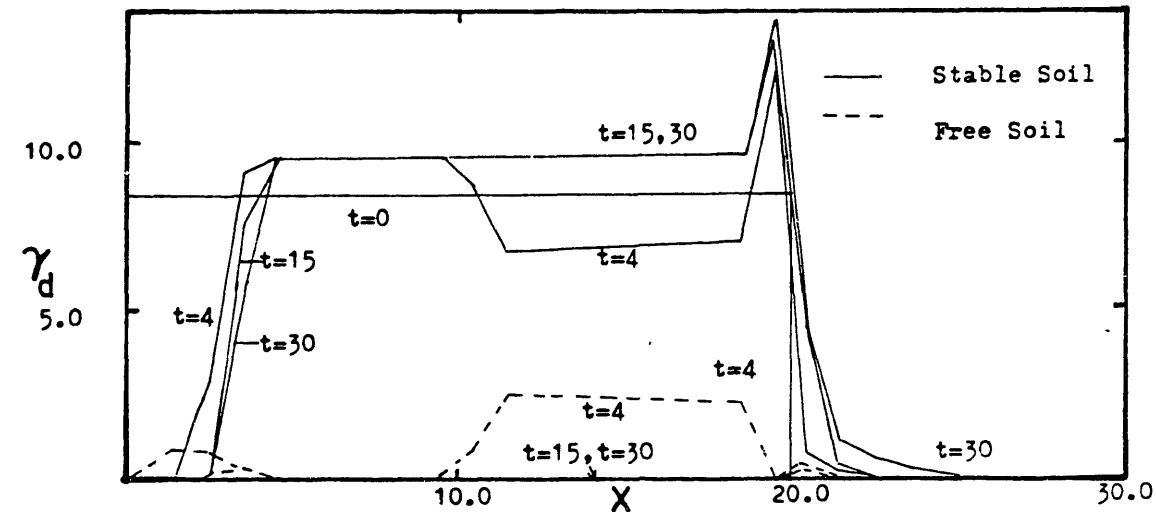

(b) Coarser Base Soil

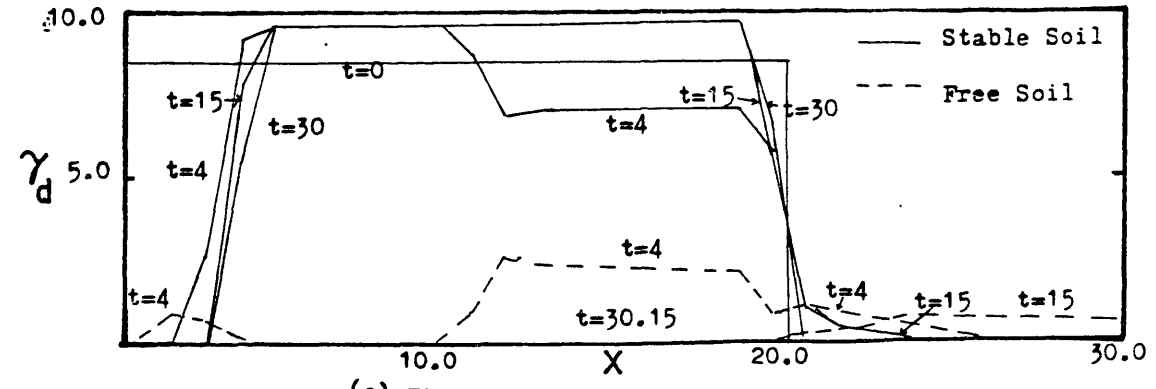

(c) Finer Base Soil

Fig. 2.24 Results of Calculation for Case A

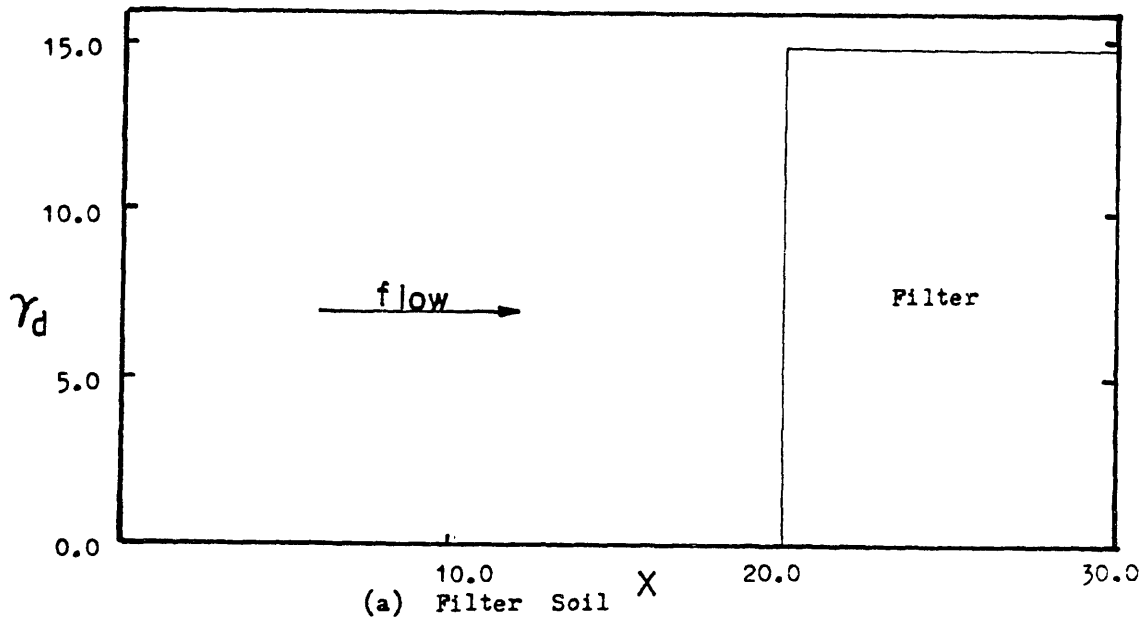

(a) Filter Soil

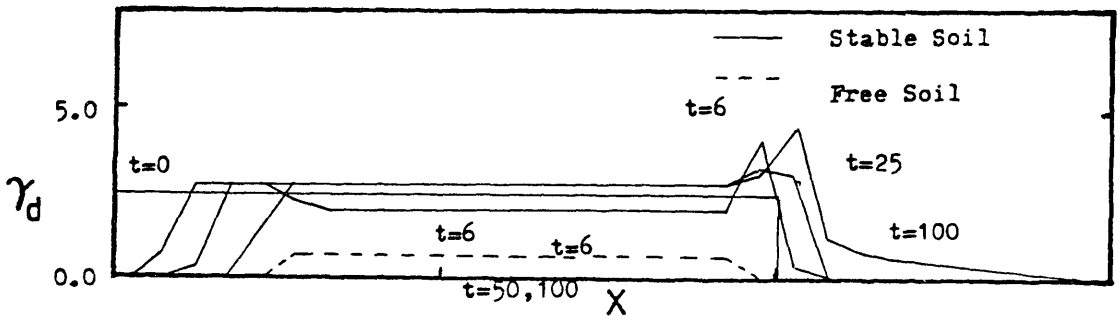

(b) Coarser Base Soil

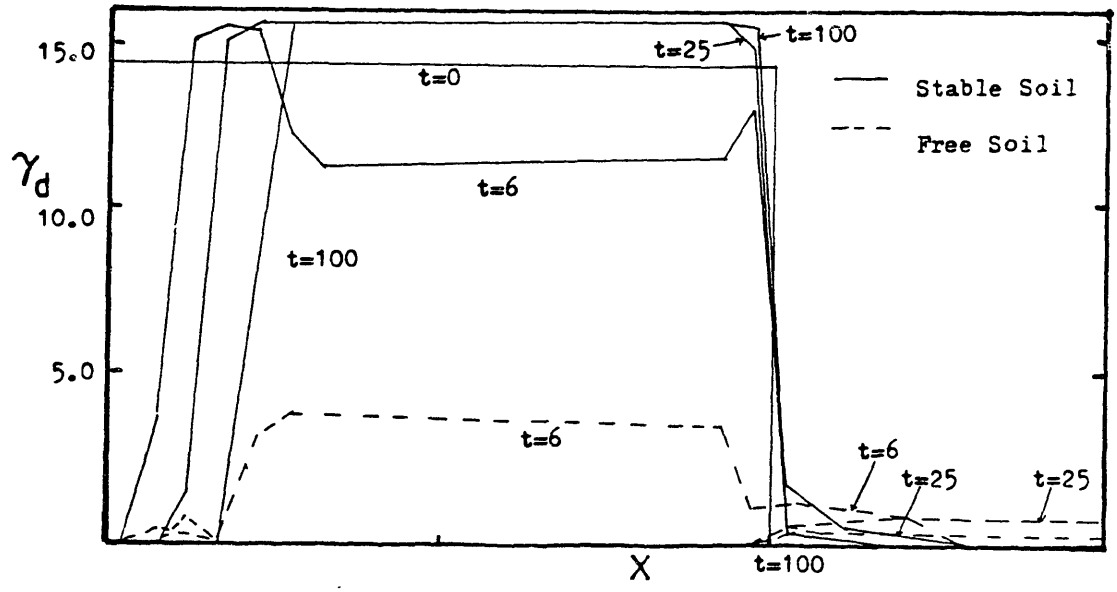

(c) Finer Base Soil

Fig. 2.25 Results of Calculation for Case B

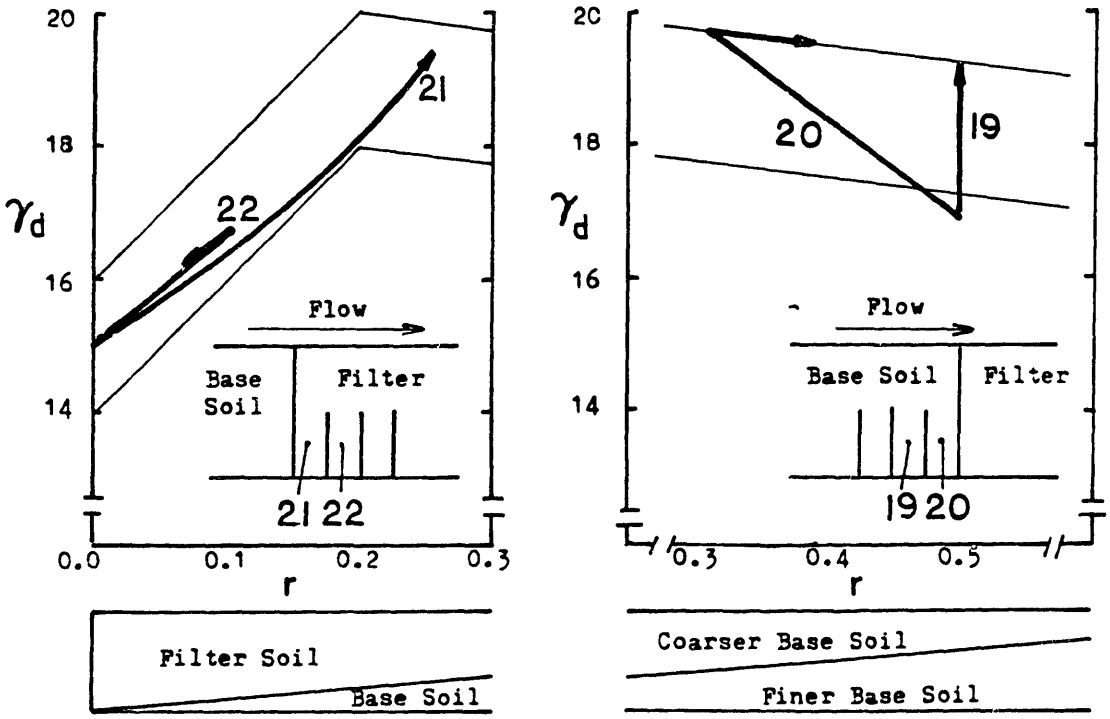

(a) The State Diagram for Base Soil Consist of 50% Finer Soil (Case A)

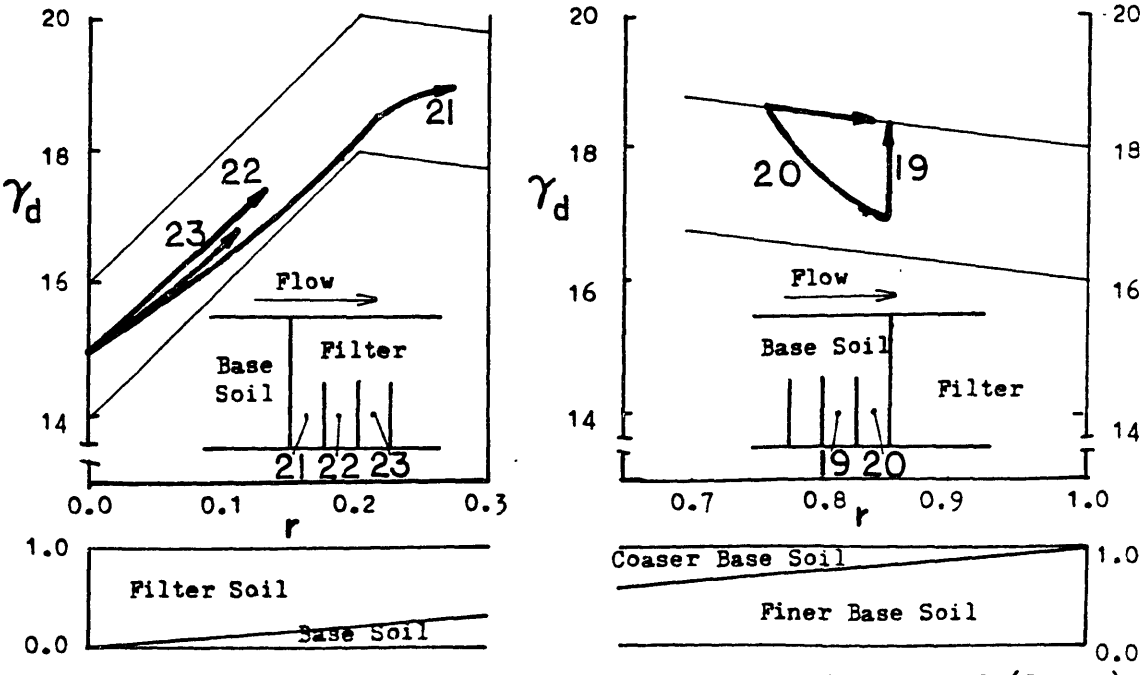

(b) The State Diagram for Base Soil Consist of 85% Finer Soil (Case B)

Fig. 2.26 The State Diagram of the Clogging Process

CHAPTER III. STATISTICAL ANALYSIS OF LABORATORY DATA

In the light of the physical insights obtained in the previous chapter, a statistical analysis of existing laboratory data on filter performance is carried out in this chapter. General characteristics of the data base are described in Section 3.1. Logistic regression, which is the main tool of analysis, is explained in Section 3.2. Finally, in Section 3.3, numerical results are presented. The objectives of the analysis are (i) to evaluate the performance of conventional filter criteria, and (ii) to propose improvements.

3.1 Data Base

We begin in Section 3.1.1 with some definitions and notations. The soil parameters that are included in the analysis as possibly influential on filter performance are discussed in Section 3.1.2. Finally, some preliminary considerations on the data base are presented in Section 3.1.3.

3.1.1 Definitions and Notation

400 experimental results on filter behavior from 13 references are summarized in Table 3.1. As previously mentioned in Chapter I, these cases can be divided into two groups: the earlier experiments (before the early (60's) aim at establishing what we now call "conventional filter criteria". The work by Bertram (1940), Hurley &

Newton (1940), USCE (1941, 48, 53) and Karpoff (1955) fall into this category; by contrast, recent experiments more often aim at investigating the filtering mechanism and special topics. For example, the experiments by Vaughn & Soares (1981) have the objective of determining the ability of filters to retain fines washed out from crack walls of the core material.

In this section, discussion of the data is limited to aspects related to the statistical anaysis. A more detailed description of each laboratory experiment is given in Appendix A.

References are identified through numbers, as indicated in the "source" column of Table 3.1; for example [40A] indicates Bertram(1940).

In Table 3.1(a), the result of each experiment is classified categorically as "stable", "nonstable" or "clogging"; specifically, if there is no migration of base soil particles into the filter, the system is classified as "stable"; if particles of the base soil wash easily through the filter, the system is considered "non-stable". "Clogging" is a condition somewhat intermediate between these two states: some base soil particles migrate into the filter, but these particles clog the free path and the system gradually becomes stable without significant loss of base soil. In most of the literature, it is

quite easy to distinguish between these three classes of results, alhtough their description differs from one reference to another.

Whether "clogging" constitutes failure or not depends on the purpose of the filter. If the filter is expected to perform as a drain, then "clogging" is an undesirable (failure) state; whereas if the filter is just intended to prevent migration of base soil particles, it may be considered acceptable. In the statistical analysis of the data, we consider separately these two interpretations, whereas conclusions are drawn mainly based on results for clogging = monstable, because this is a more frequent and conservative assumption.

In most of the literature,it is reported that filter performance can be classified as "stable", "non-stable", or "clogging" through visual inspection. However, if classification is not based on an objective criterion, subjective factors may influence the results. For example, Hurley & Newton (1940) judged some filters as "stable" even if they lost some of the fines, provided that they finally reached a stable condition; on the other hand, Leatherwood & Peterson (1954) used as a criterion the change in the loss of hydraulic head across the base soil-filter interface. This is considered to be a very sensitive method to judge performance. The way in which these differences are taken into account in the statistical

analysis is by explicitly allowing for "laboratory bias" (see Section 3.2.2).

3.1.2 Soil Parameters in the Data Base

The grain size distribution of base soil and filter, the porosity of the filter, and the hydraulic gradient may be expected to be the main factors in determining the performance of the filter. In the present statistical analysis, only the grain size distributions of base soil and filter are used; this information is available for all the cases of Table 3.1, and is the only one on which the conventional filter criteria are based.

The hydraulic gradient has been ignored because:

(i) Many authors have investigated the influence of hydraulic gradients on filter performance, concluding in all cases that this parameter affects the rate of the phenomenon, but does not appreciatively change the final state of the system.

(ii) Not all experimental studies report reliable measurements of hydraulic gradients.

Porosity (or void ratio) of the filter is also excluded from statistical analysis. The reason is that, unfortunately, this parameter is available from only very few data sources.

3.1.3 Preliminary Considerations on the Data Base

The gradations of base soil and filters are considered to be important factors in the stability of the filter. A widely used measure of soil gradation is the uniformity coefficient, U_o = D60/D10. The combinations of U_o for the base soil and the filter are summarized in Table 3.1 (b). (For the notation, see the footnote of the table). About half of the data refers to very uniform base soil (U_o < 2) and very uniform filter (U_o < 2). The rest of the data is fairly evenly distributed among the other five categories.

Later in the analysis, we shall find that the reported behavior of filters for the data sets [61], [75] and [82] is quite different from that of the other data sets; for this reason, these three sets of data will be excluded from the main portion of the analysis. One possible explanation for the difference is that the anomalies sets have relatively high fines content (size less than 0.074mm) in the base soil. This can be seen in Table 3.1(c), which classifies each experiment by the size of DB10 larger or smaller than the #200 seive (0.074mm).

A summary of the 277 data sets that remain after exclusion of sources [61], [75] and [82] is given in

the last row of Table 3.1.

Some plots of these 277 data points are shown next. Figure 3.1 plots DB60/DB10 against DF60/DF10, which gives essentially the same information as Table 3.1(b). There is a high concentration of data in the DB60/DB10 < 2 and DF60/DF10 < 2 region, but the rest of the points are fairly well distributed over the uniformity coefficients plane.

The uniformity coefficient represents a property of the finer portion of the grain size distribution, since it is the ratio between D60 and D10. On the other hand, the conventional filter criteria (Terzaghi's criteria) is based on DF15/DB85, suggesting that the coarser portion of the base soil is more important. In order to display the diversity of the coarser portion of the base soil, DB95/DB75 is plotted against DF60/DF10 in Fig. 3.2. This figure shows that except for the concentration in the lower DB95/DB75 and lower DF60/DF10 region, the points are widely distributed. Figure 3.3 shows that the correlation between DB95/DB75 and DB60/DB10 is not very high, implying that the finer portion gradation of the base soil is not a good indicator of the coarser portion gradation.

In Figure 3.4, DB85 is plotted against DF15. DF15 varies between 0.1 and 20mm. and DB85 between 0.07 and 10 mm. Terzaghi's criteria (DF15/DB85 < 5) is also shown

in the figure. Many of the figures in this chapter use the same symbols: "*" indicates stable,"+" clogging and " [ ]" unstable cases.

3.2 Logistic Regression Model

Logistic regression is a convenient technique to analyze the dependence of a binary response variable on a set of control variables. The model is introduced in Section 3.2.1. In Section 3.2.2, statistics are defined, which are useful in assessing the adequacy of the fitted model. Finally in Section 3.2.3, indicator variables, which are useful in considering laboratory biases in the analysis, and the stepwise regression procedure are introduced.

3.2.1 Regression with a Binary Response Variable

Consider the problem of predicting a binary response variable Y (either 0 or 1) from a vector of control variables $\underline{x} = [x_1, x_2, \ldots, x_p]^T$. Because Y is a binary variable, the distribution of $(Y|\underline{x})$ is defined entirely by $P[Y = 1|\underline{x}] = E[Y|x]$, i.e., by the regression of Y on $\underline{x}$. For simplicity, we assume that $E[Y\ \underline{x}]$ is a function of on a linear combination of the components of $\underline{x}$, i.e.,

$$E[Y|\underline{x}] = F(\beta_o + \sum_{j=1}^{k} \beta_j x_j) \qquad (3.2.1)$$

where β_o, β_1, ... , β_p are coefficients to be determined and F is a function between 0 and 1.

Three commonly used functions F are given in Table 3.2. The logistic function is especially popular, mainly due to the existance of simple sufficient statistics (Cox [1970], pp. 18-19) and to numerical stability (insensitivity to outlier observations). The probit model consists of using for F a normal C.D.F. The probit and logit produce similar results, except in the tails, which are thicker for the logistic function (Cox, [1970] pp. 27-28). The extreme value model is developed to analyze longitudinal data and is based on the assumption that the log of the occurrence rate is constant within each interval and is equal to $\beta_o + \sum_j \beta_j x_j$ (DuMouchel & Waternaux [1982]).

The logistic model is the one used in the present analysis. For this model,

$$E[Y|\underline{x}] = \frac{e^{\lambda}}{1+e^{\lambda}} \qquad (3.2.2a)$$

where

$$\lambda = \beta_o + \sum_{j=1}^{k} \beta_j x_j \qquad (3.2.2b)$$

Alternatively,

$$\lambda = \ell n \left(\frac{E[Y|\underline{x}]}{1-E[Y|\underline{x}]}\right) \qquad (3.2.3)$$

The most satisfactory method to estimate parameters β_o, β_1, ..., β_p is maximum likelihood. The log likelihood

function is given by (Cox [1970], Dobson [1983]).

$$\ell(\beta_o, \beta_1, \ldots, \beta_p) = \sum_{i=1}^{n} y_i(\beta_o + \sum_{j=1}^{p} \beta_j x_{ij}) - \sum_{i=1}^{n} \ell n(1 + \exp[\beta_o + \sum_{j=1}^{p} \beta_j x_{ij}]) \quad (3.2.4)$$

where n is the number of data sets. The function can be maximized by setting to zero the partial derivatives of ℓ, i.e., by solving the following set of equations:

$$\frac{\partial \ell}{\partial \beta_r} = \sum_{i=1}^{n} y_i x_{ir} - \sum_{i=1}^{n} \frac{x_{ir}}{1 + \exp[\beta_o + \sum_{j=1}^{p} \beta_j x_{ij}]} = 0$$

$$(r = 0, 1, 2, \ldots p) \quad (3.2.5)$$

where $x_{io} = 1$. The solutions can be obtained numerically, e.g., by the Newton-Raphson method.

3.2.2 Regression Statistics

Some statistics have been developed to evaluate logistic regression models and to compare alternative sets of explanatory variables x_i. A brief review of these statistics is given below.

(1) Likelihood Ratio Statistics

Consider two logistic models M_o and M_1 where M_o is nested in M_1 in the sense the control vector $\underline{x}_o$ in

model M_o is included in vector $\underline{x}_1$ used in M_1:

$$\text{Model } M_o\text{: } E[Y|\underline{x}_o] = F(\beta_o + \sum_{j=1}^{q} \beta_j x_j) = F(\underline{\beta}_o \underline{x}_o) \tag{3.2.6a}$$

$$\text{Model } M_1\text{: } E[Y|\underline{x}_1] = F(\beta_o + \sum_{j=1}^{p} \beta_j x_j) = F(\underline{\beta}_1 \underline{x}_1) \tag{3.2.6b}$$

Where $p > q$. We want to test

H_o: Model M_o correct.

against

H_1: Model M_1 correct.

If the sample size is large, this can be done

$$LR = 2[\ell(\hat{\underline{\beta}}_1) - \ell(\hat{\underline{\beta}}_o)] \tag{3.2.7}$$

where $\ell(\hat{\underline{\beta}}_1)$ and $\ell(\hat{\underline{\beta}}_o)$ are log likelihood functions of M_1 and M_o respectively. Asymptotically, the distribution of LR is χ^2 with p-q degrees of freedom. Therefore, a test at significant level α is performed by accepting H_o if $LR \leq \chi^2_{\alpha\ p-q}$. This test is especially useful in stepwise regression, which will be described later.

Two of special cases of the LR statistic are especially useful. One is obtained by model M_o by setting $P(Y = 1|\underline{x}) = 0.5$, which implies we just randomly predict the outcomes of Y regardless of $\underline{x}$. Then the log likelihood function for this case yields

$$\ell(\hat{\underline{\beta}}_o) = \ell n(\tfrac{1}{2})^n = -n\ \ell n 2$$

and the likelihood ratio statistic, Eq. (3.2.7), yields

$$LR_o = 2\,[\,\ell(\hat{\beta}_1) + n\ \ell n 2] \qquad (3.2.8)$$

In this way, we can test the significance of model M_1 compared to no information condition (i.e., Model M_o) by following the hypotheses testing procedure.

The other is obtained by not using any regression variables in model M_o, i.e., model M_o, E [Y] is constant. In this case

$$\ell(\hat{\underline{\beta}}_o) = \ell n\,[\,(\frac{n_1}{n_o+n_1})^{n_1}\ (\frac{n_o}{n_o+n_1})^{n_o}]$$

$$= n_1 \ell n(n_1) + n_o \ell n(n_o) - n \ell n(n)$$

where n_o: number of data whose response is 0

n_2: number of data whose response is 1

$n = n_o + n_1$

and the likelihood ratio statistic becomes

$$LR_1 = 2\,[\ell(\hat{\beta}_1) - n_1 \ell n(n_1) - n_o \ell n(n_o) + n \ell n(n)] \qquad (3.2.9)$$

(2) Likelihood Ratio Indices

Because of the non-linear form of the logistic model it is not immediately obvious how one could define an analogue to the coefficient of determination in

multiple linear regression.

McFadden (1974) has proposed the likelihood index ratio, ρ^2, whose general form is

$$\rho^2 = 1 - \frac{\ell(\hat{\underline{\beta}}_1)}{\ell(\hat{\underline{\beta}}_2)} \qquad (3.2.10)$$

Two special cases of ρ^2 which correspond to LR_o (Eq. (3.2.8)) and LR_1 (3.2.9) are

$$\rho_o^2 = 1 - \frac{\ell(\hat{\underline{\beta}}_1)}{(-n\ell n^2)} \qquad (3.2.11)$$

and

$$\rho_1^2 = 1 - \frac{\ell(\hat{\underline{\beta}}_1)}{(-n_1 \ell n n_1 - n_o \ell n n_o + n \ell n n)} \qquad (3.2.12)$$

The likelihood ratio indices are analogous to R^2 in ordinary linear regression and should be used with similar cartion when comparing different models, especially because ρ^2 are not adjusted for the number of fitted parameters.

The statistics introduced so far, LR and ρ^2, can be used in the comparison of nested models. Horowitz (1982) has proposed the modified likelihood ratio index, $\bar{\rho}_o^2$, for comparing non-nested models. This index is given by

$$\bar{\rho}_o^2 = 1 - \frac{\ell(\underline{\beta}_1) - p/2}{(-n\ell n 2)} \qquad (3.2.13)$$

where p is the number of parameters in M_1 plus one. The number of parameters is included in the index as a penalty so that it can be used in making comparisons of any models.

(3) Percent Correctly Predicted (PCP)

A data point $(\underline{x}_i, y_i)$ is said to be correctly predicted if

$$y = 1 \text{ and } F(\underline{x}_i) > 0.5, \text{ or}$$

$$y = 0 \text{ and } F(\underline{x}_i) < 0.5 .$$

The PCP statistic is simple to calculate and is easy to interpret intuitively. However, it is not a very discriminating quantity because it only depends on the 0.5 value of F.

(4) t Statistic

For each parameter β_i, the t statistic is defined as

$$t = \hat{\beta}_i / \sigma_i \qquad (3.2.14)$$

where

$$\sigma_i = \{ - \frac{\partial^2 \ell(\underline{\beta})}{\partial \beta_i^2} \Big|_{\underline{\beta}=\hat{\underline{\beta}}} \}^{-1/2}$$

is the standard error of β_i. The hypotheses H_o: $\beta_i = 0$ can be tested at level α by comparing $|t|$ with the $(1-\alpha/2)$ frac-

tion of the t distribution with n-(p+1) degree of freedom.

3.2.3 Indicator Variables and Stepwise Regression

In the next section, it will sometimes be necessary to include laboratory bias. This is mainly due to the subjectivity of the criteria used for classifying the results of the experiments (see Section 3.1.1). This bias can be taken into account by introducing indicator variables among the explanatory variables. Let I_k be an indicator variable such that

$$I_k = \begin{cases} 1 & \text{for data from lab.k} \\ 0 & \text{otherwise} \end{cases}$$

These variables can be included in the logistic model by writing

$$E[Y|\underline{x}] = \frac{e^{\lambda}}{1+e^{\lambda}} \qquad (3.2.15a)$$

where

$$\lambda = \beta_o + \sum_{j=1}^{p} \beta_j x_j + \sum_{k=1}^{K-1} \beta_{(p+k)} I_k \qquad (3.2.15b)$$

where K is the number of laboratories or of data sources. The effect of I_k is to shift the logistic regression curve according to the labotayory effect. The regression statistics presented previously can be used to judge the significance of each laboratory bias.

It is important in the regression analysis to be able to identify the most influential parameters among many candidate parameters. This can be done by using a technique called stepwise regression. Two variants of stepwise regression are the forward selection and the backward elimination procedure.

Forward selection works as follows:

[F1] Start from the best single parameter regression, i.e., from the regression with the parameter that gives the highest likelihood ratio LF_1.

[F2] Add the parameter that gives the best improvement of the likelihood ratio statistic, LR, as long as the improvement is statistically significant. This can be judged by comparing LR with $\chi^2_{\alpha,1}$.

[F3] Eliminate any parameters that no longer make a significant contribution to the model. This can also be decided on the basis of LR.

[F4] Repeat steps F2 and F3 until no further parameter is added or eliminated.

The backward elimination procedure is as follows:

[B1] Fit the logistic model including all candidate parameters.

[B2] Eliminate the least significant parameter using LR until no parameter can be eliminated without significantly changing LR, i.e., by comparing LR with $\chi^2_{\alpha,1}$.

[B3] Add back parameters that significantly improve the fit of the model.

[B4] Repeat steps B2 and B3 until no additional parameters can be added or eliminated.

It is important to note that these are local (one-step) optimization procedures and, therefore, may not converge to the same parameter selection. Indeed, there may be cases when the model could be significantly improved by simultaneously adding several parameters, whereas no significant imporvement results from adding one parameter. Therefore, it often happens that the number of parameters selected by the backward procedure is greater than that selected by the forward procedure.

3.3 Results of Statistical Analysis

This section presents results from applying logistic regression to the data of Section 3.1.

The performance of conventional filter criteria is evaluated first as a preliminary analysis in Section 3.3.1; this is done by carying out

the regression analysis using only the soil parameters that appear in the conventional criteria. The best form of such criteria is determined and uncertainty on the coefficients is quantified. The main aim of this preliminary analysis is to illustrate the feature of logistic regression model.

In Section 3.3.2 the data is analyzed to identify anomalous subsets and to remove some of the data for further analysis.

Analyses to improve current filter criteria based on grain size characteristics other than DF15 and DB85 are presented in Section 3.3.3. The stepwise regression procedure plays an important role here. Parameters obtained are interpreted in the light of physical considerations from Chapter 2. An improved filter criterion is proposed, and uncertainty involved in it is quantified.

3.3.1 Preliminary Analysis to Evaluate Conventional Filter Criteria

The purpose of this section is to evaluate the degree to which variables such as DF15/DB85 and DF50/DB50, can separate stable filters from non-stable ones.

Figures 3.5 and 3.6 show plots of DF15 vs. DB85 and DF50 vs. DB50 respectively; these are the characteristic grain sizes used in conventional filter criteria.

The criteria are also shown in the figures. Although the criteria roughly separate "stable" from "non-stable" data, there is considerable intermixing between the two classes of points.

Which is the best among conventional criteria? What is the probability of misclassification? Are the results from one laboratory significantly different from those from other laboratories? There are the questions we address in this section.

The stepwise regression procedure described in Section 3.2.2 is used to select the best parameter or set of parameters among those used in conventional criteria: DF15/DB85, DF50/DB50, DF15/DB15, DF60/DF10 and DB60/DB10. The uniformity coefficients of base soil and filter are included because some of the criteria account for the gradation of soils. If a uniformity coefficient were an important explanatory variable, then the stepwise regression procedure would select it together with filter/base soil grain size ratios. The regression analyses are done with all 400 data under both: (i) "clogging"="nonstable" (Analysis I-1), and (ii) "clogging"="stable" (Analysis I-2) assumptions (see Sections 3.1.1).

Results are shown in Table 3.3 for both cases. Since all the results of regression analyses will be pre-

sented in the same format, it is worthwhile to explain some notation here. "Data" indicates the data sets used in the analysis. "Assumption" indicates whether "clogging" is considered "stable" or "nonstable". "Candidate parameters" are these parameters considered in stepwise regression. "$\hat{\beta}$" is the regression coefficient calculated for each parameter, and "t" is the t-statistics defined in Eq. (3.2.14). Finally, "mean" and "s.d." give the mean value and standard deviation of the parameter for the data set being considered. The hypothesis $H_o: \beta_i = 0$ is rejected at significance level α if $t > t_{\alpha/2,\, n-p'}$ where n is the number of data points and p' is the number of parameters introduced in the analysis plus one. In the present case, $t_{0.01/2\,,\ 400-2} = t_{0.005,398} = 2.58$, which implies that H_o is rejected hencethat the parameter DF15/DB85 is very significant.

ρ_o^2 and $\bar{\rho}_o^2$ are the likelihood ratio index and the modified likelihood index as defined by Eqs. (3.2.11) and (3.2.13). The former is useful in the comparison of nested models; the latter, the comparison of non-nested models (see Section 3.2.2). From the relatively small value of these statistics, one may conclude that the chosen parameters are not producing sharp separation between stable and nonstable cases. In later analysis, both ρ_o^2 and $\bar{\rho}_o^2$ will become as large as 0.67, indicating a significant improvement of the model. PCP denotes "Per-

cent correctly predicted", as defined in Section 3.2.2.

In the case presently analyzed, DF15/DB85 is selected as the best parameter; no other parameter is retained by the stepwise regression procedure using a χ^2-test at the 1% significance level. Results using DF50/DB50 are shown in Table 3.4 for comparison (Analyses I-3 and I-4). The models in terms of DF15/DB85 and of DF50/DB50 can be compared using $\bar{\rho}_o^2$ or PCP. As explained in Section 3.2.2, the former is a more appropriate statistics. All statistics (i.e., ρ_o^2, $\bar{\rho}_o^2$ and PCP) indicate that the model in terms of DF15/DB85 gives a much better fit to the data.

In Fig. 3.7, the results are plotted on the DF15-DB85 plane together with 400 data points. Terzaghi's criteria (DB15/DB85 < 5) lies on the conservative side for both assumptions. Based on these regression analyses one can calculate the probability of failure P_ρ associated with Terzaghi's criterion. This probabilty is $P_\rho = 0.309$ for Analysis I-1 and 0.257 for Analysis I-2. Probability of failure contours can be drawn by following the procedure shown in the figure: the contours presented in Fig. 3.7 are based on Analysis I-1.

Although DF15/DB85 seems to be a good criterion to separate "stable" filters from "nonstable" filters, there is considerable mixing of points between two classes. Our final aim is to find a parameter or a set of parameters which can separate better these two classes of

points. Before doing so, we investigated the characteristics of each data set; for not all the data has the same quality; some may be biased or be affected by large erros.

3.3.2 Investigation of Each Data Set

Analyses are made to see whether there are data sets with anomalous characteristics. Stepwise regression with indicator variables to account for laboratory biases plays a major role in this analysis. DF 5/DB85 is used as a separating parameter. One should notice that the presence of a "laboratory bias" does not necessarily imply that the data set is biased; the bias can be induced by characteristics of the grain size distributions other than DF15/DB85 that are particular to that data set.

As in the case without laboratory effects, two cases are considered: "clogging" = "non-stable" (Analysis II-1) and "clogging"="stable" (Analysis II-2). The results are shown in Table 3.5.

Since the number of explanatory variables has increased the regression statistics have improved (for example ρ_o^2 has increased from 0.225 to 0.390 in the case of Analysis II-1 and from 0.309 to 0.378 in the case of Analysis II-2. The absolute value of the t-statistic for

each laboratory indicator variable is an indicator of significance of the bias: the larger this statistic, the more significant the bias. The sign of $\hat{\beta}$ shows the direction of the shift of the logistic curve for that laboratory; if it is negative the curve is shifted toward larger DF15/DB85.

Data sets [40A], [49], [75] and [82] are identified as anomalous in both analyses. Set [84] is found to be anomalous only in Analysis II-1 and set [40B] only in Analysis II-2.

The experimental set-ups of data sets [75] and [82] are very different from the rest of the data. They used flocculated clay instead of base soil agaisnt filter (see Appendix A for details). It is, therefore, not surprising that these two sets of data have been singled out as anomalous by the anaysis.

It is also known that the critical DF15/DB85 values separating nonstable from stable filters found in set [40A] are unconservative with respect to all other experiments (see Appendix A). The reason for this is not clear, but is possibly linked to the use of extremely uniform soils for both the base soil and the filter.

No obvious explanation can be found for groups [49], [84] and [40B]. The diversity of filter performance from laboratory to laboratory suggests that separating the data in terms of only the parameter DF15/DB85

may not be sufficient; i.e., there might be other parameters that can separate the data more efficiently. Identification of such parameters is the objective of the next section.

The results of Analyses II-1 and II-2 are plotted in Figs. 3.8(a) and 3.8(b) respectively. Looking separately at the data for each laboratory, one may conclude that all the data sets are reasonably well separated by DF15/DB85, except for [61]. The inclusion of many cohesive base soils in this group (see Table 3.1(c)) could provide an explanation. In order to avoid biasing the results of the analysis, in all subsequent runs, group [61] has been removed from the data base.

The sets [75] and [82] are also removed because they utilize completely different experimental set-ups.

With these three groups excluded, we are left with 277 data points; this is the data base the rest of the analyses are based on (see Table 3.1).

3.3.3 Improvement of Filter Criteria

In order to construct better filter criteria based on grain size, the stepwise regression procedure is used to select the most explanatory combination of grain sizes among a large number of candidate sizes.

First, analyses based on parameters with single grain size are performed (Analyses III-1 to 4); the aim

here is to find the grain sizes that significantly affect the filtering phenomenon. The backward elimination procedure is used in these analyses, to make sure that all the significant grain sizes are retained in the final parameter selection (see Section 3.2.2). However, it is somewhat difficult to give physical interpretation to the results because (i) each parameter is a single grain size and (ii) the number of parameters selected is rather large usually 5 or 6 parameters To overcome this difficulty, a second series of analyses is carried out. In the second series (Analyses IV-1, 2, V-1, 2), the candidate parameters are ratios of two grain sizes (most of the grain sizes are among those selected in the first series). The forward selection procedure is adopted in this case so that only the minimum necessary number of parameter is selected using ratios facilitate the physical interpretation of the results.

A few additional analyses are performed whose purpose is to evaluate the probability of malfunctioning of the filter. Finally, an improved filter criteria is proposed based on the present analysis.

As mentioned earlier, the data sets [61], [75] and [82] are not included in the data base.

(1) Significant Grain Sizes

Tables 3.6(a) and 3.6(b) show results for "clogging"= "nonstable" (Analysis III-1) and "clogging" = "stable" (Analysis III-2) respectively. The results are also illustrated in Figs. 3.9(a) and 3.9(b). The separation of the two data categories improved considerably compared to the previous analyses (e.g., Figs. 3.8(a) and (b)). The candidate grain sizes are given in Table 3.6. Logarithm of them have been taken because usally parameters in the criteria are expressed by ratios of grain size and they can be written in a linear from if logarithm is taken. Since we have increased the number of explanatory variables, the regression statistics have improved; however, in these analyses, we are more interested in the combination of variables selected and in their relative significance.

It is remarkable that the same grain sizes have been selected in both cases. Even more interesting is the fact that only one grain size, DF15 has been chosen for the filter. In contrast, six grain sizes are selected for the base soil, of which four are from the coarser portion (> DB70) of the grain size distribution.

The fact that only DF15 is selected for the filter suggests that this quantity is a good measure of the filter void sizes,or at least of the size of particles the filter

can retain. The same fact supports the conclusion by Vanmarcke and Honjo (1985) that DF15 is highly correlated to the expected distance between particles (see Section 1.2.1 (3)). It also suggests that the standard requirement that "the grain size curve of the filter should roughly parallel that of the base soil" (see Section 1.1) may not be critical for filter stability.

The other important fact that emerges from these analyses is that the details of the coarser portion of the base soil grain size distribution are important. This is in accordance with the conclusion in Section 2.3.2, that internal stability of the base soil is controlled by the coarser portion of the grain size distribution. The diameters DB95, DB90, DB85, DB70 are considered to give information concerning this portion. On the other hand, DB50 and DB10 may be viewed as indicators of the spread of the base soil, which may be important in determining internal stability of the base soil.

In the previous analyses (i.e., the Analyses III-1 and III-2), actual grain sizes are used. One may argue in physical bases that a better choice of parameters would be in terms of relative grain sizes. For this purpose, all grain sizes are normalized in Analyses III-3 and III-4 by dividing them by DF15. DF15 is used as the normalizing value, because this is the only size selected for the filter.

Results are presented in Tables 3.6(c) and 3.6(d).

Analyses III-1 and III-3, for "clogging"="Nonstable", give very similar results in terms of the regression statistics $\bar{\rho}_o^2$ (0.462 vs. 0.467) and PCP (84.1(%) vs. 85.2(%)). However, there is some difference in the parameters selected: the major parameters of interest, such as DB95, DB90, and DB85 are selected with relatively high t-statistics (which implies relatively high significance). Two parameters are selected for the filter, namely DF80 and DF30, but their t-statistics are relatively small.

For Analyses III-2 and III-4, where "clogging"= "stable" is assumed, the similarity is even greater ($\bar{\rho}_o^2$: 0.581 vs. 0.562, PCP:86.6 (%) vs. 86.6 (%)): no parameter has been selected from the filter, and the DB values are the same, except for DB95 which is replaced in Analysis III-4 by DB80. The same conclusions for Analyses III-1 and III-2 apply for Analyses III-3 and III-4.

(2) Significant Grain Size Ratios

Although the separation of the data in Analyses III-1 to 4 (Table 3.6) is very good, it is difficult to give a physical interpretation to the results. Our next objective is to find combinations of grain sizes selected by the analysis that are physically meaningful.

Again, the stepwise regression procedure is used to

select the best set of parameters among many candidate parameters. The forward selection procedure is used for the reason mentioned earlier. All the candidate parameters are the ratios between two grain sizes of which the larger size usually is in the numerator. Parameters that conserve more than two grain sizes are not considered, in order to avoid difficulty in the physical interpretation. Grain sizes are mainly among those selected in Analyses III-1 to 4 but a few other sizes are also used. The set of 22 parameters that were finally considered as candidate explanatory variables are listed in Table 3.7.

Table 3.7(a) gives the results under the assumption that "clogging" = "nonstable". Only two parameters, namely DF15/DB85 and DB95/DB90, are selected when testing is at the 1% significance level.

The very high significance of DF15/DB85 indicated by the t-statistic (7.99) confirms that this is the main explanatory varible of filter performance. A physical interpretation of this parameter has been given elsewhere (see Sections 1.2.1(2), (3) and 2.3.1). In short, DF15 can be interpreted as a representative pore size of the filter. On the other hand, DB85 is a grain size such that, if the filter retains it, the whole base soil stabilizes through the quick formation of a self-healing

filter. Therefore, the ratio DF15/DB85 is a good indicator of filter performance.

As a secondary parameter, DB95/DB90 is selected. Before discussing the physical meaning of this parameter, let us consider some more results obtained in the statistical analysis. If one increases the significance level in the forward selection, more parameters are retained as significant. The one selected is DB95/DB85 (Table 3.7(b)). It is surprising that two parameters are chosen from such a narrow percentile range (i.e., between DB85 and DB95).

Another interesting result is that one can actually obtain the second best, third best, etc. pairs of parameters from the result of the stepwise regression calculation. These pairs are listed in Table 3.7(c). Up to the eighth best pair; all ratios involve grain sizes between DB70 and DB95. Although the pair (DB15/DB85, DB95/DB90) has a slightly higher $\bar{\rho}_o^2$ value (0.388), the difference in goodness of fit with the other pairs is negligible if one fits the data to one of these eight models and then tests the hypothesis "H_o: the present model is correct" against "H_1: one of the other seven models is correct", the nul hypotheses (H_o) is always accepted.

The previous results strongly suggest that the coarser portion of the grain size distribution for the

base soil critical for filter performance. This result corresponds to the conclusion in Section 2.3.2, that the internal stability of the base soil is primarily controlled by the grain size distribution around DB85.

All 277 data point is plotted in Fig. 3.10 on the DF15/DB85 - DB95/DB90 plane; this is the best two parameter combination selected by the regression analysis. Of course, the ratio DB95/Db90 measures the gradient of the grain size curve between the 90 and 95 percentiles. The milder the gradient, the more the soil is susceptible to piping. Because soil particles larger than DB85 are considered to play a major role in the formation of self-healing filters and because the ratio DB95/DB90 gives information about this portion, the variable selection by stepwise regression appears to be reasonable. However, it is somewhat hard to understand why the average gradient between particles with only 5% difference should control the phenomenon. Moreover, since the grain size distribution is estimated from points determined through seive analysis, there exists considerable uncertainty in the measurement of this quantity. These are sufficient reasons to exclude the use of DB95/DB90 in a practical filter criterion in spite of the fact that this parameter produces the best regression statistics (i.e., $\bar{\rho}_o^2$).

The combinations presented in Table 3.7(c) can be con-

sidered as candidate pairs to replace the (DF15/DB85, DB95/DB90) combination. The pair (DF15/DB85, DB95/DB75) is chosen, based on the following considerations:

(i) All the grain sizes included in the secondary parameter are between DB70 and DB95. The ratio DB95/DB75 adequately covers this range.

(ii) The parameter is based on particles with a 20% difference. This reduces measurement uncertainty.

(iii) DB95/DB75 can be interpreted as the local average gradient of the base soil grain size distribution around DB85. Therefore, this quantity is considered to give the degree of separation between base soil larger and smaller than DB85: the more separated the two portions, the larger the value of DB95/DB75; see Fig. 3.11. Thus the physical interpretation of the parameter is as follows: DB85 is the critical grain size, and the self-healing filter layer mainly consisting of particles larger than DB85. If this layer cannot retain the finer portion, then the filter is internally unstable. This self-healing ability depends on the degree to which the two portions are separated and DB95/DB75 is a measure of this separation.

The results of regression analysis using this pair of parameters is presented in Table 3.7(d). In Fig. 3.12, the data is plotted on the DF15/DB85 - DB95/DB75 plane. As one can expect from the regression statistics ($\bar{\rho}_o^2$, PCP), the model separates the two cases almost as well as the model based on DB95/DB90, the latter is shown in Fig. 3.10. Some discussion of the outlier points will be given later.

Results from assuming "clogging" = "stable" are shown in Table 3.8 (Analysis IV-2). In this case, four parameters, namely DF15/DB85, DB85/DB75, DB90/DB70 and DB95/DB90, are selected at the significance level of 1%. The regression statistics are rather high compared to Analysis IV-1 in Table 3.7(d). This is considered to be due to laboratory biases, which will be considered later. The grain sizes included in the parameters are between DB70 and DB95, and the result is essentially showing a similar trend as for "clogging" = "non-stable" (Analysis IV-1).

As stated previously in Section 3.1, the assumption "clogging" = "nonstable" is more frequent and conservative than "clogging" = "stable". Therefore, we mainly use the results obtained from the former assumption in investigating the improved filter cirteria.

In Fig. 3.13 through 3.22, the data from each lab-

oratory is plotted separately on the DF15/DB85-DB95/DB75 plane. Using these figures, some considerations can be made about outliers:

A total of 63 experimental results from Bertram (1940) are plotted in Fig. 3.13. Only 2 cases failed at DF15/DB85=8.8, whereas 20 cases were judged to be stable at the same ratio. These results exhibit the highest critical values of DF15/DB85 among all the cases considered in the present study. The use of extremely uniform soils ($U \simeq 1.2$) for both the base and the filter might be reasponsible for the results.

Hurley & Newton (1940)'s results are plotted in Fig. 3.14. This is the case in which the ratio DB95/DB75 is the highest and the critical value of DF15/DB85 is one of the lowest among the data included in the analysis. As mentioned in Appendix A, Hurley and Newton used the same base soil adopted in all their tests. In spite of this, these base soils display some variation (see Fig. 3.23). In the analysis, the finest grain size distribution among these reported has been used (see Fig. 3.23). This is a conservative choice. A characteristic of the grain size distribution is that its coarser portion is widely graded, whereas the finer portion is relatively narrow graded ($DB60/DB10 \simeq 4$). Regarding these results, Soares (1980) points out: "It seems

that the base materials were not well graded despite their uniformity coefficient. The curves could be too concave in the upper part (in the region of partiles with DB>DB60) and this could be the reason for such low values of the ratio DF15/DB85. Also it seems that self-filtering is not only controlled by the 15 percent coarser particles. A certain amount of the other particle sizes must exist to establish the equilibrium at the interface". This statement is consistent with results of the present analysis, in particular with the use of the parameter DB95/DB75 in addition to DF15/DB85 in the prediction of filter performance. Hurley & Newton's results are the main data set in support of this conclusion.

The 13 experimental results of USCE (1941) are shown in Fig. 3.15. The critical ratio DF15/DB85 is in this case rather low compared to other experiments. Soares (1980) indicated that the small thickness of the base soil used in the test (less than 2/1") could be responsible for this poor performance for, if the base soil is too thin, it cannot provide enough material to form a self-healing layer at the base soil-filter interface. Lund (1949) made the same experiments with the soil against the screen to investiage this problem, and concluded that at least 2 inches of base soil is necessary to simulate natural filter conditions (see Appendix A).

The USCF results can, therefore, be considered to be biased.

Later results from USCE (1948) are shown in Fig. 3. 16. Cases [48 20] (nonstable) and [48 19] (stable) have a high DB95/DB75 ratio. These tests used the same base soil-filter combination, and only differ on the direction of flow downward for [48 19] and upward for [48 20]. It was noticed that, as soon as vibrations were applied to the stable sample [48 19], "immediate failure of the base took place by subsidance and piping into the filter." This fact indicates that the condition represented by these experiments is a critical one. The grain size distribution of the base soil is shown in Fig. 3.23; the shape is remarkably similar to that of [40B].

In Fig. 3.17, USCE (1953) data are presented. The test was planned to check the stability of standard concrete sand filter; as a result, it includes no non-stable case and only one clogging case. This data does not seem to have any bias.

Lund (1949)'s results are shown in Fig. 3.18. This data is generally considered to be reliable and for this reason has been used in several recent studies, i.e., Vaughan & Soares (1982) and Sherard, et al (1984a). The experiment is well organized and Lund's paper provides interesting physical insights (for example, the physical

interpretation of DB85). Lund was the first author to experiment with soil against screen (see Appendix A). Six data points have relatively high DB95/DB75 ratio. The associated grain size distributions for the base soil are presented in Fig. 3.24. Based exclusively on this data, one could not reach any positive conclusion on the effect of DB95/DB75. An interesting feature of Lund's results is that "clogging" cases are more mixed with "nonstable" than with "stable" cases; this may suggest that the "clogging" condition is closer to unstability than to stability.

Figure 3.19 shows results by Leatherwood & Peterson (1954). In this experiment, the evaluation of stability was based on the change of hydraulic head loss across the base soil-filter interface. This is a conservative way to judge stability. The authors themselves state: "The technique employed by the investigators reported herein is believed to be more sensitive (than the conventional visual inspection)". It is almost certain that the cases judged by them as "clogging" would have been considered "stable" if one had used visual inspection. For example, loss of head might have resulted in the formation of a self-healing filter. Therefore, all the cases reported in this experiment as "clogging" will be treated in later analysis as "stable".

Figure 3.20 shows results by Korpoff (1955). At a first glance, it might appear that the results are biased. Recently, Sherard, et al (1984a) criticized this experiment claiming that the way in which Korpoff judged failure (by Korpoff's terminology, "visual failure") does not correspond to failure. Rather, they may correspond to "a small movement of base fines into the filter needed to allow base particles to enter and become trapped in the filter voids" (in our terminology, self-healing process). Sherard, et al, justify this observation by pointing at the fact that, in most cases, flow increased linearly with hydraulic head even after "visual failure". In some cases (such as [55 Al-1], [55 C-2], [55 C-3], [55 A-5], a gradual reduction of flow increment occurred indicating gradual clogging of the filter by the base soil (see Fig. 3.20 (b)). Sherard, et al, also tried to duplicate the test [55 C1-2], which has a widely graded base soil (see Fig. 3.23). In two replications, for which DF15/DB85 was 5.7 and 7.6, they found the specimens to be stable. They finally concluded: "We believe that all the Korpoff's tests should have been considered as successful (stable), though some were near the failure boundary".

Although Sherard, et al's analysis is rather persuasive, the facts should be pointed out:

(i) Their use of the relationship between hydraulic head and flow as a criterion for stability is inconsistent, in the sense that this relationship is not significantly different for stable or nonstable cases such as [55 A-5] (whose DF15/DB85 = 11). The implication is that "visual failure" could mean "nonstable", and the hydraulic head-flow relationship is not necessarily a good measure to distinguish between "stable" and "nonstable" filter.

(ii) In the case of [55 C1-2] Karpoff presents a picture of the failure state of the specimen and sieve analysis indicated a 10% intrusion of base soil material into the filter. The grain size distribution for base soil is presented in Fig. 3.23; the similarity between this curve and that of other failure cases with low DF15/DB85 (e.g., [40 B] series and [48 20]) is remarkably good in the coarser portion (upper DB70 region). Because of these facts, it is difficult to judge whether case [55 C1-2] was actually stable. One should regard this case at least as being very close to the nonstable boundary.

The writer agrees with the general conclusion of Sherard, et al that the criteria used by Korpoff in judging stability is somewhat conservative. However, it seems impossible now to reevaluate his results.

Figure 3.21 plots results by Belyesherskii, et al (1972). Since in this case there is no experiment close to the border line, these results do not contribute much in evaluating critical condition. The results are consistent with other experiments.

Sherard, et al (1984a)'s results are presented in Fig. 3.22. They are of good quality, but unfortunately include only very uniform base soils.

In consideration of the previous laboratory biases, the final calculations have been made under the following conditions:

(i) As a general rule, "clogging" is assumed to be equivalent to "nonstable". This is a common and conservative assumption.

(ii) Data set [40A] removed because, as already mentioned, it is biased. Fortunately, there is a large amount of other experimental results in the same range of DB95/DB75 (i.e., DB95/DB75≃1.1).

(iii) All "clogging" cases in [54] are considered to be "stable", for reasons given previously.

(iv) Laboratory bias terms are included for data sets [41] and [55] (see Section 3.2.3). This means that the logistic curve that gives the probability of filter failure is shifted for these two data sets relatively to the rest of the data. The shift is associated with a difference in the criteria used to evaluate filter performance or to other peculiarities of the soils used. The significance of each laboratory difference can be judged by using the associated t-statistics.

The result of the analysis is shown in Table 3.9 (Analysis V). The regression statistics ρ_o^2(=0.677), $\bar{\rho}_o^2$ (=0.660) and PCP (=90.7%) all attain values higher than in any previous anaysis. The t-statistics indicate high significance of each explanatory variable.

A plot of the 0.5 failure probability line on the DF15/DB85 - DB95/DB75 plane is shown in Fig. 3.25. As one could expect, mixing between the two classes of points has been considerably reduced by the introduction of the ratio DB95/DB75 and of the bias term.

(3) Probability of Filter Malfunctioning

The fitted logistic curve together with the distribution of the data is presented in Fig. 3.26. The logistic curve gives the probability of filter malfunctioning for a given specimen. For given ratios DF15/DB85 and DB95/DB75, one first calculates

$$\lambda = 1.60 \frac{DF15}{DB85} + 1.39 \frac{DB95}{DB75} - 14.75 \qquad (3.3.1)$$

and then finds the probability of filter malfunctioning from

$$P_j = \frac{e^{\lambda}}{1+e^{\lambda}} \qquad (3.3.2)$$

For DB95/DB75 fixed to its sample average value of 1.95, the probability of malfunctioning depends on DF15/DB85 as shown by line A in Fig. 3.27. According to the fitted model, the probability of malfunctioning of the filter for Terzaghi's limit (i.e., DF15/DB85=5) is about 2%.

In practice, one must often calculate the probability of filter malfunctioning under rather safe conditions (in the tail portion of the distribution). This probability is obviously sensitive to the form of the regression model used. A reasonable alternative to the present model might be a linear logistic regression in terms of log (DF15/DB85) instead of DF15/DB85.

Results of logistic regression analysis using log (DF15/DB85) and DB95/DB90 as explanatory variables are presented in Table 3.10 (Analysis VI). The regression statistics are very similar to those obtained in Analysis V (Table 3.9): ρ_o^2, 0.660 vs. 0.667; $\bar{\rho}_o^2$, 0.660 vs. 0.644; pcp, 90.7(%) vs. 91.1(%). Line B in Fig. 3.27 corresponds to the present analysis. For DF15/DB85 larger than 4; the two lines are very close. However, significant differences exist for DF15/DB85 < 3.

Since P_f is a function of both DF15/DB85 and DB95/DB75, one can draw equal probability contours on the DF15/DB85 - DB95/DB75 plane. Contour lines are shown in Fig. 3.28 for both Model A (solid lines) and Model B (dotted linesO. The two models exhibit very similar behavior for $Pf \geq 10^{-2}$. However, below this value, they behave very differently. Of course, results for probabilities P_f less than 10^{-2} are considerably uncertain because of the limitation of the data.

(4) Improve Filter Criterion

Conventional filter criteria are considered to be developed for uniform base soils (i.e., low DB95/DB75); this can be understood from the fact that most of the data points are concentrated in the lower DB95/DB75 range (see Fig. 3.25). An improved filter criterion is proposed which

can account for the effect of higher DB95/DB75 values. The criterion is derived based on the condition that safety provided by the improved criteria for all ranges of DB95/DB75 should be the same as that provided by the conventional filter criteria for uniform base soils.

An improved design criterion which satisfies the condition stated above can be obtained by using Fig. 3.28. Since the conventional criterion, DF15/DB85 < 5 (see Section 1.1), is established based on the experiments done in smaller DB95/DB75, one may find the corresponding probability of filter malfunctioning is about 10^{-2} by looking at Fig. 3.28. It, therefore, makes sense to propose our criterion based on this line because the contour has the same safety margin agaisnt failure for all ranges of DB95/DB75. Unfortunately, there are some discrepancies between 10^{-2} contour obtained by (DF15/DB85, DB95/DB75) model and log (DF15/DB85, DB95/DB75) model in larger DB95/DB75 ranges. Therefore, a border region is proposed as an improved design criteria instead of a line as shown in Fig. 3.29;

$$\text{Average:} \quad \frac{DF15}{DB85} = 5.6 - 0.6 \frac{DB95}{DB75} \qquad (3.3.3)$$

$$\text{Most Conservative:} \quad \frac{DF15}{DB85} = 5.75 - 0.75 \frac{DB95}{DB75} \qquad (3.3.4)$$

$$\text{Most Conservative:} \quad \frac{DF15}{DB85} = 5.5 - 0.50 \frac{DB95}{DB75} \qquad (3.3.5)$$

The larger discrepancy of 10^{-2} contour predicted by the two models is higher DB95/DB75 range is caused by the scarceness of the experimental data in this region. To establish more accurate criterion in this region, experimental work is necessary.

3.4 Summary and Conclusions

Following considerations in Chapter II based on physical arguments, a statistical analysis of laboratory data on filter performance has been carried out in this chapter. The purposes of the analysis are:

(i) to evaluate the performance of conventional filter design criteria;

(ii) to derive improved design criteria.

The data base consists of 400 data from 13 sources (Table 3.1). These include experiments done in the 40's and 50's to establish what is now known as "the conventional filter criteria" as well as recent experiments to investigate the mechanism of filtering. The results of the experiments can be classified as "stable", "nonstable", and "clogging" (Table 3.1(a)). Only grain sizes of the base soil and the filter are used as explanatory variables in the statistical analysis because (i) they are the parameters used in the conventional filter criteria, and (ii) these are the only parameters that are reliably available for all 400 cases. About

half of the data corresponds to very uniform base soil (DB60/DB10 < 2) protected by very uniform filter (DF60/DF10 < 2). The remainder of the data is rather uniformly distributed over a range of uniformity coefficients (Table 3.1(b)). In nearly all cases used in the statistical analysis, the base soil has DB10 > 0.074 mm (Table 3.1(c)); therefore, the conclusions drawn from this analysis are applicable only to cohesionless base soil.

Logistic regression models have been fitted to the data by the method of maximum likelihood. Each such model gives the probability of filter malfunctioning on a function of a chosen set of explanatory variables.

Several statistics are used to evaluate the results of the analysis. The likelihood ratio index (ρ_o^2), the modified likelihood ratio index ($\bar{\rho}_o^2$) and the percent correctly predicted (PCP). Theoretical use of ρ_o^2 is appropriate for the comparison of nested models, whereas $\bar{\rho}_o^2$ for the comparison of non-nested models. PCP can be used in both cases, but it is not a very sensitive statistic. The highest values of these statistics over the models considered in the course of this study are $\rho_o^2 = 0.677$, $\bar{\rho}_o^2 = 0.660$ and PCP = 91.1(%).

Laboratory biases have been introduced into the analysis by using indicator variables. A stepwise version

of logistic regression has been used to choose the best model among a given set of nested models.

First, the conventional filter criteria have been evaluated by using stepwise regression. It has been found that DF15/DB85 is the most discriminating parameter among those employed in conventional filter criteria. Stepwise regression has been applied also to investigate the characteristics of each data set. The imporant finding concerning this analysis is that data sets [61], [75] and [82] behave very differently from other data sets. The fact that the experimental set-up for [75] and [82] is completely different from the other data sets is an apparent course for this behavior. Data set [61] is rather unreliable, due to the inclusion of many cohesive base soil cases. In order not to bias the results, data sets [61], [75] and [82] have been removed from the data base (see Table 3.1). The sample size has thus been reduced to 277.

An analysis has been made to improve the available filter criteria. Stepwise regression analysis, with many grain sizes of the base soil and the filter as candidate explanatory variables, produced two very important results (Analyses IV-1 & 2 in Table 3.6(a) and (b)).

(i) Only DF15 is significant for the filter. This means that DF15 represents the void characteristics of the filter.

(ii) DB95, DB90, DB85, DB70, DB50 and DB10 are selected for the base soil. The implication is that for filtering, what counts is the coarser portion of the base soil (larger than DB70).

These results agree with physical considerations in the previous chapters. The first result corresponds to the fact that the void size is highly correlated with small grain sizes, such as DF10 or DF15. The second result reflects the fact that the coarser particles of base soil play a major role in the self-healing filter formation. The effectiveness of the self-healing filter, which is important for the internal stability of the base soil, is also controlled by this portion of the base soil. From both statistical and physical considerations, it has been concluded that (DF15/DB85, DB95/DB75) is the best parameter combination to explain the phenomenon. The physical interpretation of these two parameters is as follows:

(i) DF15 represents the pore size of the filter, where DB85 is a grain size such that if DB85 is retained by the filter, the whole base becomes stable after the quick formation of a self-healing filter. Therefore, the ratio DF15/DB85 must be a good indicator of filter performance.

(ii) The ratio DB95/DB75 is the local average gradient of the grain size distribution, centered at DB85. Since the self-healing filter mainly consists of particles larger than DB85, the ratio DB95/DB75 is a measure of the separation (or gap) between the portions coarser and finer than DB85. The ratio is termed a self-healing index.

The data set from each laboratory has been plotted separately on the DF15/DB85 - DB95/DB75 plane in order to detect anomalous groups and outlier results. As a result of this analysis, data sets [40A], [41] and [55] have been found to possibly contain bias. The results from three different laboratories include non-stable filter cases with high DB95/DB75 ratio; the base-soil grain size distributions of these cases are very similar (see Fig. 3.23), implying that the result cannot be contributed to any laboratory bias, but is due to the nature of the base soil grain size distributions have been made.

Based on the above considerations, final anayses have been made with DF15/DB85, DB95/DB75, and the biases of [41] and [55] as explanatory variables. [40A] has been removed from the data base to avoid bias. The probability of filter malfunctioning can be calculated based

on this result:

$$P_f = \frac{e^{\lambda}}{1+e^{\lambda}}$$

where

$$\lambda = 1.60 \frac{DF15}{DB85} + 1.39 \frac{DB95}{DB75} - 14.75.$$

This result is also illustrated in Figs. 3.27 and 3.28. The border line (i.e., $P_f = 0.5$) between stable and nonstable filters can be obtained by setting $\lambda=0.0$:

$$\frac{DF15}{DB85} = 9.22 - 0.87 \frac{DB95}{DB75}.$$

The line is shown in Fig. 3.25.

An improved design criterion has been proposed which can account for the effect of DB95/DB75. It is proposed based on the condition that the proposed criterion should have the equal margin of safety against failure to that conventional Terzaghi's criterion (DF15/DB85 < 5) has. A band is proposed on the DF15/DB85 - DB95/DB75 plane of which the average is given by

$$\frac{DF15}{DB85} = 5.60 - 0.6 \frac{DB95}{DB75} .$$

The band is presented in Fig. 3.29. The wider spread of the band in the larger DB95/DB75 range is due to uncertainty caused by the scarceness of the experimental

data in this region; more experimental results are needed for the accurate prediction.

The findings in this chapter can be summarized as follows. DF15/DB85, the parameter, the conventional Terzaghi's criteria is based on the fundamental parameter that separates stable from nonstable filters. However, a second parameter DB95/DB75 is found to be significant. The second parameter gives information on the self-healing and the internal stability properties of the base soil. The implication is that the conventional filter criteria (DF15/DB85 < 5) is conservative for base soils with low DB95/DB75, but is unconservative for soils with high DB95/DB75, i.e., for soils with widely graded coarser portions. The improved filter criterion in Fig. 3.29 is based on the condition that safety should be the same as that provided by the conventional filter criteria in the case of uniform base soil.

Finally, one should emphasize the usefulness of a formal statistical analysis in this type of complex problems; the secondary parameter DB95/DB75 could not have been found easily without it.

Table 3.1 Basic Characteristics of the Data Base

Source	(a) Results				(b) Base Soil / Filter Combination									(c) DB10	
	Stable	Nonstable	Clogging	Total	EU/EU	EU/U	EU/G	U/EU	U/U	U/G	G/EU	G/U	G/G	<0.074	>0.074
Bertram [40A]	30	29	4	63	63	-	-	-	-	-	-	-	-	-	63
Hurley & Newton [40B]	13	9	-	22	-	-	-	15	6	1	-	-	-	-	22
U.S.C.E. [41]	8	4	1	13	-	4	9	-	-	-	-	-	-	-	13
U.S.C.E. [48]	23	4	-	27	-	4	2	-	4	7	-	4	6	-	27
U.S.C.E. [53]	11	-	1	12	4	-	2	-	-	1	4	-	1	3	9
Lund [49]	27	19	24	70	50	-	-	14	-	-	6	-	-	-	70
Leatherwood & Peterson [54]	9	-	4	13	12	-	-	1	-	-	-	-	-	-	13
Karpoff [55]	16	8	-	24	6	-	-	-	-	-	5	2	11	17	7
Kawakami et.al. [61]	57	20	25	102	23	14	9	8	8	-	15	16	9	45	57
Belyeshevskii et.al. [72]	11	2	-	13	-	-	-	1	3	9	-	-	-	-	13
Vaughan [75]	3	3	-	6	-	-	-	-	-	-	4	-	2	6	-
Vaughan & Soares [82]	7	6	2	15	9	1	5	-	-	-	-	-	-	15	-
Sherard et.al. [84]	9	5	6	20	10	9	1	-	-	-	-	-	-	-	20
Total	224	109	67	400	177	32	28	39	21	18	34	22	29	86	314
Total exclude [61],[75]&[82]	157	80	40	277	145	17	14	31	13	18	15	6	18	20	257

(Note) EU: Extremely Uniform ($U_0 < 2$), U: Uniform ($2 < U_0 < 4$), G: Graded ($4 < U_0$)

TABLE 3.2 MODELS USED IN BINARY RESPONSE REGRESSION

Model	Tolerance distribution $f(\underline{x}\ \underline{\beta})$	Cumulative distribution $F(\underline{x}\ \underline{\beta})$	Rationale(s)[+]
Logistic	$f(\underline{x}\ \underline{\beta}) = \frac{e^{\underline{x}\ \underline{\beta}}}{k[1+e^{\underline{x}\ \underline{\beta}}]^2}$	$P = \frac{e^{\underline{x}\ \underline{\beta}}}{1 + e^{\underline{x}\ \underline{\beta}}}$	Most common; simple sufficient statistics. numerically stable; related to discriminant analysis (Cox, [1966]).
Probit	Normal $N(\underline{x}\ \underline{\beta}, 1)$	$P = \Phi\ (\underline{x}\ \underline{\beta})$	Historical; assumes a normal distribution of individual tolerances.
Extreme Value	$f(\underline{x}\ \underline{\beta}) = \alpha\ \exp[\underline{x}\ \underline{\beta} - e^{\underline{x}\beta}]$	$P = 1 - \exp[-\exp(\underline{x}\beta)]$	Survival curve interpretaton; the hazard rate is $\exp(\underline{x}\ \underline{\beta})$. Also called complementary log-log or log hazard rate.

[+]Rationales are cited from DuMouchel & Waterhaux (1982).

Table 3.3 Prelimimary Analysis (Analyses I-1 & I-2)

Analysis I-1

Data: All data, N=400 (Stable 224, Nonstable 176)

Assumption: Clogging=Nonstable

Parameter candidates: DF15/DB85, DF50/DB50, DF15/DB15, DF60/DF10, DB60/DB10

Stopping criterion: Chi-square 1% significace level, Backward procedur

Parameters	$\hat{\beta}$	t	mean	variance
DF15/DB85	0.283	8.90	6.88	4.95
CONST.	-2.22	-9.03		

$\rho_0^2 = 0.225$, $\overline{\rho}_0^2 = 0.222$, PCP = 72.5 (%)

Analysis I-2

Data: All data, N=400 (Stable 291, Nonstable 109)

Assumption: Clogging=Stable

Parameter candidates: DF15/DB85, DF50/DB50, DF15/DB15, DF60/DF10, DB60/DB10

Stopping criterion: Chi-square 1% significace level, Backward procedur

Parameters	$\hat{\beta}$	t	mean	variance
DF15/DB85	0.234	7.81	6.88	4.95
CONST.	-2.82	-10.11		

$\rho_0^2 = 0.313$, $\overline{\rho}_0^2 = 0.309$, PCP = 79.0 (%)

Table 3.4 Regression on DF50/DB50 (Analysis I-3 & I-4)

Analysis I-3

Data: All data, N=400 (Stable 224, Nonstable 176)

Assumption: Clogging=Nonstable

No stepwise regression

Parameters	$\hat{\beta}$	t	mean	variance
DF50/DB50	0.0317	4.07		
CONST.	-0.860	0.176		

$\rho_o^2 = 0.051$, $\bar{\rho}_o^2 = 0.047$, PCP = 57.8 (%)

Analysis I-4

Data: All data, N=400 (Stable 291, Nonstable 109)

Assumption: Clogging=Stable

No stepwise regression analysis

Parameters	$\hat{\beta}$	t	mean	variance
DF50/DB50	0.0279	3.92		
CONST.	-1.56	-8.38		

$\rho_o^2 = 0.191$, $\bar{\rho}_o^2 = 0.181$, PCP = 71.8 (%)

Table 3.5(a) Analysis on laboratory difference (Anaysis II-1)

Analysis II-1

Data: All data, N=400 (Stable 224, Nonstable 176)

Assumption: Clogging=Nonstable

Parameter candidates: DF15/DB85, [40A], [40B], [49], [54], [55], [61], [72], [75], [82], [84]

Stopping criterion: Chi-square 1% significace level, Backward procedur

Parameters	$\hat{\beta}$	t	mean	variance
DF15/DB85	0.760	9.07	6.88	4.95
[40A]	-5.21	-6.85		
[49]	-2.15	-4.31		
[75]	3.74	4.11		
[82]	-6.63	-5.82		
[84]	-2.58	-4.02		
CONST.	-3.86	-9.71		

$\rho_o^2 = 0.390$, $\bar{\rho}_o^2 = 0.378$, PCP = 82.5 (%)

Table 3.5(b) Analysis on laboratory difference (Anaysis II-2)

Analysis II-2

Data: All data, N=400 (Stable 291, Nonstable 109)

Assumption: Clogging=Stable

Parameter candidates: DF15/DB85, [40A], [40B], [49], [54], [55], [61], [72], [75], [82], [84]

Stopping criterion: Chi-square 1% significace level, Backward procedur

Parameters	$\hat{\beta}$	t	mean	variance
DF15/DB85	0.425	8.20	6.88	4.95
[40A]	-1.54	-3.24		
[40B]	1.73	3.38		
[49]	-1.30	-3.06		
[75]	3.77	4.17		
[82]	-3.17	-3.42		
CONST.	-3.84	-10.03		

$\rho_o^2 = 0.391$, $\bar{\rho}_o^2 = 0.378$, PCP = 83.8 (%)

Table 3.6(a) Analysis of significant grain sizes (Analysis III-1)

Analysis III-1

Data: All data except [61], [75] and [82]
N=277 (Stable 157, Nonstable 120)

Assumption: Clogging=Nonstable

Parameter candidates: log DB(10,15,30,50,60,70,80,85,90,95),
log DF(5,10,15,20,30,50,70)

Stopping criterion: Chi-square 1% significace level,
Backward procedur

Parameters	$\hat{\beta}$	t	mean	variance
log DF15	5.81	7.29	0.838	0.065
log DB10	-8.21	-3.70	-1.95	1.02
log DB50	33.0	3.77	-1.39	0.947
log DB70	-33.6	-3.84	-1.13	1.07
log DB85	26.8	3.44	-0.893	1.24
log DB90	-41.6	-3.21	-0.770	1.32
log DB95	19.1	2.83	-0.631	1.41
CINST.	-10.9	-6.73		

$\rho_o^2 = 0.462$, $\bar{\rho}_o^2 = 0.441$, PCP = 84.1 (%)

Table 3.6(b) Analysis of significant grain sizes (Analysis III-2)

Analysis III-2

Data: All data except [61], [75] and [82]
N=277 (Stable 197, Nonstable 80)

Assumption: Clogging=Stable

Parameter candidates: log DB(10,15,30,50,60,70,80,85,90,95),
log DF(5,10,15,20,30,50,70)

Stopping criterion: Chi-square 1% significace level,
Backward procedur

Parameters	$\hat{\beta}$	t	mean	variance
log DF15	7.63	7.11	0.838	0.065
log DB10	-8.67	-3.56	-1.95	1.02
log DB50	38.1	3.87	-1.39	0.947
log DB70	-46.9	-4.55	-1.13	1.07
log DB85	42.0	4.07	-0.893	1.24
log DB90	-54.5	-3.41	-0.770	1.32
log DB95	23.2	2.86	-0.631	1.41
CINST.	-17.2	-7.15		

$\rho_o^2 = 0.581$, $\bar{\rho}_o^2 = 0.560$, PCP = 86.6 (%)

Table 3.6(c) Analysis of significant grain sizes (Analysis III-3)

Analysis III-3

Data: All data except [61], [75] and [82]
N=277 (Stable 157, Nonstable 120)

Assumption: Clogging=Nonstable

Parameter candidates: DF30/DF15, DF50/DF15, DF60/DF15, DF80/DF15, DB10/DF15, DB30/DF15, DB50/DF15, DB60/DF15, DB70/DF15, DB80/DF15, DB85/DF15, DB90/DF15, DB95/DF15, DB99/DF15

Stopping criterion: Chi-square 1% significace level, Backward procedur

Parameters	$\hat{\beta}$	t	mean	variance
DB95/DF15	163.3	5.06	0.476	1.33
DB90/DF15	-360.9	-5.13	0.378	0.739
DB85/DF15	148.2	4.12	0.314	0.453
DB60/DF15	-678.5	-4.11	0.176	0.0603
DB50/DF15	1190.7	4.25	0.147	0.027
DB30/DF15	-522.3	-4.34	0.112	0.0117
DF80/DF15	-1.52	-3.46	3.60	29.9
DF30/DF15	9.80	3.25	1.32	0.272
CONST.	-3.00	-1.20		

$\rho_o^2 = 0.467$, $\bar{\rho}_o^2 = 0.443$, PCP = 85.2 (%)

Table 3.6(d) Analysis of significant grain sizes (Analysis III-4)

Analysis III-4

Data: All data except [61], [75] and [82]
N=277 (Stable 197, Nonstable 80)

Assumption: Clogging=Stable

Parameter candidates: DF30/DF15, DF50/DF15, DF60/DF15, DF80/DF15, DB10/DF15, DB30/DF15, DB50/DF15, DB60/DF15, DB70/DF15, DB80/DF15, DB85/DF15, DB90/DF15, DB95/DF15, DB99/DF15

Stopping criterion: Chi-square 1% significace level, Backward procedur

Parameters	$\hat{\beta}$	t	mean	variance
DB90/DF15	-171.9	-4.46	0.378	0.739
DB85/DF15	620.3	4.62	0.314	0.453
DB80/DF15	-623.9	-4.59	0.272	0.295
DB50/DF15	249.6	3.42	0.147	0.027
DB10/DF15	-161.9	4.08	0.086	0.0072
CONST.	6.50	6.59		

$\rho_o^2 = 0.562$, $\bar{\rho}_o^2 = 0.547$, PCP = 86.6 (%)

Table 3.7 Analysis of significant grain size ratios (Analysis IV-1)

Analysis IV-1

Data: All data except [61], [75] and [82]
N=277 (Stable 157, Nonstable 120)

Assumption: Clogging=Nonstable

Parameter candidates:
DF15/DB85, DB95/DB90, DB95/DB85, DB95/DB80
DB95/DB75, DB90/DB80, DB90/DB70, DB90/DB50
DB85/DB75, DB85/DB70, DB85/DB60, DB85/DB50
DB85/DB10, DB80/DB50, DB80/DB10, DB50/DB30
DB50/DB10, DB70/DB50, DB70/DB10, DF80/DF15
DF30/DF15, DF15/DB50, DF15/DB95, DF15/DB75

Stopping criterion: Chi-square 1% significace level,
Forward procedur

(a) The best combination selected by the procedure

Parameters	$\hat{\beta}$	t	mean	variance
DF15/DB85	0.572	7.99	7.48	21.5
DB95/DB90	3.56	3.88	1.17	0.040
CONST.	-8.84	-5.90		

$\rho_o^2 = 0.396$, $\bar{\rho}_o^2 = 0.388$, PCP = 83.8 (%)

(b) The best combination by three parameters

Parameters	β	t	mean	variance
DF15/DB85	0.628	7.85	7.48	21.53
DB95/DB90	17.53	3.05	1.17	0.040
DB95/DB85	-6.00	-2.49	1.37	0.201
CONST.	-17.42	-4.46		

$\rho_o^2 = 0.412$, $\bar{\rho}_o^2 = 0.401$, PCP = 84.5 (%)

(C) Some of other best combinations by two parameters

	Parameters	LR		PCP
1	DF15/DB85, DB95/DB90	-116.04	0.388	83.75
2	DF15/DB85, DB85/DB75	-117.03	0.383	83.03
3	DF15/DB85, DB95/DB80	-117.24	0.382	83.39
4	DF15/DB85, DB95/DB75	-117.28	0.381	84.12
5	DF15/DB85, DB85/DB70	-117.42	0.381	82.67
6	DF15/DB85, DB95/DB85	-117.64	0.380	83.03
7	DF15/DB85, DB90/DB80	-117.78	0.379	83.03
8	DF15/DB85, DB90/DB70	-117.80	0.379	83.03

(d) DF15/DB85, DB95/DB75 Model

Parameter	$\hat{\beta}$	t	mean	variance
DF15/DB85	0.543	8.06	7.48	21.53
DB95/DB75	0.563	3.66	1.75	1.16
CONST.	-5.44	-7.36		

$\rho_o^2 = 0.389$, $\bar{\rho}_o^2 = 0.381$, PCP = 84.1 (%)

Table 3.8 Analysis of significant grain size ratios (Analysis IV-2)

Analysis IV-1

Data: All data except [61], [75] and [82]
N=277 (Stable 197, Nonstable 80)

Assumption: Clogging=Stable

Parameter candidates:
DF15/DB85, DB95/DB90, DB95/DB85, DB95/DB80
DB95/DB75, DB90/DB80, DB90/DB70, DB90/DB50
DB85/DB75, DB85/DB70, DB85/DB60, DB85/DB50
DB85/DB10, DB80/DB50, DB80/DB10, DB50/DB30
DB50/DB10, DB70/DB50, DB70/DB10, DF80/DF15
DF30/DF15, DF15/DB50, DF15/DB95, DF15/DB75

Stopping criterion: Chi-square 1% significace level,
Forward procedur

Parameters	$\hat{\beta}$	t	mean	variance
DF15/DB85	0.736	7.67	7.48	21.5
DB85/DB75	35.4	4.34	1.20	0.072
DB90/DB70	-13.68	-4.27	1.54	0.541
DB95/DB90	10.65	3.39	1.17	0.040
CONST.	-41.04	-5.60		

$\rho_o^2 = 0.539$, $\bar{\rho}_o^2 = 0.526$, PCP = 85.6 (%)

Analysis IV-2'

Parameters	$\hat{\beta}$	t	mean	variance
DF15/DB85	0.566	7.63	7.48	21.53
DB95/DB75	0.933	5.20	1.75	1.16
CONST.	-7.44	-7.80		

$\rho_o^2 = 0.470$, $\bar{\rho}_o^2 = 0.463$, PCP = 82.7 (%)

Table 3.9 Final Analysis: DF15/DB85-DB95/DB75 (Analysis V)

Analysis V

Data: All data except [40A], [61], [75] and [82]
N=214 (Stable 131, Nonstable 83)

Assumption: Clogging=Nonstable. For [54], "clogging" is corrected to "stable" (4 cases).

No stepwise regression

Parameters	$\hat{\beta}$	t	mean	variance
DF15/DB85	1.60	6.09	6.12	16.55
DB95/DB75	1.39	4.55	1.95	1.32
[41]	3.63	3.46		
[55]	4.54	3.51		
CONST.	-14.75	-5.91		

$\rho_o^2 = 0.677$, $\bar{\rho}_o^2 = 0.660$, PCP = 90.7 (%)

Table 3.10 Final Analysis: log(DF15/DB85)-DB95/DB75 (Analysis VI)

Analysis VI

Data: All data except [40A], [61], [75] and [82]
N=214 (Stable 131, Nonstable 83)

Assumption: Clogging=Nonstable. For [54], "clogging" is corrected to "stable" (4 cases).

No stepwise regression

Parameters	$\hat{\beta}$	t	mean	variance
LOG(DF15/DB85)	23.15	6.01	0.663	0.145
DB95/DB75	1.37	4.45	1.95	1.32
[41]	3.37	3.20		
[55]	4.90	3.45		
CONST.	-22.68	-5.89		

$\rho_o^2 = 0.660$, $\bar{\rho}_o^2 = 0.644$, PCP = 91.1 (%)

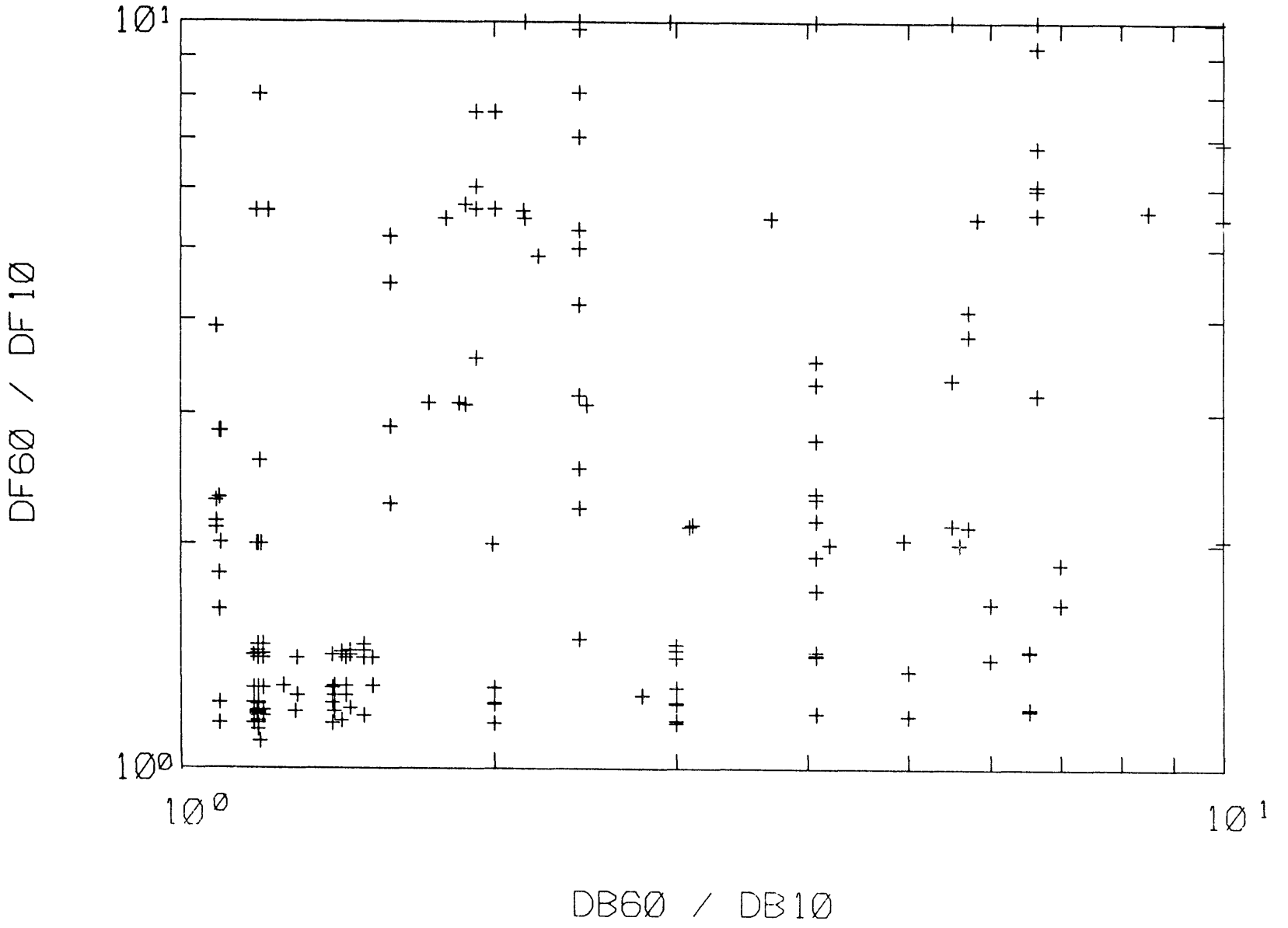

Fig. 3.1 DB60/DB10 vs. DF60/DF10 for all the Data except [61], [75] and [82] (N=277)

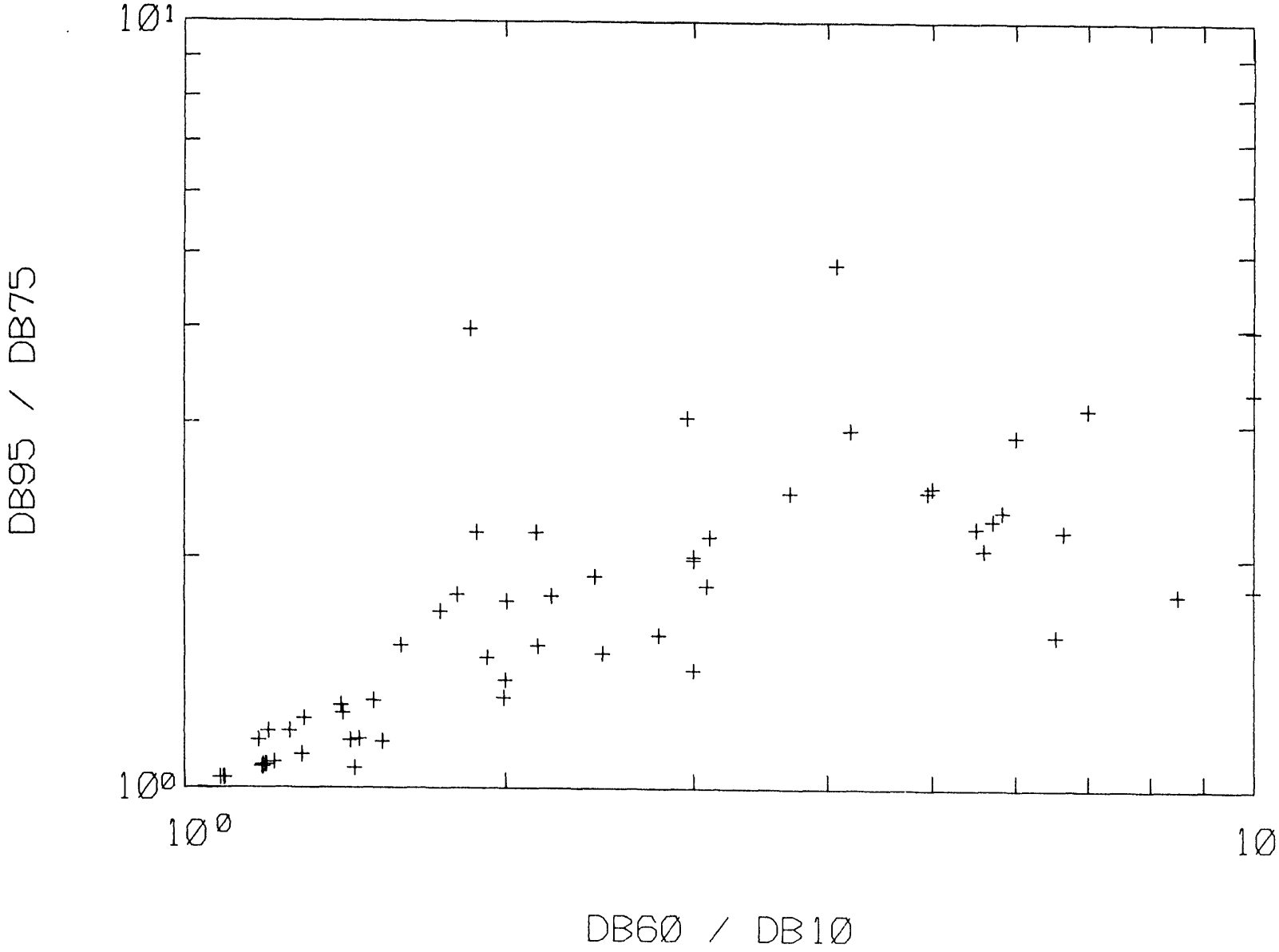

Fig. 3.2 DB60/DB10 vs. DB95/DB75 for all the Data except [61], [75] and [82] (N=277)

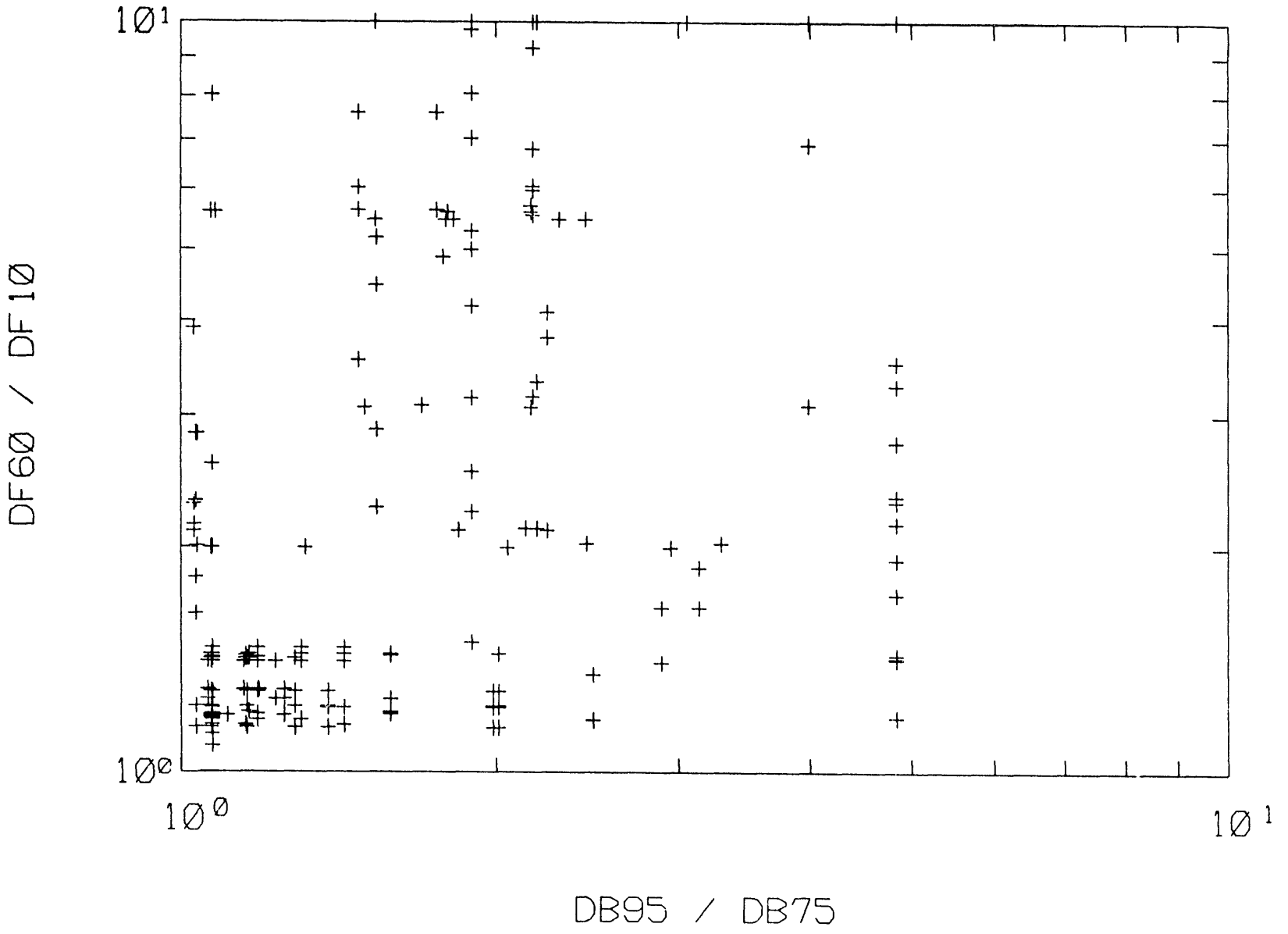

Fig. 3.3 DB95/DB75 vs. DF60/DF10 for all the Data except [61], [75] and [82] (N=277)

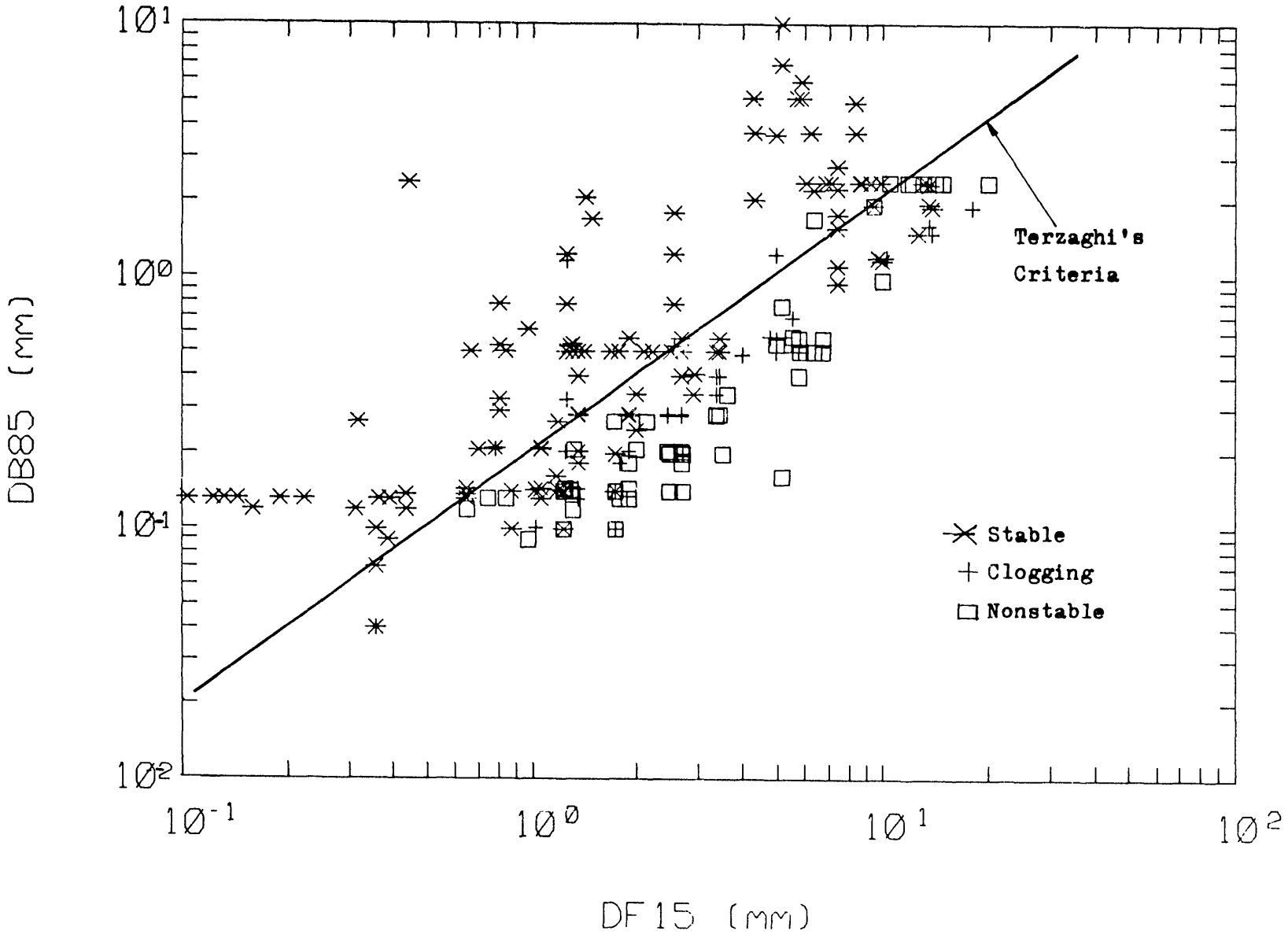

Fig. 3.4 DF15 vs. DB85 for all the Data except [61], [75] and [82] (N=277)

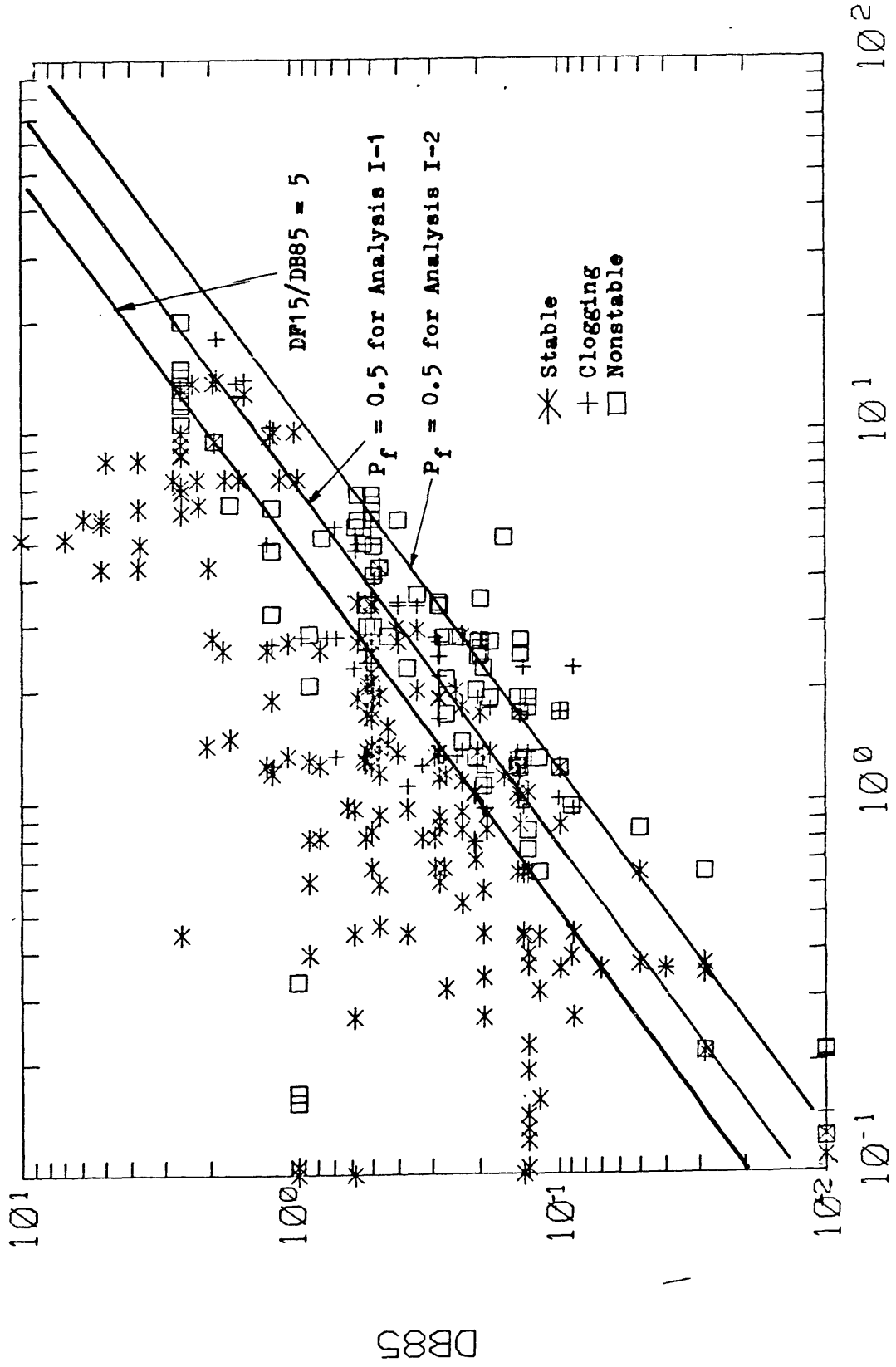

Fig. 3.5 DF15 vs. DB85 for all the data (N=400)

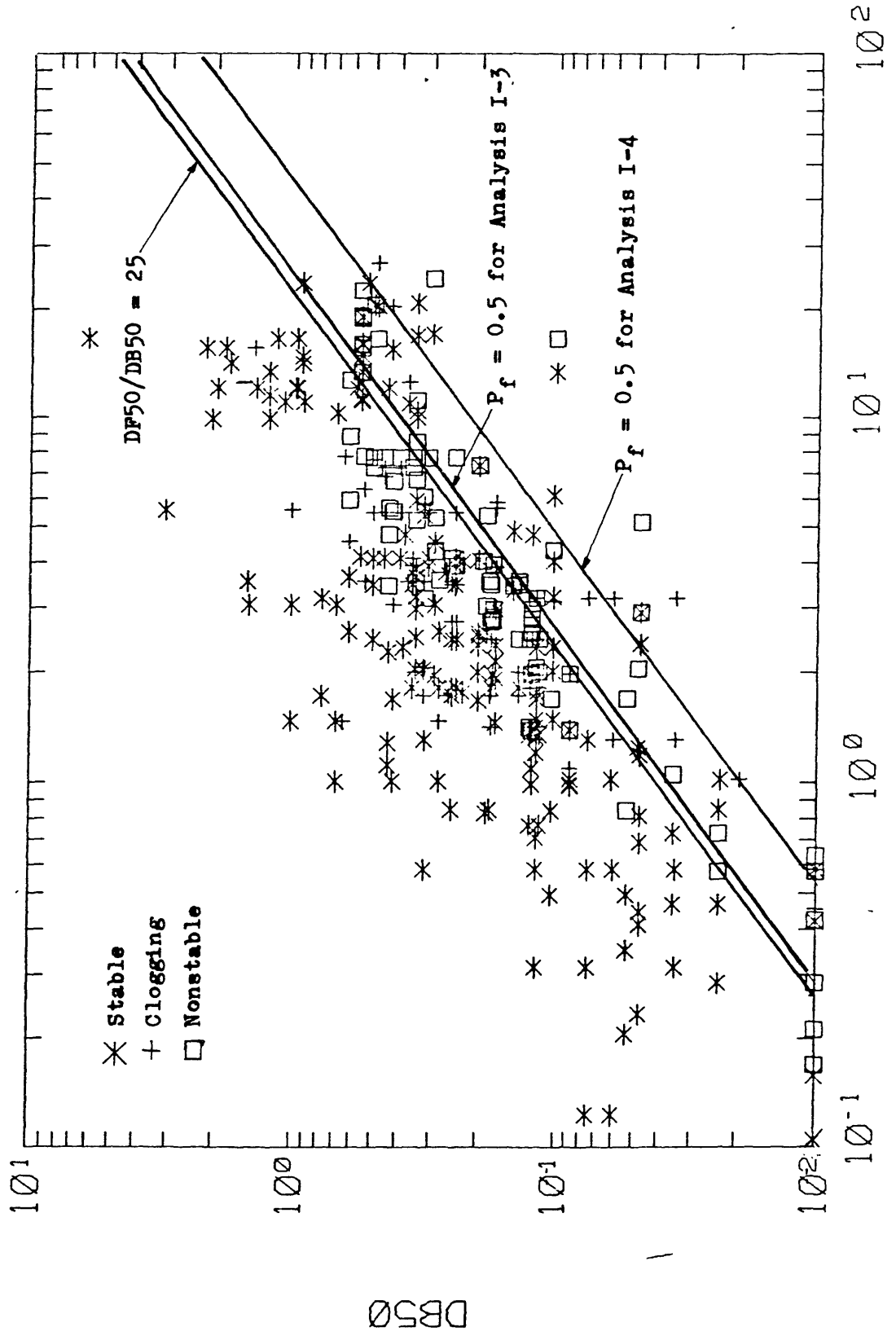

Fig. 3.6 DF50 vs. DB50 for all the Data (N=400)

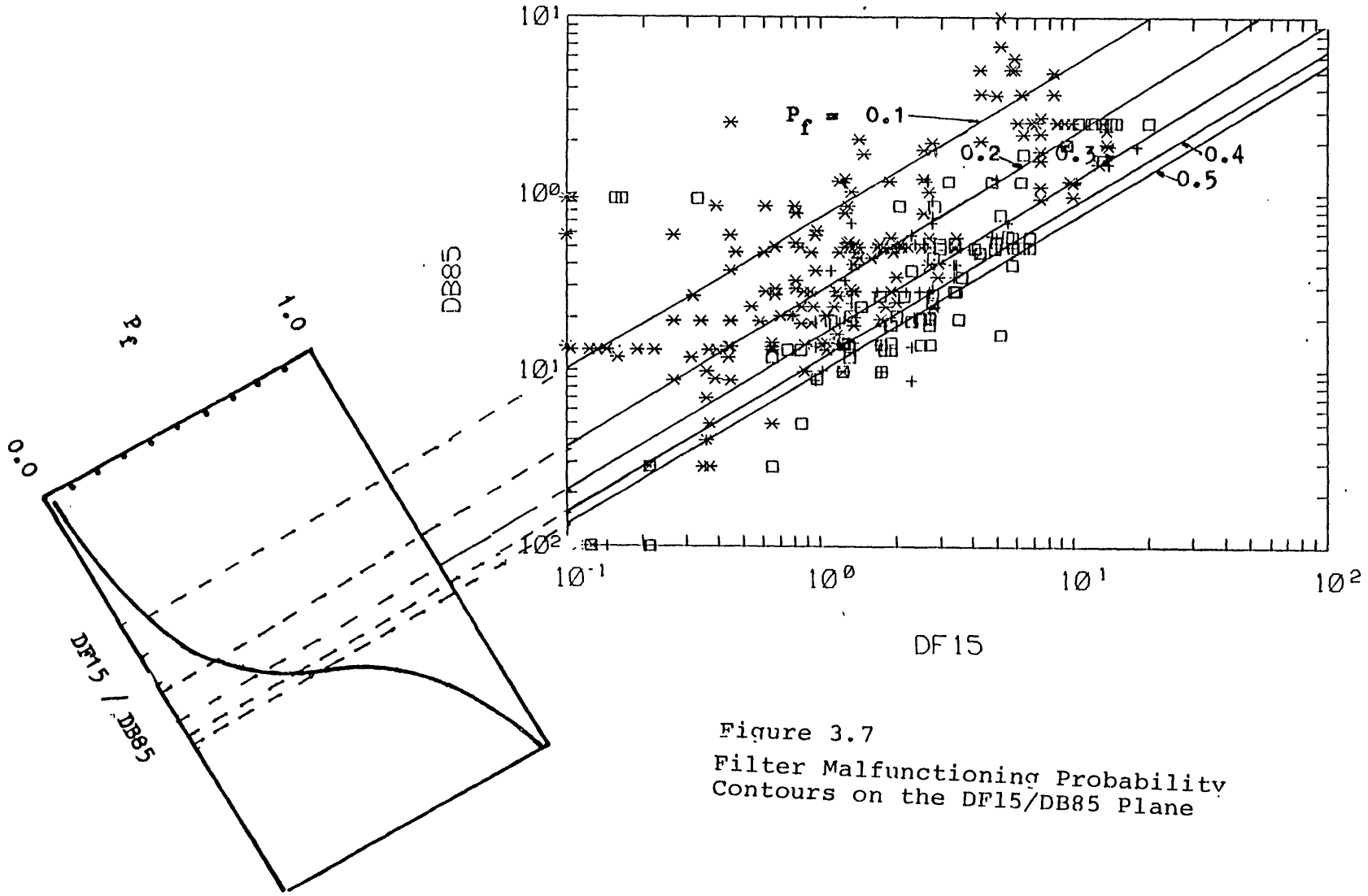

Figure 3.7
Filter Malfunctioning Probability
Contours on the DF15/DB85 Plane

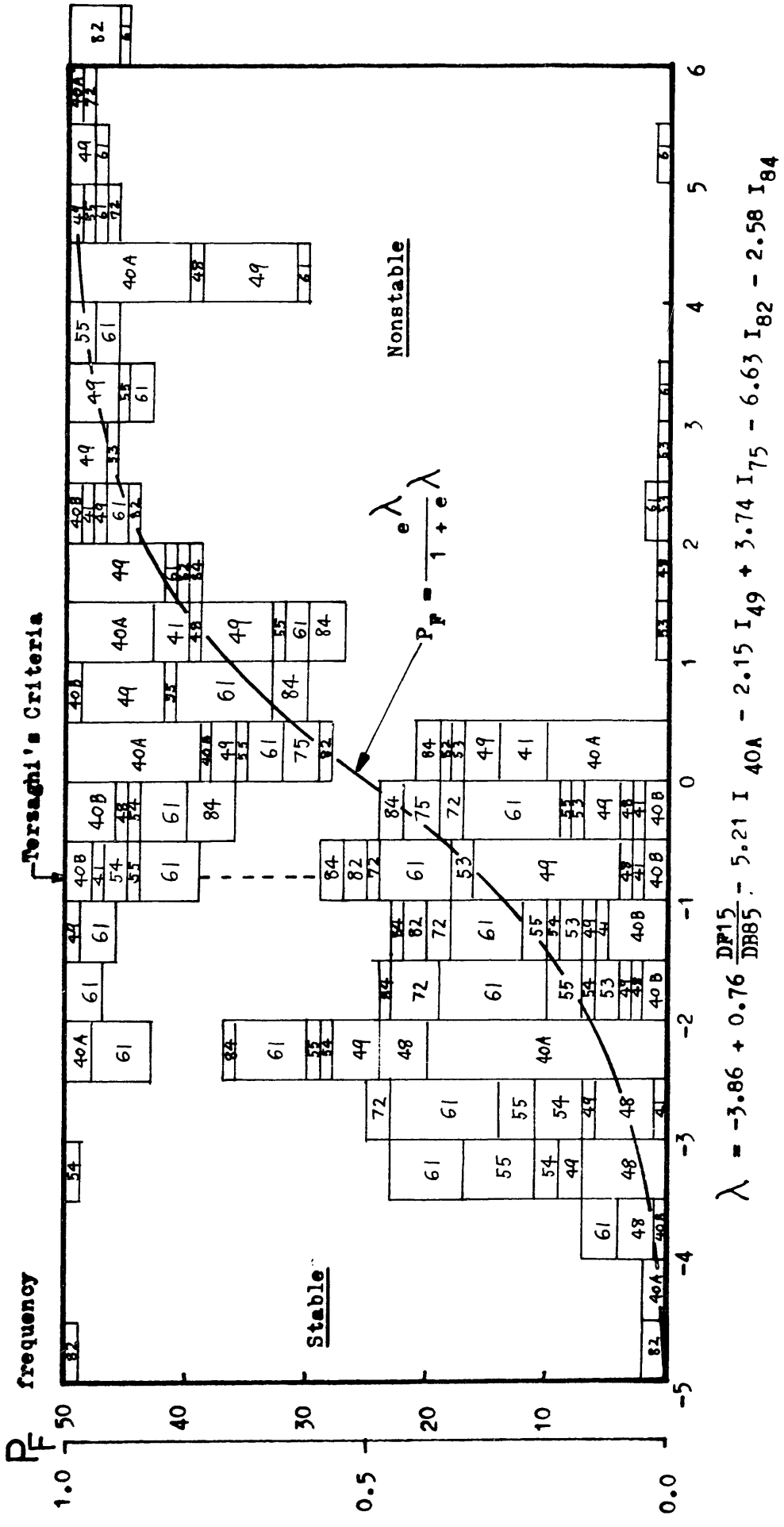

Fig. 3.8 (a) Result of Analysis II-1

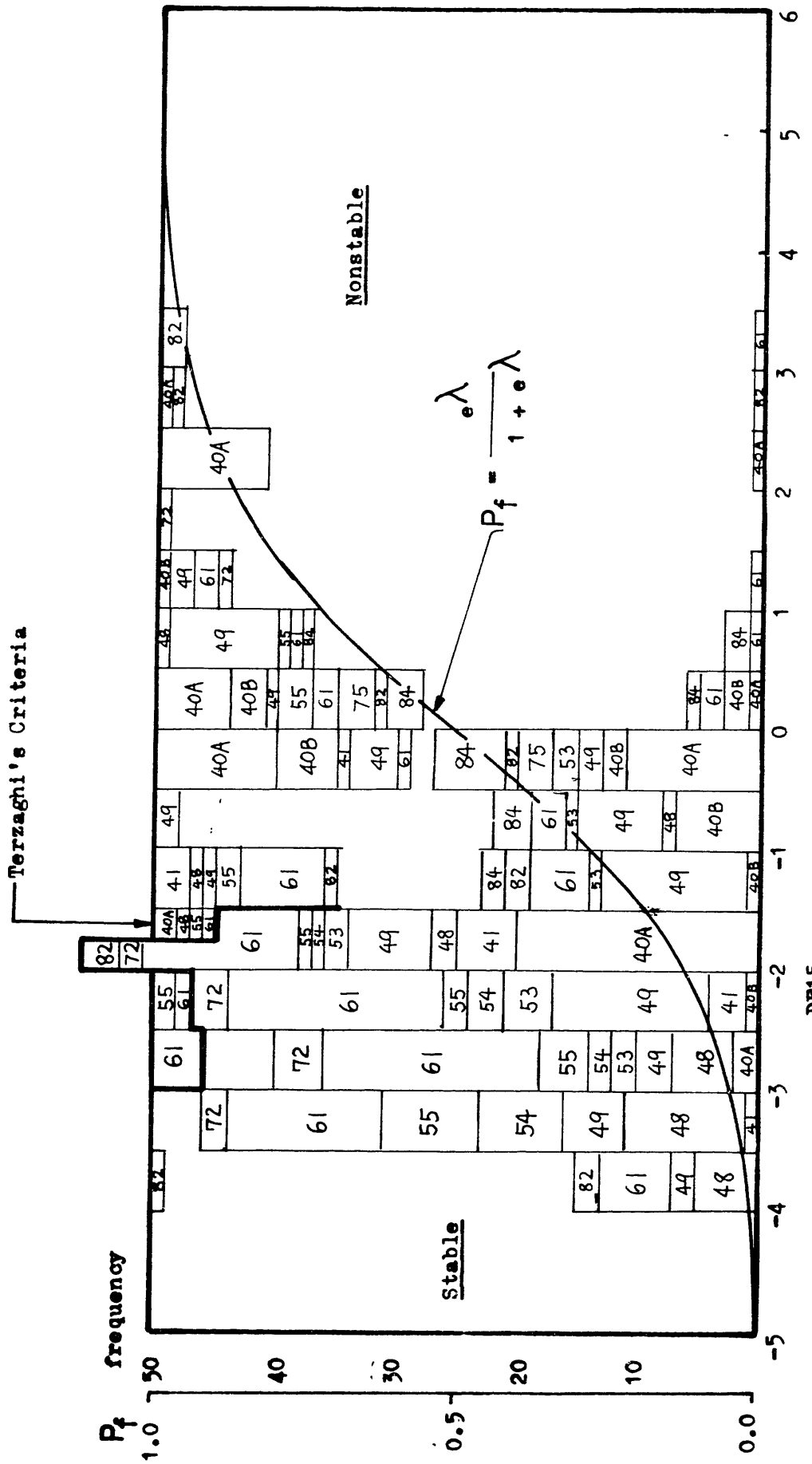

Fig. 3.8 (b) Result of Analysis II-2

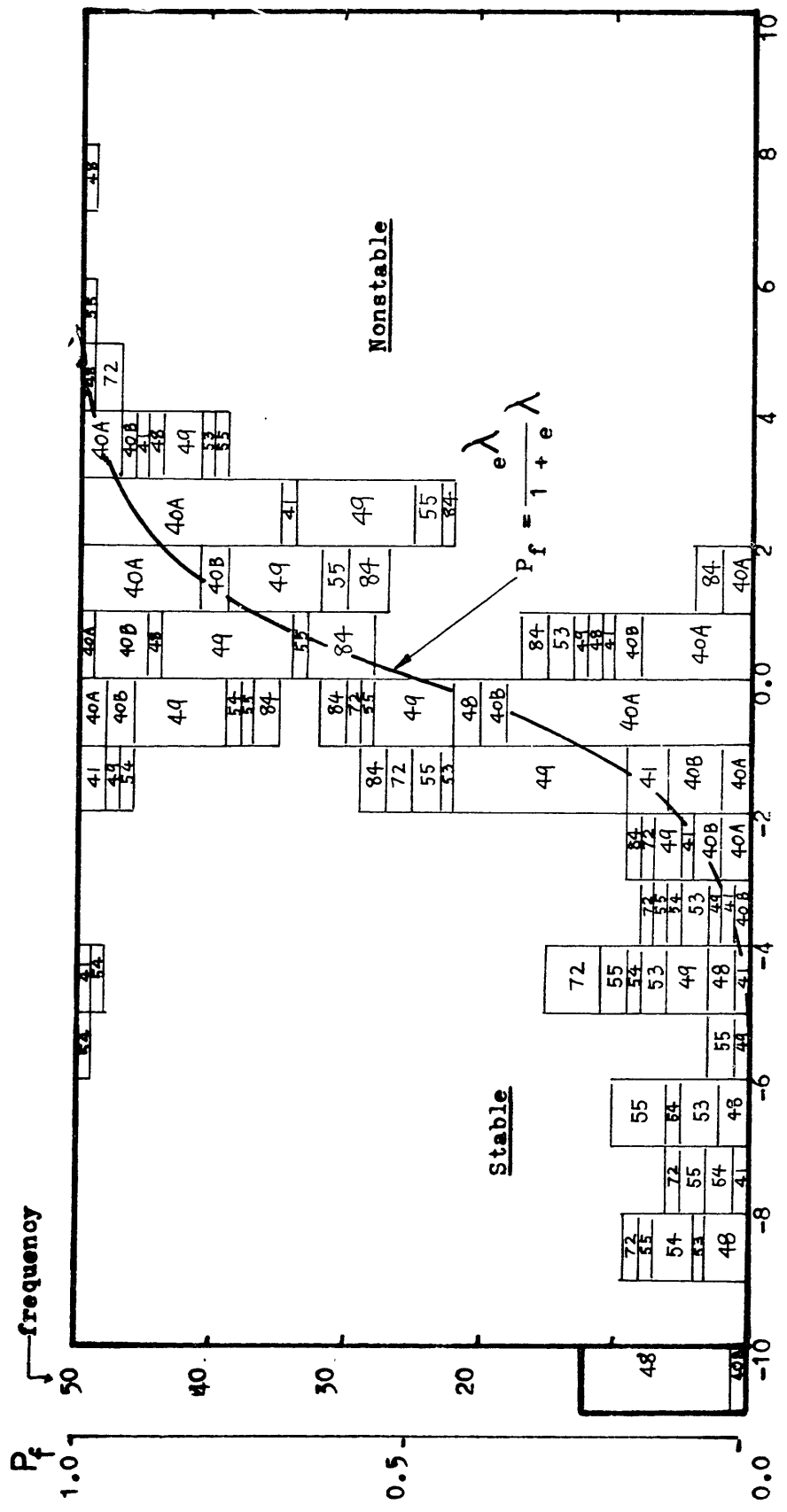

$\lambda = -10.9 + 5.81 \log DF15 - 8.21 \log DB10 + 33.0 \log DB50 - 33.6 \log DB90 + 26.8 \log DB85 - 41.6 \log DB90 + 19.1 \log DB95$

Fig. 3.9 (a) Result of Analysis III-1

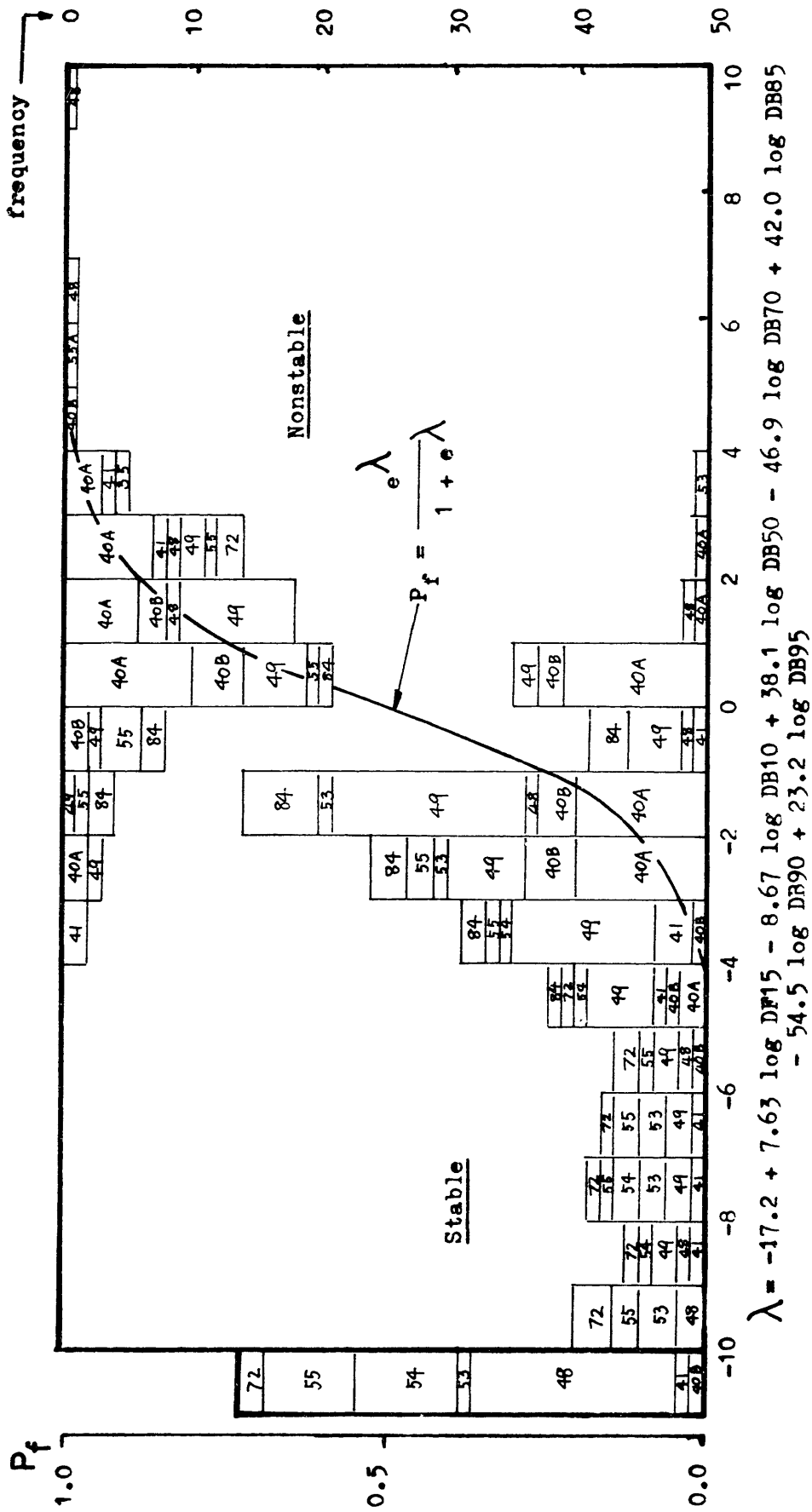

Fig. 3.9 (b) Result of Analysis III-2

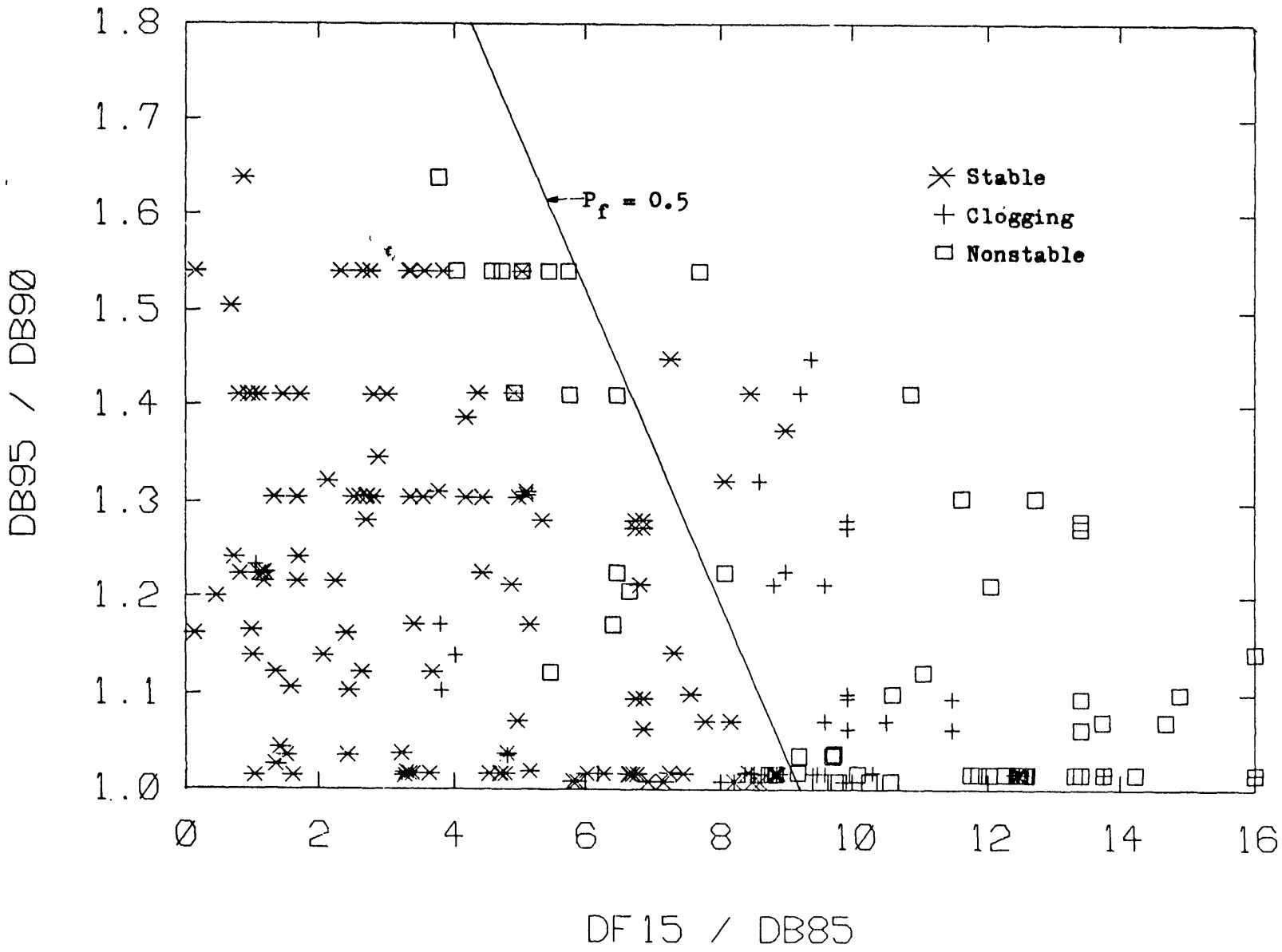

Fig. 3.10 DF15/DB85 vs. DB95/DB90 for all the Data except [61], [75] & [82] (N=277) and P_f = 0.5 line

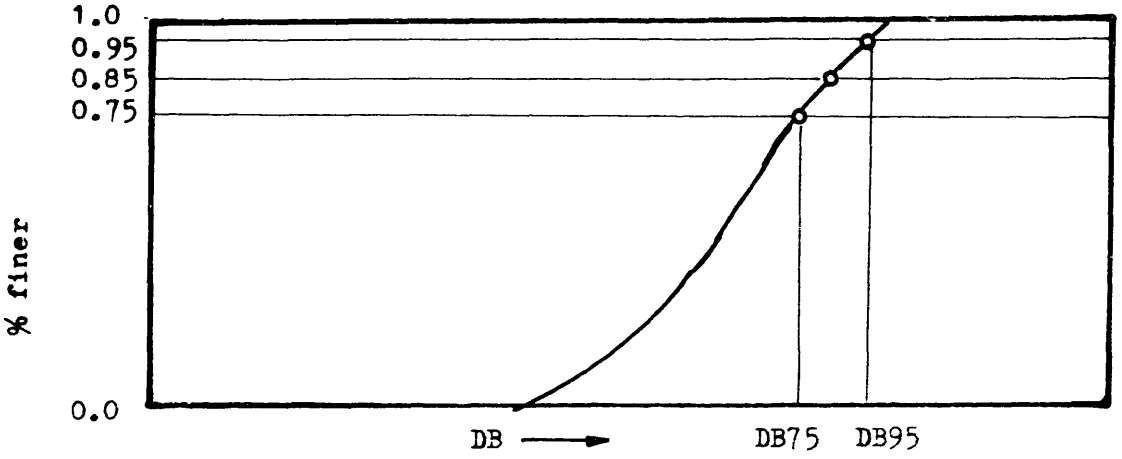

(a) An Example of Smaller DB95/DB75

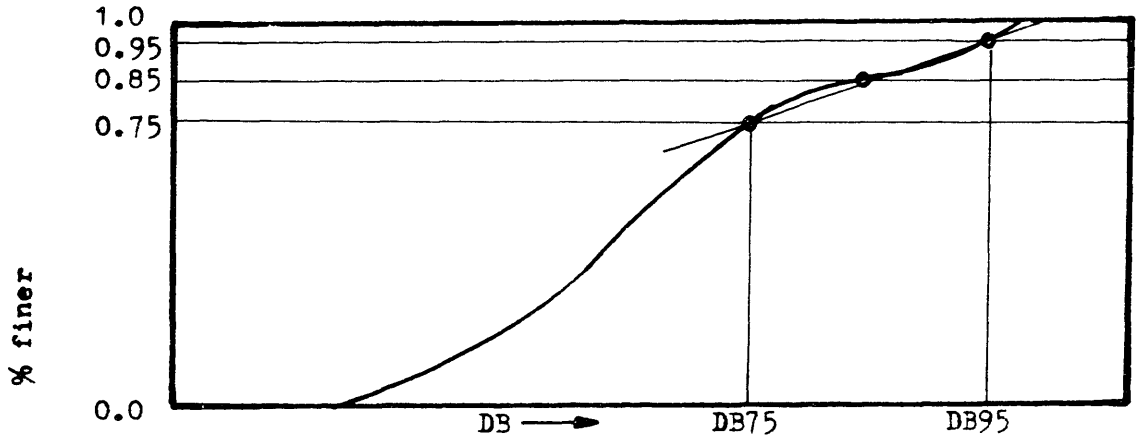

(b) An Example of Larger DB95/DB75

Fig. 3.11 Physical Interpretation of DB95/DB75

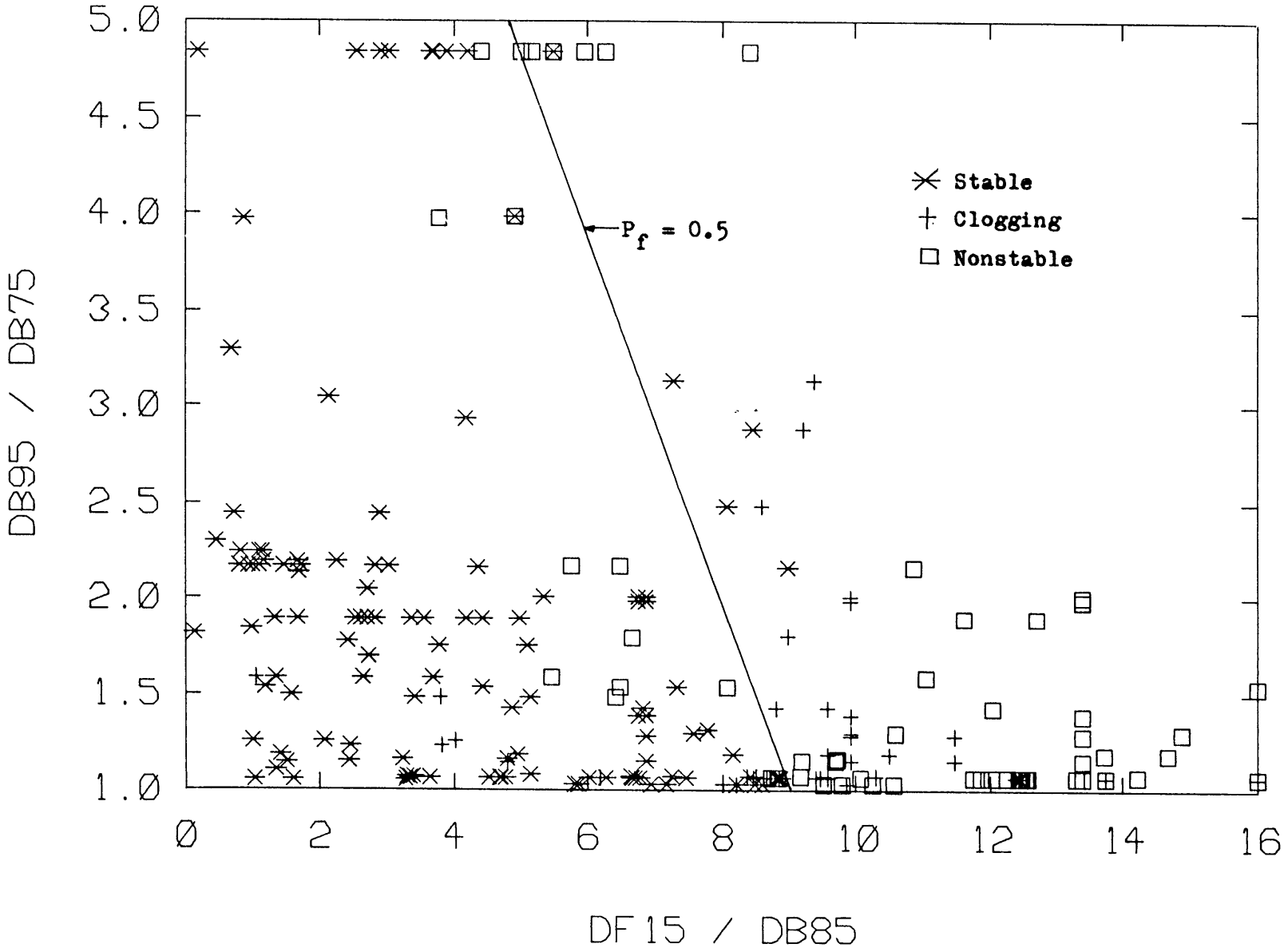

Fig. 3.12 DF15/DB85 vs. DB95/DB75 for all the Data except [61], [75] & [82] (N=277) and P_f = 0.5 line

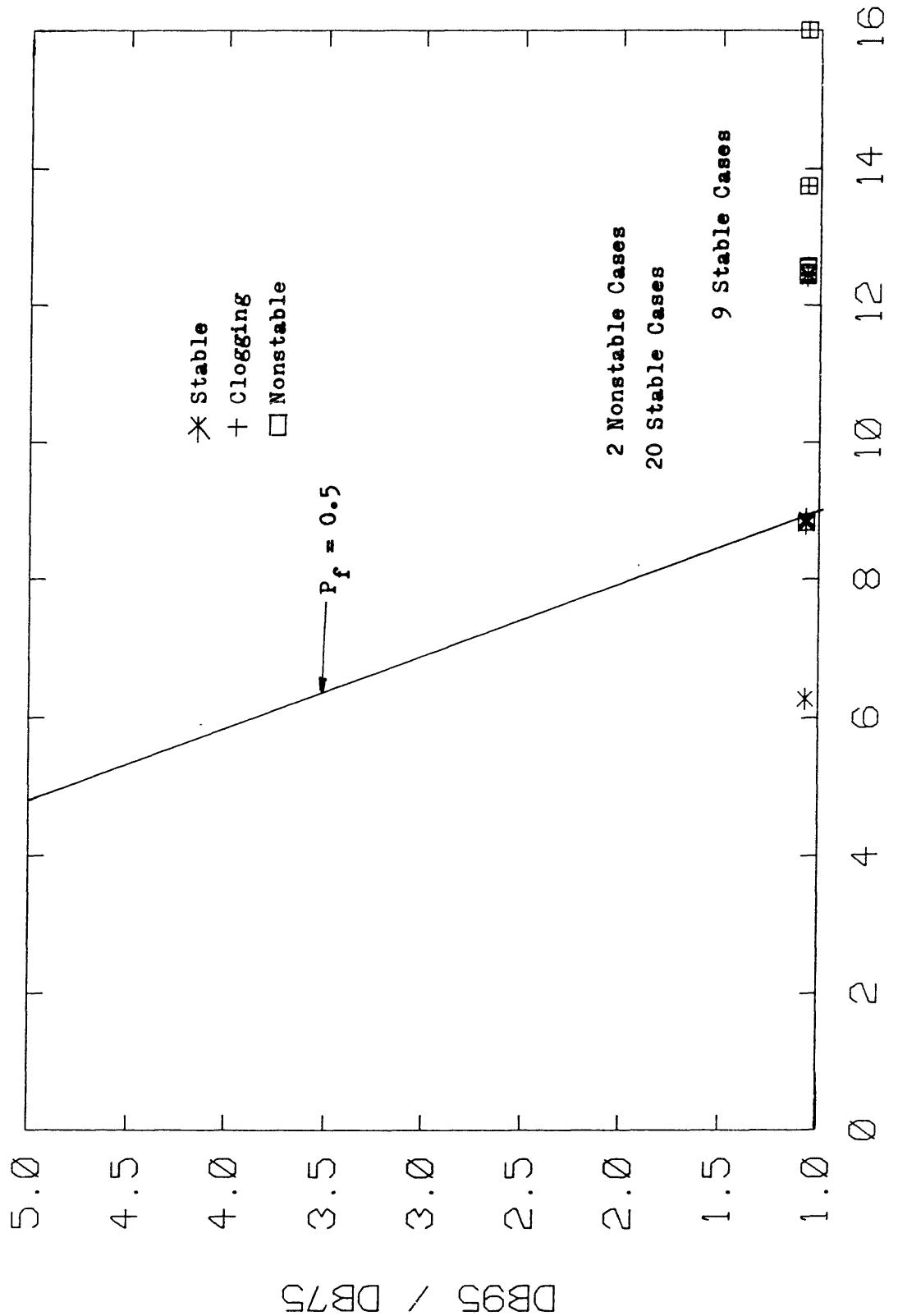

Fig. 3.13 DF15/DB85 vs. DB95/DB75 for [40A]

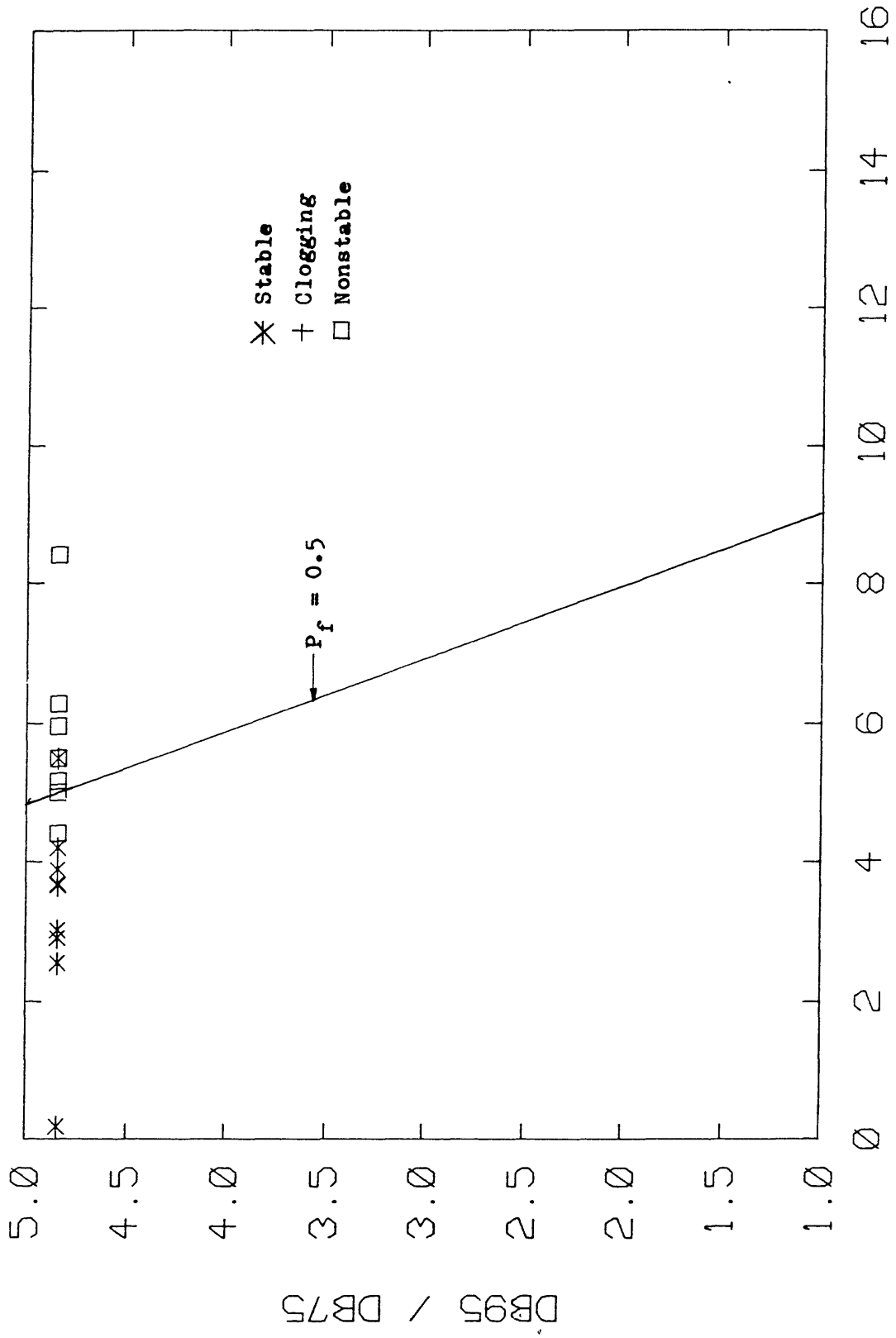

Fig. 3.14 DF15/DB85 vs. DB95/DB75 for [40B]

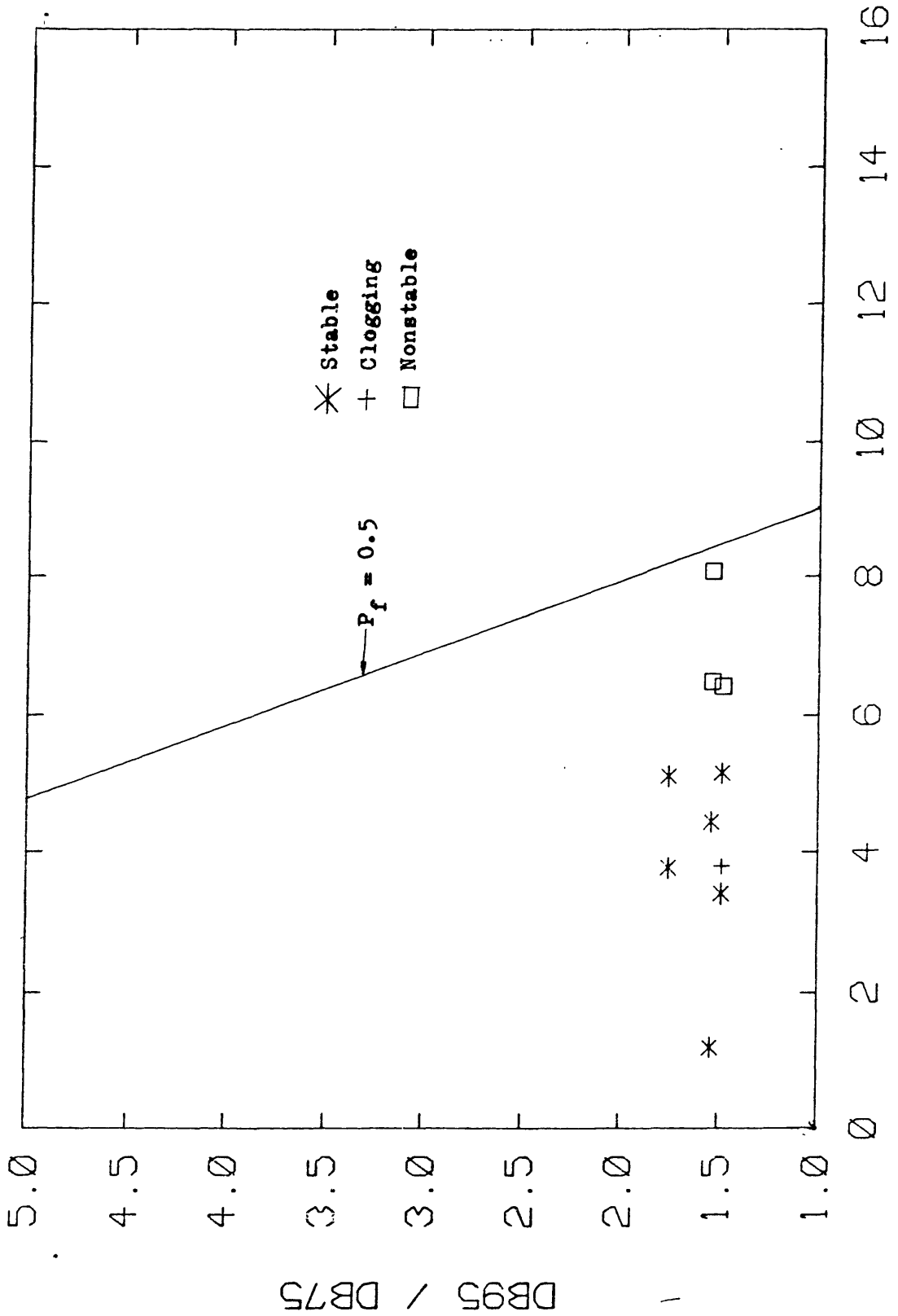

Fig. 3.15 DF15/DB85 vs. DB95/DB75 for [41]

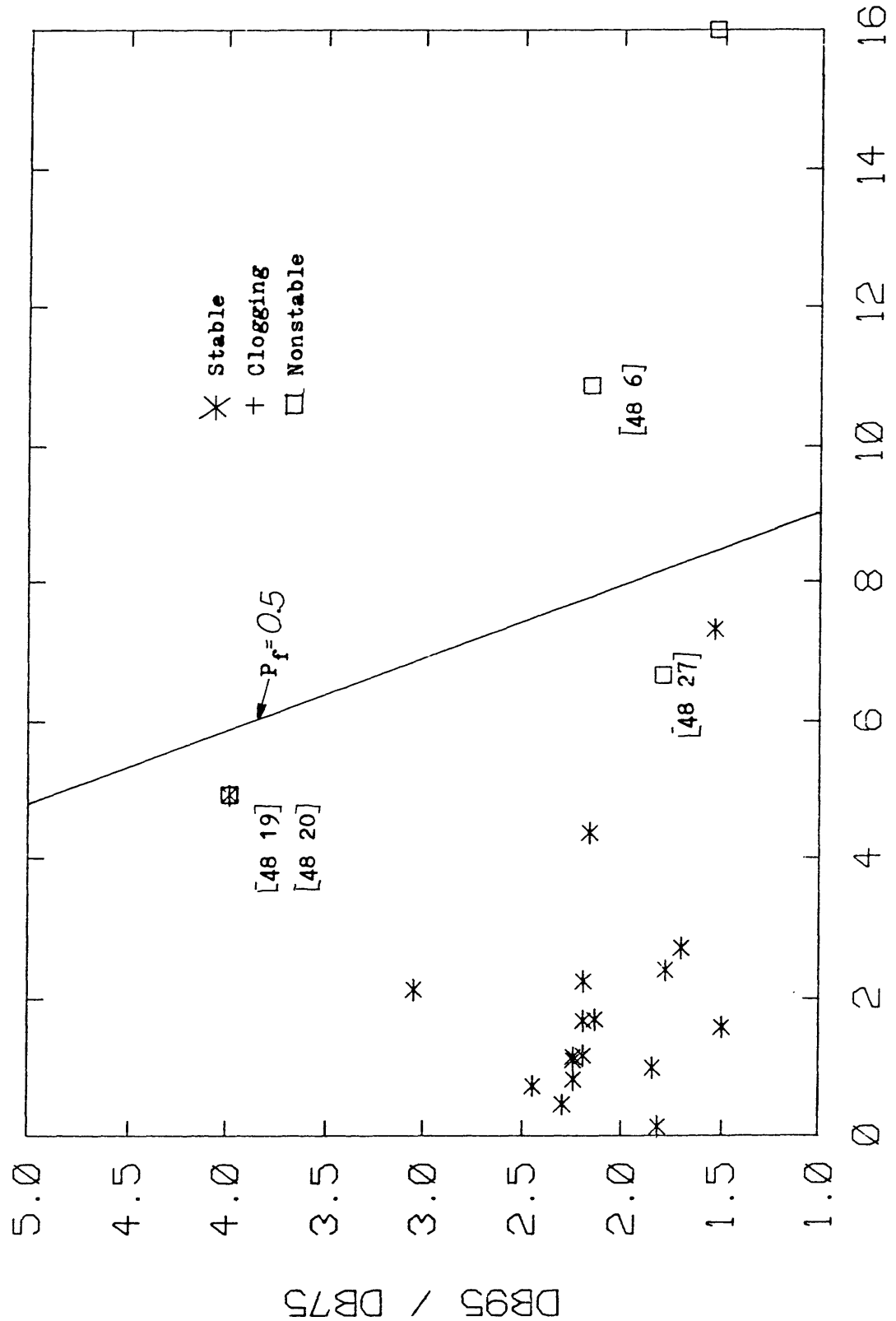

Fig. 3.16 DF15/DB85 vs. DB95/DB75 for [48]

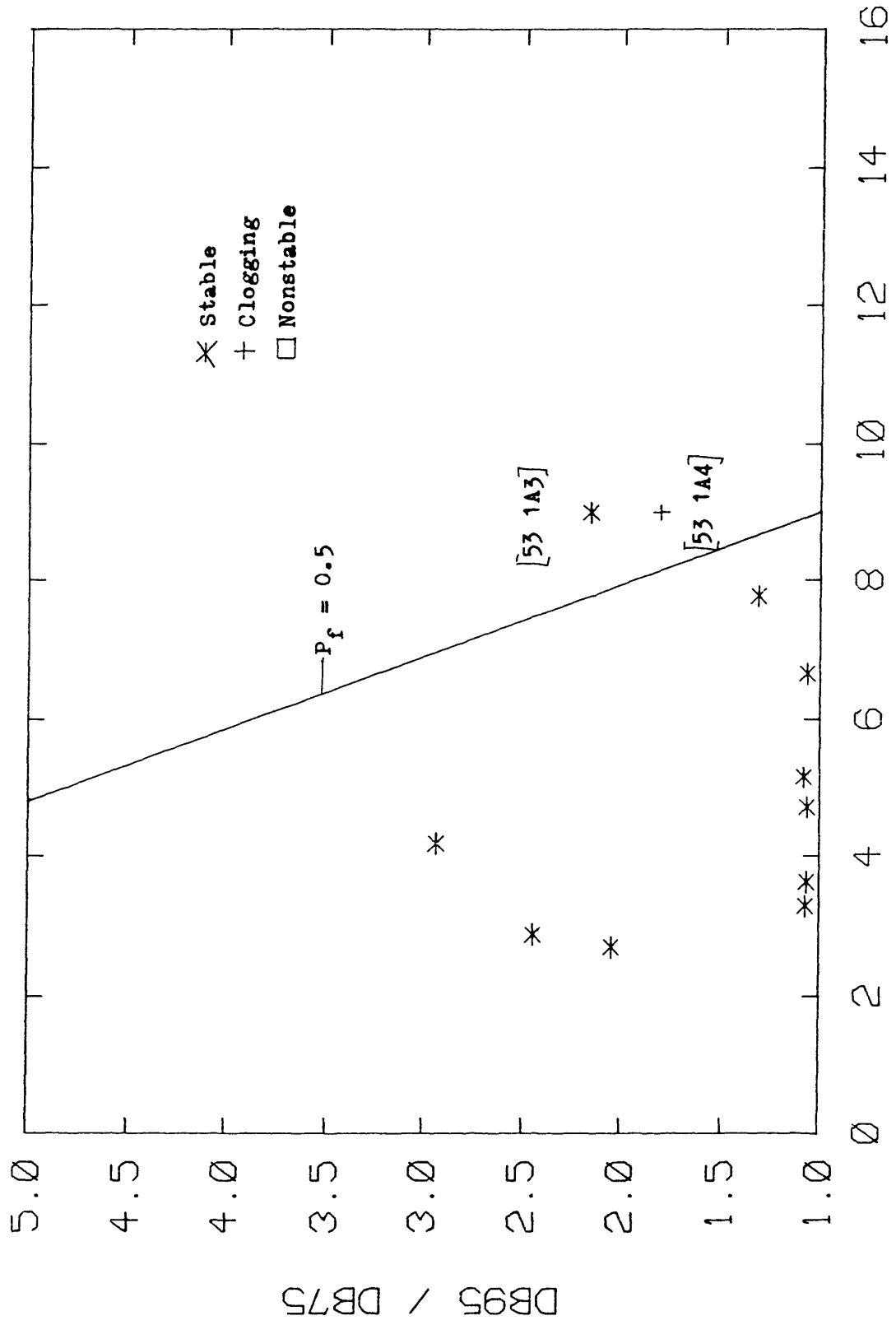

Fig. 3.17 DF15/DB85 vs. DB95/DB75 for [53]

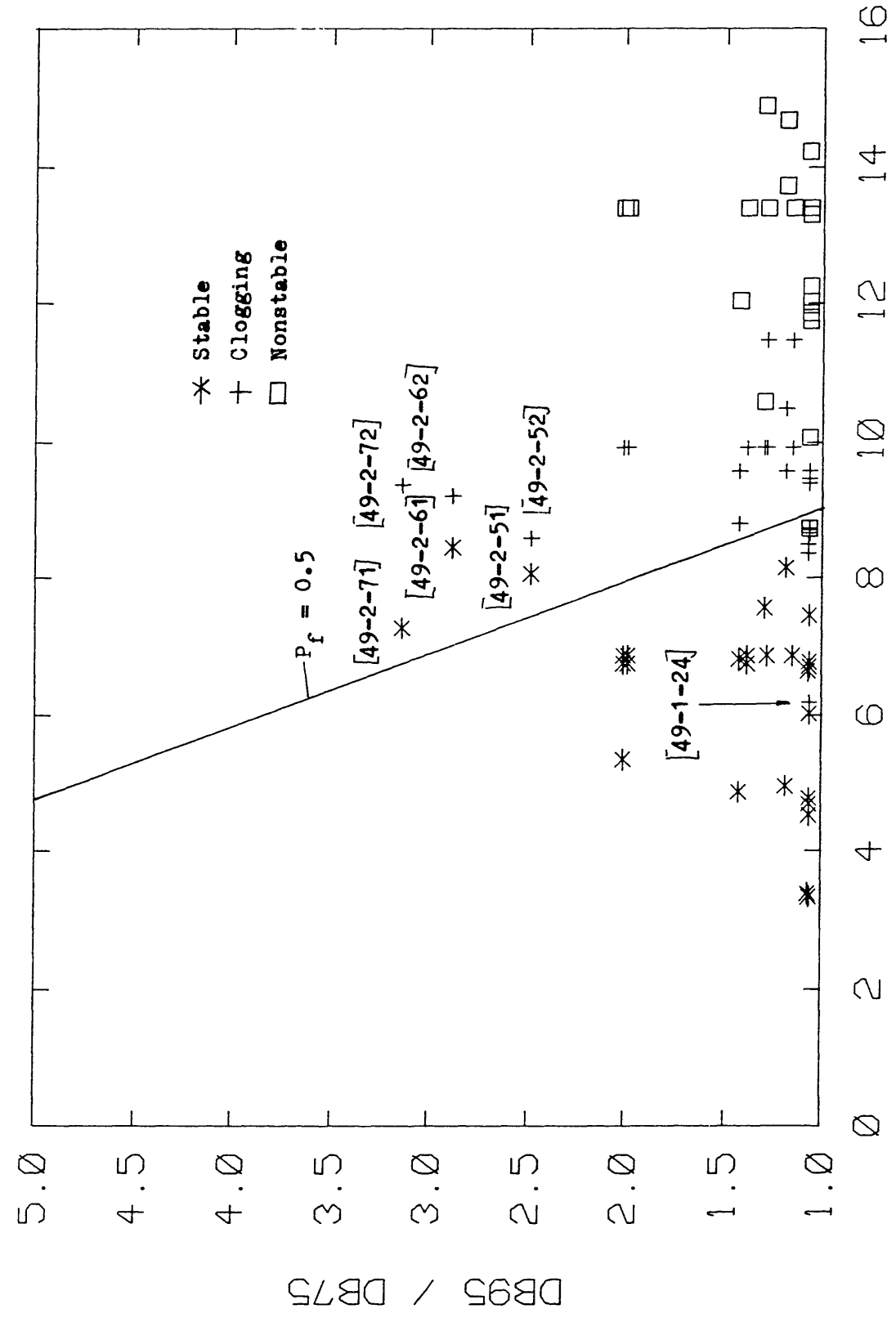

Fig. 3.18 DF15/DB85 vs. DB95/DB75 for [49]

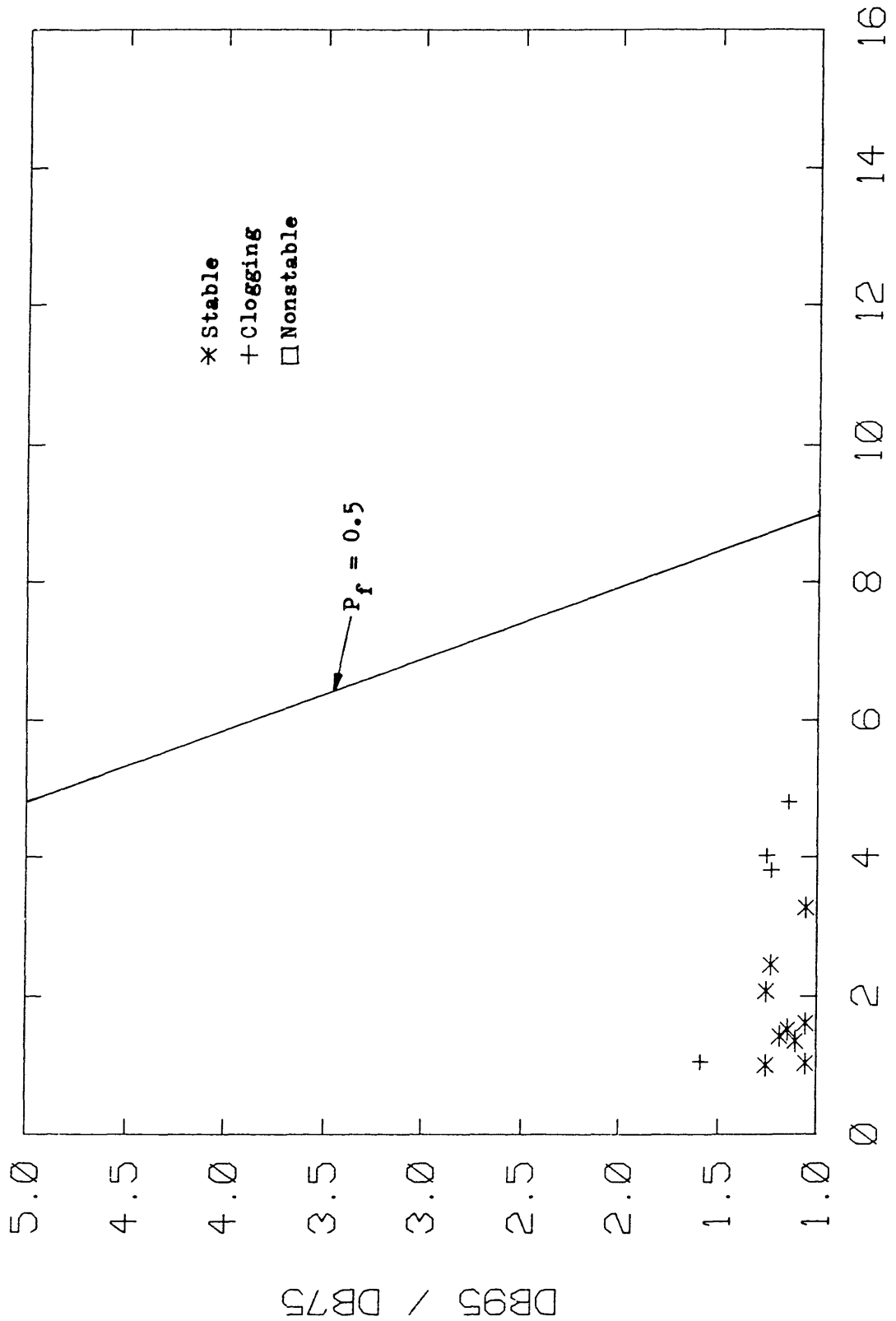

Fig. 3.19 DF15/DB85 vs. DB95/DB75 for [54]

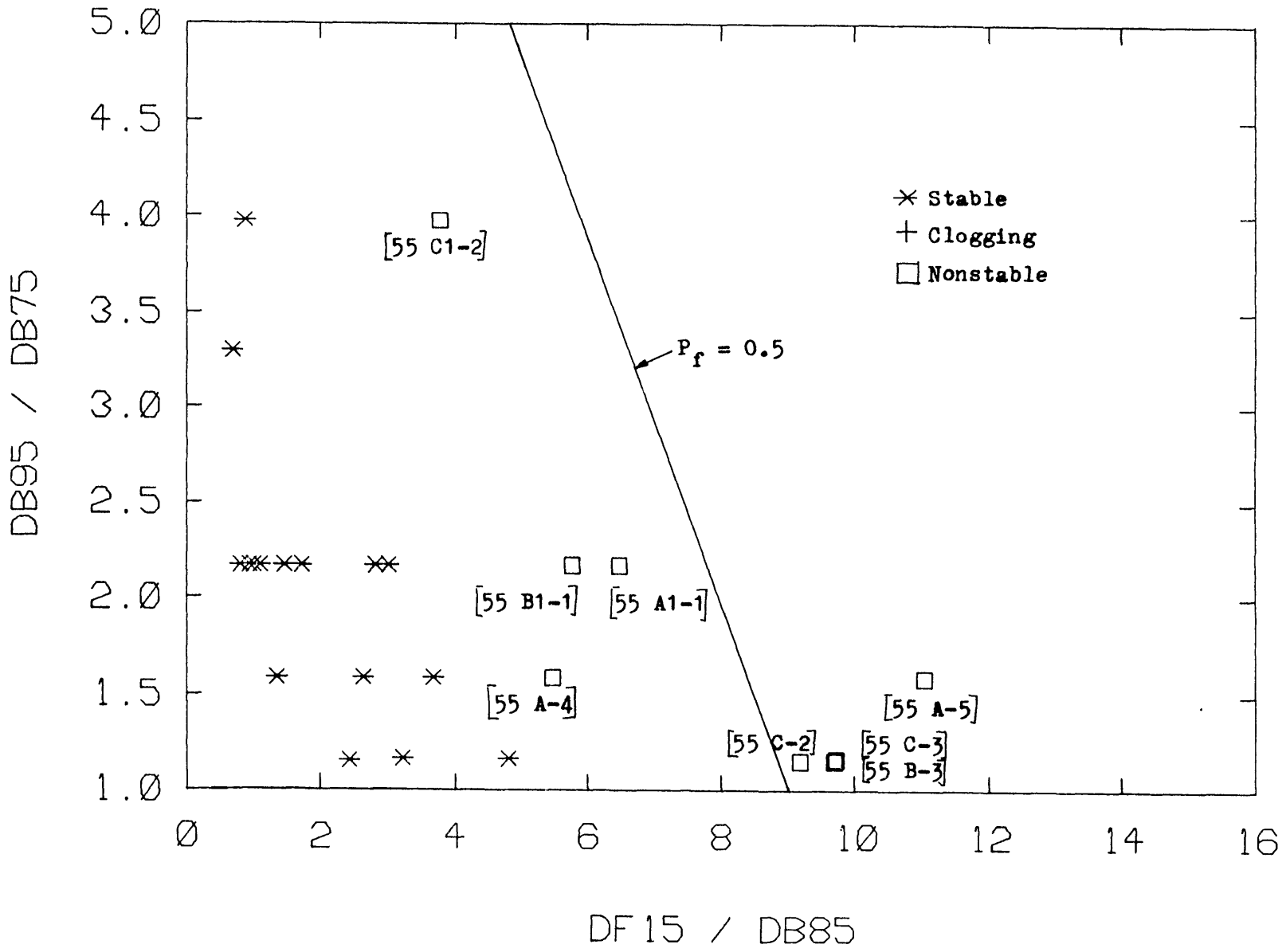

Fig. 3.20 DF15/DB85 vs. DB95/DB75 for [55]

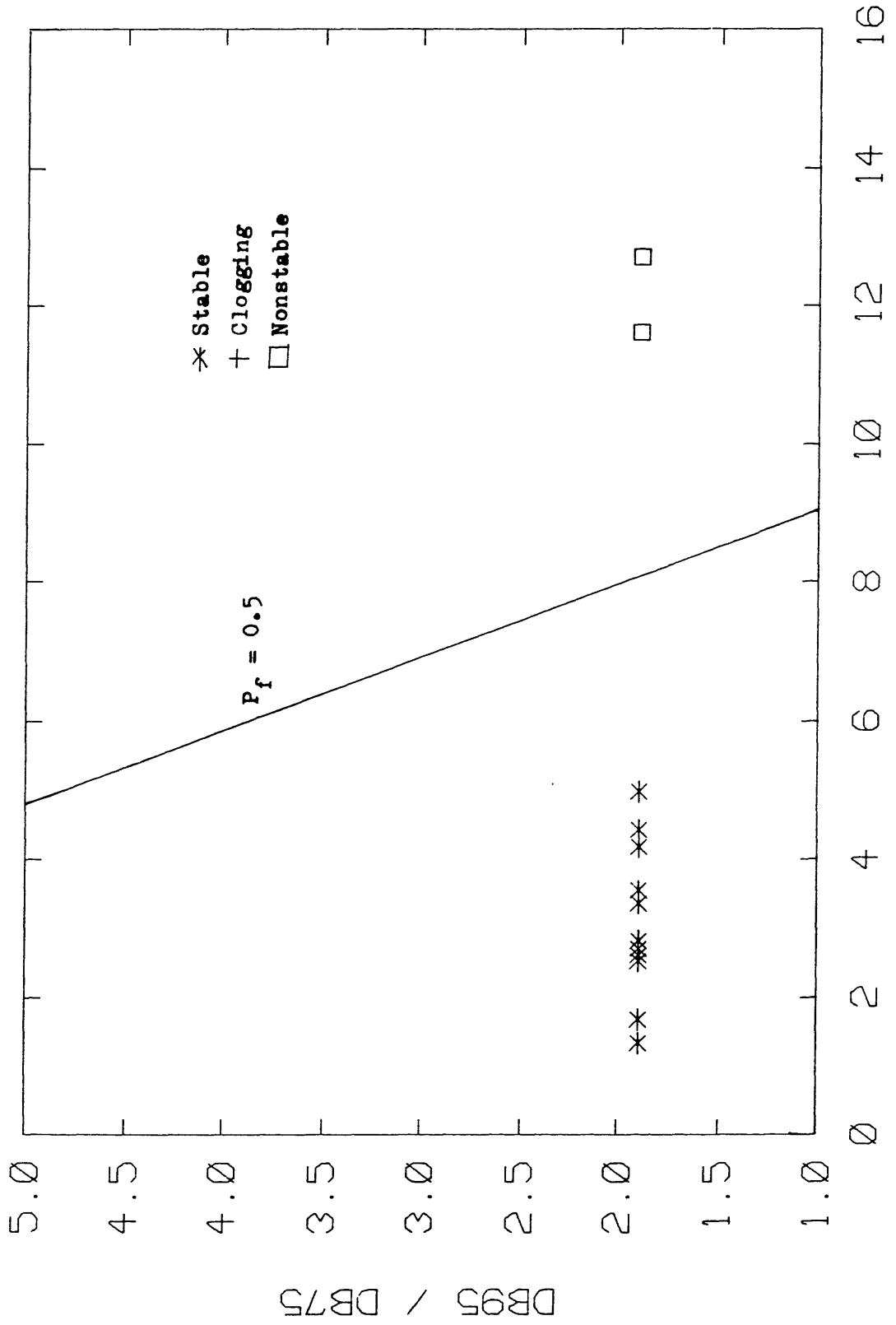

Fig. 3.21 DF15/DB85 vs. DB95/DB75 for [72]

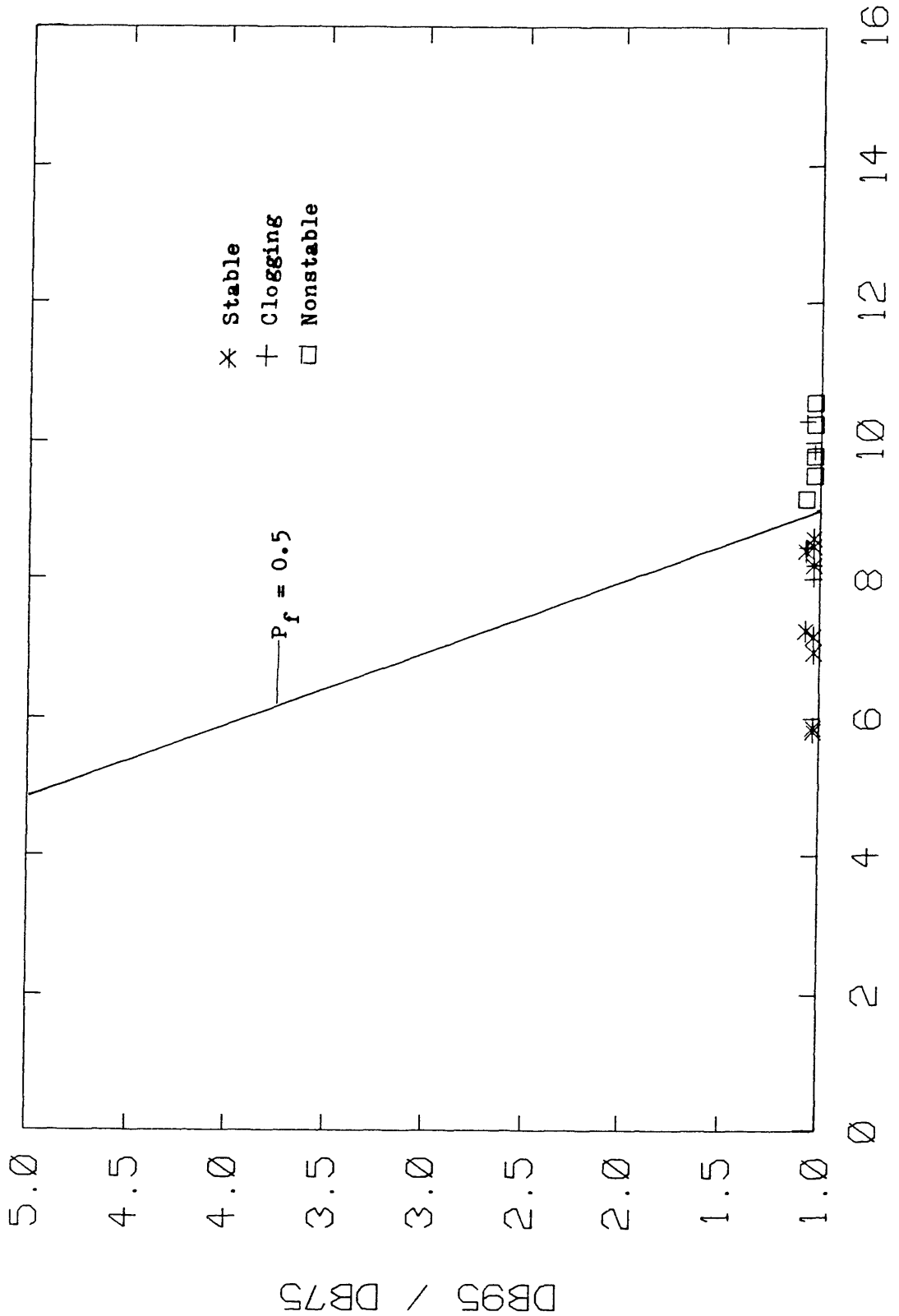

Fig. 3.22 DF15/DB85 vs. DB95/DB75 for [84]

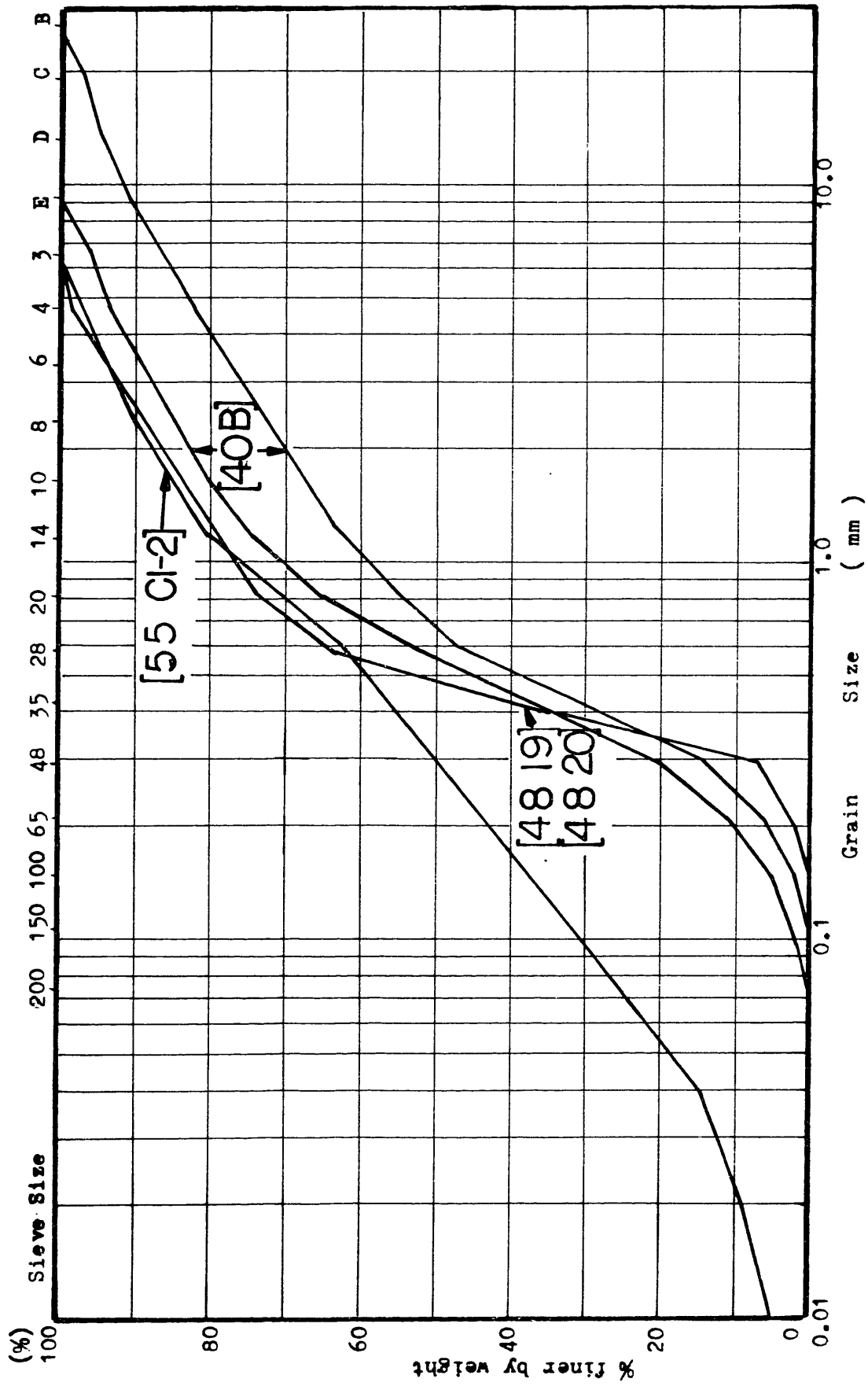

Fig. 3.23 Base Soil Grain Size Distributions with Higher D395/D375 (#1)

Fig 24

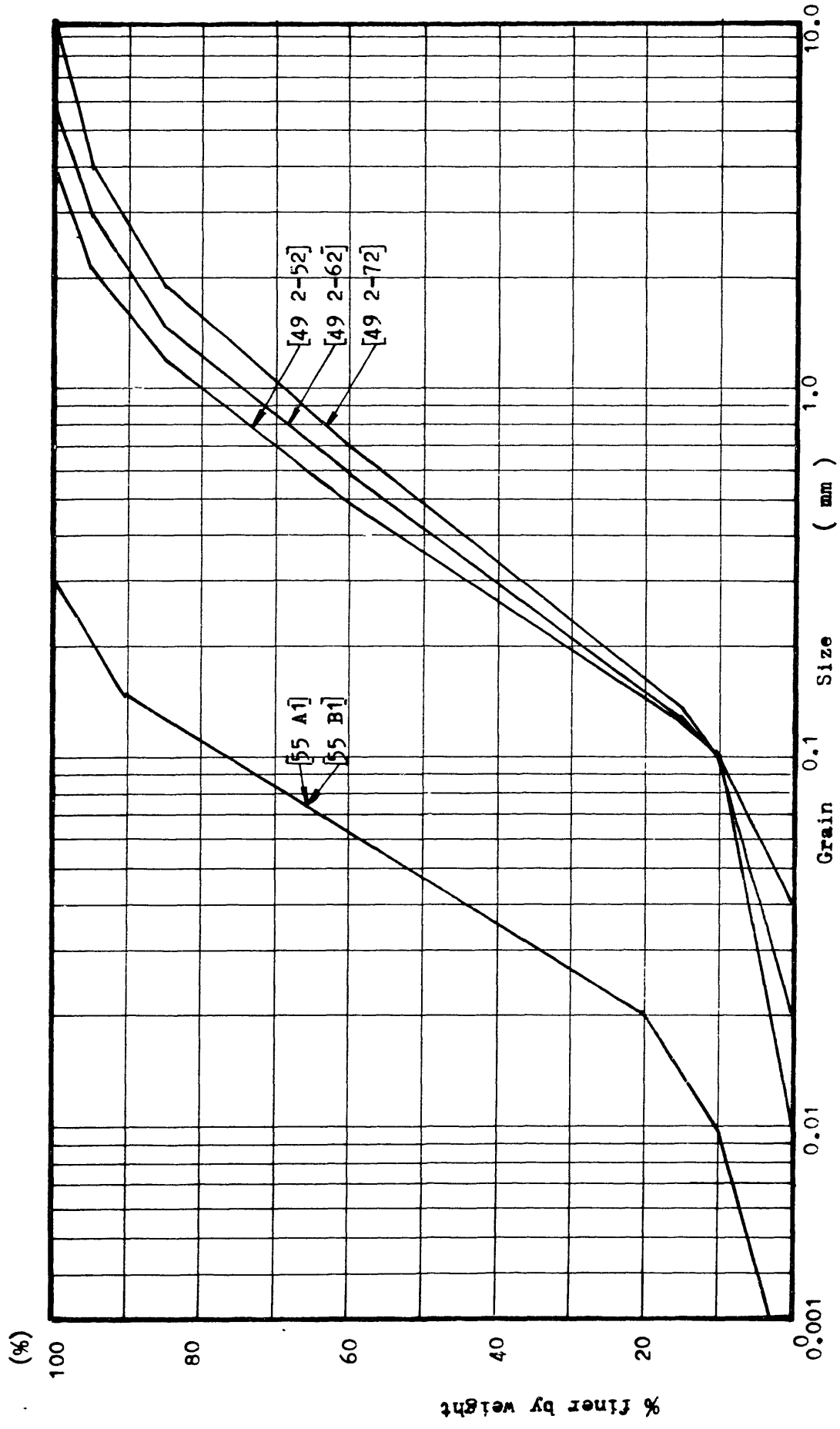

Fig. 3.24 Base Soil Grain Size Distributions with Higher DB95/DB75 (#2)

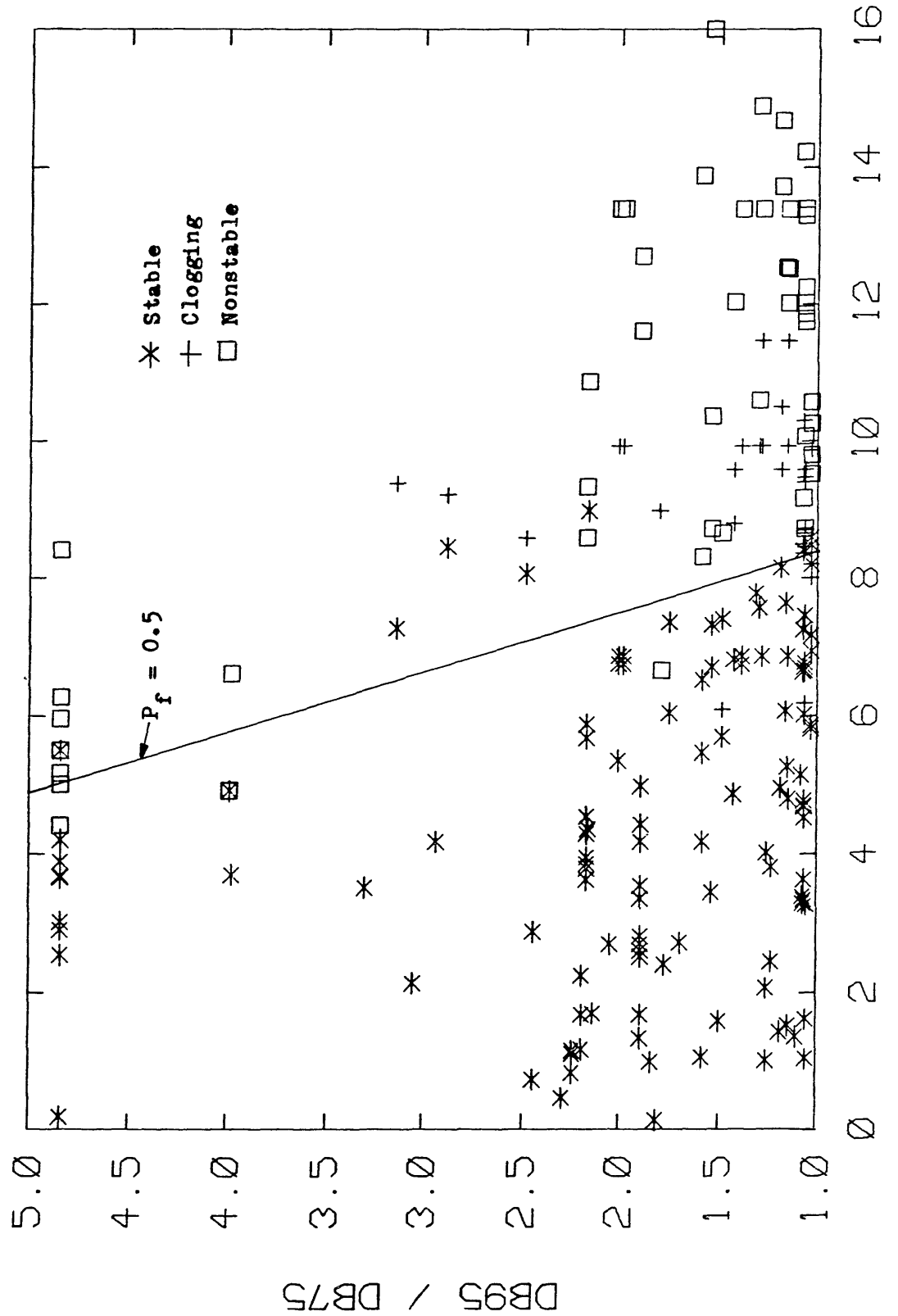

Fig. 3.25 DF15/DB85 vs. DB95/DB75 for all the Data except [40A], [61], [75] and [82] (N=214); Laboratory Biases [41] and [55] adjusted, and Pf=0.5 line shown

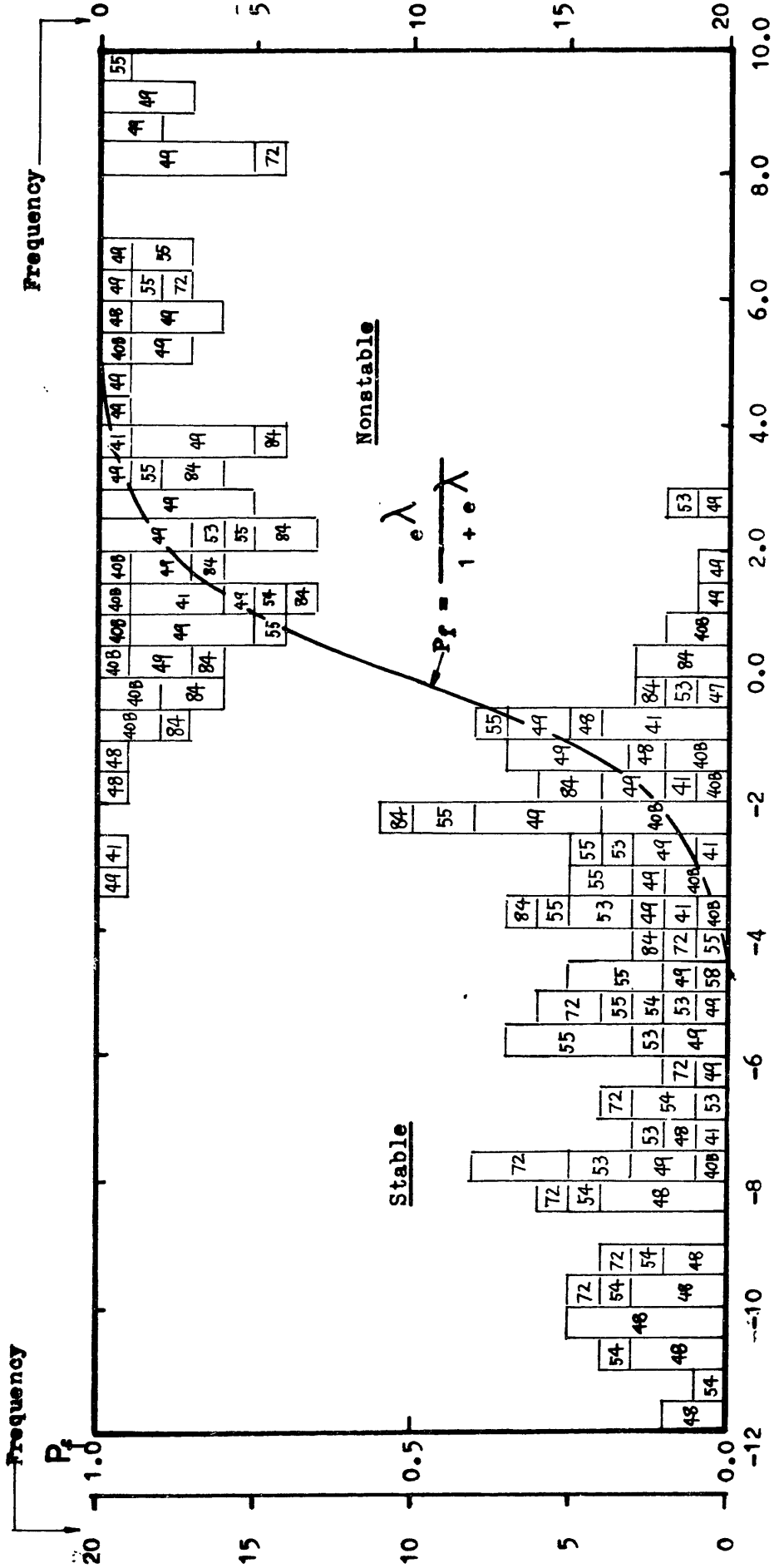

Fig. 3.26 The Fitness of the Final Regression Analysis (Analysis V)

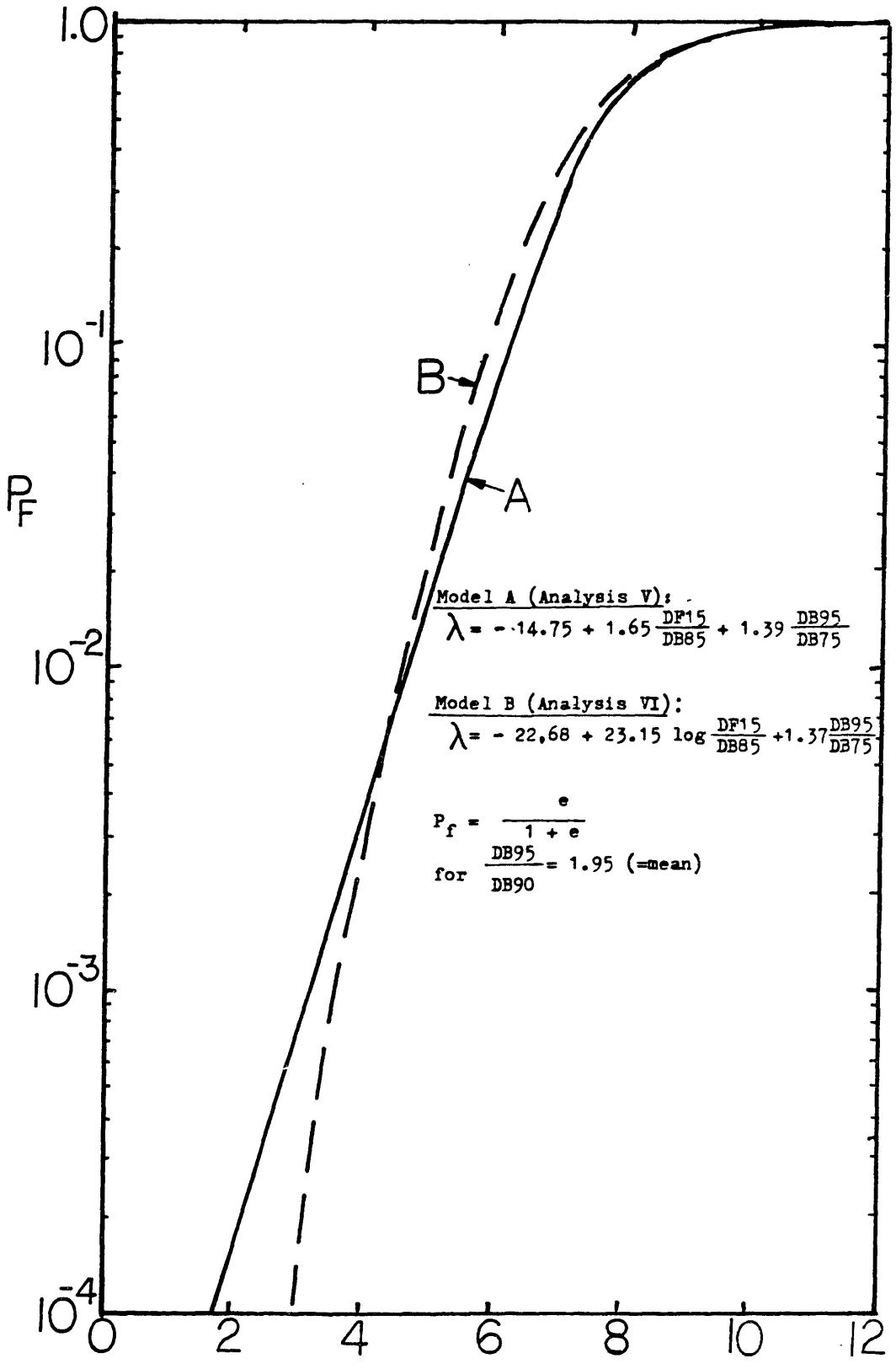

Fig. 3.27 The Probability of Malfunctioning of Filter for DB95/DB90 = 1.95

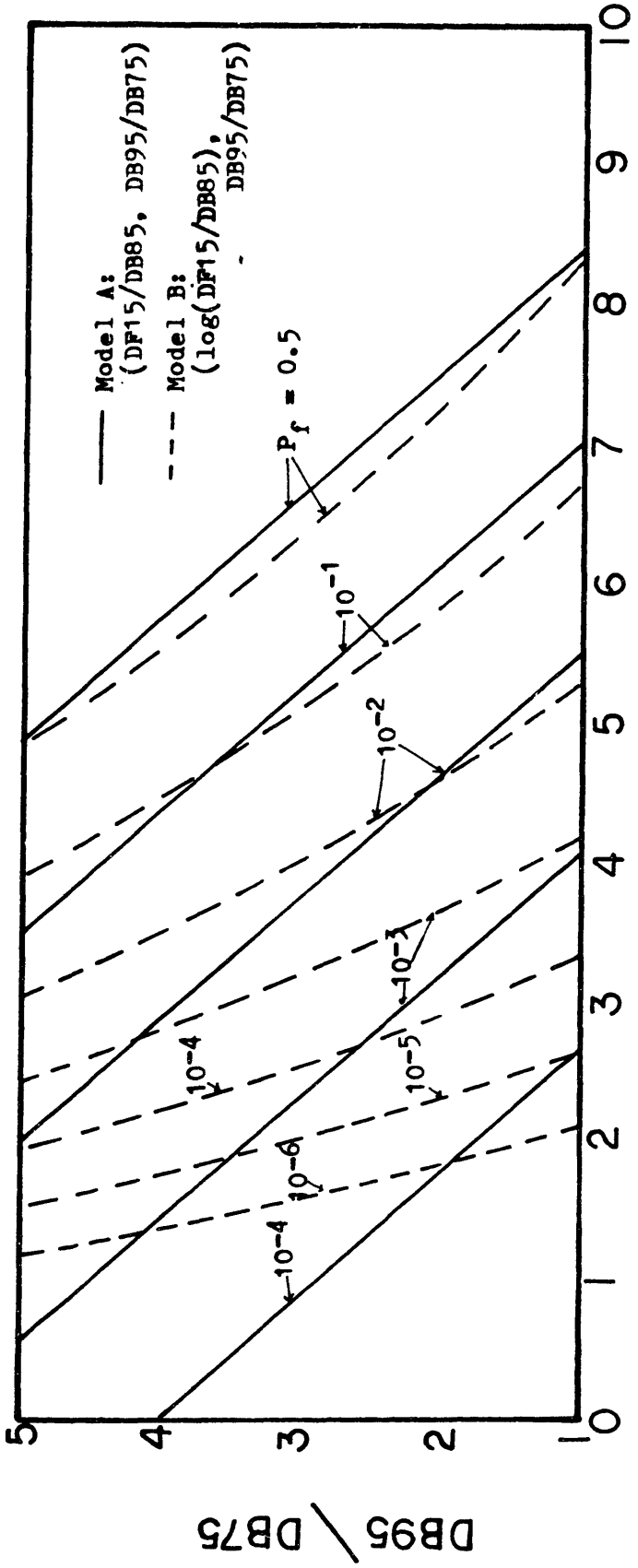

Fig. 3.28 Contours of the Probability of Filter Malfunctioning on DF15/DB85 - DB95/DB75 plane.

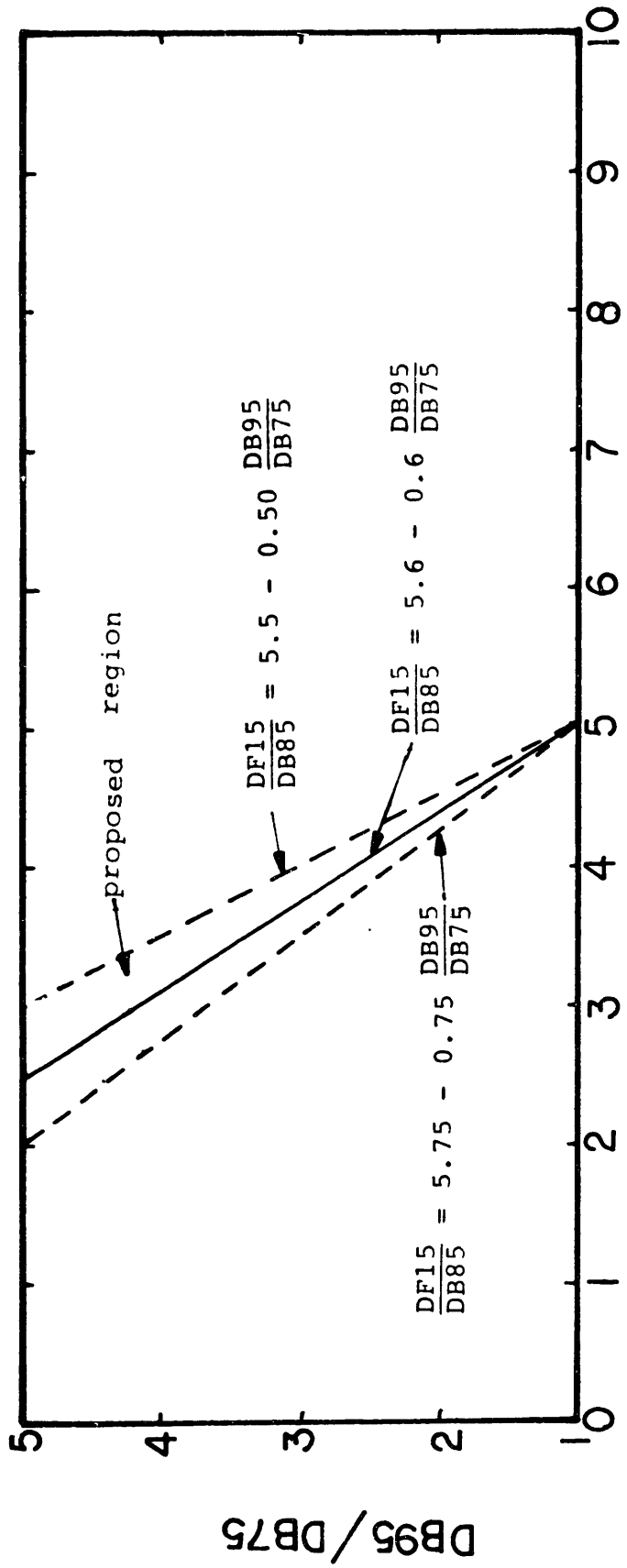

Fig. 3.29 The Region of the Improved Design Criteria

CHAPTER IV. PROBABILITY OF FILTER SYSTEM MALFUNCTIONING: GENERALIZED WEAKEST LINK MODEL

In the previous two chapters, we have studied the physical behavior of soil particles in the filtering process, and analyzed laboratory data by the logistic regression model. An improved filter criterion has also been obtained. However, the scale of the phenomenon we have considered so far is limited to that of a specimen. In this chapter, a model is proposed to evaluate the probability of malfunctioning of filters for a whole earth structure.

A fundamental feature of the dam filter problem is that the structure is considered to have failed if malfunctioning of the filter occurs at any point. This is one example of problems De Mello (1977) referred to in his Rankine Lecture as "controlled by the statistics of extreme value conditions", i.e., it is the extreme value, not the average value, of some parameter that controls the performance of the filter.

In order to account for this feature, a "generalized weakest link model" is developed. The qualifier "generalized" is added because the model is continuous in space and is not simply a series of discrete elements.

The model is potentially applicable to the systems whose behavior is determined by the extreme value of functions of one or two variables (e.g. 1-D and 2-D continous

space).

4.1 Introduction

Consider first a one-dimensional problem, e.g. a string in tension (Fig. 4.1). Let X(s) denote the state of the string at location s, such that X(s) = 1 if the load at s exceeds the resistance at the same location and X(s) = 0 otherwise, then for a strength of length S:

$$\Phi_f = \text{Prob}\{x(s) = 1 \text{ for at least one } s \text{ in } [0,S]\}.$$

Because of the geometry of dam filter system, we are interested in two dimensional extensions of this model. For this purpose, a binary random process is defined on a two dimensional lattice. Special attention is given to autoregressive models on the plane, for which explicit expression for Φ_F can be found. Taking the limit on the spacing between the lattice points tends to zero, a continuous model is derived.

A review of binary random processes on lattice is given first in Section 4.2. This review is useful for explaining the necessity of approximations introduced in the final model. A generalized weakest link on the plane is derived in Sectin 4.3. An analysis of the model and numerical simulations are given in Section 4.4.

4.2 Review of Lattice Models

A general review of autoregressive random fiels on one dimensional (1-D) and two dimensional (2-D) lattices is given in Section 4.2.1. Since models have been developed extensively for the case when the random sequence X_{ij} ($i=1, \ldots, n_1$, $j = 1, \ldots, n_2$) is continuous (especially for the case when the variables x_{ij} are Gaussian), discussion is limited to this continuous variables case first.

In the second portion of this section (4.2.2), Besag's (1974) general characterization of conditional lattice models is introduced. Binary process on a lattice are included as a special class of models. Ising model, which is binary variable model on square lattice and is very popular in physics, is explained next (Section 4.2.3).

In the case of dam filters, one needs to obtain parameters of the binary 2-D lattice model from the marginal failure probability at each lattice point. The problem is similar to obtaining likelihood function in parameters estimation problem. In Section 4.2.4, two methods to estimate model parameters are introduced. One is the "coding method" of Besag (1974), and the other is the "one sided approximation method" by Bartlett & Besag (1969) and Bartlett (1971).

4.2.1 Simultaneous and Conditional Autoregressive Models in 1-D and 2-D: Continuous Case

Before considering 2-D models, it is convenient to review the 1-D case first. This is because in 2-D, the situation becomes complicated not only due to the increase of dimensions but also due to the fact that variables are symmetrically correlated in all directions.

A simple autoregressive time series can be defined either by

$$x_i = \beta x_{i-1} + y_i \tag{4.2.1}$$

or

$$E[x_i | x_{i-1}] = \beta x_{i-1} \tag{4.2.2}$$

where y_i is an i.i.d random variable whose expectation is zero,

β is the autoregressive coefficient.

However, the identity of these two expressions is lost when one assumes x_i is correlated symmetrically to both x_{i-1} and x_{i+1}, Eqs. (4.2.1) and (4.2.2) correspond to two different ways to define autoregressive models on discrete points in 1-D space; they are called the simultaneous autoregressive (SAR) and conditional autoregressive (CAR) models. Later, one finds that the former definition is an alternative expression of the second order Markov series (Yule process), whereas the latter can be derived from the

first order Markov series.

The simultaneous autoregressive (SAR) model has originated from early work by Whittle (1954). Its 1-D form is

$$x_i = \beta(x_{i-1} + x_{i+1}) + y_i \qquad (4.2.3)$$

where

x_i is a random varialbe at site i

y_i is an i.i.d. random variable at site i, whose expectation is zero.

β is the auto-regressive coefficient.

It is immediately apparent that Eq. (4.2.3) is a special form of second order Markov series (Yule Process). The procedure to obtain mean power spectral functions based on the representation theorem is applied (Lumley & Panofsky. [1964]): For x_r and y_r, there exists another random process $Z_x(w)$ and $Z_y(w)$, and they can express x_r and x_y as

$$x_r = \sum_{r=-\infty}^{-\infty} e^{irw}\, dz_x(w)$$

$$y_r = \sum_{r=-\infty}^{\infty} e^{irw}\, dz_y(w) \qquad (4.2.4)$$

where $dz_x(w)$ and $dz_y(w)$ are increments of the processes. Both processes $Z_x(w)$ and $Z_y(w)$ have orthogonal increments, i.e.,

$$\overline{dZ_x(\omega_1)\ dz_x^*(\omega_2)} = 0 \qquad \text{if } \omega_1 \neq \omega_2$$

$$\overline{dZ_y(\omega_1)\ dz_y^*(\omega_2)} = 0 \qquad \text{if } \omega_1 \neq \omega_2.$$

By substituting Eq. (4.2.4) to Eq. (4.2.3), one obtains

$$\sum_{r=-\infty}^{+\infty} e^{ir\omega}\, dz_x = \beta\{\sum_{r=-\infty}^{+\infty} e^{i(r-1)\omega}\, dz_x + \sum_{r=-\infty}^{+\infty} e^{i(r+1)\omega}\, dz_x\} + \sum_{r=-\infty}^{+\infty} e^{ir\omega}\, dz_y$$

Because of the orthogonal property of the increments,

$$dZ_x = \beta(e^{-i\omega} + e^{i\omega})\, dZ_x + dZ_y$$

$$= 2\beta\cos\omega\, dZ_x + dZ_y$$

Therefore,

$$dZ_x = \frac{dZ_y}{(1 - 2\beta\cos\omega)}\ .$$

The mean power spectral density function of the sequence x_r, $S_{xx}(\omega)$, is

$$S_{xx}(\omega) = \overline{dZ_x(\omega)\ dZ_x^*(\omega)}$$

$$\alpha\ \frac{1}{(1-2\beta\cos\omega)^2} \qquad (4.2.5)$$

Notice that $S_{yy}(\omega)$ is constant.

The other possibility is to use a conditional auto-regressive model (CAR), as suggested by Bartlett (1955). The 1-D form is given by

$$E[X_i | X_{i-1}, X_{i+1}] = \gamma(x_{i-1} + x_{i+1}] \qquad (4.2.6)$$

It is possible to show that Eq. (4.2.6) can be derived from a first order Markov series as follows: A 1st order Markov series has the form

$$x_i = \rho x_{i-1} + y_i \qquad (4.2.7)$$

where y_i is an i.i.d. random variable whose expectation is zero. If one multiplies by ρ both sides of Eq. (4.2.7) written for i + 1, one obtains

$$\rho x_{i+1} = \rho^2 x_i + \rho y_{i+1} \qquad (4.2.8)$$

Subtracting Eq. (4.2.8) from Eq. (4.2.7) gives

$$(1 + \rho^2)x_i = \rho(x_{i-1} + x_{i+1}) + (y_i - \rho y_{i+1})$$

$$x_i = \frac{\rho}{1+\rho^2}(x_{i-1} + x_{i+1}) + \frac{1}{1+\rho^2}(y_i - \rho y_{i+1}) \qquad (4.2.9)$$

Since $E[y_i] = E[y_{i+1}] = 0$

$$E[x_i | x_{i-1}, x_{i+1}] = \frac{\rho}{1+\rho^2}(x_{i-1} + x_{i+1}) \qquad (4.2.10)$$

Therefore, Eq. (4.2.6) is derived from the first order Markov series in Eq. (4.2.7) with $\gamma / \rho(1 + \rho^2)$. The fact that 1-D CAR model can be derived from the first order Markov process gives one reason for using the one sided model +0 approximate 2-D CAR model (see Section 4.4.4). By comparing Eq. (4.2.9) to Eq. (4.2.3), one can see CAR model no longer has the i.i.d. error term which SAR model has. One the other hand, CAR model has simpler correlation structure (i.e., the first order Markov series) than SAR model has (the second order Markov series). The mean power spectral density function can be obtained from Eq. (4.2.9) by following the same procedure as before:

$$(1-\rho^2)dZ_x = \rho(e^{i\omega}+e^{-i\omega})dZ_x + (1-\rho e^{i\omega})dZ_y$$

$$\{(1+\rho^2) - 2\rho\{\cos\omega\}\ dZ_x = (1-\rho e^{i\omega})dZ_y$$

Therefore,

$$dZ_x = \frac{1-\rho e^{i\omega}}{(1+\rho^2)-2\rho\cos\omega}\ dZ_y \ .$$

Finally,

$$S_{xx}(\omega) = \overline{dZ_x\ dZ_x^*}$$

$$\alpha\ \frac{(1-\rho\cos\omega)^2+(\rho\sin\omega)^2}{\{(1+\rho^2)-2\rho\cos\omega\}^2}$$

$$= \frac{1}{(1+\rho^2)-2\rho\cos\omega}$$

$$\alpha \frac{1}{1 - 2\gamma\cos\omega} \qquad (4.2.11)$$

Comparison of Eqs. (4.2.5) and (4.2.11) shows that CAR models have a different mean power spectral density function (therefore, a different correlation structure) than SAR models, even in the 1-D case.

The simplest 2-D SAR model is defined as

$$x_{ij} = \beta_1 (x_{i-1,j}+x_{i+1,j}) + \beta_2 (x_{ij-1}+x_{i,j+1}) + y_{ij} \qquad (4.2.12)$$

The mean power spectral density function of this process can be obtained through the same procedure as for the 1-D case. By this procedure, the function is proportional to

$$[1 - 2(\beta_1 \cos \omega_1 + \beta_2 \cos \omega_2)]^{-2} \qquad (4.2.13)$$

One difficulty with this model is that, even if y_{ij} and hence x_{ij} are Gaussian, the estimation of β_1 and β_2 from data is not a simple least squares problem, due to the complicated Jacobian when transforming from the independent y_{ij} to the observed x_{ij} (Bartlett [1975]). Whittle (1954) obtained an asymptotic expression for this Jacobian, which he applied to obtain the likelihood function of β_1 and β_2.

In its general form the 2-D CAR model, can be given as

$$\text{Prob.}(x_{ij} \mid \text{rest}) = \text{Prob.}(x_{ij} \mid x_{i-1,j},\ x_{i+1,j},\ x_{i,j-1},\ x_{i,j+1}) \tag{4.2.14}$$

This model is sometimes referred to as a Markov Field. Some of the difficulties the model exhibits are:

(i) It has been proved by Besag (1972) that the only case in which the conditional variable x_{ij} can be a linear combination of the neighboring values is when the x_{ij}'s are normal variables. That is, a relationship of the type

$$E[x_{ij} \mid x_{ij-1},\ x_{ij+1},\ x_{i-1j},\ x_{i+1j}] = \gamma_1(x_{ij-1} + x_{ij+1}) + \gamma_2(x_{i-1j} + x_{i+1j}) \tag{4.2.15}$$

holds only if the x_{ij}'s are Gaussian. This model is usually called auto-normal scheme.

(ii) There is no general way to evaluate the joint p.d.f. on the lattice; thus, the likelihood function usually cannot be obtained.

By using a class of linear conditional spatial-temporal models, Bartlett (1975) showed that the spectral density function of CAR models is proportional to

$$\cdot [1 - 2\beta_1 \cos \omega_1 - 2\beta_2 \cos \omega_2]^{-1}$$

which is similar to Eq. (4.2.11) in the 1-D case.

As previously mentioned, many difficulties arise in the extension of autoregressive lattice models from the line to the plane (1-D to 2-D). A more general formulation of conditional lattice model proposed by Besag (1974) is presented next; the formulation is valid for both continuous and binary lattice process x_{ij}.

4.2.2 General Specification of Conditional Lattice Models

Besag (1974) developed a convenient and rather general procedure to formulate conditional lattice models. The procedure is the same for continuous as for binary (more in general, discrete) variables. The procedure Besag proposed based on the Hammersley-Clifford theorem, which gives a rather general expansion of any probability function that satisfies a certain loose condition (i.e., the positive condition). By using this expansion, one can produce groups of different conditional lattice models. Besag's procedure is briefly summarized here.

Let i denote a point of the lattice which consists of n sites. Site j ($j \neq i$) is said to be a neighbor of site i if and only if $P(x_i | x_1, x_2, \ldots, x_{i-1}, x_{i+1}, \ldots x_n)$ depends on the variable x_j. Second,

any set of sites which either consists of a single site or else in which every site is a neighbor of every other site in the set is called clique. The clique plays a crucial role in the Hammersley-Clifford theorem. Finally, the positive condition is defined: if $P(x_i) > 0$ for each i, then $P(x_1, \ldots x_n) > 0$. Under the positive condition, it is easy to see from the definition of conditional probability that

$$\frac{P(\underline{x})}{P(\underline{y})} = \prod_{i=1}^{n} \frac{P(x_i | x_1, \ldots x_{i-1}, y_{i+1}, \ldots y_n)}{P(y_i | x_1, \ldots x_{i-1}, y_{i+1}, \ldots y_n)} \tag{4.2.16}$$

where $\underline{x} = (x_1, \ldots, \ldots x_n)$

$\underline{y} = (y_1, \ldots, y_n)$.

Let us assume $x_i < \infty$. Furthermore, without loosing generality, assume $P(x_i = 0) > 0$. Vectors $\underline{x}$ and $\underline{x}_i$, and a function $Q(\underline{x})$ are defined as follows:

$$\underline{x} = (x_1, x_2, \ldots, x_n)$$

$$\underline{x}_i = (x_1, \ldots x_{i-1}, 0, x_{i+1}, \ldots x_n)$$

and

$$Q(\underline{x}) = \ell n\, P(\underline{x}) - \ell n P(\underline{0}) \tag{4.2.17}$$

where $\underline{0} = (0, \ldots 0)$.

The Hammersley-Clifford theorem says that under the assumptions made above, $Q(\underline{x})$ can be written in a general ex-

pansion form:

$$Q(\underline{x}) \sum_{1<i\leq n} x_i G_i(x_i) + \sum_{1\leq i<j\leq n} \sum x_i x_j G_{i,j}(x_i,x_j) + \ldots$$

$$\ldots + x_1 x_2 \ldots x_n G_{1,2,\ldots n}(x_1,x_2,\ldots x_n) \tag{4.2.18}$$

where

$$x_i G_i(x_i) = \ell nP(0,0,\ldots 0,x_i,0\ldots 0) - \ell nP(0,\ldots 0)$$

$$x_i x_j G_{ij}(x_i,x_j) = \ell nP(0,\ldots 0,x_i,0,\ldots 0,x_j,0\ldots 0)$$

$$- \ell nP(0,\ldots 0,x_i,0\ldots 0) - \ell nP(0,\ldots 0,x_j,0,\ldots 0)$$

$$+ \ell nP(0,\ldots 0), \quad \text{etc.}$$

and the function $G_{i,j,\ldots,s}$ in Eq. (4.2.18) may be non-null if and only if the sites i,j,...,s form a clique. Subject to this restriction, the G-functions may be chosen arbitrarily. Therefore, given the neighbors of each site, we can immediately write down the most general form for $Q(\underline{x})$. A proof of the theorem can be seen in Besag (1974).

Based on the Hammersley-Clifford theorem, we can general classes of conditional lattice models. It can be done by using a very convenient form of equation which can be obtained from Eqs. (4.2.16) and (4.2.17):

$$
\begin{aligned}
&\exp\,[\,Q(\underline{x}) - Q(\underline{x}_i)\,] \\
&= \exp,\,[\,\ell nP(\underline{x}) - \ell nP(\underline{0}) - \ell nP(\underline{x}_i) + \ell nP(\underline{0})\,] \\
&= P(\underline{x})/P(\underline{x}_i) \\
&= \frac{P(x_i \mid x_1, \ldots x_{i-1}, x_{i+1}, \ldots x_n)}{P(0 \mid x_1, \ldots x_{i-1}, x_{i+1}, \ldots x_n)}
\end{aligned}
\qquad (4.2.19)
$$

By using this equation, one can derive the conditional probability of x_i from knowledge of $Q(\underline{x})$.

A specially useful class of models, so called auto-models, can be derived under the assumption that the probability structure of the system depends only on contributions from cliques containing no more than two sites.* Under this assumption, Eq. (4.2.18) becomes:

$$
Q(\underline{x}) = \sum_{1 \le i \le n} x_i G_i(x_i) + \sum_{1 \le i < j \le n} \sum x_i x_j G_{ij}(x_i x_j) \qquad (4.2.20)
$$

Therefore, applying Eq. (4.2.19) to this equation yields

---

*In Besag's original paper, an additional assumption that the conditional probability distribution belongs to the exponential family of distributions. However, this assumption seems "more a matter of convenience than of necessity", and is not considered here. (See Bartlett's discussion on Besag's paper, J. Roy. Stat. Soc. B36 (1974), p. 231).

$$\frac{P(x_i|x_1,\ldots x_{i-1},x_{i+1},\ldots x_n)}{P(0|x_1,\ x_{i-1},\ x_{i+1},\ldots x_n)}$$

$$= \exp\left[\, x_i\{G_i(x_i) + \sum_{j=1}^{n} G_{ij}(x_i,x_j)x_j\}\right] \tag{4.2.21}$$

where $G_{ii}(x_i,x_i)$ is assumed to be zero.

One can generate a number of models based on Eq. (4.2.21); two such models are presented here.

(1) Auto-Binary Models

If x_i is a binary variable (0 or 1) and cliques consist only of single sites and of pairs of sites, then the auto-logistic model follows:

$$Q(\underline{x}) = \sum_{1\le i\le n} \alpha_i x_i + \sum_{1\le i<j\le n}\sum \beta_{ij}\, x_i x_j \tag{4.2.22}$$

From Eq. (4.2.20),

$$\frac{P[\,x_i=1|\text{rest}]}{P[\,x_i=0|\text{rest}]} = \exp\left[\, 1\cdot\{\alpha_i + \sum_{j=1}^{n} \beta_{ij}x_j\}\right]$$

We have another condition that

$$P[\,x_i=1|\text{rest}] + P[\,x_i=0|\text{rest}] = 1$$

By solving these two equations simultaneously, one obtains

$$P[x_i|\text{rest}] = \frac{\exp\{x_i(\alpha_i + \sum_{j=1}^{n}\beta_{ij}x_j)\}}{1 + \exp[\alpha_i + \sum_{j=1}^{n}\beta_{ij}x_j]}$$

where $\beta_{ij} = 0$ for $i=j$.

Therefore, the explicit form of a conditional auto-regressive binary model on a lattice (sometimes called Markov field) is

$$P[x_{ij}\ x_{i-1,j}, x_{i+1j}, x_{ij-1}, x_{ij+1}]$$

$$= \frac{\exp[x_{ij}\{\alpha+\beta_1(x_{i-1,j}+x_{i+1,j})+\beta_2(x_{ij-1}+x_{ij+1})\}]}{1 + \exp[\alpha+\beta_1(x_{i-j}+x_{i+1j}) + \beta_2(x_{ij-1}+x_{ij+1})]} \qquad (4.2.23)$$

Equation (4.2.23) is called Ising Model (Eq. (4.2.23) is its conditional form) and is considered in more detail in the next section.

One could extend the model to make x_{ij} depend on more than the nearest neighbors, but the model would cease to be one of the linear logistic types.

(2) Auto-Normal Models

In many applications, it may be reasonable to assume that the joint distribution of site variables is multivariant normal; one model of this type is the auto-normal model:

$$P(x_i|\text{rest}) = (2\pi\sigma^2)^{-1/2} \exp\left[-\frac{1}{2\sigma^2}\{(x_i-\mu_i) - \Sigma_j \beta_{ij}(x_j-\mu_j)\}^2\right]$$

This model can be transformed to the form of Eq. (4.2.18) by using Eq. (4.2.19).

In this case, the joint distribution can be derived from the conditional distribution. Again, simultaneous autoregressive (SAR) models yield different joint distributions than CAR models (Besag [1974], Ripley [1981]).

4.2.3 The Ising Model

The 2D binary model considered here was introduced by the German physicist Ernst Ising to study certain empirically observed facts in ferromagnetic materials.

Suppose a piece of metal which is assumed to consist of many small depoles is exposed to a magnetic field. At each site there is a small depole which is in one of two positions; "up" or "down". Ising defined the energy of whole systems to be

$$E = -\{\alpha \sum_{ij} x_{ij} + (\beta_1 \sum_{ij} x_{ij}x_{i-1j} + \beta_2 \sum_{ij} x_{ij}\, x_{ij-1})\} \tag{4.2.24}$$

where x_{ij} is +1 for "up" and -1 for "down", and α, β_1 and β_2 are constants. The first term inside the bracket represents the effect of the external magnetic field. For $\alpha > 0$, the energy is minimized if all the depoles

have the same direction of the external field. The second term is the energy caused by the interaction of the depoles and is smallest if the neighboring depoles have the same direction (provided that $\beta_1 > 0$ and $\beta_2 > 0$). It is assumed that only interactions between the neighboring depoles are important (Markov property).

A probability is assigned to each combination $\underline{x}$ according to

$$P(\underline{x}) = C^{-1} \exp [- E(\underline{x})/kT] \qquad (4.2.25)$$

where C is a normalizing constant ($C = \sum_{\text{All}\underline{x}} \exp [-E(\underline{x})/kT]$)

T is absolute temperature

k is a constant.

According to Eq. (4.2.25), states of smaller energy are assigned higher probability. Eq. (4.2.25) is called the Gibbs model.

It is easy to derive the conditional probability $P(x_{ij}|\text{rest})$:

$$P(x_{ij}|\text{rest}) = \frac{P(\underline{x})}{P(\text{all } \underline{x} \text{ with } x_{ij}=0) + P(\text{all } \underline{x} \text{ with } x_{ij}=1)}$$

$$= \frac{\exp [-x_{ij}\{\alpha+\beta_1(x_{i-1j}+x_{i+1j})+\beta_2(x_{ij-1}+x_{ij+1})\}]}{1+\exp [-\{\alpha+\beta_1(x_{i-1j}+x_{i+1j})+\beta_2(x_{ij-1}+x_{ij+1})\}]} \qquad (4.2.26)$$

Eq. (4.2.26) is identical to Eq. (4.2.23). For more details on the model, see Kinderman & Snell (1980).

The correlation properties of the Ising model have been studied extensively; however, it is known that "the correlation properties of the only possible binary model with the required bilateral properties (of model (4.2.26) are the most complicated" (Bartlett [1975], pp. 31-40).

4.2.4 Statistical Analysis of Binary Variables on 2-D Lattice

It can be seen from the form of Eq. (4.2.25) that the maximum likelihood estimation of parameters α, β_1 and β_2 from given binary data on 2-D lattice is not possible: if one takes the logarithm of Eq. (4.2.25) (i.e., the log likelihood function) and then take partial derivative of it by α, β_1 and β_2, they all become constants, meaning the function is monotonic in the α-β_1-β_2 space. To overcome this difficulty, some bypassing techniques are porposed; they are reviewed here.

(1) Coding Method: Conditional Likelihood Function

This method, proposed by Besag (1974), uses a simple conditional likelihood function in place of the usual likelihood function. In order to fit the model to data, one begins by labelling the interior site of the lattice alternatively as "x" and "." as shown in Fig. 4.3. It is straightforward that the variables associated

with "x" sites (or "." sites) are mutually independent, and, therefore, the conditional likelihood function is obtained:

$$\prod_{ij \text{ for all x site}} P(x_{ij} | x_{i-1,j},\ x_{i+1,j}\ x_{i,j-1},\ x_{i,j+1})$$

Besag estimated the unknown parameters so that this function is maximized. The same procedure applies for "." sites. It might be reasonable, in practice, to carry out both cases and then combine the results appropriately (e.g., by taking an average).

(2) One-Sided Approximation to the Likeihood Function

Another way to obtain (quasi-) likelihood functions is to use a one-sided approximation of the two-sided model. It was previously shown that for the 1-D case, the conditional auto-regressive (CAR) mdoel is identical to a lst order Markov series (see Eqs. (4.2.6) through (4.2.10)). Unfortunately, this correspondence ceases to hold in 2-D. However, one-sided 2-D models may still provide useful approximation.

One simple and intuitive way to do this is to introduce the one-sided model which has a similar form as 1-D case (Eq. (4.2.7)), as follows (Bartlett &

Besag [1969], Bartlett [1971]):

$$P(x_{ij} = 1|\text{rest}) = C + \alpha(x_{i-1,j} + x_{i,j-1}) \quad (4.2.27)$$

where c and α are constants.

Provided that x_{ij} is a 0-1 variable, $E[x_{ij}|\text{rest}] = P(x_{ij} = 1|\text{rest})$. Then the expectation of Eq. (4.2.27) is

$$E[x_{ij}] = C+\alpha\{E[x_{i-1},] + E[x_{i,j-1}]\}$$

If the field is homogeneous,

$$E[x_{ij}] = P(x_{ij} = 1) = C/(1-2\ ) \quad (4.2.28)$$

The autocovariance function of the one sided model may be obtained as

$$w_{rs} = \alpha(w_{r-1,s} + w_{r,s-1}) \quad (4.2.29)$$

where

$$w_{rs} = E[x'_{ij}\ x'_{i-r,\ j-s}],\ x'_{ij} = x_{ij} - E[x_{ij}]$$

Another way to obtain one-sided approximations is to consider an analogy with the 1-D continuous variables case (Bartlett & Besag [1969], Bartlett [1971]): for 1-D CAR continuous variable models we have seen that the spectral density function is proportional to $[1-2\gamma\cos\omega]^{-1}$ (see Eq. (4.2.11); based on this , Bartlett suggested, for the 2-D lattice system, to use one sided approximation with spectral density functions proportional to

$$[1 - \gamma(\cos\omega_1 - \cos\omega_2)]^{-1}$$

$$= [1 - \gamma\{e^{i\omega_1} + e^{i\omega_2} + e^{-i\omega_1} + e^{-i\omega_2}\}]^{-1}$$

A first-order approximation to this spectral density function can be obtained as follows: since

$$[1 - \gamma(e^{i\omega_1} + e^{i\omega_2})]^{-1}\,[1-\gamma(e^{-i\omega_1} + e^{-i\omega_2})]^{-1}$$

$$= [1 + 2\gamma^2 - \gamma(e^{i\omega_1} + e^{i\omega_2} + e^{-i\omega_1} + e^{-i\omega_2})$$

$$+ \gamma^2(e^{-i\omega_1}e^{i\omega_2} + e^{i\omega_1}e^{-i\omega_2})]^{-1}$$

To eliminate the unwanted terms on the right hand side of the equation, one may consider

$$[1-\gamma(e^{i\omega_1}+e^{i\omega_2})-\gamma^2 e^{-i\omega_1}e^{-i\omega_2}]^{-1}$$

$$[1-\gamma(e^{-i\omega_1}+e^{-i\omega_2})-\gamma^2 e^{i\omega_1}e^{-i\omega_2}]^{-1}$$

$$= [1+2\gamma^2-\gamma(e^{i\omega_1}+e^{i\omega_2}+e^{-i\omega_1}+e^{-i\omega_2}) + 0(\gamma^3)]^{-1} \quad (4.2.30)$$

Thus, the unwanted term is less than the order of γ^3. One sided approximation form that correspond to Eq. (4.2.30) is

$$E[x_{ij}|\text{rest}] = \gamma(x_{i-1,j} + x_{i,j-1}) + \gamma^2 x_{i+1,j-1} \quad (4.2.31)$$

One might be a little suspicious about the argument presented because of the fact that they are based on a continuous variable system on lattice. Unfortunately, there is no way we can extend this argument to binary variables on lattice, we just postulate the form to this case also:

$$P[x_{ij}=1|\text{rest}] = \gamma(x'_{i-1,j}+x'_{i,j-1}) + \gamma^2 x'_{i+1,j-1} \tag{4.2.32}$$

where $x'_{ij} = x_{ij} - E[x_{ij}]$.

Notice γ is restricted to give $0 \leq P[x_{ij}=1|\text{rest}] \leq 1$.

4.3 Derivation of the Model

The following problem is studied in this section. Let $z(s)$ be a quantity which varies randomly in space, and the failure probability function $P_f(z)$ is a function of these variables. From these two pieces of information, we can obtain marginal failure probability at each point of space, $P_f(s)$. Our task here is to evaluate the failure probability of whole system (i.e., Φ_F) from this marginal failure probability field $P_f(s)$.

For example, let $z(s)$ be DF15/DB85 on core-filter interface plane. Since we have a failure probability function P_f(DF15/DB85), the distribution of marginal failure probability on the interface plane can be obtained, i..e, $P_f(s)$. The aim is to evaluate the probability of malfunctioning of filter at anywhere in this whole plane, Φ_F.

As mentioned earlier, we shall evaluate by introducing a binary random field $x(\underline{s})$ such taht $x(\underline{s}) = 1$ denotes filter malfunctioning at $\underline{s}$ and $x(\underline{s}) = 0$ denotes satisfactory performance at the same location. The expectation of $x(\underline{s})$

$$P_f(\underline{s}) = E[x(\underline{s})] \tag{4.3.1}$$

is the probability of malfunctioning at $\underline{s}$, whereas Φ_F is given by

$$\Phi_F = \text{Prob.}[x(\underline{s}) = 1 \text{ for some } \underline{s} \text{ in } S] \tag{4.3.2}$$

in which S denotes the spatial region of interest.

Our interest is mainly in the evaluation of Φ_F for S a region in 2-D space. For this purpose, we find it useful to model $x(\underline{s})$ through one of the binary random process introduced in the last section. We start by considering $\underline{s}$ to be points of a lattice and then take the limit as the spacing of the lattice goes to zero to generate a model in continuous space. For convenience, we begin with homogeneous fields, for which $P_{\underline{f}}(\underline{s}) = \overline{P}_{\underline{f}}$ is rate function of $\underline{s}$.

4.3.1 Homogeneous Field: $E[x(\underline{s})] = \text{const.}$

A rectangular lattice of m x n points is defined on the plane at each point (i,j) a binary random variable (i.e., 0 or 1) x_{ij} is defined under the present assumption of homogeneity

$$E[x_{ij}] = P[x_{ij} = 1] = \overline{P}_{\underline{f}} \qquad (4.3.3)$$

for all i j. It was mentioned in the last section that the two-sided conditional autoregressive binary model is one that corresponds to the logistic relationship:

$$E[x_{ij} | x_{i-1,j}, x_{i+1,j}, x_{i,j-1}, x_{i,j+1}]$$

$$= \frac{\exp[\{\alpha+\beta_1(x_{i-1,j}+x_{i+1,j})+\beta_2(x_{i,j-1}+x_{i,j+1})\}]}{1+\exp[\alpha+\beta_1(x_{i-1,j}+x_{i+1,j})+\beta_2(x_{i,j-1}+x_{i,j+1})]} \qquad (4.3.4)$$

The correlation structure of this model is very complicated

and the parameters α, β_1 and β_2 are difficult to estimate (see Section 4.2.3). Moreover, even if one could estimate α, β_1 and β_2 and kT in Eq. (4.2.21), one would find it difficult to calculate Φ_F because of the form of the joint distribution of the variables x_{ij}.

The difficulties of calculating Φ_F are similar to those encountered in parameter estimation and suggest that similar approximations might work.

Consider first the "coding method" by Besag (1974). Because of the defined, correlation structure of the model, the conditional system failure probability can be written as (see Fig. 4.3)

$$\Phi_F\big|_{\text{all "." sites are 0}}$$

$$= 1.0 - \prod_{i,j \text{ for all "x" sites}} P(x_{i,j}=0 \,|\, x_{i-1,j}=0, x_{i+1}=0, x_{i,1,j}=0, x_{i,j+1}=0) \tag{4.2.5}$$

In order to obtain the system failure probability, one needs the joint distribution of all "x" sites, which, unfortunately, is almost impossible to obtain from the available information. It seems, for our purpose, this method does not give very good results.

A more fruitful approach is to use one-sided approximations. Two such approximations were reviewed in Section

4.1.4. According to the simulation study of Bartlett and Besag (1969) there is not much difference between the two approximations and for this reason, we prefer here to work with the model of Eq. (4.1.23), which is simpler and more intuitive. Their model has the form

$$E[x_{ij}|x_{i-1,j}, x_{i,j-1}] = \alpha + \frac{1}{2}(\beta_1 x_{i-1,j} + \beta_2 x_{i,j-1}) \tag{4.3.6}$$

Taking expectation,

$$E[x_{ij}] = \alpha + \frac{1}{2}(\beta_1 E[x_{i=1,j}] + \beta_2 E[E_{i,j-1}])$$

and under the condition of homogenity,

$$\bar{P}_f = \alpha + \frac{1}{2}(\beta_1 + \beta_2)\bar{P}_f$$

Therefore,

$$\alpha = \{1 - \frac{1}{2}(\beta_1 + \beta_2)\ \bar{P}_f$$

The autocovariance function of this model can be obtained easily: multiply both sides of Eq. (4.3.6) by $x_{i-r,j-s}$,

$$E[x_{ij}|x_{i-1,j}, x_{i,j-1}]\ x_{i-r,j-s}$$

$$= \alpha x_{i-r,j-s} + \frac{1}{2}(\beta_1 x_{i-1,j} x_{i-r,j-s} + \beta_2 x_{ij-1} x_{i-r,j-s})$$

If expectation is taken of both sides, and with $W' = E[x_{ij}\ x_{i-r,j-s}]$,

$$W'_{rs} = \alpha\bar{P}_f + \frac{1}{2}(\beta_1 W'_{r-1,s} + \beta_2 W'_{r,s-1}).$$

This equation has solution

$$W'_{rs} = \bar{P}_f(1 - \bar{P}_f)\ \beta_1^r\ \beta_2^s + \bar{P}_f^2$$

The autocovariance function $W_{rs} = \text{Cov}[x_{ij}, x_{i-r,j-s}]$ is related to W'_{rs} and P_f was

$$W_{rs} = E[x_{ij}\ x_{i-r,j-s}] - \{E[x_{ij}]\}^2$$

$$= W'_{rs} - \bar{P}_f^2 .$$

Therefore,

$$W_{rs} = \bar{P}_f(1 - \bar{P}_f)\ \beta_1^2\ \beta_2^s \qquad (4.3.8)$$

according to Eq. (4.3.8) β_1 and β_2 have a straightforward physical interpretation: these parameters give the one-step correlation of the process in the direction of the two indices of the lattice. Also the correlation structure shows an exponential decay as one might expect from having assumed a Markov definition of order 1. This simple interpretation of β_1 and β_2 makes it easier to estimate such parameters.

Suppose that β_1 and β_2 have been estimated either by statistical means or judgmentally since $\bar{P}_f$ is also given, one can calculate α from Eq. (4.3.7). This defines completely the model.

The failure probability for the system of m x n lattice points can be found as follows:

$$\Phi_F = 1 - P\,[\,x_{ij}=0 \text{ for all } i=1,\ldots m; j=1,\ldots n]$$

$$= 1-(1-\bar{P}_f)\{1-\bar{P}_f(1-\beta_1)\}^{m-1}\{1-\bar{P}_f(1-\beta_2)\}^{n-1}$$

$$\cdot\{1=\bar{P}_f(1 - \frac{\beta_1+\beta_2}{2})\}^{(m-1)(n-1)} \qquad (4.3.9)$$

Note that Eq. (4.3.9) make the following approximations along the bottom and left boundaries of the lattice (see Fig. 4.4):

$$E\,[\,x_{il}|x_{i-1,1}] = \alpha + \beta_1\, x_{i-1,1} \qquad (4.3.10a)$$

$$E\,[\,x_{1j}|x_{1,j-1}] = \alpha + \beta_2 x_{1,j-1} \qquad (4.3.10b)$$

which imply one sided Markov series with correlation coefficients β_1 and β_2 are assumed along the boundaries.

Finnaly, we consider the limit of Eq. (4.3.9) as the number of lattice points is increased to infinity within thc region of interest. More precisely, we first consider

$$\Phi_F(k,\ell) = 1-\{1-\bar{P}_f(1-\beta_1^k)\}^{\frac{m}{k}-1}\cdot\{1-\bar{P}_f(1-\beta_2^{\ell})\}^{\frac{m}{\ell}-1}$$

$$\cdot\,[\,1-\bar{P}_f\{1-\tfrac{1}{2}(\beta_1^k+\beta_2^{\ell})\,]^{\frac{m}{k}-1)(\frac{n}{\ell}-1)}\cdot(1-\bar{P}_F) \qquad (4.3.9')$$

where $1/k$ and $1/\ell$ are the number of points between the

original lattice points in the horizontal and vertical direction, respectively. As $k \to 0$ and $\ell \to 0$, the last equation becomes (for detailed derivation, see Appendix B):

$$\Phi_F = 1 - \{\beta_1^{m\bar{P}_f} \cdot \beta_2^{n\bar{P}_f} \exp\left[-nm\left(\frac{\bar{P}_f}{2}\right)^2 \ell n\beta_1 \ell n\beta_2\right]\}(1-\bar{P}_f) \tag{4.3.11}$$

$\beta_1^{n\bar{P}_F}$ and $\beta_2^{m\bar{P}_F}$ come from the boundaries, whereas exp [·] term results from the inside lattice. $(1-\bar{P}_f)$ is the marginal nonfailure probability of the initial point. Under conditions of symmetry with respect to the two axes (i.e., for $\beta_1=\beta_2=\beta$) Eq. (4.3.11) gives

$$\Phi_F = 1 - \{\beta^{(m+n)\bar{P}_f} \exp\left[-mn\left(\frac{\bar{P}_f}{2}\ell n\beta\right)^2\right]\}(1-\bar{P}_f) \tag{4.3.12}$$

The condition $\beta_1=\beta_2$ does not correspond to exact isotropy as will be mentiond later. For 1-D conditions (i.e., $\beta_2=1$), Eq. (4.3.11) gives

$$\Phi_F = 1 - \beta_1^{m\bar{P}_f}(1 - \bar{P}_f) \tag{4.3.13}$$

Some calculated results based on Eq. (4.3.12) are presented in Fig. 4.5(a)-(c): the results are for a square are (L x L) for $\bar{P}_f = 10^{-2}$, 10^{-3} and 10^{-4} respectively. All three figures exhibit similar results. If $\beta = 1.0$, the whole area acts as one element. Therefore, Φ_F is identical with $\bar{P}_f$. On the other hand, if $\beta = 0.0$, the system acts just the same as a chain consists of infinite numbers of links; as a result, $\Phi_F = 1.0$. It is very

interesting to see the system failure probability, Φ_F, is much influenced by β even for very low β (e.g., 0.1 or 0.5). Some numerical simulation results are presented in the next section.

The model developed here will be used in evaluating malfunctioning of filters of a dam in the case study.

4.3.2 Non-homogeneous Field

Suppose now that

$$E[x_{ij}] = P_{fij} \tag{4.3.14}$$

i.e., that the probability of filter malfunctioning depends on the location (i,j). In this case the random field x_{ij} is nonhomogeneous. The objective is to obtain the failure probability of the system, Φ_F, through generalization of Eq. (4.3.11).

Although the marginal failure probability fluctuates in space, we assume for simplicity that the correlation structure is homogeneous. This should be a reasonable approximation. In the case of nonhomogeneous fields, we use a one-sided approximation of the type

$$E[x_{ij}|x_{i-1,j}, x_{i,j-1}] = (\alpha+\alpha_{ij}) + \frac{1}{2}(\beta_1 x_{i-1,j} + \beta_2 x_{i,j-1}) \tag{4.3.14}$$

where α, β_1, β_2 are auto-regressive coefficients for the homogeneous component of the model.

α_{ij} is a function of space such that

$$\sum_{i=2}^{m} \sum_{j=2}^{m} \alpha_{ij} = 0 \qquad (4.3.15)$$

Taking expectation of both sides of Eq. (4.3.14) with respect to $x_{i-1,j}$ and $x_{i,j-1}$, one obtain

$$E[x_{ij}] = \alpha + \alpha_{ij} + \frac{1}{2}(\beta_1 E[x_{i-1,j}] + \beta_2 E[x_{i,j-1}])$$

i.e.,

$$P_{fij} = \alpha + \alpha_{ij} + \frac{1}{2}(\beta_1 P_{fi-1,j} + \beta_2 P_{fi,j-1}) \qquad (4.3.16)$$

In order to obtain the homogeneous portion of the field, Eq. (4.3.16) is averaged over space; indicating this averaging by a bar,+

$$\bar{P}_f = \alpha + \frac{1}{2}(\beta_1 + \beta_2)\bar{P}_f \qquad (4.3.17)$$

where $$\bar{P}_f = \sum_{i=1}^{m} \sum_{j=1}^{n} P_{f\,i,j} \qquad (4.3.18)$$

Therefore,

+There is a slight inconsistency among Eqs. (4.3.15), (4.2.17) and (4.2.18) due to boundary effects. The inconsistency is negligible if the lattice under consideration is large enough. Since we are ultimately interested in the continuous model (i.e., a lattice with infinite points), this inconsistency is not of concern.

$$\alpha = \{1 - \frac{\beta_1 + \beta_2}{2}\} \bar{P}_f \qquad (4.3.19)$$

It is assumed that the homogeneous portion has the same covariance function as the homogeneous field case, i.e.,

$$W_{rs} = \bar{P}_f (1 - \bar{P}_f) \beta_1^r \beta_2^s \qquad (4.3.20)$$

The non-homogeneous component can be calculated by subtracting Eq. (4.3.17) from Eq. (4.3.16):

$$(P_{f\ i,j} - \bar{P}_f) = \alpha_{ij} + \frac{1}{2}\{\beta_1 (P_{fi-j,j} - \bar{P}_f) + \beta_2 (P_{fi,j-1} - \bar{P}_f)\} \qquad (4.3.21)$$

If one defines $P'_{fi,j}$ as

$$P'_{f\ ij} = P_{f\ i,j} - \bar{P}_f$$

then one can obtain α_{ij} from

$$\alpha_{ij} = P'_{fi,j} - \frac{1}{2} (\beta_1 P'_{fi-1,j} + \beta_2 P'_{f\ i,j-1}) \qquad (4.3.22)$$

The failure probability of the system, Φ_F, can be obtained following the same procedure as in the homogeneous case (Fig. 4.4):

$$\Phi_F = 1.0 - (1 - P_{f0,0}) \prod_{i=2}^{m} \{1 - (\alpha + \alpha_{i1})\} \{ \prod_{j=2}^{n} \{1 - (\alpha + \alpha_{1j})\}$$

$$\cdot \prod_{i=2}^{m} \prod_{j=2}^{n} \{1 - (\alpha + \alpha_{ij})\}$$

$$= 1.0 - \prod_{i=1}^{m} [\, 1.0 - \{\bar{P}_f (1 - \beta_1) + (P'_{fi,j1} - \beta_2 P'_{fi-1,1})\}]$$

$$\cdot \prod_{j=1}^{n} [\, 1.0 - \{\bar{P}_f(1-\beta_2) + (P'_{f1,j} - \beta_2 P'_{f1,j-1})\}]$$

$$\cdot \prod_{i=2}^{m} \prod_{j=2}^{n} [\, 1.0 - \{\bar{P}_f(1 - \frac{\beta_1+\beta_2}{2}) + P'_{fij} - \frac{1}{2}(\beta_1 P'_{fi-1,j} + \beta_2 P'_{fi,j-1})\}$$

$$\cdot (1 - \bar{P}_f - P'_{f1,1}) \qquad (4.3.23)$$

In deriving Eq. (4.3.28), dependencies along the boundaries have been assumed to be of the form

$$E[\, x_{i,1} | x_{i-1,1}] = (\alpha + \alpha_{i1}) + \beta_1 \, x_{i-1,1} \qquad (4.3.24a)$$

$$E[\, x_{1,j} | x_{1,j-1}] = (\alpha + \alpha_{ij}) + \beta_2 x_{1,j-1} \qquad (4.3.24a)$$

The limit of Eq. (4.3.23) is calculated following the same procedure as in the homogeneous case (see Appendix B for the derivation). Note that some additional (but minor) assumptions are necessary due to non-homogeneity of the field. The final result is

$$\Phi_F = 1.0 - [\, (1-P_{00}) \beta_1^{\bar{P}_f m} \beta_2^{\bar{P}_f n} \exp[\, \tfrac{1}{2} \bar{P}_f^2 mn \ln\beta_1 \ln\beta_2]$$

$$\cdot \{1-(P'_f(m,o) - P'_f(0,0))\}\{1-(P'_f(o,n) - P'_f(0,0))\}$$

$$\cdot [\, 1 - \tfrac{1}{2}\{\int_o^m P'_f(x,m)\,dx + \int_o^m P'_f(m,y)\,dy$$

$$- \int_o^m P'_f(x,0)\,dx - \int_o^n P'_f(0,y)\,dy\}] \qquad (4.3.25)$$

The first portion of Eq. (4.3.25) is exactly the same as Eq. (4.3.11), which is the solution for the homogeneous field. The next two terms account for the nonhomogeneous effect along the boundary, and the last term account for that of the inside lattice.

4.4 Numerical Simulation and Discussion

In order to study the properties of the model proposed in the last section, a simple numerical simulation program has been written. Focus has been mainly on two problems:

(i) The relationship between the degree of spatial correlation (i.e., β_1 and β_2) and the average size of the failure zones here are often called "patches".

(ii) The influence of the one-sided approximation on the results and specifically on departure from isotropy.

A flow chart of the numerical simulation procedure is shown in Fig. 4.6. The correlation model used to generate the bottom and the left boundaries of the lattice is the same as that explained earlier while deriving the model (see Eq. 4.3.10)).

Some simulation results are shown in Figs. 4.7(a)-(e) for 50 x 50 lattices, a point failure probability of 0.05,

and for different β_1 and β_2.

Figures 4.7(b) and (c) have (nearly) isotropic correlation structures. As β becomes larger, the average size of the patches increases. There is some discrepancy between the probability $\overline{P}_f$ and the fraction of area where $x_{ij} = 1$. This discrepancy is larger for the larger β and is due to the relatively small size of the simulation region.

Figures 4.7(d) and (e) show cases with anisotropic correlation. In this case, the patches are elongated in the direction with larger β.

Table 4.1 presents results from simulations on 200 x 200 lattices, with Pf = 0.01 and five different values of $\beta_1 = \beta_2 = \beta$. The average area of the patches increases in approximately an exponential way with β^2.

In order to study the anisotropy introduced by the one-sided approximation, zones and sizes are analyzed. In particular, we consider the pattern of five grid points in Fig. 4.8. Each point of the pattern has a letter associated with it. The pattern is identified by a string of 0's and 1's in the order (j,k,l,m); for example (0,1,0,0) correspond to 0's at points j,ℓ and m, and 1 at point k. The number assigned to i is given separately.

The idea of studying these patterns to test anisotropy is that, if one counts, patterns which include the same

number of 0's and 1's, such as (1,0,0,0), (0,1,0,0), (0,0,1,0) and (0,0,0,1), for i=1 and i=0, the number of times each pattern is generated should be nearly the same for all patterns if the generated lattice is large enough and if it is isotropic.

Figures 4.9(a)-(c) show such results. Figure 4.9(a) refers to the case when $\overline{P}_f = 0.10$ and $\beta_1 = \beta_2 = 0.1$; the size of the lattice is 200 x 200. In this case, the frequencies of realizations for the patterns with the same number of 0's (or 1's) are nearly the same, which is an indication of near isotropy. However, Figs. 4.9(b) and (c)(for which $\beta = 0.5$ and $\beta = 0.9$ respectively), display some degree of anisotropy. Anisotropy is more pronounced for Fig. 4.9(c) due to the higher value of $\beta(=0.9)$ and is stronger for patterns that include two 1's. In particular, there is a relatively high frequency of (0,0,1,1) and (1,1,0,0) cases for both i=0 and 1. This is due to the high correlation between k and j, and between m and ℓ in the one-sided approximation. In patterns with three i's, anisotropy is less pronounced.

Another way to visualize anisotropy is to use the average projection of the patches for different values of β. Their average projections are shown in Fig. 4.10. Note that the scale is the same for all five cases in the figure. As β increases, the average size of the patches increases and their shape becomes less circular.

One may conclude that the anisotropy induced by the one-sided scheme is not significant if the correlation is weak (say, for $\beta < 0.7$); whereas if β is high then the patches tend to be elongated.

4.5 Summary and Conclusions

A dam filter is considered not to perform properly if it "fails" at least one point. This is the basic notion behind the proposed weakest link model. For the purpose of calculating the probability of failure of the system, Φ_F, a binary indicator random field, $x(\underline{s})$, is introduced whose mean value gives the probability of local malfunctioning. In terms of $x(\underline{s})$, failure probability Φ_F, is

$$\Phi_F = \text{Prob. } [\, x(\underline{s}) = 1 \text{ for some } \underline{s} \varepsilon S]$$

where S is the spatial extent of the filter (a range of the core-filter interface plane).

Binary random fields $x(\underline{s})$ on 2-D lattices are studied first. Some of the difficulties in describing and analyzing these models are reviewed in some detail, and one-sided approximations are introduced to make the model tractable. Finally, properties of indicator random fields in continuous space are derived through limiting operation. The models are specified in terms of only few parameters, which control the local probability of failure and the

degree of correlation in space of the random field $x(\underline{s})$. The latter is related to size and spacing of failure "patches". Homogeneous models are considered first and then extensions are made to non-homogeneous models. The latter allows one to analyze cases in which the probability of filter malfunctioning depends on spacial location.

The consequences of the one sided approximation in particular anisotropy are studied through numerical simulations. The present model will be used in Appendix C to quantify the reliability of filter systems for a particular dam.

TABLE 4.1 CORRELATION COEFFICIENT VS. SIZE OF PATCHES

Items	β	0.1	0.3	0.5	0.7	0.9
Estimated Failure Probability		0.00895	0.00965	0.00975	0.0084	0.0087
Average size of patches		1.14	1.55	2.17	3.21	10.58
Total number of patches		323	259	183	107	33

Simulation Conditions: Mean Probability of Failure ($\bar{P}_f$) = 0.01

Correlation Isotropic: $\beta=\beta_1=\beta_2$

200 x 200 Lattice generated

(a) Ordinary Weakest Link Model

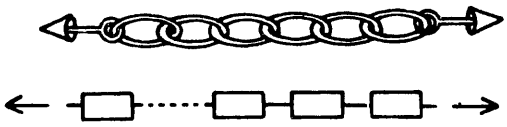

$$\Phi_F = 1.0 - \prod_{i=1}^{N} (1.0 - P_{fi})$$

where Φ_F: the System Failure Probability

P_{fi}: Failure Probability of i th Link

Extention to Continuous Space

(b) 1 - Dimension (e.g. strength of a string)

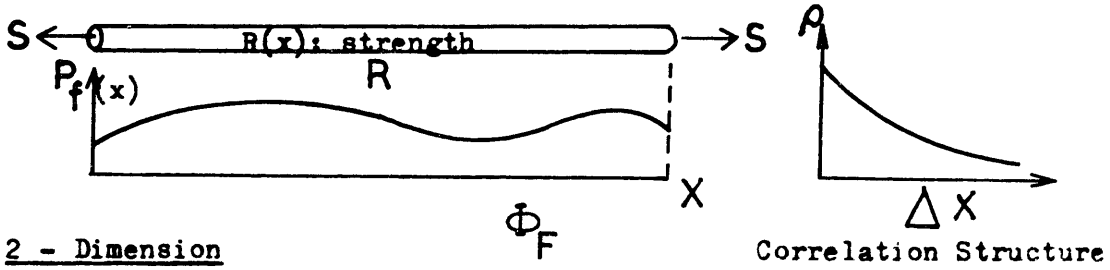

(c) 2 - Dimension

(e.g. Piping Potential on Core-Filter Interface)

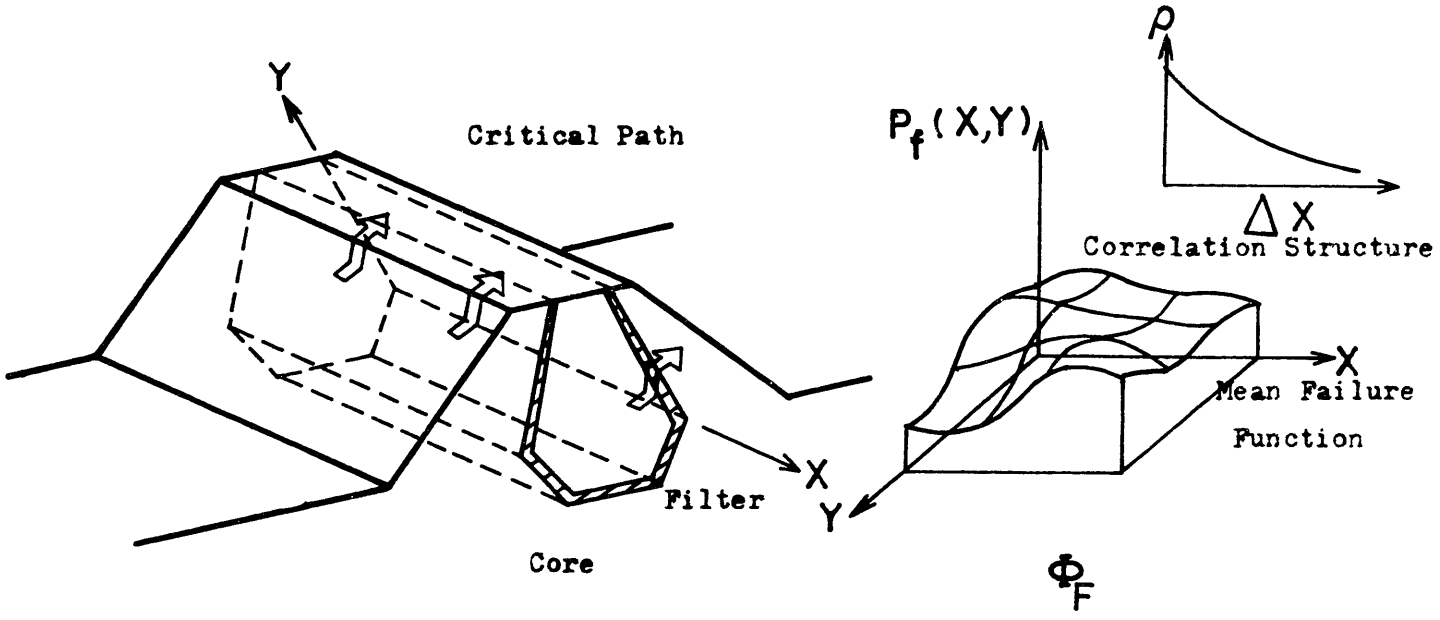

Fig. 4.1 Procedure to Calculate the Probability of Malfunctioning of the Filter System

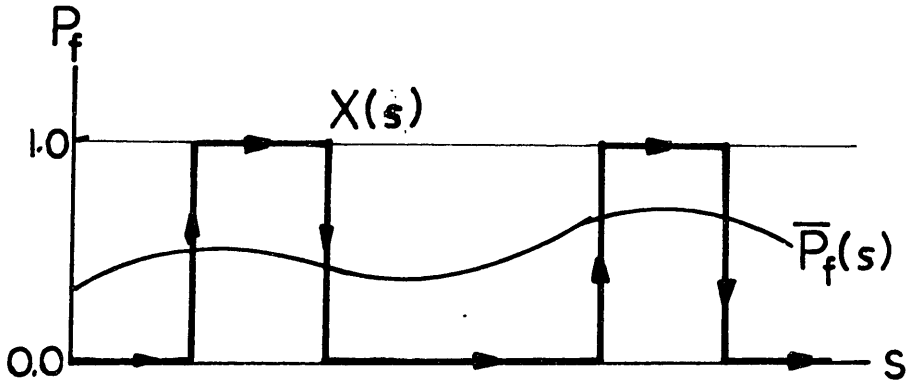

Fig. 4.2 Binary Process with Given Mean Value Function

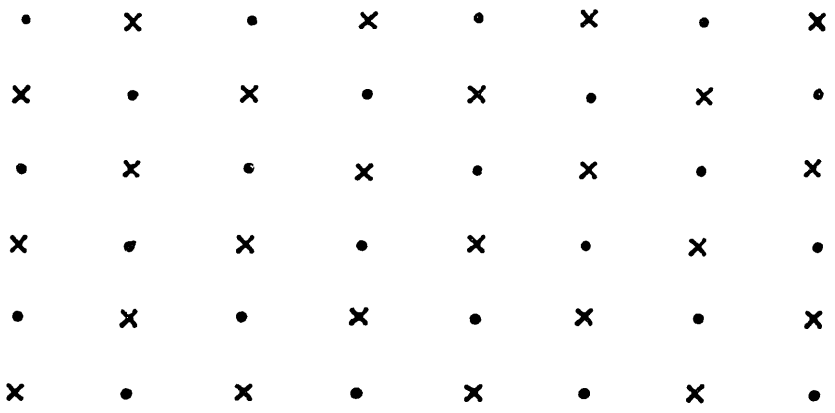

Fig. 4.3 Coding Pattern for a Nearest Neighbour Scheme

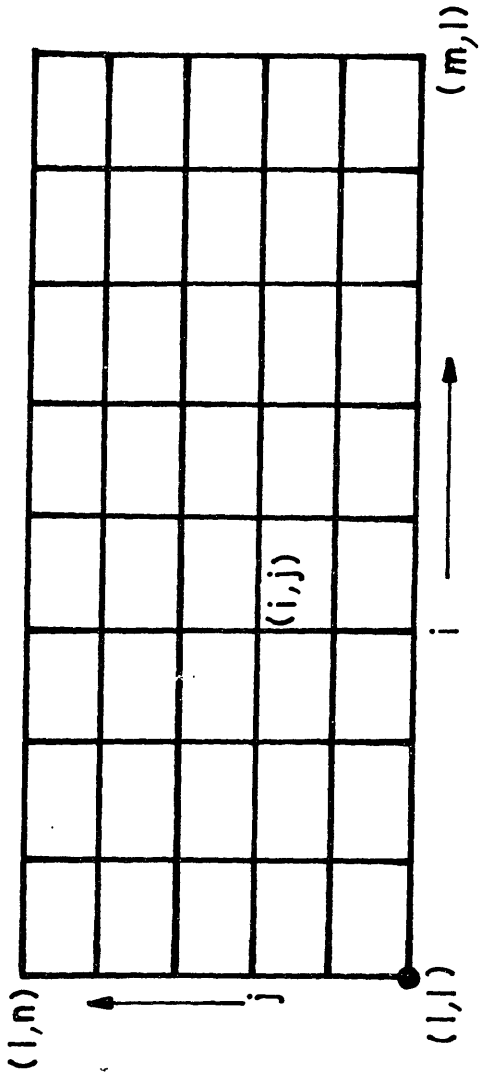

Fig. 4.4 Initial and Boundary Condition for One-sided Approximation

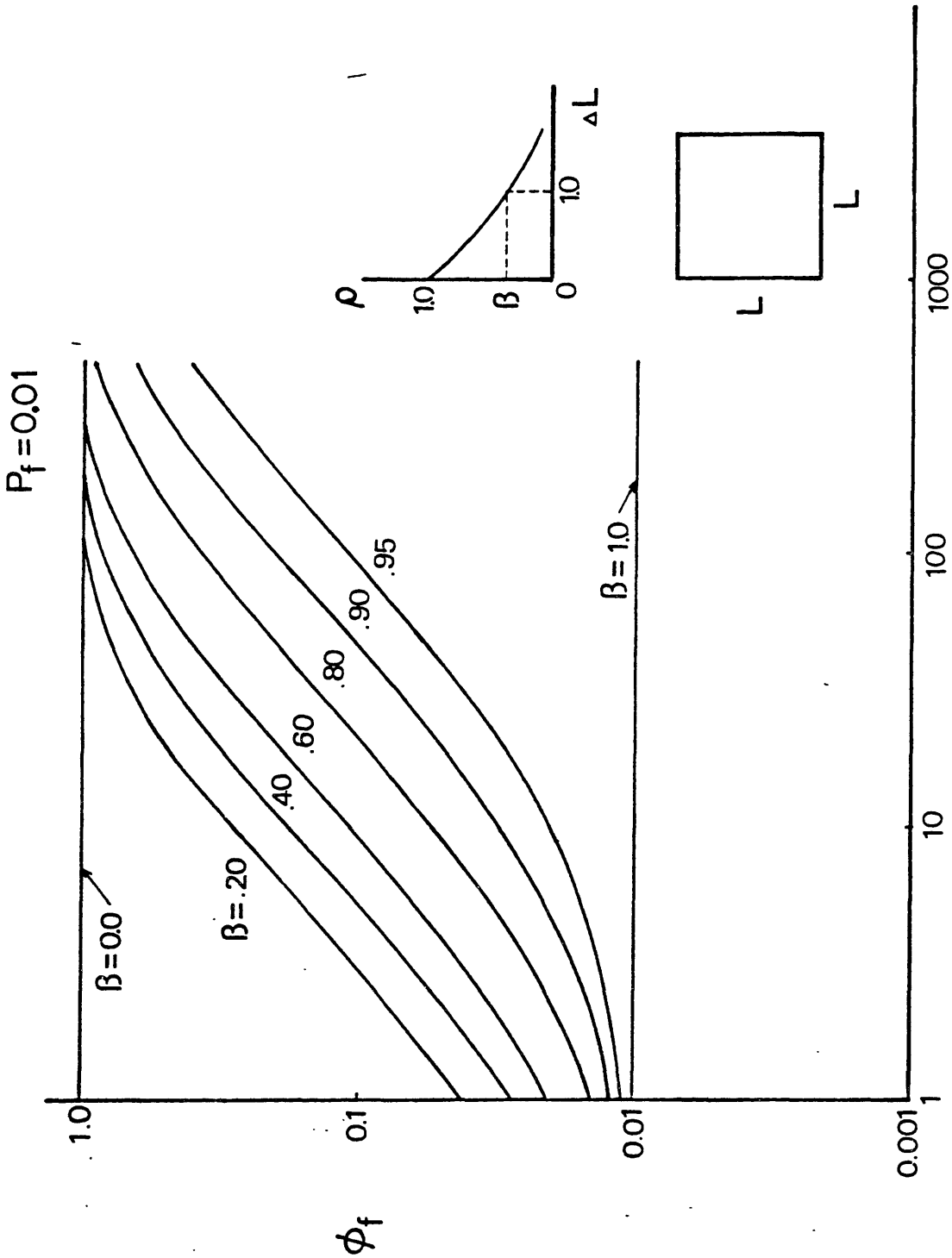

Fig. 4.5 (a) System Failure Probability for a Homogeneous Square Area $P_f = 10^{-2}$

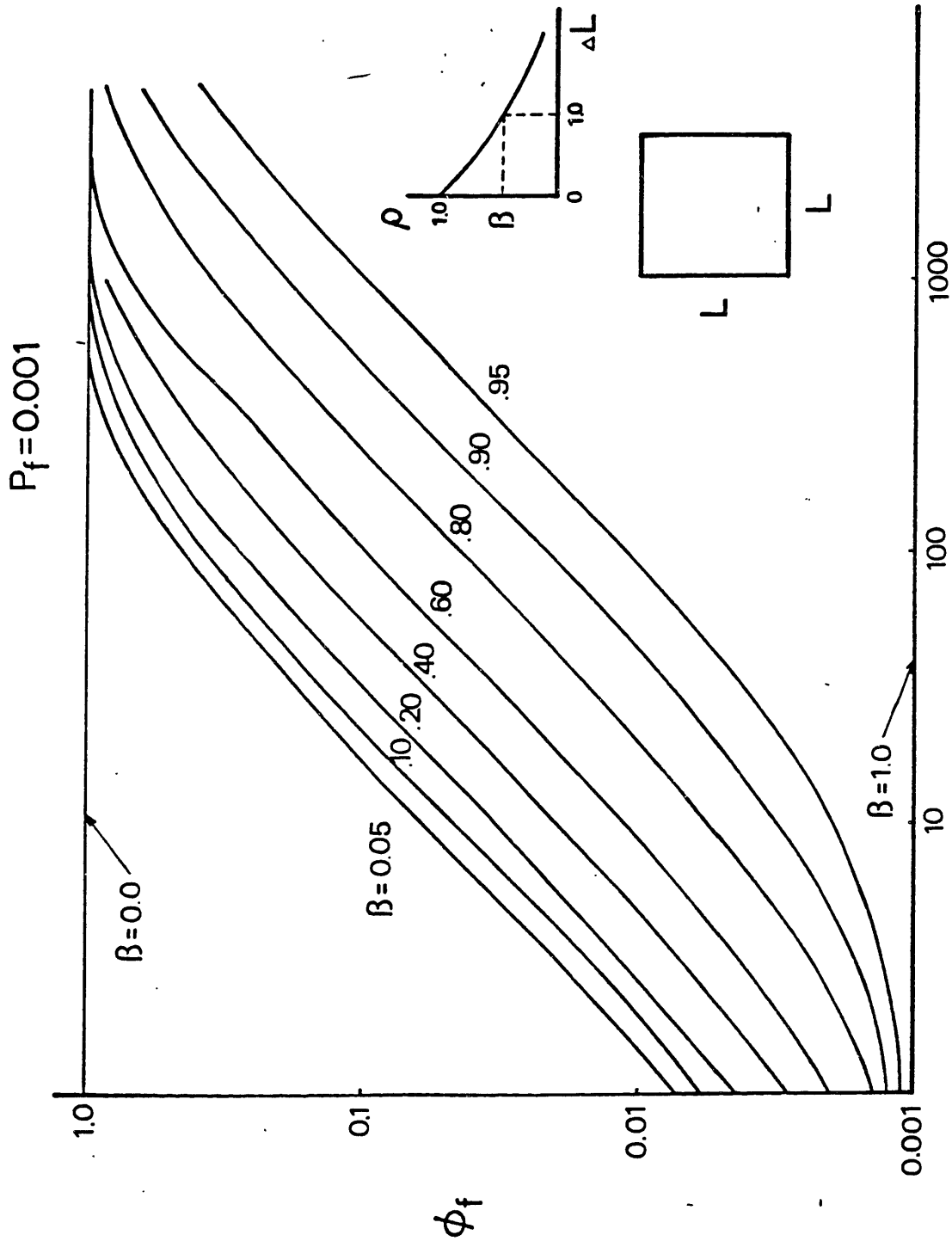

Fig. 4.5 (b) System Failure Probability for a Homogeneous Square Area $P_f = 10^{-3}$

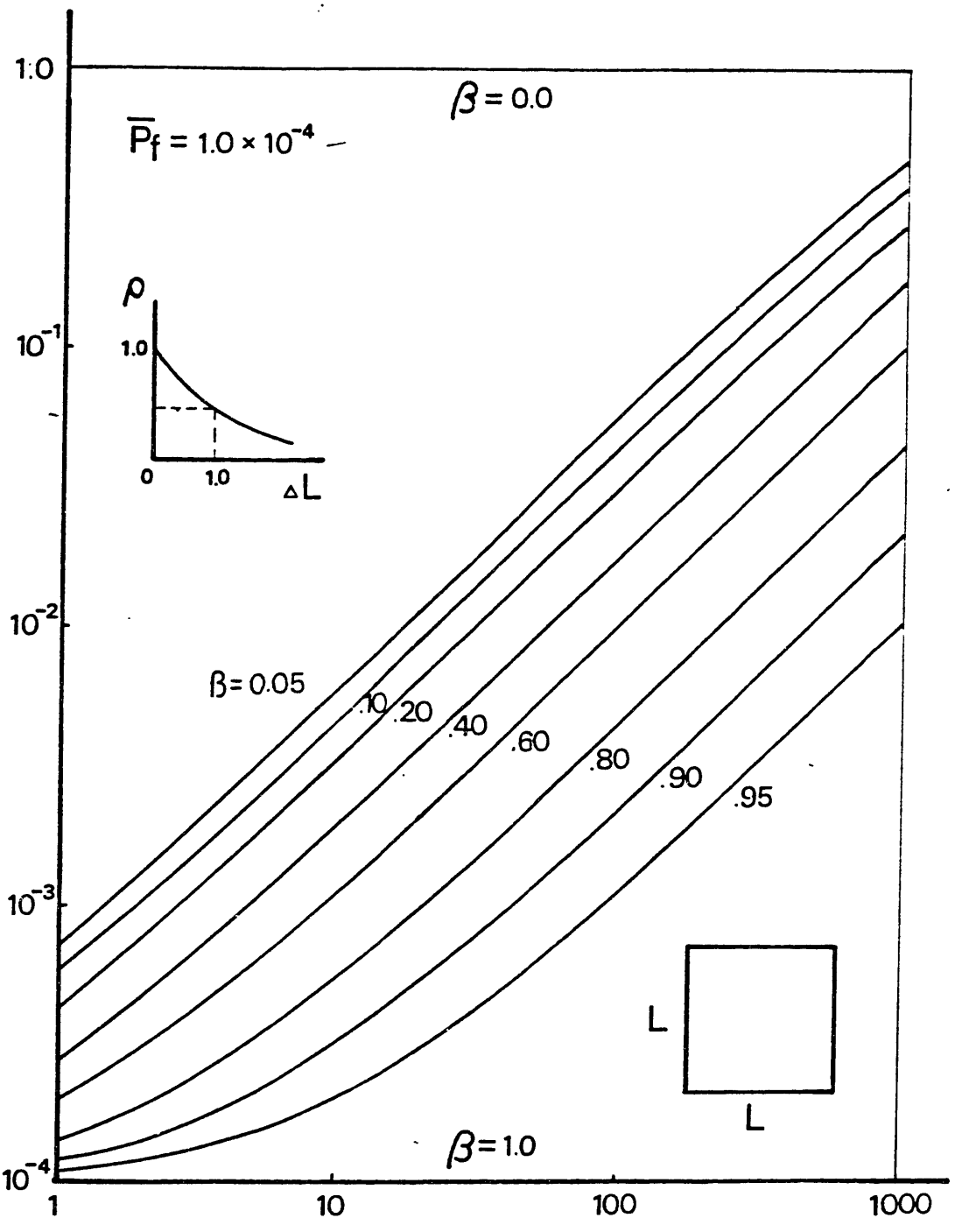

Fig. 4.5 (c) System Failure Probability for a Homogeneous Square Area $P_f = 10^{-4}$

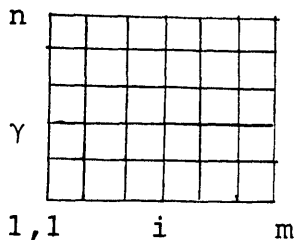

Step 1: Data Input; $\bar{P}_F$, β_1, β_2, m, n

Step 2: Generation of the Initial Point

If Random > $\bar{P}_F$, x(1,1) = 0

Otherwise , x(1,1) = 1

Step 3: Generation of Horizontal Boundary (i Boundary)

$$P_{FH} = (1-\beta_1)P_F + \beta_1 x(i-1,1)$$

If Random $\geq P_{FH}$ x(i,1) = 0

Otherwise x(i,L) = 1 $i \varepsilon [2,m]$

Step 4: Generation of Vertical Boundary (j Boundary)

$$P_{FV} = (1-\beta_2)\bar{P}_F + \beta_2 x(1,i-1)$$

If Random $\geq P_{FV}$ x(1,j) = 0

Otherwise x(1,j) = 1 $j \varepsilon [2,n]$

Step 5: Generation of Main Part

$$P_F = (1 - \frac{1}{2}(\beta_1 + \beta_2))\bar{P}_F + \frac{1}{2}\beta_1 x(i-1,j) + \frac{1}{2}\beta_2 x(i,j-1)$$

If Random $\geq P_F$ x(i,j) = 0

Otherwise x(i,j) = 1 $i \varepsilon [2,m]$

$j \varepsilon [2,m]$

Step 6: Output the results

Step 7: Stop

Note: "Random" is a random number generator in [0,1].

FIGURE 4.6 FLOW CHART FOR NUMERICAL SIMULATION OF THE BINARY PROCESS ON A LATTICE BY ONE-SIDED APPROXIMATION

N1 = 50 Beta1 =0.100
N2 = 50 Beta2 =0.100
Mean Probability of Failure =0.05000
Estimated Pf from the sample=0.05240

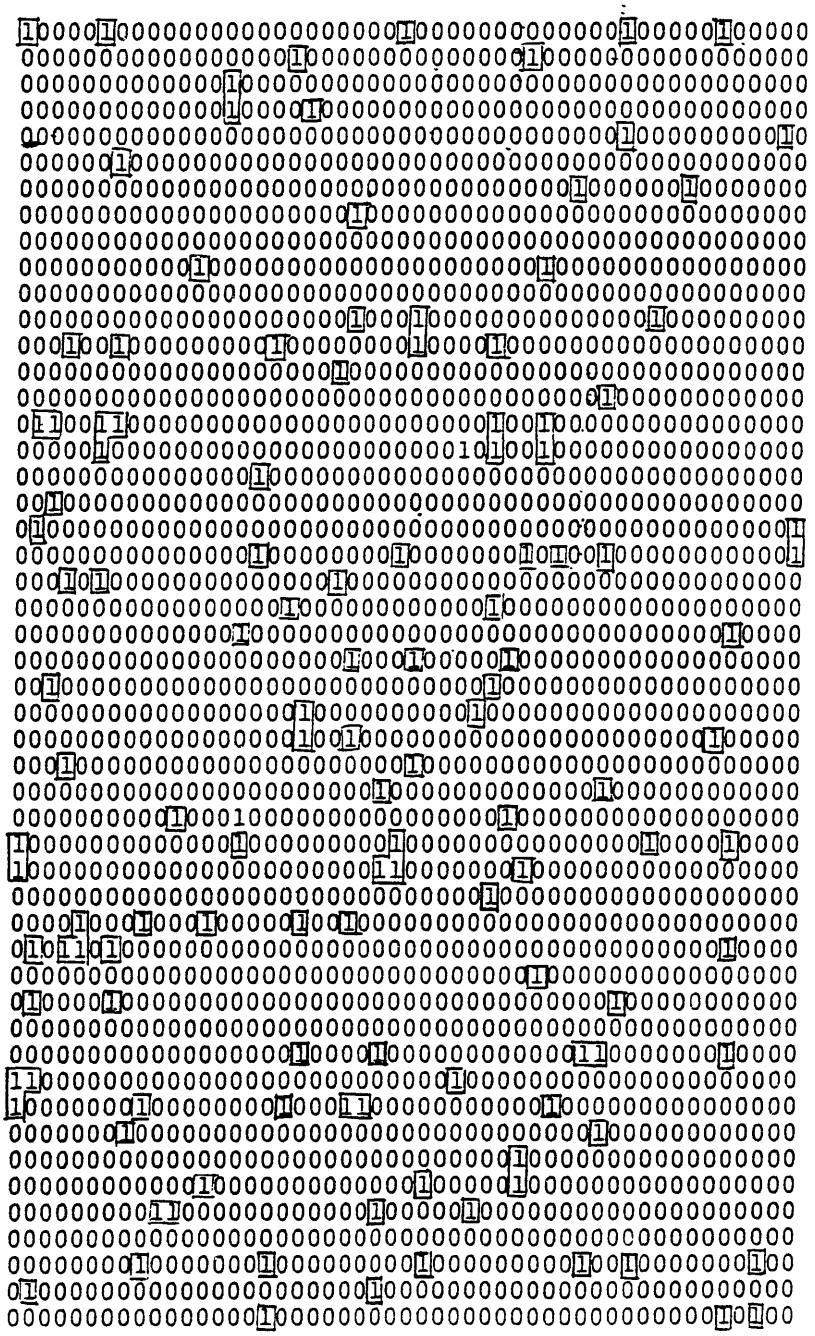

Fig. 4.7 (a) Results of Numerical Simulation:
$P_f = 0.05, \beta_1 \beta_2 = 0.1$

N1 = 50 Beta1 =0.500
N2 = 50 Beta2 =0.500
Mean Probability of Failure =0.05000
Estimated Pf from the sample=0.05520

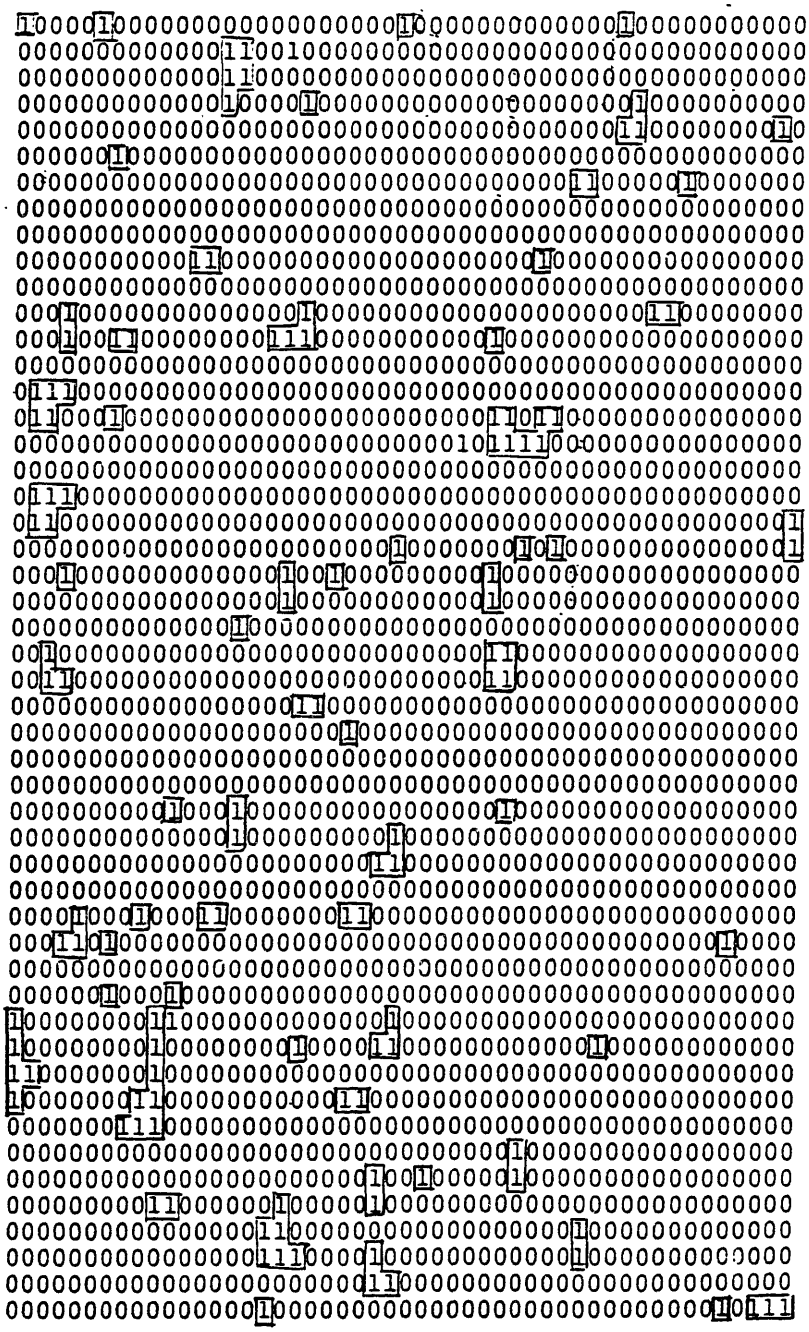

Fig. 4.7 (b) Results of Numerical Simulation:

$$P_f = 0.05, \beta_1 = \beta_2 = 0.5$$

N1 = 50 Beta1 =0.900
N2 = 50 Beta2 =0.900
Mean Probability of Failure =0.05000
Estimated Pf from the sample=0.03440

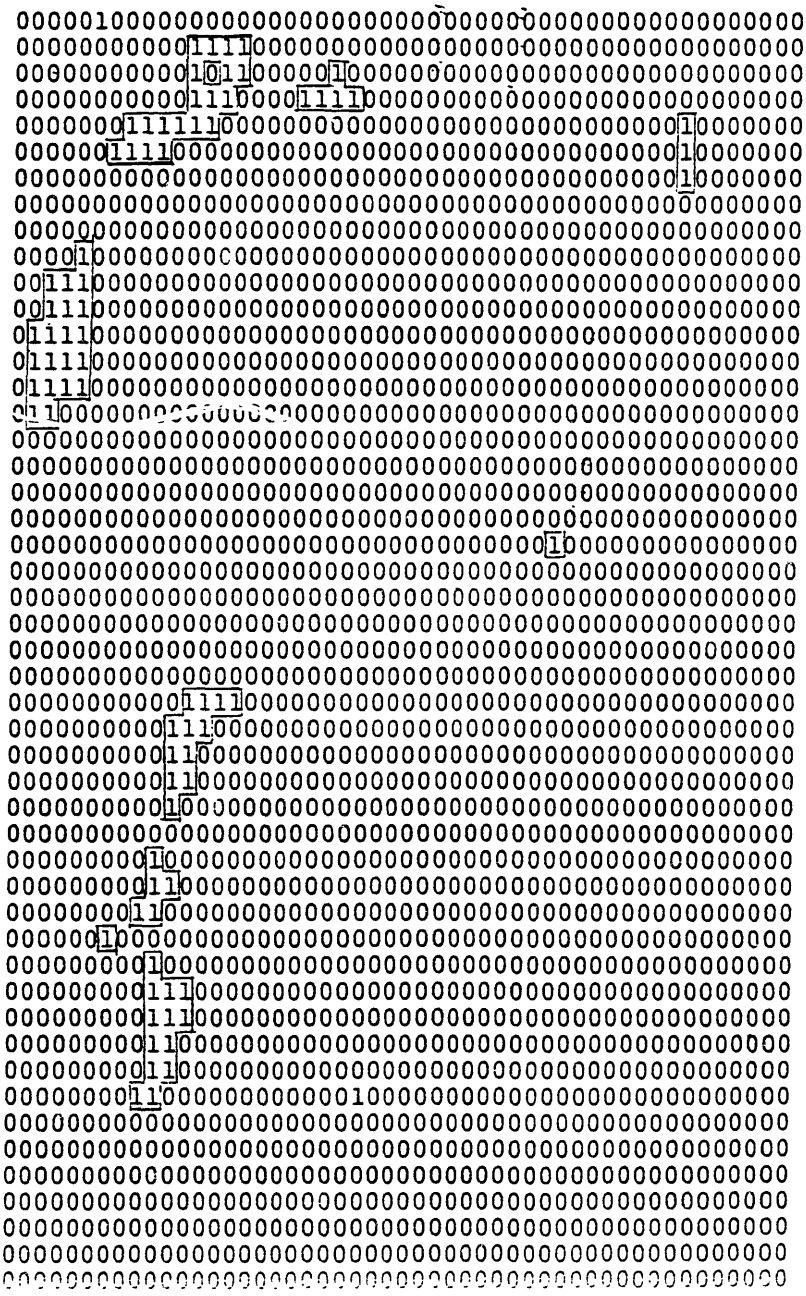

Fig. 4.7 (c) Results of Numerical Simulation:

$$P_f = 0.05, \beta_1 = \beta_2 = 0.9$$

N1 = 50 Beta1 =0.950
N2 = 50 Beta2 =0.100
Mean Probability of Failure =0.10000
Estimated Pf from the sample=0.09880

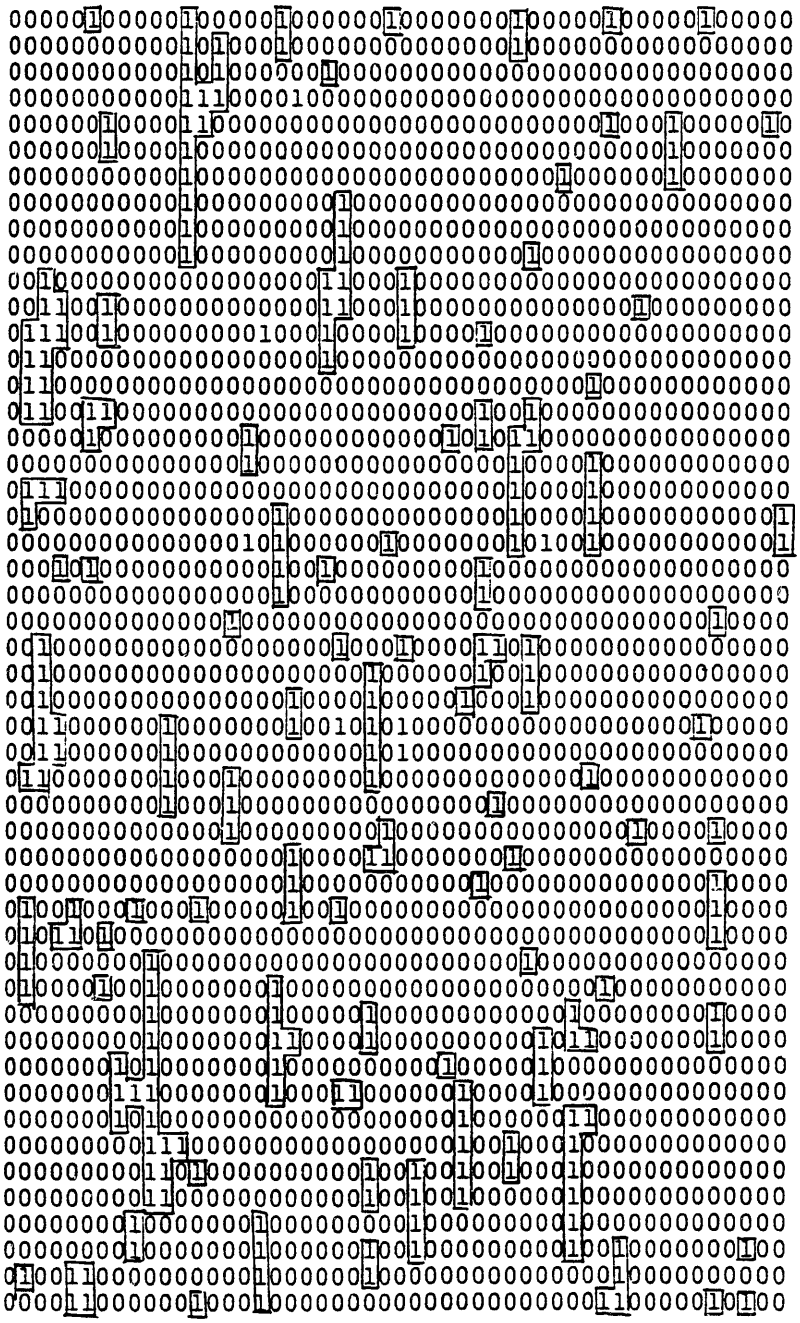

Fig. 4.7 (d) Results of Numerical Simulation:
$P_f = 0.10, \beta_1 = 0.95, \beta_2 = 0.1$

N1 = 50 Beta1 =0.100
N2 = 50 Beta2 =0.950
Mean Probability of Failure =0.10000
Estimated Pf from the sample=0.10800

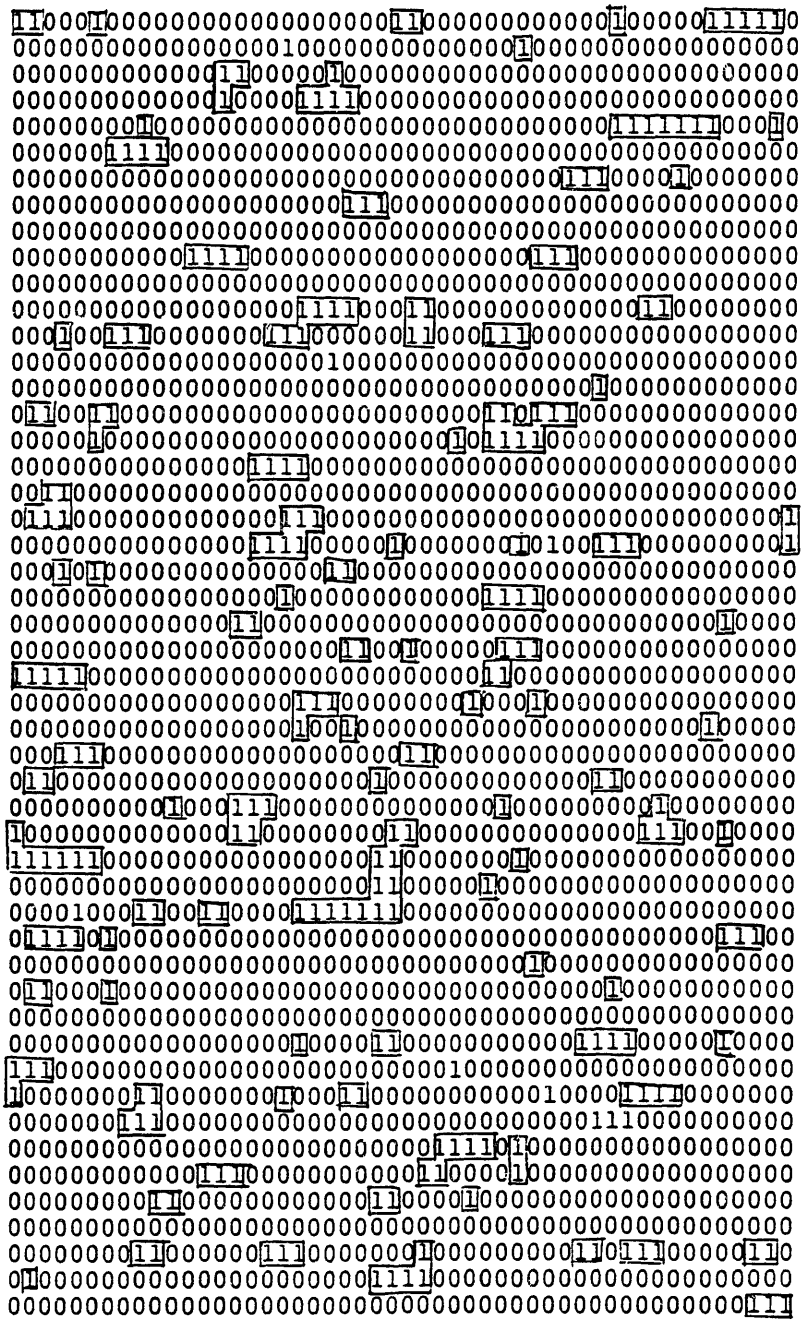

Fig. 4.7 (e) Results of Numerical Simulation:
$P_f = 0.10, \beta_1 = 0.10, \beta_2 = 0.95$

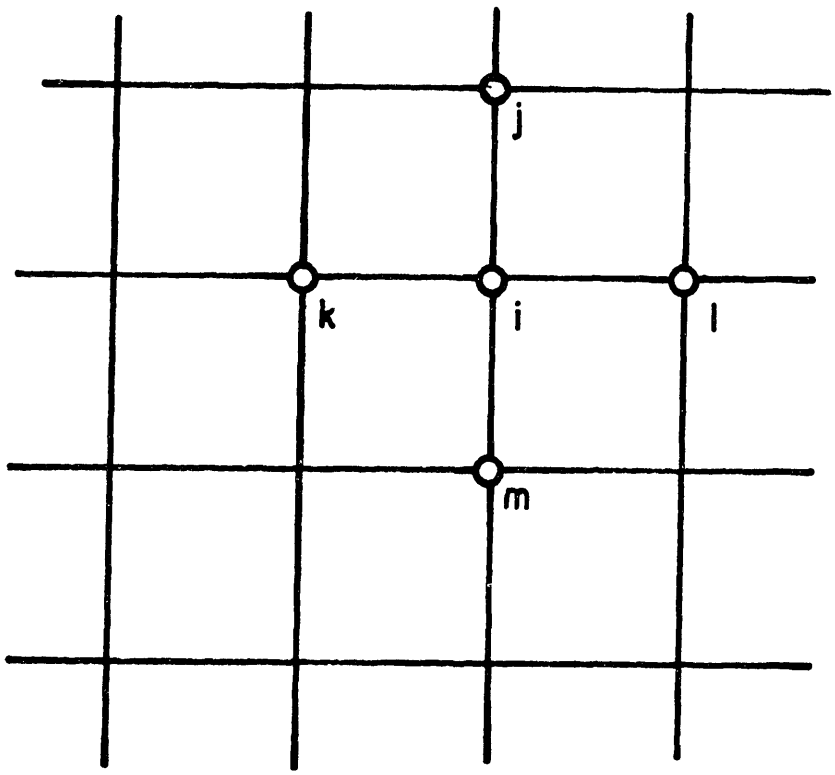

Fig. 4.8 Pattern of Grid Points Used in Testing Anisotropy of the Model

N1 = 200 Beta1 =0.100
N2 = 200 Beta2 =0.100
Mean Probability of Failure =0.10000
Estimated Pf from the sample=0.09980

j
k i l
m

j	k	l	m / i = 0	1	Total
0	1	0	0	2427	364	2791
0	0	0	1	2484	350	2834
0	0	1	0	2429	364	2793
1	0	0	0	2458	374	2832
0	1	0	1	270	62	332
0	1	1	0	270	59	329
0	0	1	1	249	68	317
1	1	0	0	279	63	342
1	0	0	1	228	66	294
1	0	1	0	282	54	336
0	1	1	1	32	14	46
1	1	0	1	23	7	30
1	1	1	0	27	7	34
1	0	1	1	30	9	39
0	0	0	0	23808	2042	25850
1	1	1	1	3	2	5

Fig. 4.9 (a) Results of Simulation to Test Approximation
Induced Anisotropy: $P_f = 0.10$, $_1 = _2 = 0.10$

N1 = 200 Beta1 =0.500
N2 = 200 Beta2 =0.500
Mean Probability of Failure =0.10000
Estimated Pf from the sample=0.09618

j
k i l
m

j	k	l	m / i = 0	1	Total
0	1	0	0	1801	388	2189
0	0	0	1	1810	392	2202
0	0	1	0	1903	317	2220
1	0	0	0	1844	368	2212
0	1	0	1	198	146	344
0	1	1	0	132	181	313
0	0	1	1	255	249	504
1	1	0	0	296	250	546
1	0	0	1	118	180	298
1	0	1	0	134	164	298
0	1	1	1	21	87	108
1	1	0	1	30	67	97
1	1	1	0	14	94	108
1	0	1	1	20	113	133
0	0	0	0	26861	702	27563
1	1	1	1	7	62	69

Fig. 4.9 (b) Results of Simulation to Test Approximation Induced Anisotropy: $P_f = 0.10$, $_1 = _2 = 0.50$

N1 = 200 Beta1 =0.900
N2 = 200 Beta2 =0.900
Mean Probability of Failure =0.10000
Estimated Pf from the sample=0.10970

j
k i l
m

j	k	l	m / i = 0	1	Total
0	1	0	0	735	112	847
0	0	0	1	724	104	828
0	0	1	0	772	79	851
1	0	0	0	816	68	884
0	1	0	1	81	101	182
0	1	1	0	24	114	138
0	0	1	1	367	401	768
1	1	0	0	363	404	767
1	0	0	1	41	96	137
1	0	1	0	27	82	109
0	1	1	1	35	333	368
1	1	0	1	37	338	375
1	1	1	0	16	390	406
1	0	1	1	13	370	383
0	0	0	0	30868	74	30942
1	1	1	1	11	1208	1219

Fig. 4.9 (c) Results of Simulation to Test Approximation Induced Anisotropy: $P_f = 0.10$, $\rho_1 = \rho_2 = 0.90$

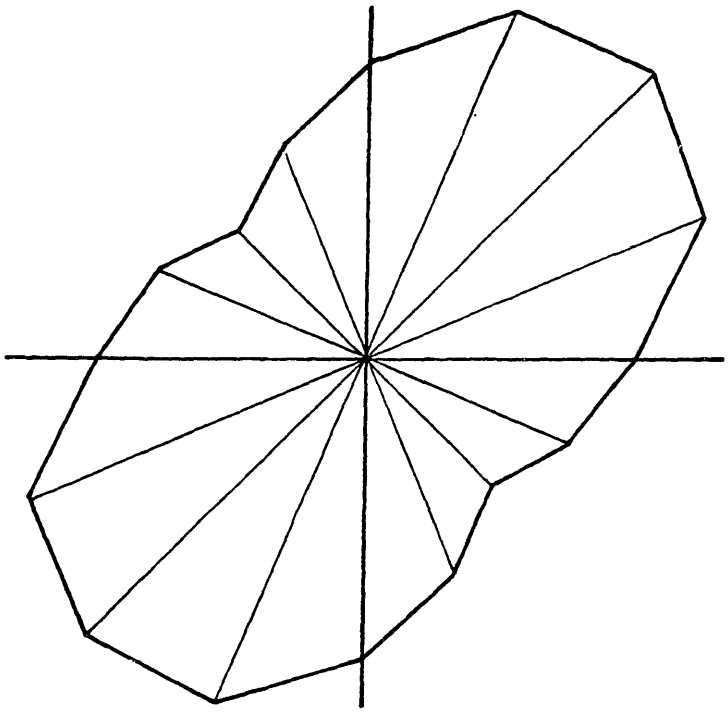

$\beta = 0.95$

Mean Size 22.5

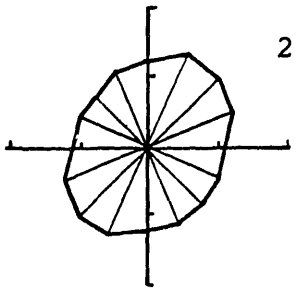

$\beta = 0.7$

Mean Size 3.93

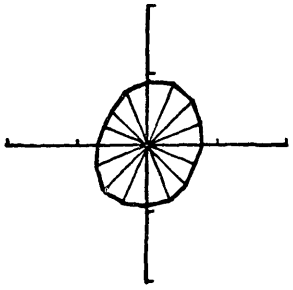

$\beta = 0.5$

Mean Size 2.57

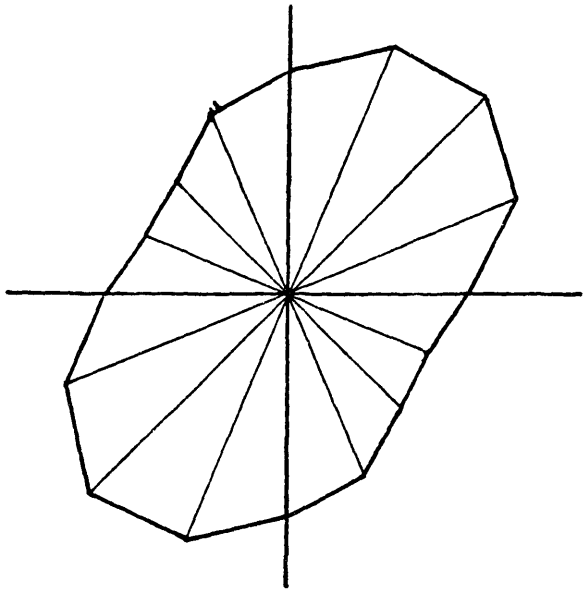

$\beta = 0.90$

Mean Size 12.2

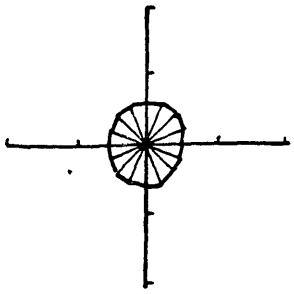

$\beta = 0.3$

Mean Size 1.97

Fig. 4.10 The Average Size of Patches of "1"'S: Results of 100 x 100 Latice Simulation, $P_f = 0.10$

CHAPTER V. SUMMARY AND CONCLUSIONS

Dam filters are usually installed between the core and the shell of earth and rockfill dams in order to prevent seepage forces to produce internal erosion of the core material. Filters must meet two basic requirements:

(i) Stability requirement: the filter material must be fine enough to prevent the particles of base material from washing into its voids.

(ii) Permeability requirement: the filter material must be pervious enough to avoid development of large seepage forces.

Two widely accepted design criteria, so called Terzaghi's filter criteria, are as follows:

(i) Stability requirement: $DF15/DB85 < 5$.

(ii) Permeability requirement: $DF15/DB15 > 5$.

Occasionally, other requirements are added. Most of the current design criteria are based on experiments made in the 1940's and 1950's.

It is the consensus of the profession that the criteria, although sometimes conservative, works well in most cases. However, because of the broadening of the applications and the requirement for more economical designs, there is a need to understand the filtering

phenomenon in more detail. In addition, there are a few cases in which the conventional criteria did not work satisfactorily.

Current research efforts can be classified as follows:

Studies that aim at using a broader spectrum of the filter and the base soil including

(i) Internal stability of widely graded and gap-graded base soils,

(ii) Design criteria for geotextile filters.

Studies seeking more economical designs, e.g.

(iii) Design of filters to protect the sea bed from wave action,

Studies to understand the mechanism involved in the filter process,

(iv) Experiments on soil against screen,

(v) Void phase description based on microscopic and geometric considerations,

(vi) Influence of spatial variability of soil parameters.

Studies on the applicability and improvement of conventional criteria,

((viii) Criteria for filters to retain fines migrated from crack walls.

The present study focuses on the mechanism of filtering on the reliability of filters and filter systems, and improving current design criteria.

Therefore, results obtained in this study are directly relevant to areas (i), (ii) and (vi).

In order to study the physical mechanism of soil particle transport, a mathematical model is introduced. The model is based on the principle of mass conservation for free and stable particles. Absorption and release of these particles are described by the retention ratio, i.e., by the ratio between the dry density of stable and free particles for each particle size. The resulting equations have the same form as the equilibrium absorption isothermals in chemical solute transport. These equations are mathematically very tractable.

Another spatial feature of the proposed model is the distance lag effect for the velocity, absorption and release of free particles. That is the state of the particles at a given location are controlled by the state of the medium a little distance Δx downstream. Under this condition, the retention ratio has the physical interpretation of ratio of particles mechanically blocked by skeleton particles located Δx downstream. A numerical scheme is used in solving the equations under given initial and boundary conditions.

The case of soil against screen has been considered to study the self-healing process of base soils. Two aspects of this process are emphasized:

(i) It is known that the self-healing process of the base soil results from the formation of a filtering layer of large particles next to the screen. This layer retains the rest of the soil from washing through. A critical quantity is the minimum size of particles that should be retained by the screen for successful formation of a self-healing layer. Experimental evidences (Soares [1980] indicates that this size lies between DB80 and DB90. The experiment of Southworth (1980) is successfully reproduced by the present model; it is also found that the combined effects of (a) the percentage of particles retained by the screen and (b) the thickness of the layer to be formed, are responsible for the considerable increase of soil lost through the screen when the screen opening increases from DB80 to DB90.

(ii) The internal stability of the base soil is another important factor in the self-healing process. If the self-healing filter cannot retain

the rest of the soil from washing through or loses too much soil before a successful filtering layer is formed, the base soil cannot be stable. This can occur in gap graded soils (Wittman, [1978]) and perhaps also widely graded soils. Numerical experiments that simulate this behavior are presented. Gradual clogging of the filter by base soil particles simulated by the model.

The physical insight gained by the physical model is helpful in evaluating and interpreting experimental results and findings from statistical analysis of the filter performance data.

400 data from 13 sources have been collected for statistical analysis (Table 3.1). The result of each experiment is either "stable", "nonstable" or "clogging". The purpose of the analysis is to quantify the probability of nonstable conditions as a function of a few influential parameters, such as certain fractiles of the grain size distributions for the filter and the base soil.

Logistic regression is used as the main tool for this analysis. A few regression statistics (the likelihood ratio index ρ_o^2, the modified likelihood ratio index $\bar{\rho}_o^2$, the percent correctly predicted PCP and the t-statistic) are used to evaluate the filtered models. Laboratory bias can be introduced in the analysis. A step-

wise version of logistic regression is used to automatically select the best model.

In a preliminary analysis, models are fitted in terms of the conventional filter parameters DF15/DB85, DF15/DB15, and DF50/DB50. At the same time, conventional criteria are evaluated. As a result of this analysis, it has been decided to remove some of the data sets (i.e., [61], [75] and [82]) because of their unreliability or because of substantial differences in the way experiments were conducted. This elimination left us with 277 cases from 10 sources. Among all the parameters, the ratio DF15/DB85 is the most explanatory one (i..e, the parameter that best separates "stable" cases from "non-stable" cases).

The search for improved filter criteria is carried out in two stages. In the first stage, many grain sizes of base soil and filters are considered as candidate parameters and stepwise regression is used to select those that are significant (Table 3.6(a) and (b)). The main results of this analysis are:

(i) Only DF15 is selected for the filter, which implies that DF15 represent well the void characteristic of the filter.

(ii) DB95, DB90, DB85, DB70, DB50 and DB10 are selected for the base soil; meaning that details of the coarser portion of the grain size

distribution for the base soil (diameters larger than DB70) are critical to the filtering process.

Qualitatively, these results agree with those of the physical model and with characteristics of the filtering process noticed earlier by other authors. In the second stage, stepwise regression is used with ratios of previously determined grain sizes as explanatory variables. The objective here is to find parameters that can be used in improved filter criteria (Table 3.7). From both statistical and physical considerations, it is concluded that the combination of DF15/DB85 and DB95/DB75 is the best one to explain the phenomenon. The physical interpretation of these two parameters is as follows:

(i) DF15/DB85: As previously mentioned, DF15 represents the pore size of the filter, whereas DB85 is a grain size, such that of this grain size is retained by the filter, the whole base soil becomes stable through the quick formation of a self-healing filter. Therefore, the ratio DF15/DB85 must be a good indicator of filter performance.

(ii) DB95/DB7: this ratio can be thought of as the local average gradient of the grain size distribution of base soil centered at DB85.

> Since the self-healing filter consists mainly of particles larger than DB85, the ratio DB95/DB75 indicates the degree of separation between the portion of soil that forms the self-healing layer and the portion of soil that is retained by such layers. The ratio DB95/DB75 is called here the self-healing index.

Finally, a logistic regression analysis have been madw ith two laboratory bias indicators (i.e., Soares [41] and [55], whose results have also been recognized as biased ones in the recent literatures) to obtain improved filter criterion and to quantify uncertainty involved in it. The final result for low values of DB95/DB75 is shown in Figs. 3.25 and 3.26 together with the data. The value of DF15/DB85 that best separates "stable" from "nonstable" cases is between 8 and 9. This is consistent with many experimental results; however, the separating value becomes lower as DB95/DB75 increases.

The probability of filter malfunctioning is a basic result of the analysis. Based on this probability, the region of the improved filter criteria on the DF15/DB85 - DB95/DB75 plane is shown in Fig. 3.29. The region of Fig. 3.29 has been calibrated so that the proposed and conventional criteria agree for a small value of DB95/DB75 (i.e., in case of uniformly graded base soil). The

proposed design criterion can be presented by the following formulas:

$$\text{Average:} \quad \frac{DF15}{DB85} < 5.6 - 0.6 \frac{DB95}{DB75}$$

$$\text{Most Conservative:} \quad \frac{DF15}{DB85} < 5.75 - 0.75 \frac{DB95}{DB75}$$

$$\text{Most Unconservative:} \quad \frac{DF15}{DB85} < 5.5 - 0.5 \frac{DB95}{DB75} \ .$$

The implications of the present study on filter design criteria are as follows:

(i) The ratio DF15/DB85, which is used in Terzaghi's criteria,is the parameter with highest explanatory power. This parameter also has a clear physical interpretation.

(ii) The ratio DB95/DB75, is less important but still significant. This ratio is related to the capability of the base soil to form a satisfactory self-healing filter. Since the conventional criteria are based on experiments using relatively uniform soils (i.e., low values of DB95/DB75), these criteria are unconservative when the base soil has widely-graded coarser portions. The proposed design criterion is based on both DF15/DB85 and DB95/DB75 (Fig. 3.29).

(iii) The use of DF50/DB50 as a parameter in filter design criteria cannot be justified, either on statistical or on physical grounds. Furthermore, the requirement that "the grain size distribution of the filter should be roughly parallel to that of the base material" appears questionable.

The results here are for cohesionless soils (specifically, DB10 > 0.074mm), and for ratios DB95/DB75 soils between 1 and 5. These limitations should be considered when applying the proposed criteria to actual cases.

A dam filter system fails if it fails at any one location.

In order to evaluate the probability of malfunctioning of a dam filter system, a Generalized Weakest Iink Model is proposed. The term "generalized" comes from the fact that the model is developed for 1-D and 2-D continuum. An indicator random field, x9$\underline{s}$), is defined such that $P[x(\underline{s}) = 1] = E[x(\underline{s})] = P_f(\underline{s})$, where $P_f(\underline{s})$ is the probability of filter failure at location $\underline{s}$. The probability of failure anywhere in a region S is then

$$\Phi_F = \text{Prob.}\,[x(\underline{s}) = 1 \text{ for any } \underline{s} \in S].$$

Binary random fields on 2-D lattices and their limits on the lattice spacing goes to zero are studied.

The difficulties of treating these models are reviewed and approximations that are amenable to simplified analysis are introduced. For these approximations, closed form expressions are found for the system failure probability Φ_F (see Eq. (4.3.11).

The same models should be applicable to other reliability problems when failure depends on the extreme value of a random function in 1-D and 2-D.

A case study is presented using construction data for Carters Dam, Georgea (Appendix C). The purpose of this case study is to illustrate the applicability of the model. The results seem to be reasonable, although they are sensitive to the tail of the logistic regression model, which is difficult to verify by empirical means.

APPENDIX A. DESCRIPTION OF FILTER EXPERIMENTS

The objective of this appendix is to review the laboratory experiments, results from which are used in the statistical analysis. Surveys on this topic are in Thanikachalan & Sakthivadival (1973, 1974), Southworth (1980) and Soares (1980). In particular Soares' thesis presents a detailed comparison of experimental procedures. In the present appendix consideration is limited to experiments in the data base of Section 3.1. Conventional soil parameters and typical grain sizes are listed in Table A.1.

(1) Bertram (1940); ab. [40A]

Test arrangement: Soil to soil arrangement, 2" and 4" ID. (inside diameter) cylinder. No shock or vibration applied.

Materials: Very uniform (U_o = 1.2) Ottawa sand (round) and crushed quartz (angular), for both case soils and filters.

Results: Many combinations of base soils and filters were examined. 30 boundary cases are tabulated in the paper. At the limit of stability, the grain size ratios DF15/DB85 and DF15/DB15 lie respectively between 6.5 and 11.5, and between 8.5 and 15 Bertram proposed a filter criterion: DF15/DB85 < 6, DF15/DB15 < 9. Comparing the critical values of DF15/DB85 with those from other experiments, Bertram's results are on the high side (only 2 out of 30 cases failed at DF15/DB85 = 9, for the other failure cases, DF15/DB85 $\geq$ 12). The use of extremely uniform soils may be responsible for the results.

Miscellaneous Comments: The test was the first systematic investigation of the filter stability problem. Bertram published his paper with a detailed account of the experimental procedure. The effectiveness of the filters was judged mainly by visual inspection. In the statistical anaysis, we considered 2 experiments, one

from each side of the stable-nonstable boundary. In some cases, it was difficult to categorize the result as stable or nonstable. In such cases, 3 experiments were considered in the analysis: one stable, one non-stable, and the third clogging, (i.e., an intermediate condition). Sina Bertram did not report all of his experimental results, the procedure described is taken. We obtained 63 cases from this experiment.

Reference: Bertram, G.E. (1940): "An Experimental Investigation of Protective Filters", Harvard Graduate School of Engineering, Soil Mechanics Series No. 7.

(2) Hurley and Newton (1940); ab. [40B]

Test Arrangement: Soil to soil test arrangement, 4" ID. cylinders.

Materials: Base Soil: a sand with DB15 = 0.3mm, and DB60/DB10≃4; Only one kind of base soil was used throughout the experiment. However, the grain size distributions had a range which it varied from experiment to experiment. It had a widely graded coarser portion (Fig. 3.2.3). Filters: selectively screened gravel, DF60/DF10≃ 1.2 ~3.3 and one with 25. The aim of the investigation was to establish filter criteria for graded base soils. These materials were considered to be representative samples of earth dam materials in the New England area.

Results: Main conclusions by the investigators are:

(i) The proposed grain size rations for stability criteria are DF15/DB15 < 32, DF15/DB50 < 15. DB50 was used instead of DB85, because the range of DB50 was found to be smaller than that of DB85.

(ii) Both ratios, DF15/DB15 and DF15/DB50, tend to decrease slightly with increasing DF60/DF10.

Miscellaneous Comments: Stability mainly determined visually. Judgment seems to be on the unconservative side compared to other experiments. For even if some migration of fines occurred through the filter, the filter was judged safe provided that stable conditions were finally attained without significant loss of base soil. Re-sieving was done after the experiment, but no significant change in the grain size distribution was observed. As mentioned earlier there was some variation of grain size distribution from experiment to experiment. In the statistical analysis, the most unconservative side of the distribution was introduced (see Fig. 3.23).

Reference: Hurley, H.W. and Newton, C.T. (1940): "An Investigation to determine the practical application

of natural bank gravel as a protective filter for an earth embankment", M.S. Thesis at M.I.T., Department of Civil Engineering.

(3) U.S.C.E. (1941): ab. [41]

Test Arrangement: Soil to soil test arrangement, 8" and 8" 3/4 ID. cylinders. The side of the cylinder was tapped with a rubber mallet after usual test procedure.

Materials: Base Soil: fine sand with DB60/DB10 = 1.6~2.0. Filter: mixtures of concrete sand and gravel. DF60/DF10 varies from 1.2 to 8.0. Various grain size curve shapes were examined (e.g., linear, S-shaped, etc.). One of the purposes of the experiment was to investigate the influence of filter gradation on the performance.

Results: Conclusions are as follows:

(i) DF15/DB85 < 5 for stability.

(ii) In order to minimize washing of the fine base material into the filter the grain size distributions of the base soil and the filter should be approximately parallel.

Miscellaneous Comments: Stability mainly judged visually. In the statistical analysis, only results before tapping were used. Soares (1980) points out that, because of the very thin (1/2") base soil layers

used in the experiment, the result might be too conservative. (In order to simulate the natural filter behavior, at least 2 inches base soil thickness is necessary to supply enough material for the self-healing process (Lund, 1949).)

Reference: U.S.C.E., Waterways Experiment Station (1941): "Investigation of Filter Requirements for Underdrains", Technical Memorandum No. 183-1.

(4) U.S.C.E. (1948): ab. [48]

Test arrangement: Soil to soil test arrangement, 8" ID. cylinders. Since some of the materials were planned to be used as riprap, vibration was applied after a steady flow test. In some cases, surging was also applied.

Materials: The purpose of the investigation was to develop criteria for filters and blankets used in Enid and Grenade Dams. Two groups of tests were carried out. Group I tests: Laboratory tests to examine all the possible combinations of the base and filters: DB10 = 0.03 - 0.9 (mm) with DB60/DB10 = 1.8 - 5.7, and DF15 = 0.9 - 8.0(mm) with DF60/DB10 = 2-15. Group II tests: design satisfactory blankets under the riprap on the upstream face of the dam. The materials were obtained by screening borrow material at the site DB = 0.05 - 0.3(mm) with DB60/DB10 = 1.8 - 25, whereas

DF15 = 1 - 9(mm) with DF60/DF10 = 3~21.

Results: The following conclusions have been obtained:

(i) For base soils and filters that are rather uniformly graded, DF15/DB85 < 5 appears to be a satisfactory design criterion.

(ii) In addition the following conditions are desirable; DF15/DB15 < 20, DF50/DB60 < 25.

Miscellaneous Comments: Because this experiment was done in order to check the proposed design for the filter, the results include only a few non-stable cases (4 out of 27). In the statistical analysis, stability of the filters was judged based only on the behavior of steady flow (i.e., tapping and surging was disregarded).

Reference: U.S.C.E. Waterways Experiment Station (1948): "Laboratory Investigation of Filters for Enid and Grenada Dams", Technical Memorandum No. 3-245.

(5) U.S.C.E. (1953): ab. [53]

Test Arrangement: Soil to soil test arrangement 2 & 5/8", 5" and 12" ID. cylinders. Vibration net applied to Series I tests, but applied to Series II tests.

Materials: Series I (3 experiments): The purpose was to determine the types of material which could

be protected effectively by a standard concrete sand filter (DF15 = 0.36mm, DF60/DF10 = 5.6). In three cases, the base soils were selectively sieved from usual concrete sand (DB60/DB10 = 1.2 - 2.1). In the other case, a slurry of the Vicksburg loses were used as base soil (DB10 = 0.03mm, DB60/DB10 = 8.5), which resulted in clogging of the filter. Series II: These tests were conducted to determine the stability of using standard concrete gravel aggregate of which grain size distribute between No. 4 (=4.7mm) and 3/4 in. as a filter (DF15 = 7.4mm, DF60/DF10=2.0). Standard concrete sand was used as the main base soil in this series (DB10 = 0.15 - 1.7(mm), DB60/DB10 = 1.2 - 5.6).

Results: Besides presenting the results of their own experiments, the authors compiled a series of previous published results. Their final conclusions are:

(i) DF15/DB85 < 5; but for very uniform base soils (DB60/DB10 < 1.5) the limit may be increased to 6.

(ii) DF50/DB50 < 25

(iii) DF15/DB15 < 20; but for widely graded base materials (DB60/DB10 > 4) the limit may be extended to 40.

Miscellaneous Comments: The main aim of this investigation was to check the stability of standard concrete sand filters. Because of this objective, the test includes no non-stable case and only one clogging case.

Reference: U.S.C.E. Water Experimental Station (1953); "Filter Experiments and Design Criteria", Technical Memorandum No. 3-360.

(6) Karpoff (1955); ab. [55]

Test arrangement: Sil to soil test arrangement. 8" ID. cylinder. Vibration applied.

Materials: The experiments are divided into two groups; one with uniform filters (DF60/DF10 = 1.2 - 1.4, 11 cases), the other with graded filters (DF60/DF10 = 2 - 33, 13 cases). In the latter tests, various grain size curve shapes were obtained through selective sieving. As for the base soils, a silt (DB10 = 0.01mm, DB60/DB10 = 6.5) and a fine sand (DB10 = 0.08mm, DB60/DB10 = 1.5) were used for the uniform tests, whereas silt(DB60/DB10 = 6.6 & 23 was mainly used for the graded tests.

Results:

(i) For uniform filters: $5 < DF50/DB50 < 10$

(ii) For graded filters: $12 < DF50/DB50 < 58$ and $12 < DF15/DB15 < 40$.

The author states that a reason for using DF50/DB50 as a representative value for the criteria is that since 50% fine is actually very close to the mean value of a grainsize distribution. Based on the fact that a uniform filter could nto retain the graded base soil (Series C1 experiment) it is also suggested that their grain size distributions should be roughly parallel.

Miscellaneous Comments: The effectiveness of the filters were judged by maximizing the permeability of the base soil-filter system. Visual observations are also used in judgment. It is not clear why DF15/DB85 was not adopted as the criterion parameter, since a value of DF15/DB85 between 3 and 6 can separate the stable results from the non-stable resuls for both uniform and graded filter cases.

Reference: Karpoff, K.P., (1955): "The Use of Laboratory Tests to Develop Design Criteria for Protective Filters", Proc. ASTM, Vol. 55, pp. 1183-1198.

(7) Lund (1949): ab. [49]

Test arrangement: Soil to soil test arrangement. 3" ID. cylinder was used for DB60/DB10 < 3, otherwise an 8" ID cylinder was used. The apparatus was gently tapped during the test.

Materials: Group I: Tests combine uniform filters (DF60/DF10 ≃ 1.2) and uniform base soils (DB60/DB10 ≃ 1.2). They are systematically combined to investigate the critical conditions. Group II: The base soils have D10 = 0.1mm and DB60/DB10 from 1.2 to 7; whereas the filters are the same as for Group I. The purpose of this group of experiments was to investigate the influence of gradation of the base soil. Group II: The base soils have DB85 = 0.5mm and DB60/DB10 from 1.2 to 3; the filters are very uniform (DF = 3.4 - 6.7mm, DF60/DF10 = 1.15 - 1.4). The aim of this part of the experiment was to analyze the influence of base soil gradation while DB85 remains constant.

Results: Lund reached the following conclusions:

(i) DF15/DB85 < 8 for DB60/DB10 < 7.

(ii) There is some evidence that the critical value of DF15/DB85 decreases with increasing DF60/DF10.

(iii) The coarser particles of the base soil should be the ones that control filteration through self-healing at the base soil-filter interface.

Miscellaneous Comments: Results were classified based on (1) change of filter permeability, and (2) visual inspection. The author classified the results in-

to three categories: STABLE - no permeability change and no migrations of base soils even under tapping of the apparatus. UNSTABLE - significant drop in permeability after gentle tapping; this was almost always accompanied by migration of base soil particles into filter. If the intrusion was less than 1/2", the condition was considered unstable. COMPLETELY UNSTABLE - when all or a significant amount of base soil was washed through the filter.

In addition to these usual soil to soil tests, Lund examined the physical meaning of using DB85 in the filter criteria by conducting soil against screen type experiments. It was found that, if the opening size of the screen exceeds DB80 to DB85, the amount of soil lost through the screen increases exponentially. This fact suggests that DB85 could be a key parameter of the self-healing" process of the base soil.

The author found in this soil against screen type tests that if the base soil thickness on the screen is less than 2", there is significant differences in stability of the base soil. Based on this fact, Lund concluded that the thickness of the base soil should be at least 2" in order to simulate "natural filter" behavior.

Reference: Lund, A (1949): "An Experimental Study of Granded Filters", Thesis presented to the University

of London in fulfillment of the requirements for the degree of Master of Science.

(8) Leatherwood & Peterson (1954); ab. [54]

Test arrangement: Soil to soil test arrangement, 6" ID. cylinder. No vibration applied.

Materials: Natural sands and gravels, artifically graded by selective sieving (DB10 ≃ 0.2-2.5mm, DB60/DB10 ≃ 1.4 with one 2.8, DF15 ≃ 0.8-5.0mm, DF60/DF10 ≃ 1.3).

Results: The limiting grain size ratios are

$$DF15/DB35 < 4.1$$

$$DF50/DB50 < 5.3$$

Miscellaneous Comments: The effectiveness of the filters was judged based on the changes in head loss at the base soil-filter interface, which is considered to be a very sensitive method. The authors themselves stated that "The technique employed by the investigators reported herein is believed to be more sensitive (than the conventional visual inspections)". As a result, the limiting grain size ratios are more conservative than in other experiments.

Reference: Leatherwood, F.N. and Peterson, D.F., Jr. (1954): "Hydraulic Head Loss at the Interface between

Uniform Sands of Different Sizes", Transactions, American Geophysical Union, Vol. 35, No. 4, pp. 588-594.

(9) Kawakami, et al (1961): ab [61]

This is a set of experiments conducted from 1957 to 1961 at Tohoku University, Sendai, Japan, under the Supervision of Prof. F. Kawakami. Only a summary paper by Kawakami & Esashi (1961) is known internationally. The data used in the present statistical analysis were taken from a thesis by Takemura & Yamamoto (1961), which completed this series of experiments. The authors give a very detailed summary of all the experiments.

Test arrangement: Soil to soil test arrangement, ID. 15cm cylinder, thickness of base soil and filters were 7.5cm and 15cm respectively.

Materials: Base Soil: sand, sandy loam and silty lome. Many had cohesion. Filters were prepared in four ways:

(i) parallel to the base soils.

(ii) non-parallel to the base soils.

(iii) For some filters that are very close to non-stable condition, the changes were made on the coarser portion of the grain size distribution while keeping constant the portion finer than DF20.

(iv) The same as (iii), but changing the finer portion (finer than DF20), while keeping the coarser portion constant.

Results: The following conclusions were drawn:

(i) DF15/DB85 is not a good criterion to separate stable from non-stable filters especially when the base soils have cohesion. The conventional criterion DF15/DB85 < 5 is unconservative for some cohesive base soils.

(ii) Comparing the filters that changed the shape of distribution finer than DF20 and the filters that changed that of coarser than DF20, it was found that the stability of the former was influenced by the change, while that of the latter was not. This suggests that the finer portion of the filter is important in the filtering process.

(iii) Comparing the filters prepared according to the procedures described in (iii) and (iv) in "Materals" section, it was found that the stability of the latter was influenced by the change while that of the former was not. This suggests that the finer portion of the filter is important in the filtering process.

(iv) The finer portion of the grain size distribution is important both for the filter and the base

soil. The authors also proposed the following criterion based on DF10 and DB10 (units is mm, and $0.009 < DB10 < 0.4$):

$$\log\left(\frac{DF10}{DB10} - 2\right) < \frac{1.9}{\log(DB10 - 0.001)\times 10^{3}}.$$

Miscellaneous Comments: The stability of filters were judged mainly based on the mechanical analysis of the filter after each experiment. Results were classified into three groups:

STABLE:	almost no base soil particle found in the filter.
UNSTABLE:	After the experiment, the filter contains more than 2% of base soil particles.
PIPING:	A considerable amount of base soil washed through the filter.

References: Kawakami, F. and Esashi, Y. (1961): "On Drainage Filter for Earth Structure", Abstract paper, 16th Annual Meeting, Japan Society of Civil Engineers (in Japanese). Takemura, S. and Yamamoto, H. (1961): "A Study on Filters", Graduate Thesis at Tohoku University, Sendai, Japan (in Japanese).

(10) Belyasherskii, et al (1972): ab. [72]

Tests Arrangement: Soil to soil test arrangement with filter layer top; 8" ID cylinder. Fluctuating flow was applied with average gradient 0.3-0.7, amplitude

of pressure fluctuation 1.85 - 3.2, and frequency 1.6 - 4.5 Hz.

Materials: Base soil was a river sand, DB10 = 0.17mm, DB60/DB10 = 2.24. Various grain size curves for the filter were used, with DF10 $\simeq$ 0.5 - 0.6 mm and DF60/DF10 $\simeq$ 2-33.

Results: A stable region on DF60/DF10 - DF50/DB50 plane was proposed as follows:

Miscellaneous Comments: The effectiveness of the filters was judged based on the amount of penetration of filters into the base soil. The condition was judged to be stable when the penetration was less than 1cm. Only two cases were judged unstable among a total of 13 cases. Description of the experimental details is poor and sometimes unclear. It seems that the conclusions are stated too strongly considering that they are based on only 13 experiments.

References: Belyashevskii, N.N., et al (1972): "Behavior and Selection of the Composition of Graded Filter in the Presence of a Fluctuating Flow", Hydrotechnical Construction, Vol. 6, pp. 541-6 (translated from Russian).

The next two sets of experimental data are the result of investigations on the design of filters for cracked clay cores of earth dams. The main investigator is P. Vaughan (see also Section 1.2.2(3)). Balderhead Dam was completed in 1965 and suffered internal erosion of well-graded glacial till core material after first filling of the reservoir. The investigation showed that cracking of the core by hydraulic fracturing followed by fine clay particles washed out from the crack wall was the mechanism responsible for failure. The filter failed

to retain soil particles migrated from the crack walls. (Filters are usually designed for intact core conditions, not for cracked conditions).

Vaughan proposed a method to design filters for cracked conditions based on a "perfect" filter principle, i.e., the filter should retain the smallest particles that could migrate from the crack walls. This principle does not necessarily mean the filters have to retain clay mineral particles. For a combination of seepage water and clay chemistry, flocculation of clay particles occurs. Therefore, it is these clay flocs that should be retained by the filter.

Cow Green Dam has a similar clay in the core. Its construction had just started when the damage of Balderhead Dam became known. Vaughan did some experiments to ensure the effectiveness of the filter of the Cow Green Dam (Vaughan (1975)). Group (11) is from this experiment. Later on, Vaughan and Soares did a more systematic study on this topic. Group (12) is the result of the latter study (Vaughan & Soares (1982)).

11. Vaughan (1975); ab. [75]

Test Arrangement: ID. 50mm cylinder. Thickness of the filter 75mm. The tube was filled with water and flow was allowed. Flocculated clay was introduced.

Materials: The flocculated clay was produced by using the clay used in the core and river water. The floc size was in the fine silt range (DB0 ~ DB50 = 0.002 - 0.006mm). Three types of filters were prepared: (1) artificially sieved uniform sand filters (DF15 = 0.06 - 0.3mm, DF60/DF10 ≃ 1.4), (2) natural sand (DF15 ≃ 0.1mm, DF60/DF10 ≃ 12), (3) natural sand after washing on No. 200 (0.074 mm) sieve (DF15 = 0.15mm, DF60/DF10 ≃ 7.7).

Results: The permeability of the filter is proposed as a filter criterion (see next section for details).

References: Vaughan, P.R., Lovenbury, H.T. and Horswill, P. (1975): "The Design, Construction and Performance of Cow Green Embankment Dam", Geotechnique 25 (3).
Vaughan, P.R., and Soares, H.F. (1982): "Design of Filters for Clay Cores of Dams", Proc. ASCE, Vol. 108, No. GT1.

(12). Vaughan & Soares (1982); ab. [82]

Test arrangement: Same as in (11) Vaughan (1975).

Materials: Suspensions of fine quartz particles (30g/ℓ) were used as base soil (DB10 = 0.0007 - 0.023mm. DB60/DB10 ≃ 1.2 - 1.7). Filters were artificially sieved and were all in the sand range (DF15 = 0.1 - 0.8mm, DF60/DF10 = 1.5 - 5.6).

Results: The authors proposed a filter criterion based on the permeability of filters; the critical value of permeability is proposed to be

$$k \leftarrow 6.7 \times 10^{-7} \times \delta^{1.52}$$

k: permeability (m/sec)

δ: particle size (m)

δ = {DB85 for cohesionless base soil or the minimum size of floccurated clay.

A filter whose permeability is less than k is considered capable of retaining particles of size larger than δ.

(13) Sherard, Dunnigam & Talbot (1984A);. [84A]

Test Arrangements: Soil to soil test arrangement, 4" I.D. cylinder. The thickness of the base material and the filter were 2" - 4" and 5" - 7" respectively.

Materials: Very uniform base soils were used (DB10 $\simeq$ 0.1 ~ 2.0mm, DB60/DB10 $\simeq$ 1.1 ~ 1.2) which were obtained by selective sieving. Filters were mostly uniform sands and gravels consisting of subrounded to subangular particles (DF15 $\simeq$ 1.0 ~ 13.5mm, DF60/DB10 $\simeq$ 1.1 ~ 3.9). 20 experiments were carried out.

Results: The authors' conclusions are as follows:

(i) The Borderline between the stable filters and nonstable ones ν, DF15 = 9 DB85. This value was also supported by the results of

Lund (1949) and Bertram (1940).

(ii) The authors compared the results with those of Karpoff (1955) and found them to be substantially different (DF15 $\simeq$ 5 DB85 was Karpoff's borderline). They attributed this discrepancy to the way in which filter stability was judged by Karpoff. They claimed that "visual failure" in Karpoff's paper just indicates base particles movement during the formation of a self-healing filter; this was supported by the fact that permeability did not increase after "visual failure".

(iii) The pore of the filter was observed by using molten wax. The channel's linear dimensions normal to the direction of flow ranged approximately from 0.1 to 0.6 DF15. Therefore, it is speculated that particles smaller than 0.10DF15 can pass through the void without being caught by the skeleton.

(iv) DF15/DB85 $\leq$ 5 is shown to be a conservative criterion and DF15 and DB85 to be appropriate characteristics of the filter and the base; Therefore, it should be continued as the main criterion for judging filter performance.

(v) Criteria that use DF50/DB85 or DF15/DB15 are not founded on sound theoretical or experimental bases.

(vi) There is no necessity for the grain distribution curves of the filter and the base soil to be parallel.

Reference: Sherard, J.L., Dunnigan, L.P. & J.R. Talbot (1984): "Basic Properties of Sand and Gravel Filters", J. of Geotechnical Eng. (ASCE), Vol. 110, No. 6.

..../ TABLE A.1 EXPLANATORY VARIABLES /

DATA NAME / RESPONSE	* DB60/DB10	* DF60/DF10	* DF15/DB85	* DB95/DB75	* DF50/DB50	* DB10	* DB85	* DF15
Bertram(1940): [40A]								
40A00-1	0.00	1.185	1.189	12.449	1.070	11.244	0.76562E-01	0.98824E-01	0.87632
40A00-2	1.00	1.185	1.196	17.628	1.070	22.510	0.76562E-01	0.98824E-01	1.7421
40A00-3	0.00	1.189	1.189	8.815	1.072	11.231	0.10766	0.13956	1.2302
40A00-4	0.50	1.189	1.196	12.483	1.072	15.971	0.10766	0.13956	1.7421
40A00-5	1.00	1.189	1.187	17.816	1.072	22.672	0.10766	0.13956	2.4865
40A00-6	0.00	1.190	1.196	8.823	1.072	11.293	0.15219	0.19745	1.7421
40A00-7	1.00	1.190	1.177	12.562	1.072	15.899	0.15219	0.19745	2.4803
40A00-8	0.00	1.185	1.189	12.449	1.070	15.829	0.76562E-01	0.98824E-01	1.2302
40A00-9	1.00	1.185	1.196	17.628	1.070	22.510	0.76562E-01	0.98824E-01	1.7421
40A0010	0.00	1.189	1.189	8.815	1.072	11.231	0.10766	0.13956	1.2302
40A0011	1.00	1.189	1.196	12.483	1.072	15.971	0.10766	0.13956	1.7421
40A0012	0.00	1.190	1.196	8.823	1.072	11.293	0.15219	0.19745	1.7421
40A0013	1.00	1.190	1.187	12.593	1.072	16.032	0.15219	0.19745	2.4865
40A0014	0.00	1.185	1.184	8.868	1.070	11.244	0.76562E-01	0.98824E-01	0.87632
40A0015	1.00	1.185	1.189	12.449	1.070	15.829	0.76562E-01	0.98824E-01	1.2302
40A0016	0.00	1.189	1.189	8.815	1.072	11.231	0.10766	0.13956	1.2302
40A0017	1.00	1.189	1.196	12.483	1.072	15.971	0.10766	0.13956	1.7421
40A0018	0.00	1.190	1.196	8.823	1.072	11.293	0.15219	0.19745	1.7421
40A0019	1.00	1.190	1.187	12.593	1.072	16.032	0.15219	0.19745	2.4865
40ACC 1	0.00	1.185	1.188	12.466	1.070	15.838	0.76562E-01	0.98824E-01	1.2319
40ACC 2	0.50	1.185	1.196	17.617	1.070	22.494	0.76562E-01	0.98824E-01	1.7410
40ACC 3	0.00	1.189	1.188	8.827	1.072	11.237	0.10766	0.13956	1.2319
40ACC 4	0.50	1.189	1.196	12.475	1.072	15.960	0.10766	0.13956	1.7410
40ACC 5	1.00	1.189	1.127	19.460	1.072	23.689	0.10766	0.13956	2.7160
40ACC 6	0.00	1.190	1.196	8.818	1.072	11.285	0.15219	0.19745	1.7410
40ACC 7	0.50	1.190	1.127	13.755	1.072	16.892	0.15219	0.19745	2.7160
40ACC 8	1.00	1.190	1.188	17.760	1.072	22.625	0.15219	0.19745	3.5066
40ACC 9	0.00	1.185	1.188	12.466	1.070	15.838	0.76562E-01	0.98824E-01	1.2319
40ACC10	1.00	1.185	1.196	17.617	1.070	22.494	0.76562E-01	0.98824E-01	1.7410
40ACC11	0.00	1.189	1.188	8.827	1.072	11.237	0.10766	0.13956	1.2319
40ACC12	1.00	1.189	1.196	12.475	1.072	15.960	0.10766	0.13956	1.7410
40ACC13	0.00	1.190	1.196	8.818	1.072	11.285	0.15219	0.19745	1.7410
40ACC14	1.00	1.190	1.127	13.755	1.072	16.892	0.15219	0.19745	2.7160
40ACC15	0.00	1.185	1.188	12.466	1.070	15.838	0.76562E-01	0.98824E-01	1.2319
40ACC16	1.00	1.185	1.196	17.617	1.070	22.494	0.76562E-01	0.98824E-01	1.7410
40ACC17	0.00	1.189	1.188	8.827	1.072	11.237	0.10766	0.13956	1.2319
40ACC18	1.00	1.189	1.196	12.475	1.072	15.960	0.10766	0.13956	1.7410
40ACC19	0.00	1.190	1.196	8.818	1.072	11.285	0.15219	0.19745	1.7410
40ACC20	1.00	1.190	1.127	13.755	1.072	16.892	0.15219	0.19745	2.7160
40AC0 1	0.00	1.185	1.188	12.466	1.070	15.838	0.76562E-01	0.98824E-01	1.2319
40AC0 2	1.00	1.185	1.196	17.617	1.070	22.494	0.76562E-01	0.98824E-01	1.7410
40AC0 3	0.00	1.189	1.188	8.827	1.072	11.237	0.10766	0.13956	1.2319
40AC0 4	1.00	1.189	1.196	12.475	1.072	15.960	0.10766	0.13956	1.7410
40AC0 5	0.00	1.190	1.196	8.818	1.072	11.285	0.15219	0.19745	1.7410
40AC0 6	1.00	1.190	1.127	13.755	1.072	16.892	0.15219	0.19745	2.7160
40AC0 7	0.00	1.185	1.188	12.466	1.070	15.838	0.76562E-01	0.98824E-01	1.2319
40AC0 8	1.00	1.185	1.196	17.617	1.070	22.494	0.76562E-01	0.98824E-01	1.7410
40AC0 9	0.00	1.189	1.185	6.281	1.072	7.984	0.10766	0.13956	0.87655
40AC010	1.00	1.189	1.188	8.827	1.072	11.237	0.10766	0.13956	1.2319
40AC011	0.00	1.190	1.196	8.818	1.072	11.285	0.15219	0.19745	1.7410
40AC012	1.00	1.190	1.127	13.755	1.072	16.892	0.15219	0.19745	2.7160
40A0C 1	0.00	1.185	1.188	12.466	1.070	15.838	0.76562E-01	0.98824E-01	1.2319
40A0C 2	1.00	1.185	1.196	17.617	1.070	22.494	0.76562E-01	0.98824E-01	1.7410
40A0C 3	0.00	1.189	1.188	8.827	1.072	11.237	0.10766	0.13956	1.2319

..../ TABLE A.1 EXPLANATORY VARIABLES /

DATA NAME / RESPONSE	* DB60/DB10	* DF60/DF10	* DF15/DB85	* DB95/DB75	* DF50/DB50	* DB10	* DB85	* DF15 *
40A0C 4 1.00	1.189	1.196	12.475	1.072	15.960	0.10766	0.13956	1.7410
40A0C 5 0.00	1.190	1.196	8.818	1.072	11.285	0.15219	0.19745	1.7410
40A0C 6 1.00	1.190	1.127	13.755	1.072	16.892	0.15219	0.19745	2.7160
40A0C 7 0.00	1.185	1.185	8.870	1.070	11.253	0.76562E-01	0.98824E-01	0.87655
40A0C 8 1.00	1.185	1.188	12.466	1.070	15.838	0.76562E-01	0.98824E-01	1.2319
40A0C 9 0.00	1.189	1.185	6.281	1.072	7.984	0.10766	0.13956	0.87655
40A0C10 1.00	1.189	1.188	8.827	1.072	11.237	0.10766	0.13956	1.2319
40A0C11 0.00	1.190	1.196	8.818	1.072	11.285	0.15219	0.19745	1.7410
40A0C12 1.00	1.190	1.127	13.755	1.072	16.892	0.15219	0.19745	2.7160
Hurley & Newton (1940): [40B]								
40B 4 0.00	4.077	25.348	0.189	4.843	7.325	0.18542	2.3600	0.44682
40B 5A 0.00	4.077	2.766	3.032	4.843	26.385	0.18542	2.3600	7.1554
40B 6 0.00	4.077	2.149	3.907	4.843	28.101	0.18542	2.3600	9.2198
40B 6A 0.00	4.077	2.341	3.663	4.843	28.314	0.18542	2.3600	8.6444
40B 6B 0.00	4.077	2.299	3.666	4.843	28.407	0.18542	2.3600	8.6512
40B 7A 1.00	4.077	1.926	5.006	4.843	34.050	0.18542	2.3600	11.814
40B 7B 1.00	4.077	1.926	5.006	4.843	34.050	0.18542	2.3600	11.814
40B 8A 1.00	4.077	1.189	5.950	4.843	28.101	0.18542	2.3600	14.041
40B 9 1.00	4.077	1.189	8.414	4.843	39.748	0.18542	2.3600	19.857
40B 16 0.00	4.077	1.189	4.206	4.843	19.868	0.18542	2.3600	9.9263
40B 16A 0.00	4.077	1.189	4.206	4.843	19.868	0.18542	2.3600	9.9263
40B 10 1.00	4.077	1.414	6.268	4.843	33.426	0.18542	2.3600	14.791
40B 11 1.00	4.077	1.421	5.179	4.843	27.703	0.18542	2.3600	12.222
40B 13 1.00	4.077	1.414	4.430	4.843	23.627	0.18542	2.3600	10.456
40B 15 0.00	4.077	1.432	3.681	4.843	19.804	0.18542	2.3600	8.6876
40B 15A 0.00	4.077	1.432	3.681	4.843	19.804	0.18542	2.3600	8.6876
40B 12A 1.00	4.077	1.415	4.429	4.843	23.623	0.18542	2.3600	10.453
40B 14 1.00	4.077	1.732	5.496	4.843	33.776	0.18542	2.3600	12.971
40B 17 0.00	4.077	1.732	5.496	4.843	33.776	0.18542	2.3600	12.971
40B 17A 0.00	4.077	1.732	5.496	4.843	33.776	0.18542	2.3600	12.971
40B 19 0.00	4.077	3.527	2.906	4.843	28.101	0.18542	2.3600	6.8590
40B 18 0.00	4.077	3.283	2.547	4.843	23.631	0.18542	2.3600	6.0110
USCE(1941): [41]								
41 3-B 1.00	1.594	4.484	8.091	1.539	28.885	0.12364	0.26524	2.1461
41 4 0.00	1.594	2.873	4.445	1.539	13.805	0.12364	0.26524	1.1790
41 5 0.00	1.594	5.190	1.197	1.539	4.487	0.12364	0.26524	0.31737
41 6 1.00	1.594	2.261	6.483	1.539	16.217	0.12364	0.26524	1.7196
41 8 1.00	1.919	3.549	6.405	1.482	23.456	0.84073E-01	0.20598	1.3193
41 12 0.00	1.919	6.048	3.423	1.482	22.731	0.84073E-01	0.20598	0.70515
41 14 1.00	1.919	3.549	6.405	1.482	23.456	0.84073E-01	0.20598	1.3193
41 15 0.50	1.919	5.625	3.817	1.482	22.731	0.84073E-01	0.20598	0.78624
41 21 0.00	1.919	7.601	5.148	1.482	33.085	0.84073E-01	0.20598	1.0605
41 19 0.00	2.008	5.625	3.780	1.760	22.735	0.80572E-01	0.20800	0.78624
41 22 0.00	2.008	7.601	5.098	1.760	33.090	0.80572E-01	0.20800	1.0605
41 23 0.00	2.008	7.601	5.098	1.755	33.090	0.80572E-01	0.20800	1.0605
41 24 0.00	2.008	7.601	5.098	1.760	33.090	0.80572E-01	0.20800	1.0605
USCE(1948): [48]								
48 1 0.00	3.081	2.114	0.987	1.843	4.858	0.90099	5.9583	5.8822
48 2 0.00	3.081	2.114	0.987	1.843	4.858	0.90099	5.9583	5.8822
48 3 0.00	3.104	2.119	1.705	2.138	8.021	0.72479	4.9079	8.3681
48 4 0.00	5.714	2.114	1.145	2.245	7.959	0.32728	5.1381	5.8822
48 5 0.00	5.499	2.119	2.258	2.194	15.105	0.25243	3.7059	8.3681
48 6 1.00	1.876	3.081	10.869	2.162	42.581	0.28021E-01	0.89094E-01	0.96835
48 7 0.00	2.455	3.081	1.577	1.502	6.315	0.15447	0.61386	0.96835
48 8 0.00	1.733	3.104	2.725	1.701	7.679	0.14245	0.29500	0.80402
48 9 0.00	5.714	4.129	0.832	2.245	9.160	0.32728	5.1381	4.2767
48 10 0.00	5.499	3.334	1.674	2.194	15.705	0.25243	3.7059	6.2035

..../ TABLE A.1 EXPLANATORY VARIABLES /

DATA NAME / RESPONSE	* DB60/DB10	* DF60/DF10	* DF15/DB85	* DB95/DB75	* DF50/DB50	* DB10	* DB85	* DF15 *
48 11 0.00	5.714	4.129	0.832	2.245	9.160	0.32728	5.1381	4.2767
48 12 0.00	1.876	5.714	4.367	2.162	25.990	0.28021E-01	0.89094E-01	0.38911
48 13 0.00	5.714	3.813	1.103	2.245	10.657	0.32728	5.1381	5.6666
48 14 0.00	5.499	15.580	1.168	2.194	25.124	0.25243	3.7059	4.3286
48 15 0.00	2.956	15.580	2.127	3.054	44.212	0.21729	2.0347	4.3286
48 16 0.00	2.205	4.885	2.414	1.782	14.156	0.13876	0.53047	1.2807
48 17 0.00	2.205	4.885	2.414	1.782	14.156	0.13876	0.53047	1.2807
48 19 0.00	1.854	3.098	4.928	3.992	40.945	0.30614	1.9114	9.4200
48 20 1.00	1.854	3.098	4.928	3.992	40.945	0.30614	1.9114	9.4200
48 22 0.00	24.982	5.473	0.159	1.821	2.706	0.47575	32.410	5.1565
48 23 0.00	24.982	5.473	0.159	1.821	2.706	0.47575	32.410	5.1565
48 24 0.00	5.814	5.473	0.473	2.302	14.193	0.43543	10.907	5.1565
48 25 0.00	3.700	5.473	0.743	2.443	17.067	0.41700	6.9423	5.1565
48 26 0.00	3.700	5.473	0.743	2.443	17.067	0.41700	6.9423	5.1565
48 27 1.00	1.797	5.473	6.668	1.795	33.702	0.29500	0.77337	5.1565
48 28 1.00	2.138	5.473	32.378	1.538	164.737	0.52880E-01	0.15926	5.1565
48 30 0.00	2.138	21.446	7.334	1.538	132.595	0.52880E-01	0.15926	1.1680
Lund (1949): [49]								
49 1-11 1.00	1.190	1.407	13.405	1.072	19.458	0.10974	0.14239	1.9087
49 1-12 1.00	1.190	1.200	8.754	1.072	11.232	0.10974	0.14239	1.2464
49 1-13 0.50	1.190	1.471	9.590	1.072	14.396	0.10974	0.14239	1.3656
49 1-14 0.50	1.190	1.200	8.754	1.072	11.232	0.10974	0.14239	1.2464
49 1-15 0.00	1.190	1.429	7.466	1.072	10.669	0.10974	0.14239	1.0630
49 1-16 0.00	1.190	1.282	4.540	1.072	6.102	0.10974	0.14239	0.64650
49 1-21 1.00	1.189	1.445	13.324	1.072	19.572	0.15528	0.20128	2.6818
49 1-22 1.00	1.189	1.161	12.261	1.072	15.362	0.15528	0.20128	2.4680
49 1-23 0.50	1.189	1.407	9.483	1.072	13.759	0.15528	0.20128	1.9087
49 1-24 0.50	1.189	1.200	6.193	1.072	7.942	0.15528	0.20128	1.2464
49 1-25 0.00	1.189	1.471	6.784	1.072	10.180	0.15528	0.20128	1.3656
49 1-31 1.00	1.190	1.287	12.044	1.072	16.225	0.21949	0.28478	3.4298
49 1-32 1.00	1.190	1.223	11.863	1.072	15.427	0.21949	0.28478	3.3783
49 1-33 0.50	1.190	1.445	9.417	1.072	13.840	0.21949	0.28478	2.6818
49 1-34 0.50	1.190	1.161	8.666	1.072	10.863	0.21949	0.28478	2.4680
49 1-35 0.00	1.190	1.407	6.702	1.072	9.729	0.21949	0.28478	1.9087
49 1-36 0.00	1.190	1.471	4.795	1.072	7.198	0.21949	0.28478	1.3656
49 1-41 1.00	1.190	1.425	14.225	1.072	20.412	0.31063	0.40337	5.7380
49 1-42 0.50	1.190	1.287	8.503	1.072	11.459	0.31063	0.40337	3.4298
49 1-43 0.50	1.190	1.223	8.375	1.072	10.896	0.31063	0.40337	3.3783
49 1-44 0.00	1.190	1.445	6.648	1.072	9.775	0.31063	0.40337	2.6818
49 1-45 0.00	1.190	1.471	3.385	1.072	5.084	0.31063	0.40337	1.3656
49 1-51 1.00	1.188	1.228	11.760	1.071	15.320	0.43991	0.56975	6.7004
49 1-52 1.00	1.188	1.425	10.071	1.071	14.433	0.43991	0.56975	5.7380
49 1-53 0.50	1.188	1.150	8.713	1.071	10.844	0.43991	0.56975	4.9644
49 1-54 0.00	1.188	1.287	6.020	1.071	8.103	0.43991	0.56975	3.4298
49 1-55 0.00	1.188	1.445	4.707	1.071	6.912	0.43991	0.56975	2.6818
49 1-56 0.00	1.188	1.407	3.350	1.071	4.859	0.43991	0.56975	1.9087
49 2-11 1.00	1.200	1.407	14.682	1.186	21.245	0.10000	0.13000	1.9087
49 2-12 1.00	1.200	1.178	13.736	1.186	17.343	0.10000	0.13000	1.7857
49 2-13 0.50	1.200	1.471	10.504	1.186	15.718	0.10000	0.13000	1.3656
49 2-14 0.50	1.200	1.200	9.588	1.186	12.264	0.10000	0.13000	1.2464
49 2-15 0.00	1.200	1.429	8.177	1.186	11.648	0.10000	0.13000	1.0630
49 2-16 0.00	1.200	1.282	4.973	1.186	6.663	0.10000	0.13000	0.64650
49 2-21 1.00	1.500	1.445	14.899	1.303	25.187	0.10000	0.18000	2.6818
49 2-22 1.00	1.500	1.407	10.604	1.303	17.707	0.10000	0.18000	1.9087
49 2-23 0.50	1.500	1.178	9.921	1.303	14.455	0.10000	0.18000	1.7857

..../ TABLE A.1 EXPLANATORY VARIABLES /

DATA NAME / RESPONSE	* DB60/DB10	* DF60/DF10	* DF15/DB85	* DB95/DB75	* DF50/DB50	* DB10	* DB85	* DF15
49 2-24 0.00	1.500	1.471	7.586	1.303	13.100	0.10000	0.18000	1.3656
49 2-31 1.00	3.000	1.223	12.066	1.432	16.208	0.10000	0.28000	3.3783
49 2-32 0.50	3.000	1.445	9.578	1.432	14.540	0.10000	0.28000	2.6818
49 2-33 0.50	3.000	1.161	8.814	1.432	11.412	0.10000	0.28000	2.4680
49 2-34 0.00	3.000	1.407	6.817	1.432	10.221	0.10000	0.28000	1.9087
49 2-35 0.00	3.000	1.471	4.877	1.432	7.562	0.10000	0.28000	1.3656
49 2-41 1.00	3.000	1.228	13.401	2.012	31.611	0.10000	0.50000	6.7004
49 2-42 0.50	3.000	1.150	9.929	2.012	22.376	0.10000	0.50000	4.9644
49 2-43 0.00	3.000	1.287	6.860	2.012	16.720	0.10000	0.50000	3.4298
49 2-44 0.00	3.000	1.223	6.757	2.012	15.897	0.10000	0.50000	3.3783
49 2-45 0.00	3.000	1.445	5.364	2.012	14.261	0.10000	0.50000	2.6818
49 2-51 0.00	5.000	1.177	8.073	2.484	29.304	0.10000	1.2000	9.6881
49 2-52 0.50	5.000	1.354	8.596	2.484	33.725	0.10000	1.2000	10.315
49 2-61 0.00	6.000	1.404	8.470	2.885	35.683	0.10000	1.5000	12.706
49 2-62 0.50	6.000	1.664	9.220	2.885	47.184	0.10000	1.5000	13.829
49 2-71 0.00	7.000	1.664	7.279	3.139	41.516	0.10000	1.9000	13.829
49 2-72 0.50	7.000	1.887	9.376	3.139	54.641	0.10000	1.9000	17.815
49 3-11 1.00	1.175	1.228	13.401	1.158	16.967	0.40000	0.50000	6.7004
49 3-12 0.50	1.175	1.425	11.476	1.158	15.985	0.40000	0.50000	5.7380
49 3-13 0.50	1.175	1.150	9.929	1.158	12.010	0.40000	0.50000	4.9644
49 3-14 0.00	1.175	1.287	6.860	1.158	8.974	0.40000	0.50000	3.4298
49 3-21 1.00	1.400	1.228	13.401	1.287	19.567	0.30000	0.50000	6.7004
49 3-22 0.50	1.400	1.425	11.476	1.287	18.435	0.30000	0.50000	5.7380
49 3-23 0.50	1.400	1.150	9.929	1.287	13.851	0.30000	0.50000	4.9644
49 3-24 0.00	1.400	1.287	6.860	1.287	10.349	0.30000	0.50000	3.4298
49 3-31 1.00	2.000	1.228	13.401	1.384	25.031	0.17500	0.50000	6.7004
49 3-32 0.50	2.000	1.150	9.929	1.384	17.718	0.17500	0.50000	4.9644
49 3-33 0.00	2.000	1.287	6.860	1.384	13.239	0.17500	0.50000	3.4298
49 3-34 0.00	2.000	1.223	6.757	1.384	12.588	0.17500	0.50000	3.3783
49 3-41 1.00	3.000	1.228	13.401	1.987	31.611	0.10000	0.50000	6.7004
49 3-42 0.50	3.000	1.150	9.929	1.987	22.376	0.10000	0.50000	4.9644
49 3-43 0.00	3.000	1.287	6.860	1.987	16.720	0.10000	0.50000	3.4298
49 3-44 0.00	3.000	1.223	6.757	1.987	15.897	0.10000	0.50000	3.3783
USCE(1953): [53]								
53 1A1 0.00	1.185	5.600	3.643	1.070	11.627	0.76562E-01	0.98824E-01	0.36000
53 1A2 0.00	1.217	5.600	5.160	1.082	16.769	0.51999E-01	0.69774E-01	0.36000
53 1A3 0.00	2.134	5.600	9.000	2.161	44.348	0.12749E-01	0.40000E-01	0.36000
53 1A4 0.50	8.484	5.600	9.000	1.801	52.378	0.29240E-02	0.40000E-01	0.36000
53 2B1 0.00	1.196	2.000	3.306	1.074	6.127	1.7112	2.2385	7.4000
53 2B2 0.00	1.189	2.000	4.721	1.072	8.713	1.2091	1.5675	7.4000
53 2B3 0.00	1.184	2.000	6.665	1.070	12.267	0.86164	1.1103	7.4000
53 2C1 0.00	1.990	2.000	7.788	1.317	20.614	0.33852	0.95017	7.4000
53 2D1 0.00	5.600	2.000	2.701	2.053	12.398	0.28000	2.7400	7.4000
53 2D2# 0.00	4.962	2.024	2.880	2.447	14.789	0.18542	2.2009	6.3397
53 2D3 0.00	4.200	2.000	4.205	2.943	27.191	0.14500	1.7600	7.4000
53 2D3# 0.00	4.200	2.000	4.205	2.943	27.191	0.14500	1.7600	7.4000
Leatherwood & Peterson (1954): [54]								
54 1 0.00	1.292	1.192	1.358	1.108	1.837	2.4860	3.6489	4.9536
54 2 0.50	1.406	1.192	4.036	1.256	5.518	0.75963	1.2273	4.9536
54 3 0.00	1.259	1.292	1.417	1.190	2.074	1.2236	1.7997	2.5504
54 4 0.00	1.406	1.292	2.078	1.256	3.004	0.75963	1.2273	2.5504
54 5 0.00	1.443	1.292	3.280	1.062	4.444	0.49951	0.77754	2.5504
54 6 0.50	1.532	1.292	4.817	1.150	7.218	0.29314	0.52949	2.5504
54 7 0.00	1.406	1.258	1.021	1.256	1.449	0.75963	1.2273	1.2528
54 8 0.00	1.443	1.258	1.611	1.062	2.143	0.49951	0.77754	1.2528
54 9 0.50	1.293	1.258	3.829	1.233	5.264	0.22723	0.32717	1.2528

..../ TABLE A.1 EXPLANATORY VARIABLES /

DATA NAME / RESPONSE	* DB60/DB10	* DF60/DF10	* DF15/DB85	* DB95/DB75	* DF50/DB50	* DB10	* DB85	* DF15 *
54 10 0.50	2.776	1.258	1.071	1.589	2.238	0.27213	1.1700	1.2528
54 11 0.00	1.443	1.406	1.033	1.062	1.479	0.49951	0.77754	0.80288
54 12 0.00	1.532	1.406	1.516	1.150	2.403	0.29314	0.52949	0.80288
54 13 0.00	1.293	1.406	2.464	1.233	3.634	0.22723	0.32717	0.80288
Karpoff (1955): [55]								
55 A-1 0.00	6.537	1.443	1.355	1.586	3.929	0.10165E-01	0.11830	0.16035
55 A-2 0.00	6.537	1.198	2.631	1.586	6.694	0.10165E-01	0.11830	0.31127
55 A-3 0.00	6.537	1.205	3.685	1.586	9.418	0.10165E-01	0.11830	0.43598
55 A-4 1.00	6.537	1.441	5.484	1.586	15.882	0.10165E-01	0.11830	0.64880
55 A-5 1.00	6.537	1.435	11.049	1.586	31.898	0.10165E-01	0.11830	1.3071
55 B-1 0.00	1.457	1.203	3.225	1.162	4.777	0.76838E-01	0.13511	0.43581
55 B-2 0.00	1.457	1.441	4.802	1.162	8.070	0.76838E-01	0.13511	0.64880
55 B-3 1.00	1.457	1.424	9.724	1.162	16.209	0.76838E-01	0.13511	1.3139
55 C-1 0.00	1.430	1.435	2.431	1.154	4.020	0.31448	0.53763	1.3071
55 C-2 1.00	1.430	1.162	9.206	1.154	13.134	0.31448	0.53763	4.9494
55 C-3 1.00	1.430	1.424	9.706	1.154	15.968	0.31448	0.53763	5.2184
55 D 0.00	10.362	2.028	0.694	3.299	6.057	0.60280E-01	2.0622	1.4303
55 A1-1 1.00	6.633	5.994	6.491	2.171	61.344	0.95000E-02	0.12909	0.83791
55 A1-2 0.00	6.633	10.574	3.037	2.171	50.323	0.95000E-02	0.12909	0.39203
55 A1-3 0.00	6.633	9.263	1.118	2.171	14.494	0.95000E-02	0.12909	0.14430
55 A1-4 0.00	6.633	3.184	0.811	2.171	4.981	0.95000E-02	0.12909	0.10474
55 A1-5 0.00	6.633	6.804	1.726	2.171	17.190	0.95000E-02	0.12909	0.22281
55 A1-6 0.00	6.633	5.554	0.959	2.171	8.691	0.95000E-02	0.12909	0.12377
55 B1-1 1.00	6.633	18.600	5.767	2.171	109.197	0.95000E-02	0.12909	0.74440
55 B1-2 0.00	6.633	14.896	1.479	2.171	25.161	0.95000E-02	0.12909	0.19086
55 B1-3 0.00	6.633	6.075	1.027	2.171	9.473	0.95000E-02	0.12909	0.13259
55 B1-4 0.00	6.633	20.204	2.833	2.171	61.344	0.95000E-02	0.12909	0.36574
55 C1-1 0.00	23.492	33.612	0.884	3.982	56.520	0.22449E-01	1.6829	1.4870
55 C1-2 1.00	23.492	6.888	3.775	3.982	80.707	0.22449E-01	1.6829	6.3538
Kawakami, Esashi et al.(1961): [61]								
61 AM-1 0.00	1.293	1.414	1.407	1.242	2.357	1.2548	1.9715	2.7739
61 BM-1 0.00	1.307	1.265	2.592	1.218	4.032	0.63303	1.0351	2.6826
61 BM-2 0.00	1.307	1.443	1.294	1.218	2.208	0.63303	1.0351	1.3397
61 CM-1 0.50	1.253	1.414	9.457	1.381	14.112	0.20922	0.29332	2.7739
61 CM-2 0.00	1.253	1.443	4.567	1.381	6.914	0.20922	0.29332	1.3397
61 CM-3 0.00	1.253	1.414	2.270	1.381	3.387	0.20922	0.29332	0.66574
61 DM-1 1.00	1.845	1.414	10.298	1.185	19.448	0.11136	0.26935	2.7739
61 DM-2 0.50	1.845	1.443	4.974	1.185	9.528	0.11136	0.26935	1.3397
61 DM-3 0.00	1.845	1.414	2.472	1.185	4.668	0.11136	0.26935	0.66574
61 EM-1 1.00	1.702	1.414	11.408	1.522	25.392	0.87040E-01	0.24316	2.7739
61 EM-2 0.50	1.702	1.443	5.509	1.522	12.439	0.87040E-01	0.24316	1.3397
61 FM-2 0.50	7.727	1.443	3.349	2.021	6.676	0.38000E-01	0.40000	1.3397
61 GM-1 0.50	4.287	1.414	4.092	1.791	10.929	0.87821E-01	0.67797	2.7739
61 GM-2 0.50	4.287	1.443	1.976	1.791	5.354	0.87821E-01	0.67797	1.3397
61 HM-1 0.50	3.007	1.414	3.737	1.629	9.491	0.14748	0.74229	2.7739
61 KM-1 0.50	2.459	1.414	2.994	1.397	6.538	0.25566	0.92653	2.7739
61 AO-1 0.50	4.227	1.581	26.042	3.658	91.269	0.13248E-01	0.88114E-01	2.2947
61 AO-2 0.50	4.227	1.534	10.968	3.658	37.631	0.13248E-01	0.88114E-01	0.96641
61 AO-3 0.00	4.227	1.458	5.083	3.658	16.829	0.13248E-01	0.88114E-01	0.44788
61 AO-4 0.00	4.227	1.265	3.044	3.658	9.127	0.13248E-01	0.88114E-01	0.26826
61 BO-1 0.50	4.050	1.581	16.990	4.125	52.694	0.16000E-01	0.13506	2.2947
61 BO-2 0.50	4.050	1.534	7.155	4.125	21.726	0.16000E-01	0.13506	0.96641
61 BO-3 0.00	4.050	1.458	3.316	4.125	9.716	0.16000E-01	0.13506	0.44788
61 BO-5 0.00	4.050	2.056	0.577	4.125	2.053	0.16000E-01	0.13506	0.77884E-01
61 CO-1 0.50	6.725	1.581	3.942	4.119	42.276	0.18394E-01	0.58218	2.2947
61 CO-2 0.00	6.725	1.534	1.660	4.119	17.431	0.18394E-01	0.58218	0.96641

..../ TABLE A.1 EXPLANATORY VARIABLES /

DATA	NAME	RESPONSE	* DB60/DB10	* DF60/DF10	* DF15/DB85	* DB95/DB75	* DF50/DB50	* DB10	* DB85	* DF15 *
61	C0-3	0.00	6.725	1.458	0.769	4.119	7.795	0.18394E-01	0.58218	0.44788
61	C0-4	0.00	6.725	1.265	0.461	4.119	4.228	0.18394E-01	0.58218	0.26826
61	C0-5	0.00	6.725	2.056	0.134	4.119	1.647	0.18394E-01	0.58218	0.77884E-01
61	A1E1	1.00	2.007	1.581	12.037	1.402	26.408	0.66770E-01	0.19064	2.2947
61	A1E2	1.00	2.007	2.425	5.816	1.402	17.216	0.66770E-01	0.19064	1.1083
61	A1E3	0.00	2.007	3.536	3.065	1.402	11.810	0.66770E-01	0.19064	0.58425
61	A1E4	0.50	2.007	1.534	5.069	1.402	10.888	0.66770E-01	0.19064	0.96641
61	A1E5	0.00	2.007	2.828	1.791	1.402	5.905	0.66770E-01	0.19064	0.34151
61	A1E6	0.00	2.007	1.458	2.349	1.402	4.869	0.66770E-01	0.19064	0.44788
61	A1E7	0.00	2.007	1.265	1.407	1.402	2.641	0.66770E-01	0.19064	0.26826
61	A2E1	1.00	1.265	1.581	6.156	1.099	10.000	0.26203	0.37277	2.2947
61	A2E2	0.50	1.265	2.425	2.974	1.099	6.519	0.26203	0.37277	1.1088
61	A2E4	0.00	1.265	1.534	2.592	1.099	4.123	0.26203	0.37277	0.96641
61	A2E6	0.00	1.265	1.458	1.201	1.099	1.844	0.26203	0.37277	0.44788
61	A3E1	1.00	2.541	1.428	6.362	1.195	12.612	0.12796	0.43734	2.7822
61	A3E2	0.00	2.541	1.981	3.649	1.195	9.095	0.12796	0.43734	1.5958
61	A3E3	0.00	2.541	1.387	3.279	1.195	6.368	0.12796	0.43734	1.4340
61	B1E2	1.00	2.609	2.686	5.304	1.746	20.463	0.28000	1.1753	6.2338
61	B1E3	1.00	2.609	2.763	4.064	1.746	14.282	0.28000	1.1753	4.7758
61	B1E4	1.00	2.609	2.344	2.728	1.746	9.552	0.28000	1.1753	3.2065
61	B1E5	0.50	2.609	2.182	2.258	1.746	7.387	0.28000	1.1753	2.6539
61	B1E6	0.00	2.609	2.637	1.605	1.746	5.898	0.28000	1.1753	1.8858
61	B1E7	0.00	2.609	3.302	1.021	1.746	4.180	0.28000	1.1753	1.2000
61	B2E1	1.00	2.416	2.217	9.891	1.288	24.673	0.15500	0.49614	4.9071
61	B2E2	1.00	2.416	2.017	8.180	1.288	19.566	0.15500	0.49614	4.0584
61	B2E3	1.00	2.416	2.226	5.974	1.288	15.117	0.15500	0.49614	2.9640
61	B2E4	0.50	2.416	1.001	4.032	1.288	5.803	0.15500	0.49614	2.0006
61	B2E5	0.00	2.416	1.934	3.830	1.288	8.580	0.15500	0.49614	1.9000
61	C111	0.00	11.001	4.319	2.327	1.929	14.491	0.94533E-02	0.23031	0.53598
61	C112	0.00	11.001	4.741	3.691	1.929	22.772	0.94533E-02	0.23031	0.85000
61	C113	0.00	11.001	4.378	4.959	1.929	31.171	0.94533E-02	0.23031	1.1420
61	C114	1.00	11.001	4.448	6.300	1.929	41.874	0.94533E-02	0.23031	1.4510
61	C115	0.00	11.001	2.946	4.112	1.929	19.587	0.94533E-02	0.23031	0.94698
61	C116	0.50	11.001	3.218	5.937	1.929	30.121	0.94533E-02	0.23031	1.3673
61	C117	0.00	11.001	3.556	7.852	1.929	39.227	0.94533E-02	0.23031	1.8085
61	C118	0.00	11.001	3.017	12.143	1.929	58.993	0.94533E-02	0.23031	2.7965
61	C221	0.00	9.392	4.472	0.452	1.605	2.541	0.57855E-01	0.86609	0.39183
61	C222	0.00	9.392	4.798	0.924	1.605	5.144	0.57855E-01	0.86609	0.80000
61	C223	1.00	9.392	4.712	2.377	1.605	12.791	0.57855E-01	0.86609	2.0583
61	C224	1.00	9.392	4.712	2.377	1.605	12.791	0.57855E-01	0.86609	2.0583
61	C225	0.00	9.392	3.403	0.708	1.605	2.924	0.57855E-01	0.86609	0.61285
61	C226	0.00	9.392	3.535	1.501	1.605	5.145	0.57855E-01	0.86609	1.3000
61	C227	1.00	9.392	2.644	2.378	1.605	7.853	0.57855E-01	0.86609	2.0600
61	C228	1.00	9.392	2.453	3.260	1.605	10.801	0.57855E-01	0.86609	2.8232
61	C331	0.00	15.617	2.343	1.987	2.293	8.399	0.16000E-01	0.46574	0.92555
61	C332	0.00	15.617	2.602	3.006	2.293	11.823	0.16000E-01	0.46574	1.4000
61	C333	0.00	15.617	2.504	9.215	2.293	36.893	0.16000E-01	0.46574	4.2919
61	C334	1.00	15.617	2.504	9.215	2.293	36.893	0.16000E-01	0.46574	4.2919
61	C335	0.00	15.617	8.000	1.002	2.293	10.000	0.16000E-01	0.46574	0.46652
61	C336	0.00	15.617	7.873	1.298	2.293	12.810	0.16000E-01	0.46574	0.60434
61	C337	0.00	15.617	2.861	2.570	2.293	12.493	0.16000E-01	0.46574	1.1972
61	C338	0.00	15.617	2.849	4.184	2.293	20.277	0.16000E-01	0.46574	1.9488
61	S111	0.00	1.973	2.022	4.567	1.387	10.074	0.68000E-01	0.18612	0.85000
61	S112	0.00	1.973	2.304	4.567	1.387	11.149	0.68000E-01	0.18612	0.85000

..../ TABLE A.1 EXPLANATORY VARIABLES /

DATA	NAME / RESPONSE	* DB60/DB10	* DF60/DF10	* DF15/DB85	* DB95/DB75	* DF50/DB50	* DB10	* DB85	* DF15 *
61	S113 0.00	1.973	2.623	4.567	1.387	12.332	0.68000E-01	0.18612	0.85000
61	S114 0.00	1.973	3.285	4.567	1.387	14.691	0.68000E-01	0.18612	0.85000
61	S115 0.00	1.973	2.353	4.975	1.387	14.043	0.68000E-01	0.18612	0.92593
61	S116 0.00	1.973	4.741	4.567	1.387	19.544	0.68000E-01	0.18612	0.85000
61	S117 0.50	1.973	2.953	5.857	1.387	20.566	0.68000E-01	0.18612	1.0902
61	S118 0.50	1.973	3.952	6.431	1.387	26.393	0.68000E-01	0.18612	1.1969
61	S221 0.00	1.778	1.857	2.632	2.374	6.724	0.18000	0.52000	1.3684
61	S222 0.00	1.778	1.817	3.879	2.374	10.515	0.18000	0.52000	2.0169
61	S223 1.00	1.778	1.694	5.676	2.374	14.650	0.18000	0.52000	2.9515
61	S224 1.00	1.778	1.890	6.517	2.374	18.160	0.18000	0.52000	3.3891
61	S225 0.00	1.778	5.000	3.310	2.374	15.488	0.18000	0.52000	1.7214
61	S226 0.00	1.778	3.430	3.997	2.374	15.488	0.18000	0.52000	2.0784
61	S227 0.50	1.778	2.673	4.528	2.374	15.488	0.18000	0.52000	2.3545
61	S228 0.50	1.778	2.236	4.950	2.374	15.488	0.18000	0.52000	2.5741
61	S331 0.00	2.011	4.100	2.179	1.528	8.528	0.94000E-01	0.28000	0.61000
61	S332 0.00	2.011	3.636	3.265	1.528	12.569	0.94000E-01	0.28000	0.91421
61	S333 0.00	2.011	4.082	4.132	1.528	17.510	0.94000E-01	0.28000	1.1569
61	S334 0.50	2.011	4.085	7.811	1.528	34.438	0.94000E-01	0.28000	2.1871
61	S335 0.00	2.011	5.918	2.179	1.528	11.345	0.94000E-01	0.28000	0.61000
61	S336 0.00	2.011	4.730	3.071	1.528	13.885	0.94000E-01	0.28000	0.86000
61	S337 0.50	2.011	5.920	4.067	1.528	22.835	0.94000E-01	0.28000	1.1388
61	S338 0.50	2.011	5.689	5.949	1.528	33.070	0.94000E-01	0.28000	1.6658
Belyashevskii et al.(1972): [72]									
72	1 0.00	2.422	5.000	2.520	1.896	11.179	0.15811	0.50000	1.2599
72	2 0.00	2.422	2.531	3.564	1.896	9.323	0.15811	0.50000	1.7818
72	3 0.00	2.422	4.202	1.682	1.896	7.178	0.15811	0.50000	0.84090
72	4 1.00	2.422	1.495	11.613	1.896	22.515	0.15811	0.50000	5.8065
72	5 1.00	2.422	2.236	12.731	1.896	32.477	0.15811	0.50000	6.3653
72	6 0.00	2.422	7.038	5.000	1.896	29.048	0.15811	0.50000	2.5000
72	7 0.00	2.422	15.657	4.446	1.896	60.278	0.15811	0.50000	2.2230
72	8 0.00	2.422	26.869	2.714	1.896	48.854	0.15811	0.50000	1.3572
72	9 0.00	2.422	3.162	3.364	1.896	10.623	0.15811	0.50000	1.6818
72	10 0.00	2.422	30.825	2.621	1.896	60.278	0.15811	0.50000	1.3104
72	11 0.00	2.422	8.060	2.828	1.896	17.163	0.15811	0.50000	1.4142
72	12 0.00	2.422	5.280	1.335	1.896	5.940	0.15811	0.50000	0.66742
72	13 0.00	2.422	9.807	4.203	1.896	30.254	0.15811	0.50000	2.1015
Vaughan (1975): [75]									
75	CG-A 0.00	6.687	11.812	0.111	29.234	69.746	0.35000E-02	0.95295	0.10555
75	CG-B 1.00	6.687	7.675	0.164	29.234	76.251	0.35000E-02	0.95295	0.15651
75	CG-C 0.00	6.687	1.399	0.064	29.234	9.129	0.35000E-02	0.95295	0.60790E-01
75	CG-D 0.00	6.687	1.414	0.087	29.234	12.668	0.35000E-02	0.95295	0.83218E-01
75	CG-E 1.00	6.687	1.414	0.175	29.234	25.337	0.35000E-02	0.95295	0.16644
75	CG-F 1.00	6.687	1.414	0.349	29.234	50.673	0.35000E-02	0.95295	0.33287
Vaughan & Soares (1982): [82]									
82	A-U1 0.00	1.162	1.666	12.277	1.276	21.058	0.68000E-02	0.90000E-02	0.11050
82	A-U2 1.00	1.162	1.548	13.812	1.276	22.501	0.68000E-02	0.90000E-02	0.12431
82	A-U3 1.00	1.162	1.745	23.556	1.276	38.014	0.68000E-02	0.90000E-02	0.21200
82	B-U3 0.00	1.410	1.745	7.449	1.315	12.269	0.17321E-01	0.28460E-01	0.21200
82	B-U4 0.00	1.410	1.447	12.958	1.315	20.109	0.17321E-01	0.28460E-01	0.36878
82	B-U5 1.00	1.410	1.182	22.866	1.315	31.476	0.17321E-01	0.28460E-01	0.65077
82	C-U4 0.00	1.685	1.447	7.376	1.451	13.351	0.23000E-01	0.50000E-01	0.36878
82	C-U5 0.00	1.685	1.182	13.015	1.451	20.898	0.23000E-01	0.50000E-01	0.65077
82	C-U6 1.00	1.685	1.388	16.971	1.451	30.104	0.23000E-01	0.50000E-01	0.84853
82	A-G1 0.00	1.162	5.610	13.980	1.276	56.095	0.68000E-02	0.90000E-02	0.12582
82	A-G2 1.00	1.162	4.106	23.763	1.276	76.641	0.68000E-02	0.90000E-02	0.21387
82	A-G3 0.50	1.162	5.415	16.075	1.276	60.898	0.68000E-02	0.90000E-02	0.14467
82	A-G4 0.50	1.162	4.522	22.896	1.276	77.356	0.68000E-02	0.90000E-02	0.20606

..../ TABLE A.1 EXPLANATORY VARIABLES /

DATA NAME	RESPONSE	DB60/DB10	DF60/DF10	DF15/DB85	DB95/DB75	DF50/DB50	DB10	DB85	DF15
82 B-G5	0.00	1.410	3.473	12.255	1.315	36.548	0.17321E-01	0.28460E-01	0.34879
82 B-G6	1.00	1.410	4.106	7.515	1.315	24.736	0.17321E-01	0.28460E-01	0.21387
Sherard, Dunnigan & Talbot (1984a): [84]									
84 # 3	0.00	1.091	2.836	8.217	1.035	17.503	0.21369	0.24355	2.0013
84 # 4	1.00	1.095	2.836	9.794	1.037	20.921	0.17822	0.20433	2.0013
84 # 6	0.00	1.095	2.005	7.176	1.037	12.448	0.35644	0.40867	2.9324
84 # 7	0.50	1.091	2.310	8.217	1.035	15.008	0.42739	0.48709	4.0027
84 # 8	0.50	1.090	1.633	8.005	1.035	11.988	0.60535	0.68894	5.5149
84 # 9	1.00	1.091	1.633	9.514	1.035	14.255	0.50877	0.57968	5.5149
84 #10	0.00	1.191	8.018	8.417	1.073	38.056	0.10874	0.14138	1.1900
84 #11	0.00	1.191	1.091	7.260	1.073	8.721	0.10874	0.14138	1.0264
84 #12	0.50	1.191	1.091	10.302	1.072	12.376	0.76635E-01	0.99631E-01	1.0264
84 #13	0.00	1.091	1.152	8.613	1.035	10.106	1.0175	1.1594	9.9849
84 #14	1.00	1.090	1.152	10.248	1.035	12.022	0.85569	0.97436	9.9849
84 #15	0.00	1.091	1.226	5.823	1.035	7.139	2.0351	2.3187	13.502
84 #16	0.00	1.091	1.226	6.930	1.035	8.497	1.7095	1.9484	13.502
84 #17	0.50	1.188	1.226	8.463	1.071	11.015	1.2318	1.5953	13.502
84 #18	1.00	1.191	2.586	9.168	1.073	20.485	0.10874	0.14138	1.2961
84 #19	0.00	1.086	3.925	5.857	1.033	17.387	0.30192	0.34148	2.0000
84 #20	0.00	1.086	2.286	8.496	1.033	16.586	0.30192	0.34148	2.9013
84 #21	0.50	1.086	2.141	9.856	1.033	18.024	0.30192	0.34148	3.3658
84 #22	1.00	1.086	2.100	10.564	1.033	18.634	0.30192	0.34148	3.6074
84 #23	0.50	1.091	1.824	8.211	1.035	11.635	0.50877	0.57968	4.7600

APPENDIX B. LIMITS OF EQ. (4.3.9) AND EQ. (4.3.23)

B.1 Limits of Eq. (4.3.9)

Eq. (4.3.9') is rewritten:

$$\Phi_F = 1-\{1-\bar{P}_F(1-\beta_1^k)\}^{\frac{m}{k}-1}\cdot\{1-\bar{P}_F(1-\beta_2^{\ell})\}^{\frac{n}{\ell}-1}$$

$$\cdot\{1-\bar{P}_F\left(1-\tfrac{1}{2}(\beta_1^k+\beta_2^{\ell})\right)\}^{(\frac{m}{k}-1)(\frac{n}{\ell}-1)}(1-P_F)$$

Let us consider $\ell n(1-\Phi_F)$ for calculational convenience:

$$\ell n(1-\Phi_F)$$

$$= \underbrace{(\tfrac{m}{k}-1)\,\ell n\{1-\bar{P}_F(1-\beta_1^k)\}}_{1} + \underbrace{(\tfrac{n}{\ell}-1)\,\ell n\{1-\bar{P}_F(1-\beta_2)\}}_{2}$$

$$+ \underbrace{(\tfrac{m}{k}-1)(\tfrac{n}{\ell}-1)\,\ell n\ \{1-P_F(1-\tfrac{1}{2}(\beta^k+\beta^{\ell}))\} + \ell n(1-\bar{P}_F)}_{3}$$

The limit is considered separately for terms 1 , 2 and 3.

For term 1,

$$\lim_{k\to o}\ (\tfrac{m}{k}-1)\,\ell n\{1-\bar{P}_F(1-\beta_1^k)\} = \lim_{k\to 0}\frac{\ell n\{1-\bar{P}_F(1-\beta_1^k)\}}{(\frac{k}{m-k})}$$

$$= \lim_{k\to o}\frac{\bar{P}_F\beta_1^k\ell n\ \beta_1}{\frac{m-k+k}{(m-k)^2}\{1-\bar{P}_F(1-\beta_1^k)\}}$$

$$= m\bar{P}_F\ell n\beta_1$$

For term 2 ,

$$\lim_{\ell \to o} \left(\frac{n}{\ell} - 1\right) \ell n\{1-\bar{P}_F(1-\beta_2^{\ell})\} = n\bar{P}_F \ell n\beta_2$$

For term 3 ,

$$\lim_{\substack{k \to o \\ \ell \to o}} \left(\frac{m-k}{k}\right)\left(\frac{n-\ell}{\ell}\right) \ell n\{1-\bar{P}_F(1-\tfrac{1}{2}(\beta_1^k+\beta_2^{\ell}))\}$$

$$= \lim_{\substack{k \to o \\ \ell \to o}} \frac{\ell n\{1-\bar{P}_F(1-\frac{1}{2}(\beta_1^k+\beta_2^{\ell}))\}}{\frac{k}{m-k} \quad \frac{\ell}{n-\ell}}$$

Applying Hospital's theorem for multivariate functions,

$$= \lim_{\substack{k \to o \\ \ell \to o}} \frac{-\frac{\bar{P}_F}{2}\beta_1^k \ell n\beta_1 \cdot \frac{\bar{P}_F}{2}\beta_2^{\ell} \ell n\beta_2}{\{\frac{m}{(m-k)^2} \cdot \frac{n}{(n-\ell)^2}\}\{1-\bar{P}_F(1-\frac{1}{2}(\beta_1^k+\beta_2^{\ell}))\}^2}$$

$$= -mn\left(\frac{\bar{P}_F}{2}\right)^2 \ell n\beta_1 \ell n\beta_2$$

From 1 , 2 and 3 ,

$$\ell n(1-\Phi_F) = m\bar{P}_F \ell n\beta_1 + n\bar{P}_F \ell n\beta_2 - mn\left(\frac{P_F}{2}\right)^2 \ell n\beta_1 \ell n\beta_2 + \ell n(1-\bar{P}_F)$$

$$(1-\Phi_F) = \beta_1^{m\bar{P}_F} \cdot \beta_2^{n\bar{P}_F} \cdot \exp\left(-mn\left(\frac{\bar{P}_F}{2}\right)^2 \ell n\beta_1 \ell n\beta_2\right) \cdot (1-\bar{P}_F)$$

Therefore,

$$\Phi_F = 1 - \{\beta_1^{m\bar{P}_F} \cdot \beta_2^{n\bar{P}_F} \cdot \exp\left[-mn\left(\frac{\bar{P}_F}{2}\right)^2 \ell n\beta_1 \ell n\beta_2\right](1-\bar{P}_F)\}$$

If $\beta_1 = \beta_2 = \beta$,

If $\beta_2 = 1$, which is 1-D case, Φ_F becomes

$$\Phi_F = 1 - \beta_1^{m\bar{P}_F}(1 - \bar{P}_F)$$

B.2 Limit of Eq. (4.3.23)

The system failure probability can be written as

$$\Phi_F = 1(1-P_{foo}) \cdot \prod_{i=1}^{mk} \{1-(P_{fil}-\beta_1^{\frac{1}{k}} P_{fi-1,1})\}$$

$$\cdot \prod_{j=1}^{n\ell} \{1-(P_{flj}-\beta_2^{\frac{1}{\ell}} P_{flj-1})\}$$

$$\cdot \prod_{i=1}^{mk}\prod_{j=1}^{n\ell} \{1-(P_{fij}-\tfrac{1}{2}\beta_1^{\frac{1}{k}} P_{fi-1j}-\tfrac{1}{2}\beta_2^{\frac{1}{\ell}} P_{fij-1})\}$$

where P_{fij} is the marginal failure distribution at point (i,j), and the distance between two points are divided by k and ℓ.

Thus

$$\begin{aligned}\ell n(1-\Phi_F) = {} & \ell n(1-P_{foo}) \\ & + \ell n \prod_{i=1}^{nk} \{1 - (P_{fil}-\beta_1^{\frac{1}{k}} P_{fi-11})\} && 1 \\ & + \ell n \prod_{j=1}^{n\ell} \{1 - (P_{fij}-\beta_2^{\frac{1}{\ell}} P_{flj-1}) && 2 \\ & + \ell n \prod_{i=1}^{mk}\prod_{j=1}^{n\ell} \{1-(P_{fij} - \tfrac{1}{2}\beta_1^{\frac{1}{k}} P_{fi-1j}-\tfrac{1}{2}\beta_2^{\frac{1}{\ell}} P_{Fij-1})\} && 3\end{aligned} \qquad (B.2.1)$$

For term 1,

$$I_1 = \ell n \prod_{i=1}^{mk} \{1-(P_{Fil}-\beta_1^{\frac{1}{k}} P_{Fi-1l})\}$$

$$= \ell n \prod_{i=1}^{mk} [\{1-(1-\beta_1^{\frac{1}{k}})\bar{P}_f\}-\{P'_{fil}-\beta_1^{\frac{1}{k}}P'_{fi-1,1}\}]$$

Let $A = \{1-(1-\beta_1^{\frac{1}{k}})\bar{P}_F\}$ and $B_i=P'_{Fil}-\beta_1^{\frac{1}{k}} P'_{Fi-1l}$.

Note that $B_i << A$.

$$I_1 = \ell n \prod_{i=1}^{mk} (A-B_i)$$

$$\simeq \frac{(mk-1)\ \ell nA}{I_{11}} + \frac{\ell n(A - \sum_{i=1}^{mk} B_i)}{I_{12}}$$

The limits ($k\to\infty$) are taken for the two terms above.

$$\lim_{k\to o} I_{11} = \bar{P}_F\ m\ \ell n\beta_1$$

and

$$\lim_{k\to o} I_{12} = \lim_{k\to o} \ell n[\{1-(1-\beta_1^{\frac{1}{k}})\bar{P}_F\} - \sum_{i=1}^{km} \{P'_{fil} - \beta_1^{\frac{1}{k}}P'_{fi-1,1}\}]$$

$$= \ell n\ \{1-P'_f(m,0) + P'_f(0,0)\}$$

Therefore,

$$\lim_{k\to\infty} I_1 = \bar{P}_F\ m\ell n\beta_1 + \ell n\{1-P'_F(m,o) + P'_F(0,0)\} \qquad (B.2.2)$$

$$\lim_{\ell\to\infty} I_2 = \bar{P}_F\ n\ell n\beta_2 + \ell n\{1-P'_F(0,n) + P'_F(0,0)\} \qquad (B.2.3)$$

For term 3

$$I_3=\ell n \prod_{i=1}^{mk}\prod_{j=1}^{n\ell}\{1-(P_{fij}-\tfrac{1}{2}\beta_1^{\frac{1}{k}} P_{fi-1j}-\tfrac{1}{2}\beta_2^{\frac{1}{\ell}}P_{fij-1})\}$$

$$= \ell n \prod_{i=1}^{mk}\prod_{j=1}^{n\ell}[\{1-(1-\tfrac{1}{2}\beta_1^{\frac{1}{k}}-\tfrac{1}{2}\beta_2^{\frac{1}{\ell}})\bar{P}_f\} - \{P'_{fij} - \tfrac{1}{2}\beta^{\frac{1}{k}} P_{fi-1j} - \tfrac{1}{2}\beta^{\frac{1}{\ell}}P_{fij-1}\}]$$

Let $A = 1 - (1-\frac{1}{2}\beta_1^{\frac{1}{k}} - \frac{1}{2}\beta_2^{\frac{1}{\ell}})\bar{P}_f$

$$B_{ij} = P'_{fij} - \tfrac{1}{2}\beta_1^{\frac{1}{k}} P'_{fi-1j} - \tfrac{1}{2}\beta_2^{\frac{1}{\ell}}P_{fij-1}$$

then

$$I_3 = \ell n \prod_{i=1}^{mk}\prod_{j=1}^{n\ell}(A-B_{ij})$$

$$\simeq \ell n[A^{mkn\ell} - A^{mkn\ell-1}\sum_{i=1}^{mk}\sum_{j=1}^{n\ell}B_{ij}]$$

$$= \underbrace{(mkn\ell-1)\ \ell nA}_{I_{31}} - \underbrace{\ell n(A - \sum_{i=1}^{mk}\sum_{j=1}^{n\ell}B_{ij})}_{I_{32}}$$

$$\lim_{\substack{k\to\infty\\ \ell\to\infty}} I_{31} = \lim_{\substack{k\to\infty\\ \ell\to\infty}} \frac{\ell n[(1-P_F)+\frac{1}{2}\bar{P}_F\beta_1^{\frac{1}{k}}+\frac{1}{2}\bar{P}_F\beta_2^{\frac{1}{\ell}}]}{\frac{1}{(mkn\ell-1)}} = \frac{1}{2}\bar{P}_f^2 mn\,\ell n\beta_1\ell n\beta_2$$

$$\lim_{\substack{k\to\infty\\ \ell\to\infty}} I_{32} = \lim_{\substack{k\to\infty\\ \ell\to\infty}} \ell n[\{(1-\bar{P}_f) + \frac{1}{2}\bar{P}_f\beta_1^{\frac{1}{k}} + \frac{1}{2}\bar{P}_f\beta_2^{\frac{1}{\ell}}\}$$

$$- \sum_{i=1}^{mk}\sum_{j=1}^{n\ell} \{P'_{fij} - \frac{1}{2}\beta_1^{\frac{1}{k}} P'_{fi-1j} - \frac{1}{2}\beta_2^{\frac{1}{\ell}} P'_{fij-1}\}]$$

$$= \ell n[1 - \frac{1}{2}\{\int_o^m P'_f(x,n)\,dx + \int_o^n P'_f(m,y)\,dy$$

$$- \int_o^m P'_f(x,0)\,dx - \int_o^n P'_f(0,y)\,dy\}]$$

Finally,

$$\lim_{\substack{k\to\infty\\ \ell\to\infty}} I_3 = \frac{1}{2} P_F^2\, mn\ell n\beta_1\ell n\beta_2$$

$$+ \ell n[1 - \frac{1}{2}\{\int_o^m P'_{f(x,m)}\,dx + \int_o^n P'_f(m,y)\,dy -$$

$$\int_o^m P'_f(x,o)\,dx - \int_o^n P'_{f(o,y)}\,dy\}]$$

(B.2.4)

Eq. (B.2.1) becomes

$$\ell n(1-\Phi_F) = \ell n(1-P_{foo})$$

$$+ \bar{P}_F m \ell n \beta_1 + \ell n\{1-P'_f(m,0)-P'_f(0,0))\}$$

$$+ \bar{P}_f n \ell n \beta_2 + \ell n\{1-(P'_f(0,n) - P'_f(0,0))\}$$

$$+ \frac{1}{2} \bar{P}_f^2 mn \ell n \beta_1 \ell n \beta_2$$

$$+ \ell n[1- \frac{1}{2} \{\int_o^m P'_f(x,m)dx + \int_o^n P'_f(m,y)dy - \int_o^m P'_f(x,0)dx - \int_o^n P'_f(o,y)\}$$

Thus,

$$\Phi_F = 1 - [(1-P_{foo}) \cdot \beta_1^{\bar{P}_F m} \cdot \beta_2^{\bar{P}n} \cdot \exp[\frac{1}{2} \bar{P}_f^2 mn \ell n \beta_1 \ell n \beta_2]$$

$$\cdot\{1-(P'_f(m,0)-P'_f(o,o)\}\{1-(P'_f(0,n)-P'_f(0,0))\}$$

$$\cdot[1-\frac{1}{2}\{\int_o^m P'_f(x,m)dx+\int_o^n P'_f(m,y)dy-\int_o^m P'_f(x,0)dx-\int_o^n P'_f(0,y)dy\}]]$$

APPENDIX C. CASE STUDY: PROBABILITY OF MALFUNCTIONS OF THE FILTER OF CARTERS DAM

Construction records from Carters Dam, Georgia, are used to estimate the probability of filter malfunctioning. Calculation is based on model and results obtained previously in Chapters II, III and IV. A brief explanation on the dam project and a description of the available data are given in Section C.1 followed in Section C.2 by preliminary statistical analyses. Finally, the probability of filter malfunctioning anywhere in the structure is calculated in Section C.3.

The present calculations are limited mainly by the amount of grain size data available for the core and the transition zone and by uncertainty on the tail behavior of the logistic models fitted to data from laboratory experiment. For this reason, the main purpose of this application is to illustrate the methodology.

C.1 Introduction

Carters Dam is located on the Coosawatt River in northwest Georgia, 75 miles north of Atlanta. The project is part of the development of the Alabama-Coosa River and tributaries for navigation, flood control, and power. The dam was built by the Mobile District, Corps. of Engineers, U.S. Army. Construction of the embankment started in April 1964 and was completed in February 1970. The lay-

out and a cross section of the dam are shown in Figs. C.1 and C.2 respectively. The overall dimensions of the dam are given in Table C.1.

The rock foundation consists of quartzites, argillite and phyllite with quarzites predominating. The overburden material (mainly lean clay) and the weathered rock (10 to 60 feet in depth on top was removed.

Carters Dam is a compacted, zoned rockfill embankment with centrally located impervious core (Fig. C.2). The core, Zone 1, consists of highly weathered and disintegrated rock. Most of the material for the core was taken from the same borrow areas. Zone 2 is a transition zone which protects the core against internal erosion by seapage; it was built using weathered rock from the excavations. The rockfill consists of 4 zones, sound quartz with up to 30% argillite and/or phyllite which was considered to be the best quality rock at the site and was used for Zone 4A; Intermediate quality rock was used for Zone 3B; and Zone 3C is made of random rock. The crest, Zone 3AA, was made of sound quartz with 30% finer than the number 4 sieve (4.7mm). Most of the material used for the dam was a by-product of excavation. Ranges of grain size distributions for Zone 1 and Zone 2 are shown in Fig. C3. For more detail, see Robeson & Crisp (1965) and U.S.A.C.E. (1976).

Construction records of the Dam are used to evaluate the probability of malfunctioning of the filter system. The available data is summarized in Table C.2. Unfortunately, the grain size distribution data is not abundant for the core and the transition zone (one sample per $(33)^3$ C.Y. and one sample per $(26)^3$ C.Y. respectively). Because of this limitation, construction control density date (one sample per $(12)^3$ C.Y.) are used to estimate the correlation in space of material properties.

The procedure for the estimation of the probability of malfunctioning is shown in Fig. C.4. First, the spatial variation of critical grain size values (e.g., DF15,DB85) is analyzed. In particular, the dam is partitioned into regions such that these grain size parameters are statistically homogeneous within each region. The mean probability of malfunctioning of the filter is the same at all points of a region. The correlation function of dry density is used as an indirect measure of the correlation of grain sizes, for which data is limited. These correlation analyses are described in Section C.2.

The failure probability at the given point of each homogeneous portion of the plane between the core and the transition zone is obtained using results from the logistic regression analysis of Chapter III.

Finally, the probability of malfunctioning of the filter system for the entire structure is obtained using the generalized weakest link model.

C.2 Statistical Analysis of Grain Sizes and Estimation of the Failure Probability at a Point

First, grain size data is analyzed for the purpose of partitioning the core and the transition zone into homogeneous regions. A cluster-analysis method known as K-menas is used for this purpose. The spatial correlation function is estimated from the construction control density data because of the relative abundance of this type of measurement. Section C.2.2 is devoted to this topic.

C.2.1 Estimation of the Probability of Malfunctioning at a point.

Grain size distribution data is available at 57 points of the core (zone 1), and at 28 points of the downstream transition zone (Zone 2). Log DB85 and Log DF15 are plotted in the sampling sequence in Figs. C.5 and C.6. Logarithm taken because (i) the finer grain sizes are considered to be more important in this phenomenon; (ii) in approximation grain sizes follow log normal distribution. Figure C.5 clearly indicates the existance of several subregions with homogeneous properties.

There are several ways in which one can partition a

set of data into homogeneous groups. The K-means method, one of the most popular nonhierarchical procedure cluster analysis is used here mainly because of its simplicity. (Johnson, R.A. & Wichern, D.W. (1982)).

The procedure consists of the following three steps:

Step 1: Partition the data into K initial clusters;

Step 2: Assign each data point to the cluster with nearest mean (Euclidean distance is often used, although other distance function are allowed). The mean values of the clusters are recalculated.

Step 3: Step 2 is repeated until no data point is reassigned.

Another way of describing the method is as follows: It is well known in ANOVA (Analysis of Variance) that a total sum of squares (S.S.) can be decomposed into a within-group (a within-cluster) and a between-clusters S.S.:

(Total S.S.) =

(S.S. within clusters)+(S.S. between clusters)

(C.2.1)

Explicitly,

$$\sum_{i=1}^{k}\sum_{j=1}^{m_i}(x_{ij}-\bar{x})^2 = \sum_{i=1}^{k}\sum_{j=1}^{m_i}(x_{ij}-\bar{x}_{i\cdot})^2 + \sum_{i=1}^{k} m_i(\bar{x}_{i\cdot}-\bar{x})^2 \qquad (C.2.2)$$

where k: number of cluster

m_i: number of data points in the ith cluster

x_{ij}: data

and where $\bar{x}$ and $\bar{x}_i$ are the averages

$$\bar{x} = \frac{1}{k}\sum_{i=1}^{n}\frac{1}{m_i}\sum_{j=1}^{m_i} x_{ij}$$

$$\bar{x}_{i\cdot} = \frac{1}{m_i}\sum_{j=1}^{m_i} x_{ij}.$$

The objective of k-means is to minimize the within-cluster S.S. for a given number of clusters.

Cluster analysis are presented in Figs. C.7(a) and (b) for log DB95 and in Figs. C.8(a)-(c) for log DF15. One of the criteria that can be used to determine the number of clusters k is to consider the ratio between the within-cluster S.S. and the total S.S. as a function of k. This function is shown in Figs. C.9(a) and C.9(b) for both cases. On the both of these Figures, it is decided to use 3 clusters for log DB85 and 5 clusters for log DF15.

The analysis applies strictly only to the sample locations. In order to obtain a complete zoning of the

dam, each point is associated with the cluster of the nearest sampled point. The final results are shown in Figs. C.10 and C.11 for log DB85 and for log DF15 respectively.

Regions that consist of combinations of a homogeneous core zone and a homogeneous transition zone, are identified as shown in Fig. C.13. For each such region, Table C.13 gives area and the mean values of DF15, DB85 and DF15/DB85 (the latter using first order approximation).

It is straight forward to calculate the mean probability of filter malfunctioning at the given point of each zone based on the result of the logistic regression analysis of Chapter III. Two differrent logistic models have been fitted to the data: One is in terms of (DF15/DB85, DB95/DB75) (see Table 3.9), the other is in terms of (log DF15/DB85), DB95/DB75) (see Table 3.10).

The models are nearly the same except for extreme value of the parameters. In all calculations, the ratio DB95/DB75 is equal to 5 because (i) the base soil has a widely dispersed grain size distribution and (ii) the data base on which the results of the regression analysis is based includes only cases with DB95/DB75 < 5. Therefore, regression results are considered less reliable beyond this value.

The results are shown in Table C-4. As expected, the two models give very different results because of the

low lattice DF15/DB85. Clearly, the data is scarcely an indication of the probability of malfunctioning under these conditions.

C.2.2 Estimation of the Spatial Correlation Function

Because of the sparsity of grain size data, indirect information on the degree of spatial correlation of data grain size is obtained from the construction control density data.

Baecher (1984) has done some statistical analyses of density data including spatial correlation analysis. The only case in which he found significant correlation was in the analysis according to the sampling sequence. Correlation in terms of spacial distance was found to be not significant. This is an expected condition because material properties are expected to be strongly correlated to the borrow sources. As a consequence, the present correlation analysis uses the sampling sequence as a parameter for ordering the data.

The correlation function is estimated as follows:

(i) The data is grouped according to $\gamma_{d\ max}$.

(ii) Bartlett's test (Bancoft & Han (1981)) is used for the hypothesis that the variance is the same for all the groups.

(iii) If Bartlett's test passes (this is found to be the case here), then the F-test is used to reduce the number of groups when the difference in groups mean is not significant.

(iv) The correlation function is estimated for each group.

These procedures are explained next in detail.

(1) Use of $\gamma_{d\ max}$ to group γ_d

During construction, only dry density γ_d and w are measured at each sample point; on the other hand, the criteria used for control are in terms of the ratio $D=\gamma_d/\gamma_{d\ max}$. $\gamma_{d\ max}$ is usually estimated from compaction tests on the borrow material. This implies that the value of $\gamma_{d\ max}$ assigned to each measured point indicates the construction engineer's classification of that particular soil. For this reason, $\gamma_{d\ max}$ is used here to classify the data into homogeneous groups. As a result, 1045 data are classified into 25 groups.

(2) Bartlett's test on the homogeneity of variance

Suppose one has k sets of independent samples of size n_i (i=1,...k). Samples of this ith set are from $N(\mu_i, \sigma_i^2)$. We want to test the null hypotheses

$$H_o: \quad \sigma_1^2 = \sigma_s^2 = \ldots = \sigma_k^2 = \sigma^2$$

against an alternative hypotheses that for $\sigma_i^2 \neq \sigma^2$ at least

one i. The mean values in i are unknown, and must be estimated from the samples.

Under the present condition the likelihood function is

$$\mathcal{L} = \prod_{i=1}^{k} \frac{1}{(2\pi\sigma_i^2)^{ni/2}} \exp\left[-\sum_{j=1}^{n_i} \frac{(x_{ij} - \mu_i)^2}{s\sigma_i^2}\right] \tag{C.2.3}$$

It is easy to show that the maximum likelihood estimators of μ_i and σ_i^2 are

$$\begin{aligned} \hat{\mu}_i &= \bar{x}_i = \frac{1}{n_i} \sum_{j=1}^{n_i} \qquad (i=1,\ldots,k) \\ \hat{\sigma}_i^2 &= \frac{1}{n_i} \sum_{j=1}^{n_i} (x_{ij} - \bar{x}_i)^2 \end{aligned} \tag{C.2.4}$$

Substitution of Eq. (C.2.4) into Eq. (C.2.3) gives the maximum of the likelihood function:

$$\begin{aligned} \mathcal{L}_{max}^{1} &= \prod_{i=1}^{k} \frac{1}{(2\pi\hat{\sigma}_i^2)^{n_i/2}} \exp\left[-\sum_{j=1}^{n_i} \frac{(x_{ij} - \bar{x}_i)^2}{\frac{2}{n_i}\sum_{j=1}^{n_i}(x_{ij}-\bar{x}_i)^2}\right] \\ &= \prod_{i=1}^{k} \frac{1}{(2\pi\hat{\sigma}_i^2)^{n_i/2}} \exp\left[-\frac{n_i}{2}\right] \end{aligned} \tag{C.2.5}$$

On the other hand, under H_o, the maximum likelihood estimators of μ_i and σ^2 are

$$\hat{\mu}_{oi} = \bar{x}_{ii}$$

$$\hat{\sigma}_o^2 = \frac{1}{N} \sum_i \sum_j (x_{ij} - \bar{x}_i)^2 \qquad \text{(C.2.6)}$$

where $N = \sum_i n_i$

Hence the maximum of the likelihood is

$$\mathcal{L}^o_{max} = (2\pi\hat{\sigma}_o^2)^{-\frac{N}{2}} e^{-\frac{N}{2}} \qquad \text{(C.2.7)}$$

Taking the ratio between Eqs. (c.2.5) and (c.2.7),

$$\gamma = \frac{\mathcal{L}^0_{max}}{\mathcal{L}^1_{max}}$$

$$= \frac{(2\pi\hat{\sigma}_o^2)^{-\frac{N}{2}} e^{-\frac{N}{2}}}{\prod_{i=1}^{k} (2\pi\hat{\sigma}_i^2)^{-\frac{n_i}{2}} e^{-\frac{n_i}{2}}}$$

$$= \frac{\prod_{i=1}^{k} (\hat{\sigma}_i^2)^{\frac{n_i}{2}}}{(\hat{\sigma}_o^2)^{N/2}} \qquad \text{(C.2.8)}$$

H_o is rejected if $\lambda \leq \lambda_\alpha$ (where λ_α corresponds to α% significant value of λ). This test is slightly biased due to the use of biased estimators $\hat{\sigma}_i^2$ and $\hat{\sigma}_o^2$. In order to correct this bias Bartlett suggests replacing the sample size n_i by n_i-1 in the expression for λ. He proposed

use of the statistic

$$B = \frac{\nu \log S_o^2 - \sum_{i=1} \nu_i \log S_i^2}{1 + \frac{1}{3(k-1)} \{ \sum_{i=1}^{k} \frac{1}{\nu_i} - \frac{1}{\nu} \}} \qquad (C.2.9)$$

where

$$\nu_i = n_i - 1, \qquad \nu = \sum_i \nu_i = N-k$$

$$S_i^2 = \frac{1}{\nu_i} \sum_{i=1}^{n_i} (x_{ij} - \bar{x}_i)^2$$

$$S_o^2 = \sum_i \nu_i S_i^2 / \nu$$

Under Ho for large sample size n_i B is approximately distributed like χ^2 with (k-1) degree of freedom. Hence H_8 is rejected if $B > \chi^2_{\alpha,k-1}$. The test is unfortunately not robust with respect to departures from normality. For detail, see for example Bancoft & Han (1981).

For the present data set, the quantity B Eq. C.2.9) has value 33.6, and Ho is accepted at the 5% significant level because $\chi^2_{d.o.f.=24} = 36.42$.

(3) F-test to reduce the number of clusters

From the previous analysis, we have concluded that all the group variances can be considered the same. Next, we want to test whether the group means can be considered the same. In this case, the null hypothesis is

$$H_o: \mu_1 = \mu_2, \ldots, \mu_k = \mu$$

and is tested against H_1: $\mu_i = \mu$ for at least one i.

This is a standard problem in analysis of variance (ANOVA), see e.g., Snedecor & Cochran [1980]. The test consists of calculating the ratio

$$F = \frac{SS_{treatment}/(k-1)}{SS_{error}/(N-k)} \qquad (C.2.10)$$

where

$$SS_{treatment} = \sum_{i=1}^{k} \sum_{j=1}^{n_i} (\bar{x}_{i.} - \bar{\bar{x}}_{..})^2$$

$$SS_{error} = \sum_{i=1}^{k} \sum_{j=1}^{n_i} (x_{ij} - \bar{x}_{i.})^2$$

and of rejecting H_o if

$$F > F_{\alpha,k-1,n-k}$$

This test has been used to reduce the number of statistically different groups from 25 to 9. Final results are shown in Fig. C.11.

(4) Estimation of the Correlation Function

Correlation functions are estimated using only groups with more than 100 data points. This reduces the number of useful groups to 5. Results are shown in Fig. C.12(a)-(e). For groups 5 and 8 (Fig. C.12(a)

(e)) showed no obvious trend, possibly due to the small sample size (Baecher, 1984).

C.3 Results

The generalized weakest link model of Chapter IV can be used now to calculate the probability of filter malfunctioning. Eq. (4.3.11) gives

$$\Phi_F = 1-\{\beta_1^{m\bar{P}_f}\beta_2^{n\bar{P}_F}\exp[-mn(\frac{\bar{P}_f}{2})^2 \ell n\beta_1 \ell n\beta_2]\}(1-\bar{P}_f) \quad (4.3.11)$$

where Φ_F: the system failure probability

$\bar{P}_F$: mean failure probability

m,n: size of the 2-D continuum.

β_1, β_2: correlation coefficients at distance $\Delta s = 1$ in two othogonal directions.

$\bar{P}_f$ varies from region to region (Section C.2.1).

Let us consider 20 ft. as unit length for calculational convenience. Because of the scarceness of the data, this procedure will not affect the result. Each latter in Fig. C.13 indicates square area with unit length sides (i.e., 20 ft. by 20 ft. square). Because of the nature of the construction procedure, we assume these unit squares are correlated only to the horizontal direction. For the vritual direction, correlation is only assumed within each square. As obtained in Section C.2.2, the correlation coefficient for points unit distance apart

is estimated to be 0.35, than Eq. (4.3.11) becomes

$$P_F = 1 - \{\beta^{(n+1)\bar{P}_f} \exp[-n(\frac{\bar{P}_f \ell n \beta}{2})^2]\}(1-\bar{P}_f)$$

The calculated results are given in Table C.4.

Results based on (DF15/DB85, DB95/DB75) model give an unreasonably high failure probability. On the other hand, the model based on (log (DF15/DB85), DB95/DB75) give probability that are negligibly small for all regions except region C for which $\Phi_F \simeq 10^{-4}$. This discrepancy in the results comes from the difficulty of evaluating $\bar{P}_f$ under very safe conditions, using statistical data from laboratory experiments (see Section 3.3.3). Results obtained under the second model (smaller failure probability) appears to be more reasonable.

TABLE C.1 LEADING DIMENSIONS OF CARTERS DAM

Crest of embankment	El. 1112.3 ft
Top water level	El. 1107.2 ft
Maximum height above foundation	445 ft (135.6m)
Length of embankment	2053 ft (625.8m)
Crest	40 ft (12.2m)
Upstream slope	1:1.9
Downstream slope	1:1.8

Total value of Embankment	14 766 000 C.Y.	(11 296 000 m^3)
Rock	12 416 000 C.Y.	(9 498 000 m^3)
impervious material	1 800 000 C.Y.	(1 377 000 m^3)
random material	550 000 C.Y.	(420 000 m^3)

TABLE C.2 LIST OF SOIL TEST DATA AVAILABLE

Classification	Size of Data	Measured Quantities
Shear tests on Core Material	57	TC Q (3 per each point), TC R(3 per each point), DS S (3 per each point) Grain size distribution, LL, PL, G, w, Compaction test (w_{opt}, $\gamma_{d\ max}$), Consolidation test (Cc, t_{50})
Construction Control Density	1175	Dry density (γ_d), Water content (w), Date measured, Spatial location, Estimated maximum dry density ($\gamma_{d\ max}$), Estimated Optimum water content (w_{opt}), Borrow source.
Large diameter density test (Transition Zone)		Dry density (γ_d), Grain size distribution, Water content (w), Spatial location, Date measured.
Zone 2		
Downstream	28	
Upstream	37	
Zone 3A	69	
Zone 3B (Rock Fill)	14	
Zone 3C	44	

Note: TC: triaxial compression DS: Direct shear Q: quick, R: rapid,
S: slow

TABLE C.3. SUMMARY OF CLUSTER ZONES

Core (Zone 1) - DB85 -

Cluster #	# of Data	Mean	s.d.
B1	16	-0.818(0.152)	0.256
B2	12	0.142(1.39)	0.189
B3	26	0.962(9.16)	0.245

Transition (Zone 2; Downstream) - DF15 -

Cluster #	# of Data	Mean	s.d.
F1	5	-1.86(0.0139)	0.252
F2	12	-1.39(0.0404)	0.101
F3	7	-0.686(0.206)	0.184
F4	3	-0.942(0.796)	0.199
F5	1	0.845(7.00)	--

Table C.4 Combinations of the core and transition zones

Combi-nation	Cluster # (Core)	Cluster # (Trans.)	Area (unit)	DF15 (mm)	DB85 (mm)	DF15/DB85	log(DF15/DB85)		DF15/DB85	
A	B1	F1	137	0.0139	0.152	0.091	0	0	4.7E-4	0.066
B	B1	F2	11	0.0404	0.152	0.27	0	0	6.3E-4	8.5E-3
C	B1	F3	49	0.206	0.152	1.36	2.9E-6	1.6E-4	3.6E-3	0.175
D	B1	F4	-	0.796	0.152	5.24	-	-	-	-
E	B1	F5	-	7.00	0.152	46.05	-	-	-	-
F	B2	F1	128	0.0139	1.39	0.01	0	0	4.2E-4	0.056
G	B2	F2	79	0.0404	1.39	0.029	0	0	4.3E-4	0.036
H	B2	F3	38	0.206	1.39	0.148	0	0	5.2E-4	0.022
I	B2	F4	-	0.796	1.39	0.573	-	-	-	-
J	B2	F5	-	7.00	1.39	5.04	-	-	-	-
K	B3	F1	113	0.0139	32.0	4.3E-4	0	0	4.0E-4	0.047
L	B3	F2	332	0.0404	32.0	1.3E-3	0	0	4.1E-4	0.134
M	B3	F3	149	0.206	32.0	6.4E-3	0	0	4.1E-4	0.063
N	B3	F4	68	0.796	32.0	0.025	0	0	4.3E-4	0.031
O	B3	F5	-	7.00	32.0	0.22	-	-	-	-

1 unit area is 20'x20' square System Failure Probability = 1.6E-4 (0.51)

Fig C 1

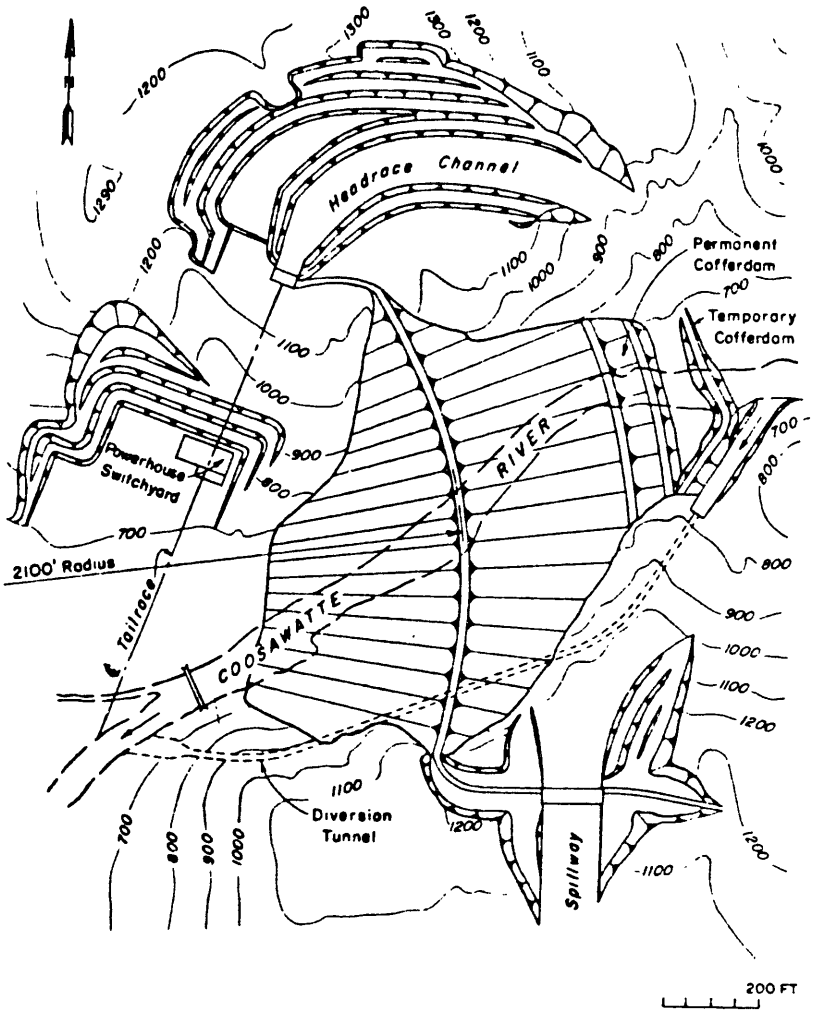

Fig. C.1 Layout of Carters Dam

EMBANKMENT MATERIALS

Zone 1 - Impervious Core - Highly weathered and Disintegrated Rock

Zone 2 - Transition Material - Weathered Rock

Zone 3A - Best Quality Rock - Sound Quartzite with up to 30% Argillite and/or Phylite

Zone 3B - Intermediate Quality Rock - Slightly Weathered Rock with up to 40% Argillite and/or Phylite

Zone 3C - Random Rock

Zone 3AA - Best Quality Rock - Sound Quartzite with 30% Finer than #4 Sieve

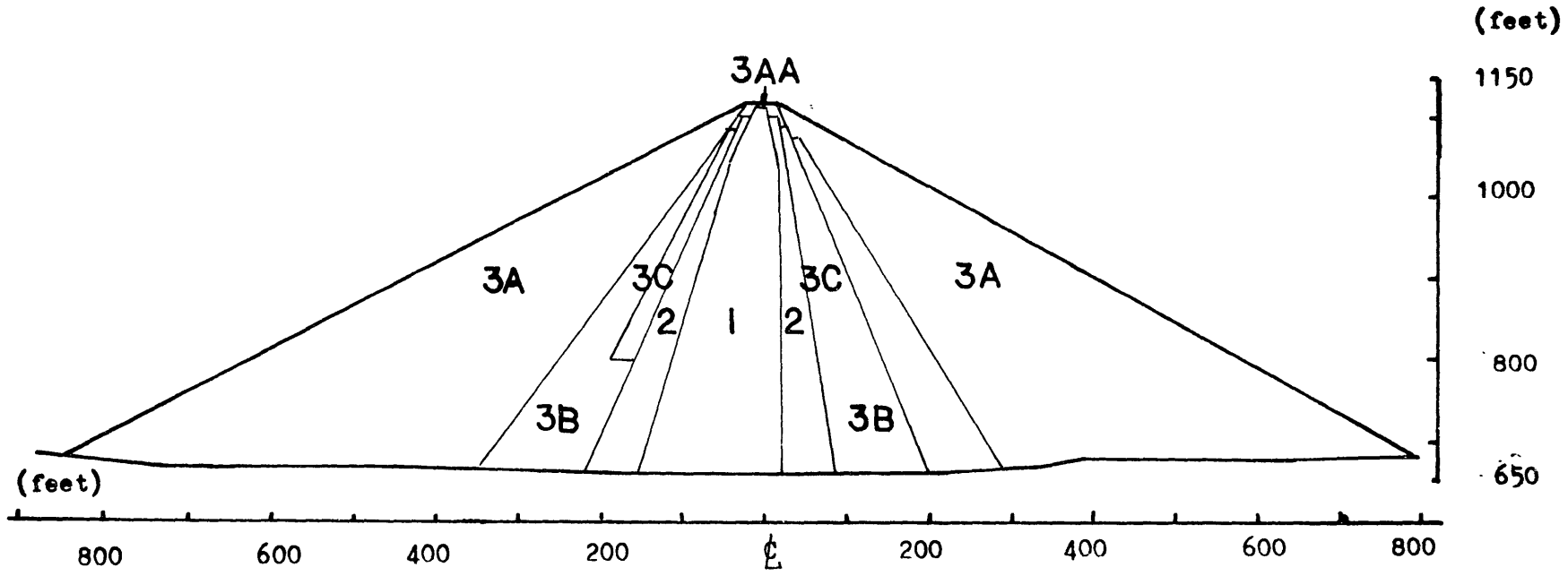

Fig. C.2 Section of Carters Dam

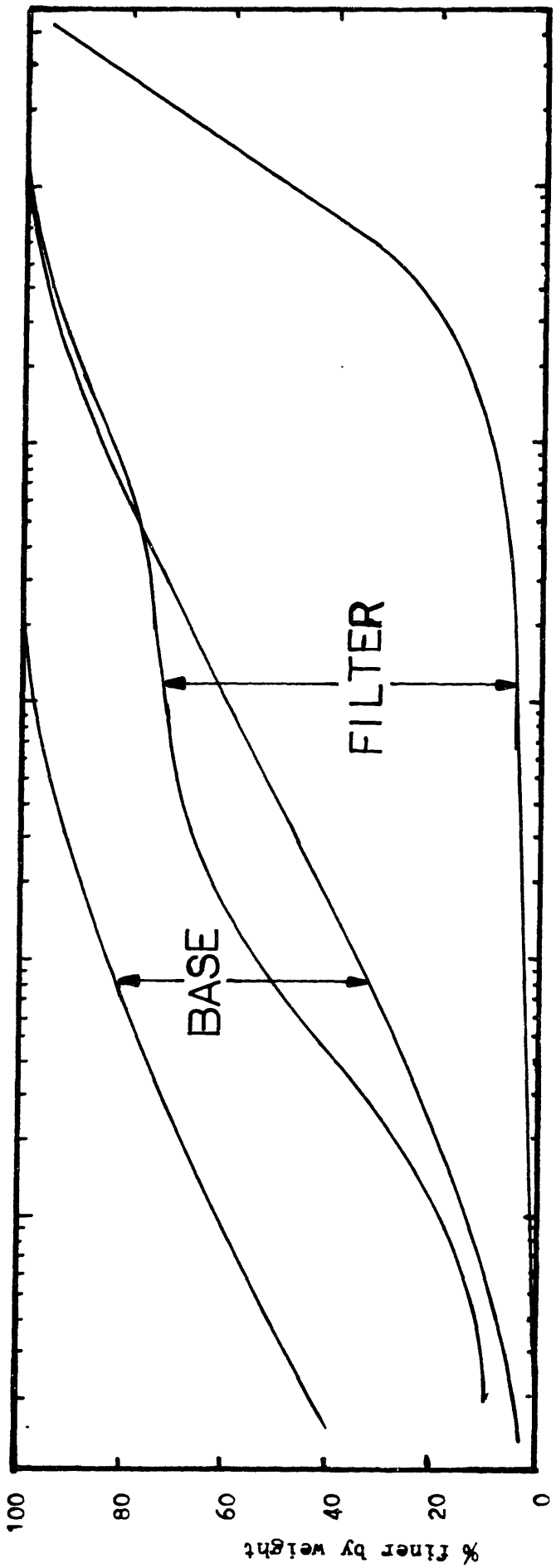

Fig. C.3 Typical Grain Size Distributions of Zone 1 and Zone 2

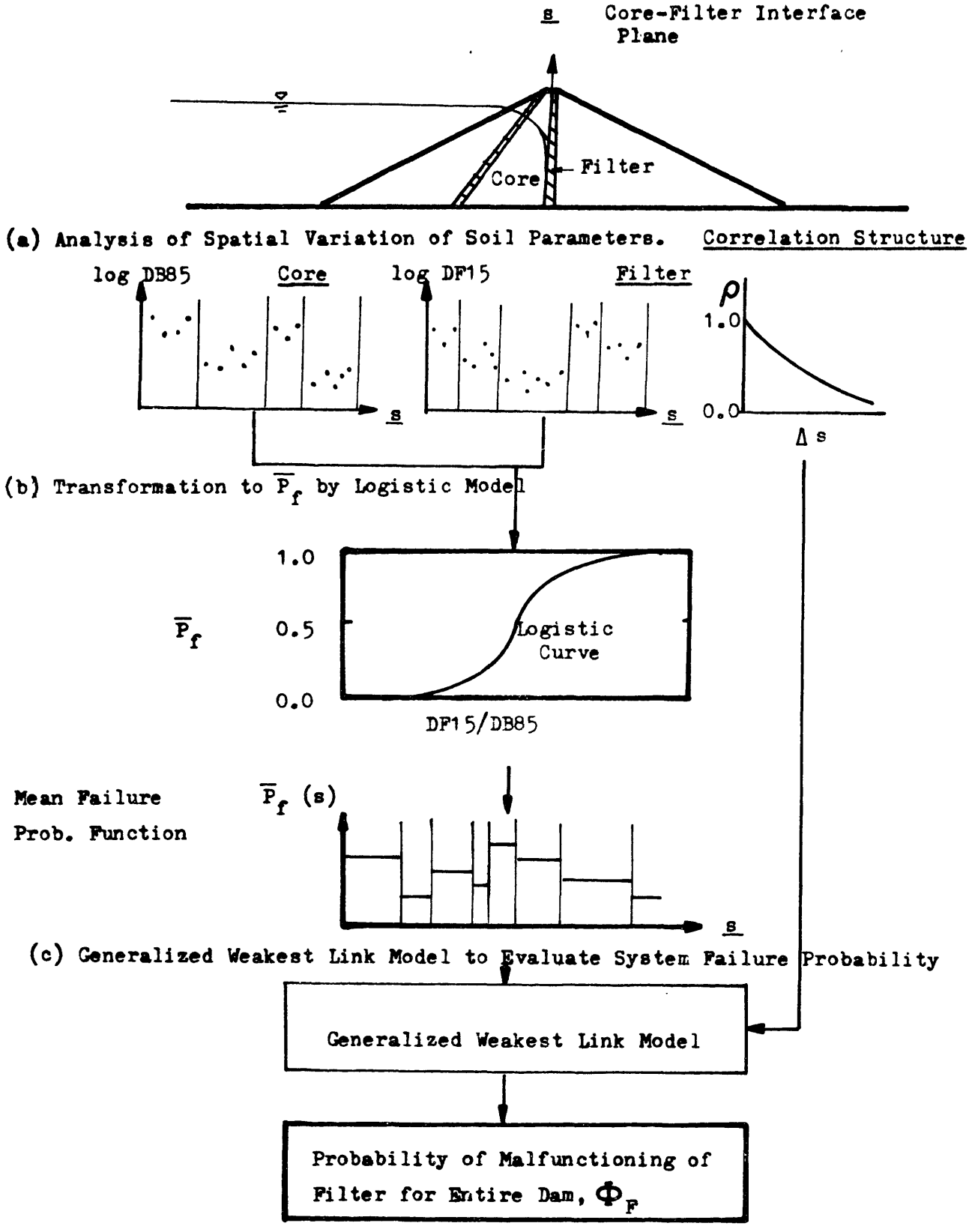

Fig. C.4 The Proposed Procedure to Calculate the Probability of Malfunctioning of Dam Filter System

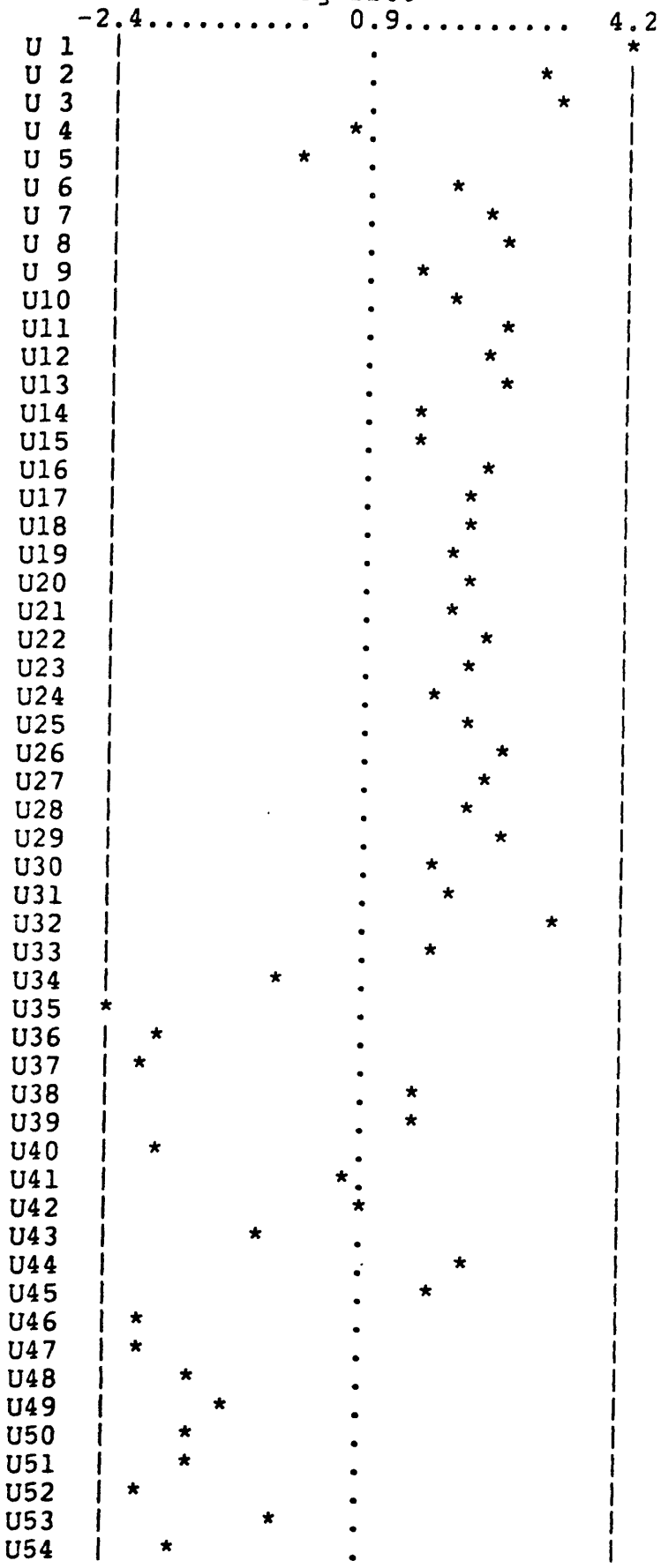

Fig. C5 The variation of log DB85 according to the Sample Sequence

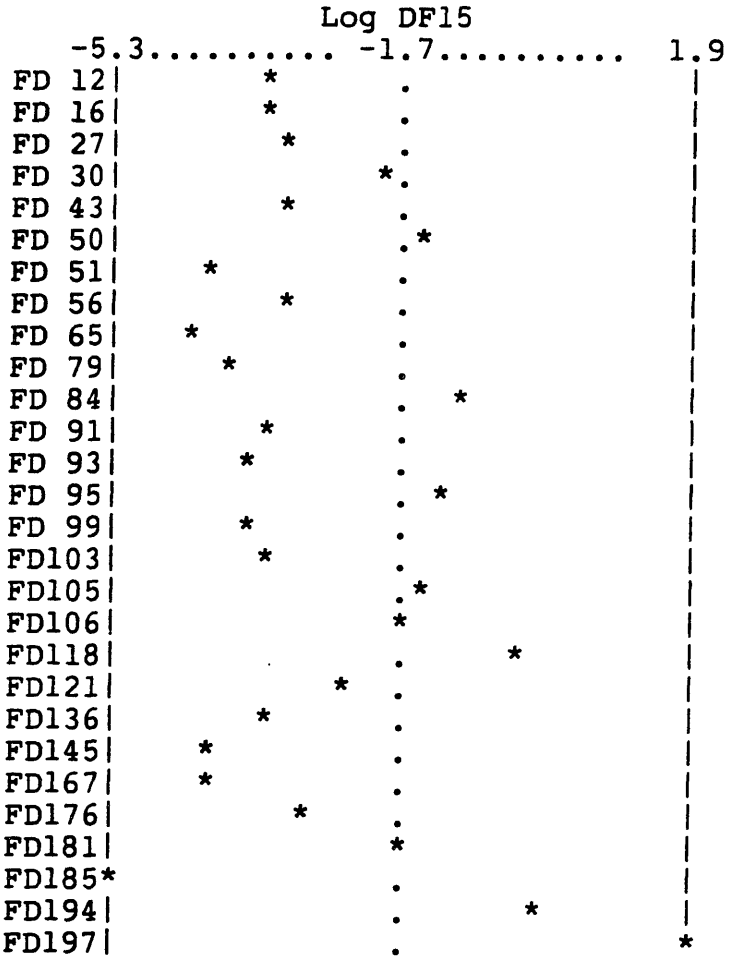

Fig. C.6 The Variation of log DF15 according to the Sample Sequence

Log DB85 Analyaia on Zone 1 by K-Means; No Weight

Output for each cluster .....

Cluster#	# of Data	S.S.	Centers
1	16	1.051878	-0.8176277
2	12	0.3948698	0.1424372
3	26	1.505676	0.9616050

Total Sum of Squares	34.49413
Sum of Squares within Clusters	2.952424
Sum of Squares between Clusters	31.54171
S.S.b.C. / T.S.S.	0.9144080

Zone 1 - Core of the Dam -

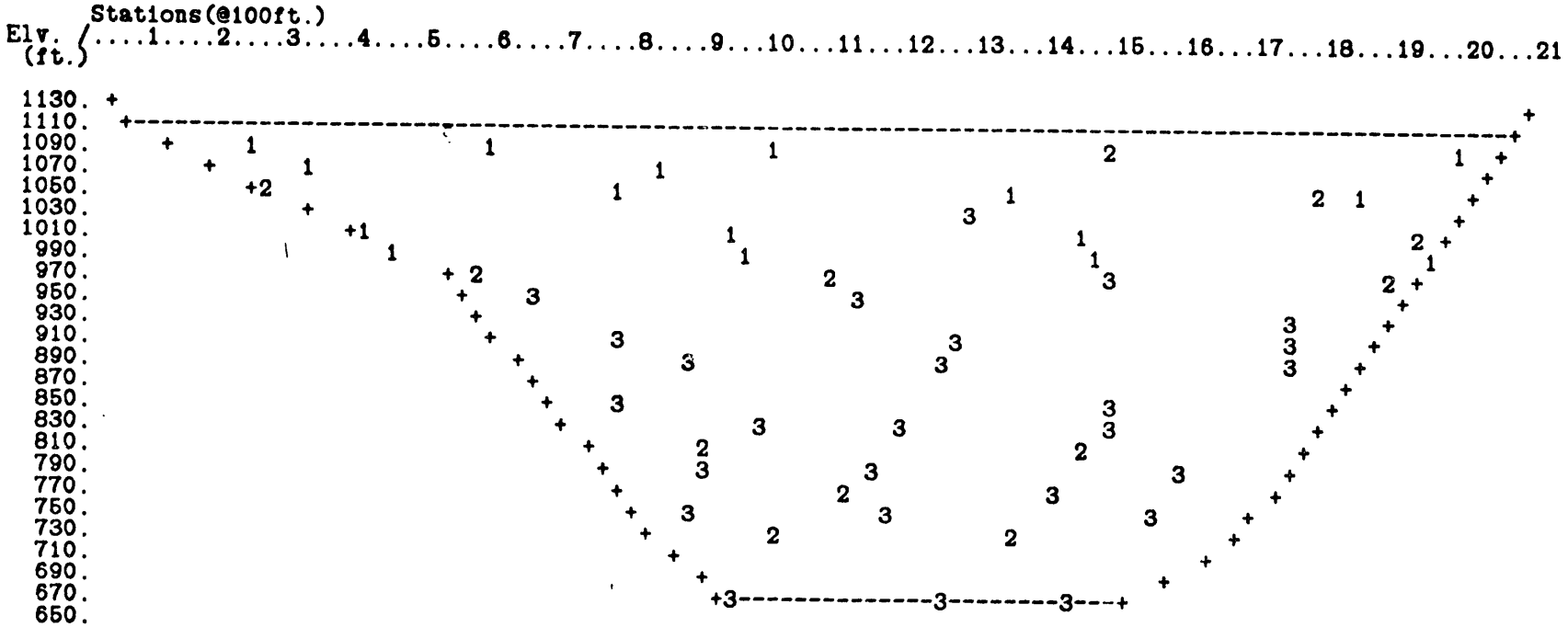

Fig. C.7(a) Results of K-means Analysis for log DB85

Log DB85 Analysis by K-Means Method; No Weight

Output for each cluster .....

Cluster#	# of Data	S.S.	Centers
1	15	0.8445467	-0.8470194
2	12	0.5150023	0.7377820e-01
3	17	0.3403457	0.7980639
4	10	0.4619483	1.188180

Total Sum of Squares	34.49413
Sum of Squares within Clusters	2.161843
Sum of Squares between Clusters	32.33229
S.S.b.C. / T.S.S.	0.9373273

Zone 1 - Core of the Dam -

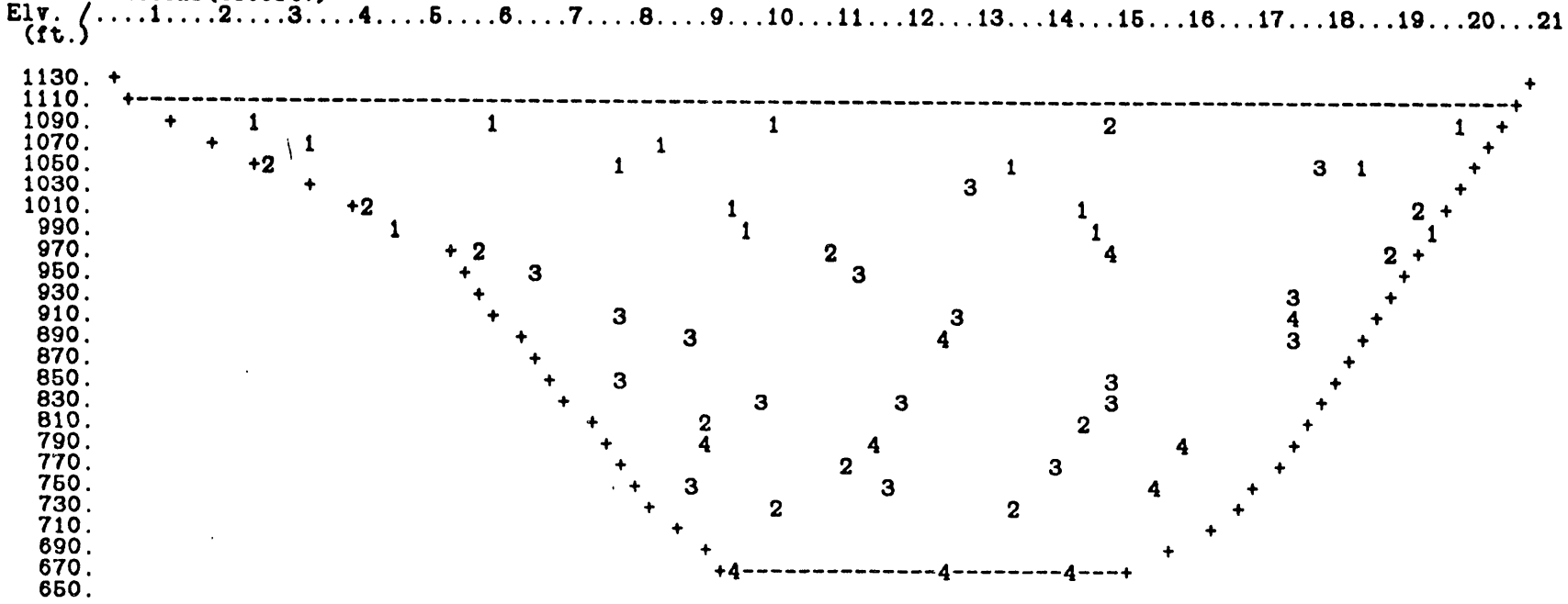

Fig. C.7(b) Results of K-means Analysis for log DB85

Fig C.8(a)

Analysis of Log DF15 of Zone 2 (downstream) by K-means Method: No weight

Output for each cluster .....

Cluster#	# of Data	S.S.	Centers
1	17	1.126381	-1.530637
2	8	0.2382727	-0.6474331
3	3	0.4356954	0.3080927

Total Sum of Squares	12.57986
Sum of Squares within Clusters	1.850349
Sum of Squares between Clusters	10.72951
S.S.b.C. / T.S.S.	0.8529117

Zone 1 - Core of the Dam -

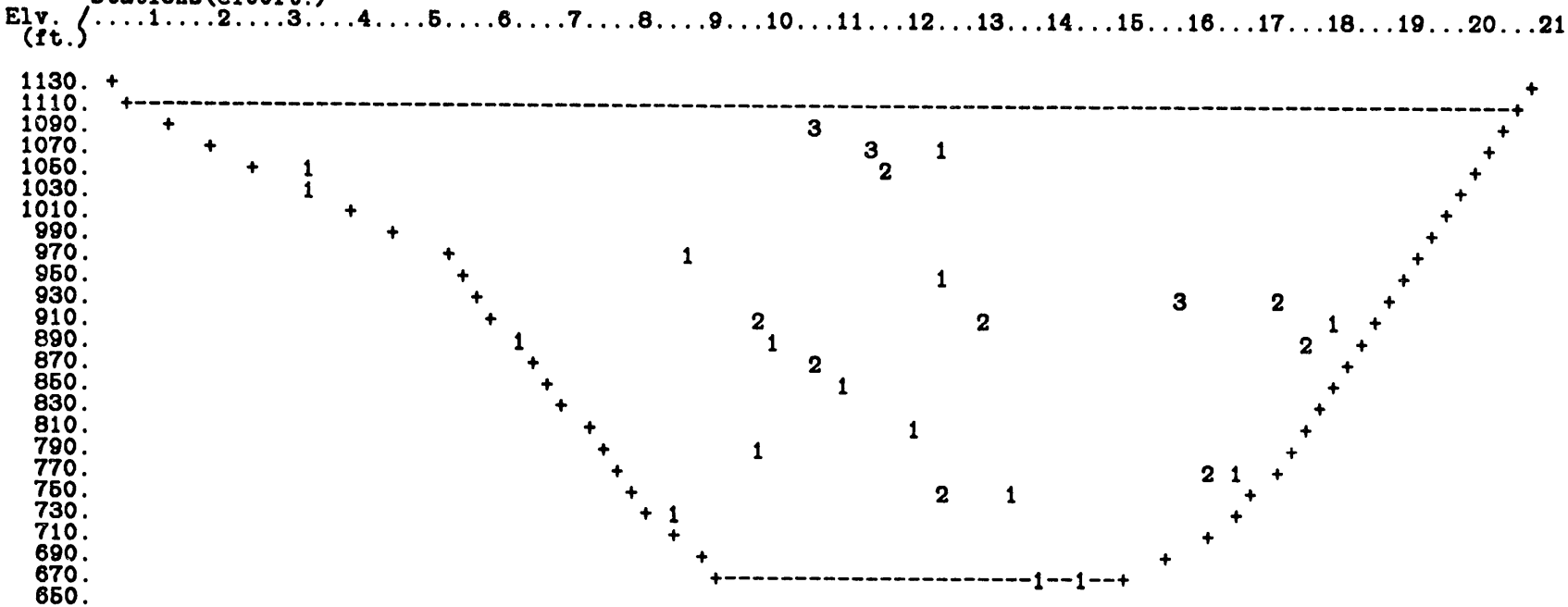

Fig. C.8(a) Results of K-means Analysis for log DF15

Analysis of Log DF15 of Zone 2 (downstream) by K-means Method: No Weight

Output for each cluster .....

Cluster#	# of Data	S.S.	Centers
1	6	0.3088375	-1.815322
2	12	0.1951792	-1.344074
3	7	0.1462125	-0.5970665
4	3	0.4356954	0.3080927

Total Sum of Squares	12.57986
Sum of Squares within Clusters	1.085925
Sum of Squares between Clusters	11.49393
S.S.b.C. / T.S.S.	0.9136776

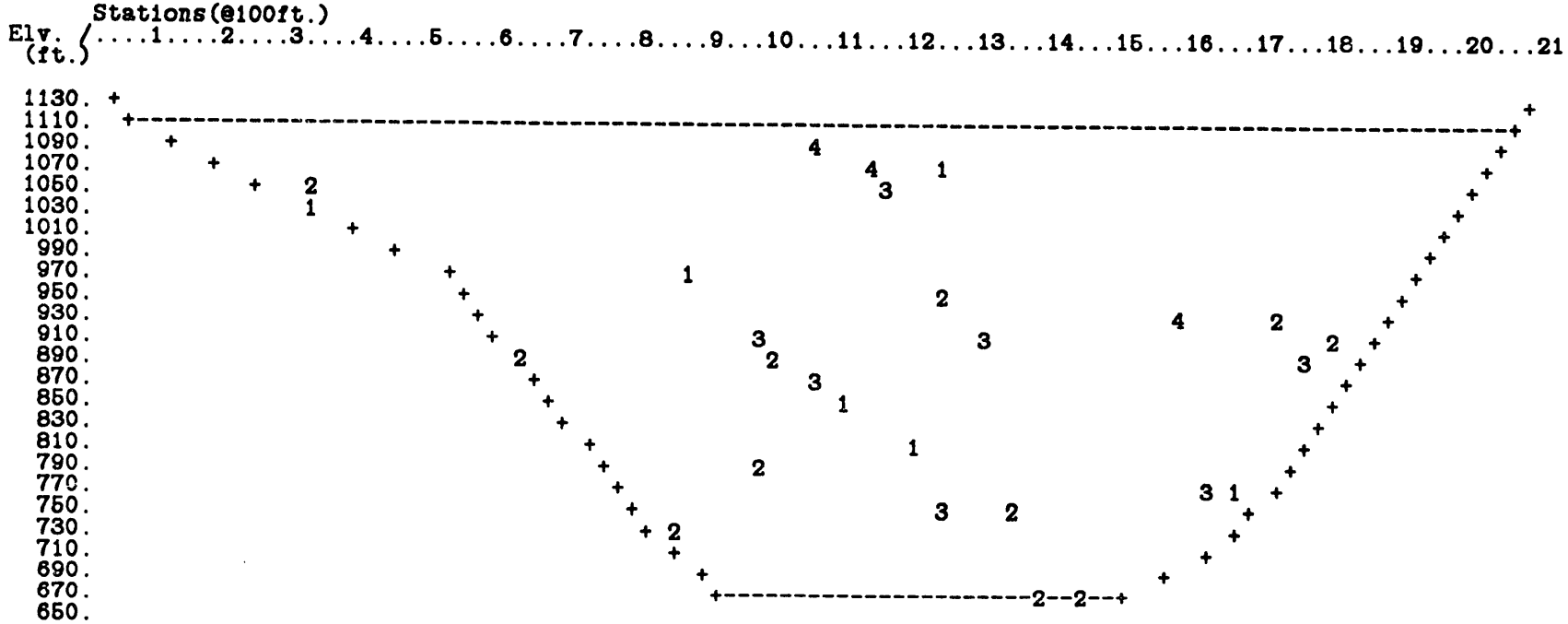

Fig. C.8(b) Results of K-means Analysis for log DF15

Fig. C.8(c)

Analysis of Log DF15 of Zone 2 (Downstream) by K-means Method; No Weight

Output for each cluster .....

Cluster#	# of Data	S.S.	Centers
1	5	0.2542599	-1.857974
2	12	0.1131409	-1.394246
3	7	0.2045365	-0.6861020
4	3	0.1186946	-0.9918971E-01
5	1	0.0000000E+00	0.8450971

Total Sum of Squares	12.57986
Sum of Squares within Clusters	0.6906320
Sum of Squares between Clusters	11.88923
S.S.b.C. / T.S.S.	0.9451002

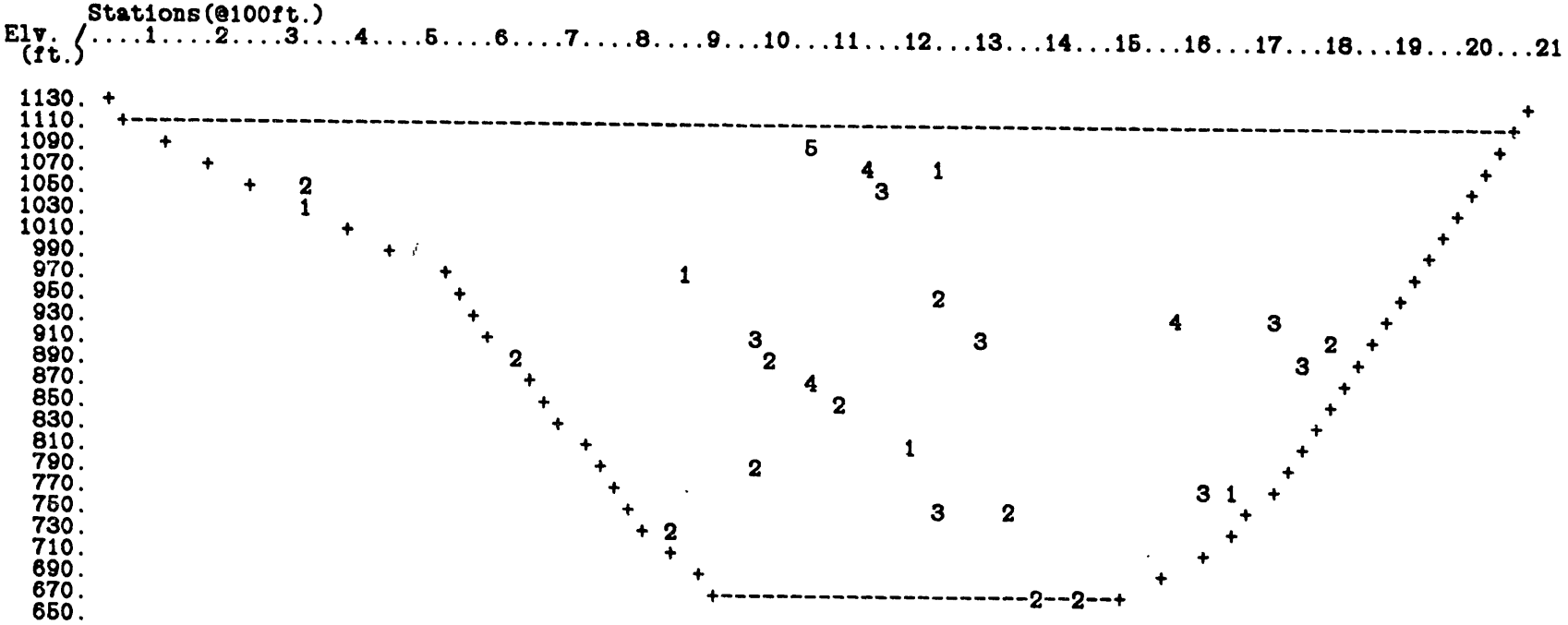

Fig. C.8(c) Results of K-means Analysis for log DF15

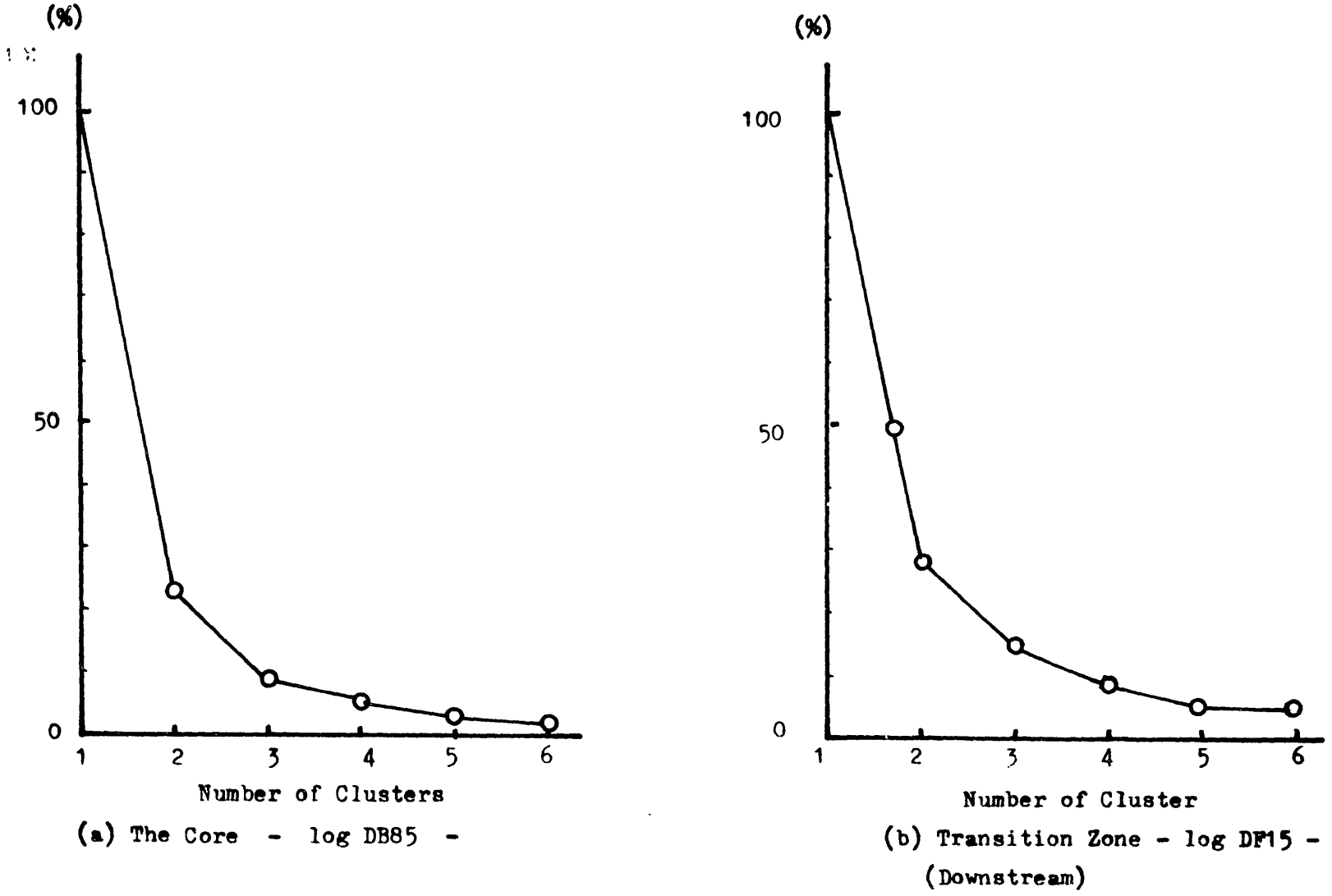

(a) The Core - log DB85 -

(b) Transition Zone - log DF15 - (Downstream)

Fig. C.9 (Variance between Clusters)/(Total Variance) vs. Number of Clusters

Log DB85 Analysis on Zone 1; Zoned based on the K-means analysis

Output for each cluster .....

Cluster#	# of Data	S.S.	Centers
1	16	1.051878	-0.8176277
2	12	0.3948698	0.1424372
3	26	1.505676	0.9616050

Total Sum of Squares	34.49413
Sum of Squares within Clusters	2.952424
Sum of Squares between Clusters	31.54171
S.S.b.C. / T.S.S.	0.9144080

Zone 1 - Core of the Dam -

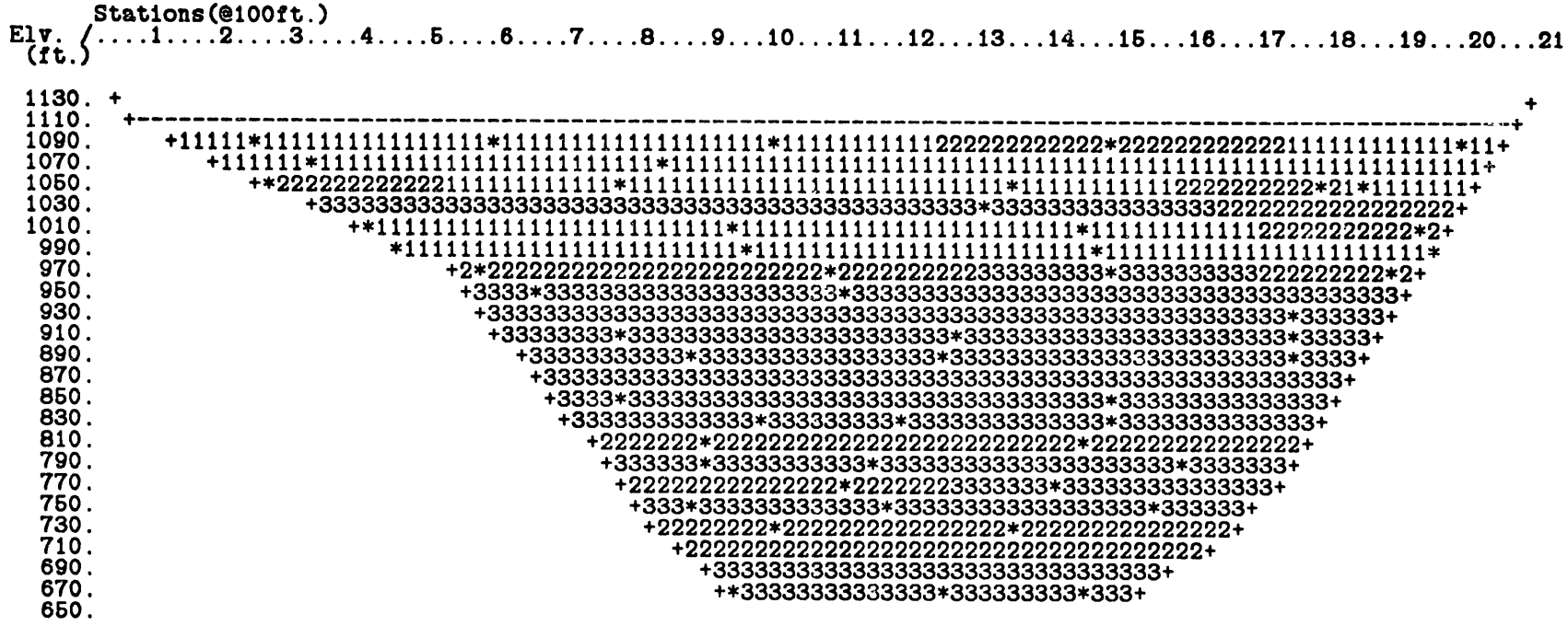

* Sample Points

Fig. 10(a) Results of K-means Clustering for log DB65

Analysis of Log DF15 of Zone 2 (Downstream) by K-means Method; No Weight

Output for each cluster .....

Cluster#	# of Data	S.S.	Centers
1	5	0.2542599	-1.857974
2	12	0.1131409	-1.394246
3	7	0.2045365	-0.6861020
4	3	0.1186946	-0.9918971E-01
5	1	0.0000000E+00	0.8450971

Total Sum of Squares	12.57986
Sum of Squares within Clusters	0.6906320
Sum of Squares between Clusters	11.88923
S.S.b.C. / T.S.S.	0.9451002

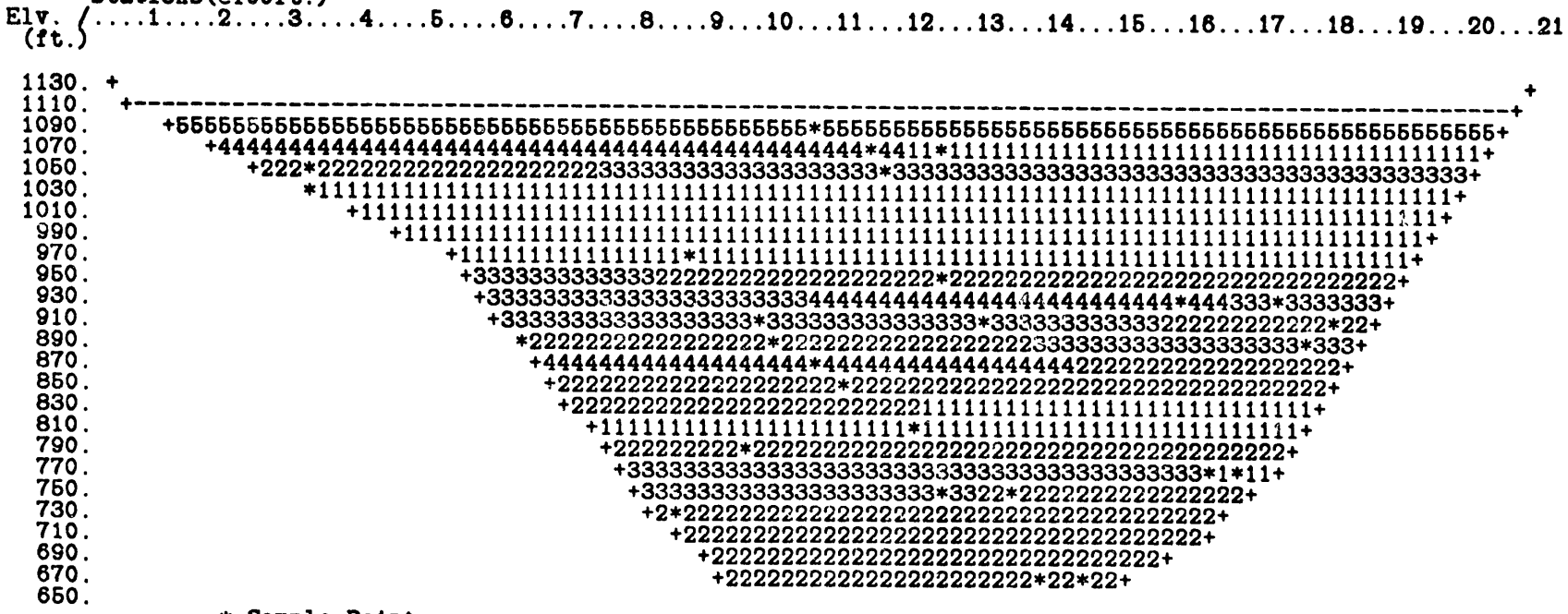

Fig. C.10(b) Results of K-means Clustering for log DB15

Zone 1 - Core of the Dam -

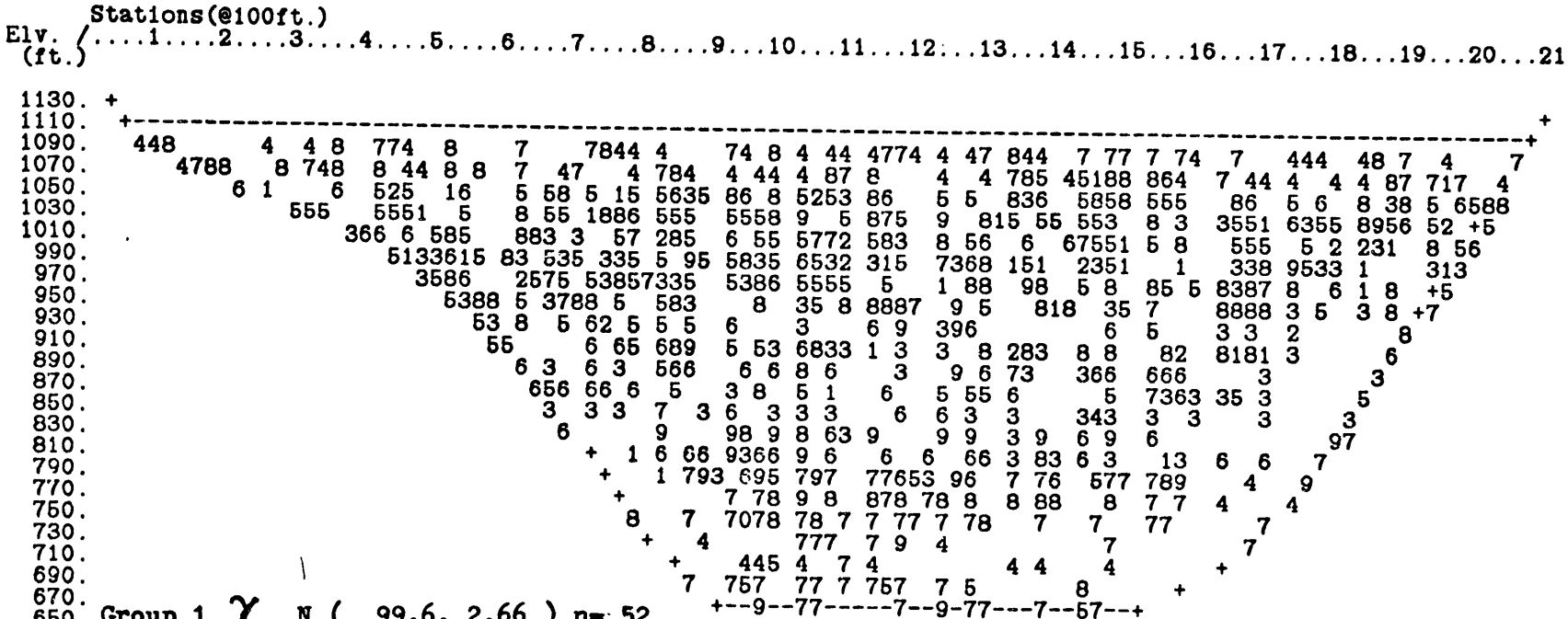

Group 1 γ_d N (99.6, 2.66) n= 52

Group 2 γ_d N (101.2, 2.66) n= 26

Group 3 γ_d N (105.2, 2.66) n=169

Group 4 γ_d N (107.4, 2.66) n= 79

Group 5 γ_d N (109.5, 2.66) n=259

Group 6 γ_d N (110.6, 2.66) n=122

Group 7 γ_d N (112.9, 2.66) n=167

Group 8 γ_d N (116.2, 2.66) n=213

Group 9 γ_d N (120.6, 2.66) n= 47

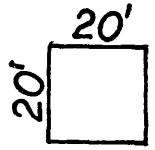

Unit Area

Fig. C.11 Results of Clustering Based on Dry Density Data

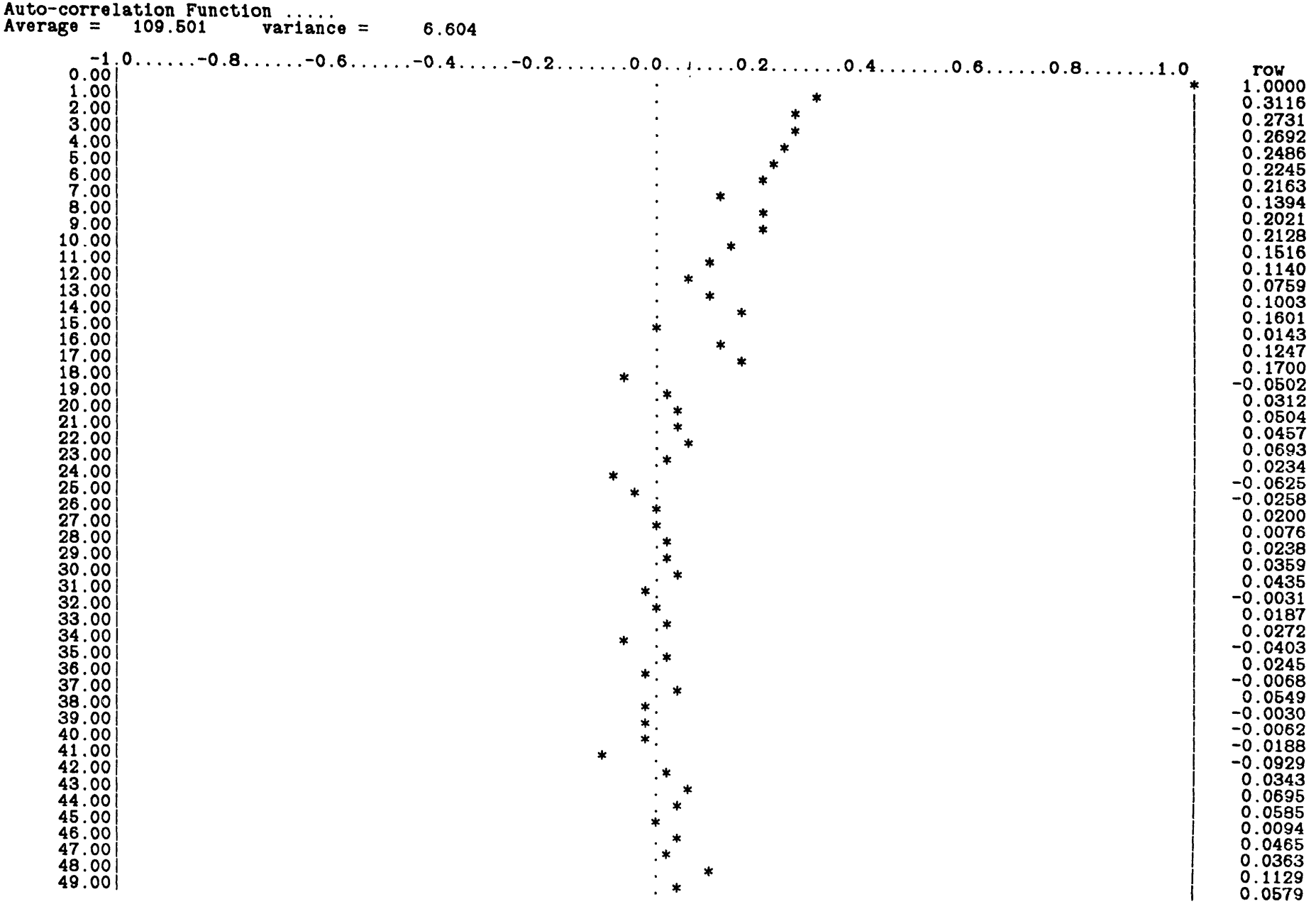

Fig. C.12(a) Estimated Auto-Correlation Function of Dry Density Data: Group 5 (N=259)

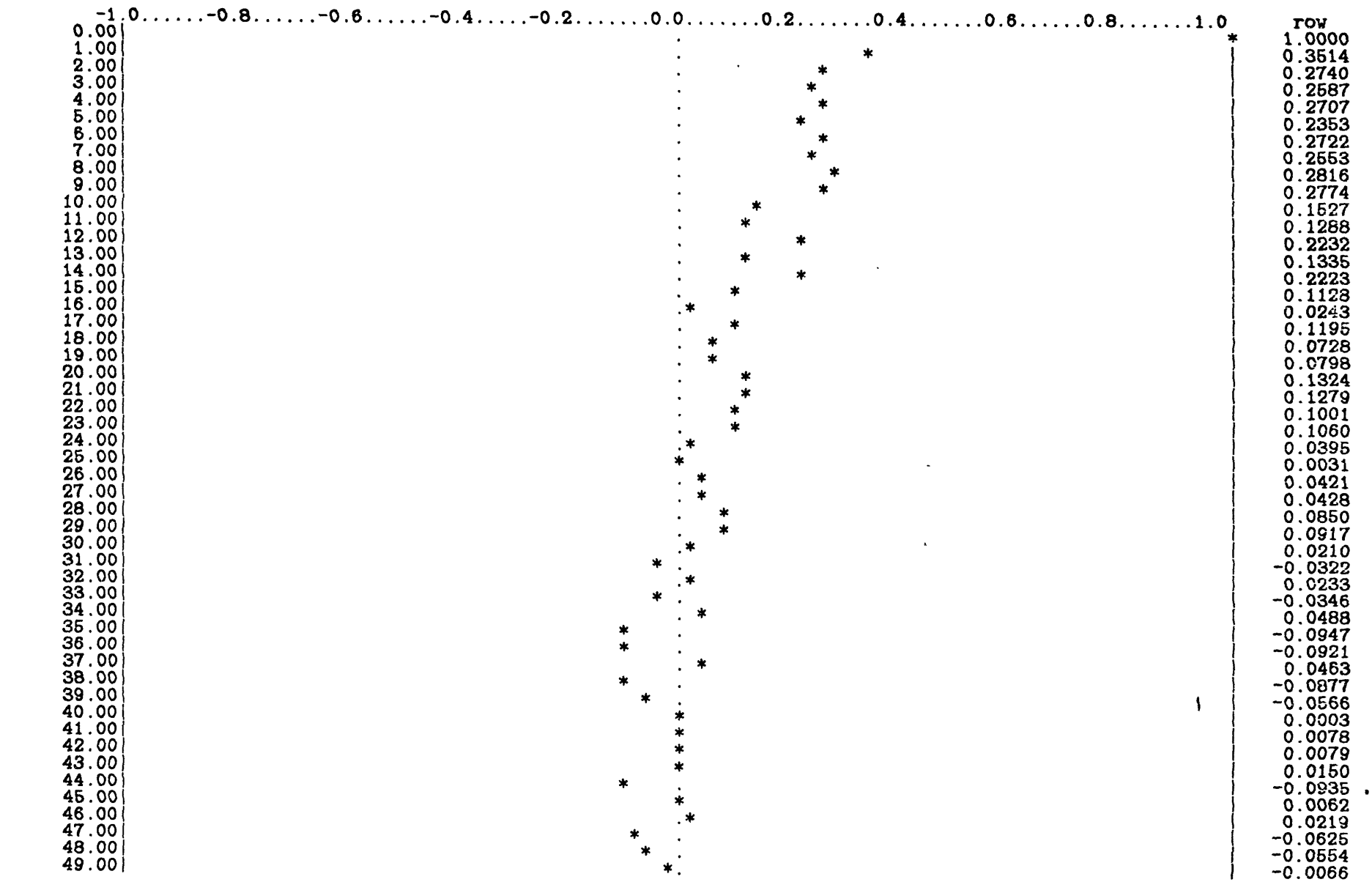

Fig. C.12(b) Estimated Auto-Correlation Function of Dry Density Data: Group 8 (N=213)

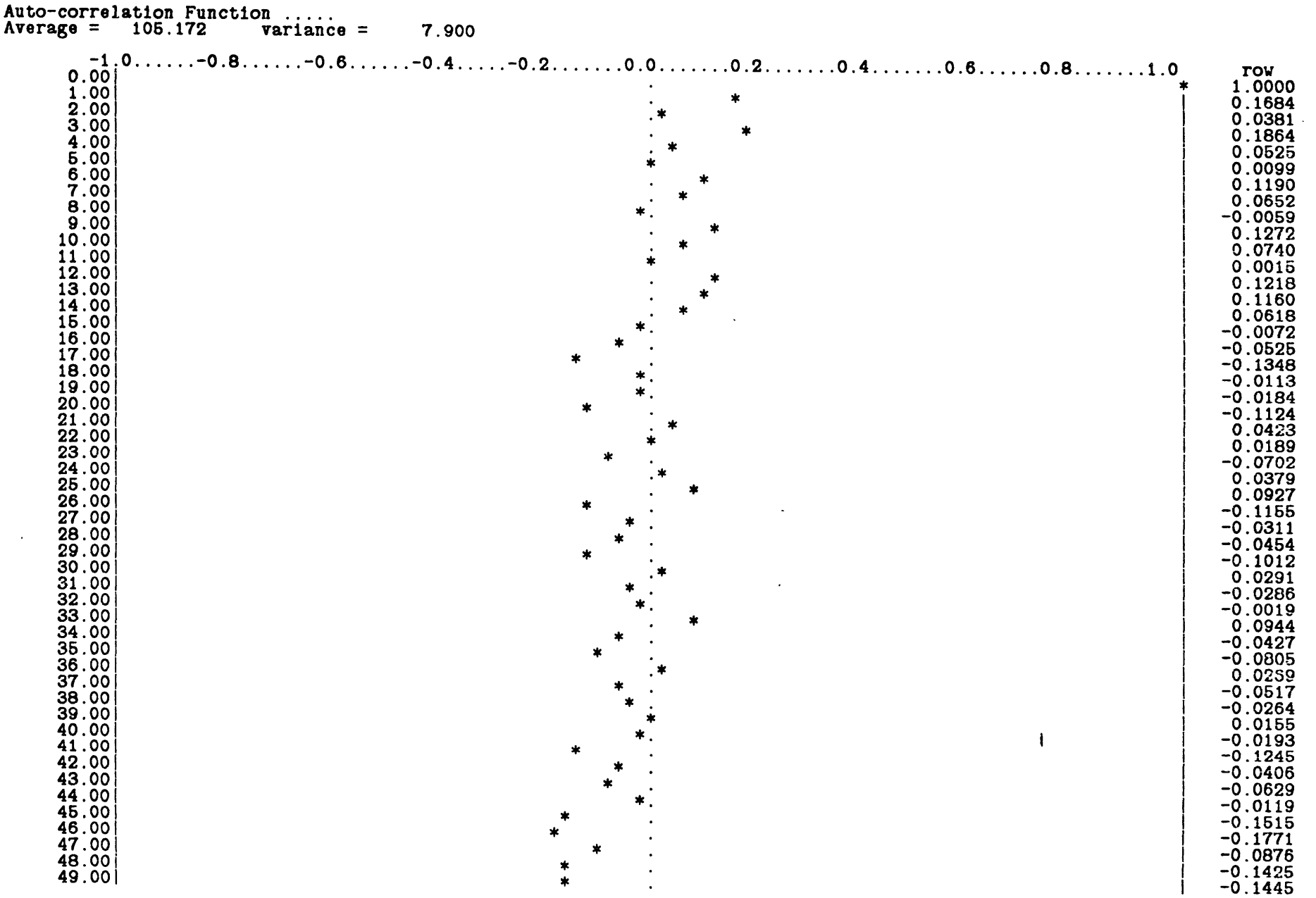

Fig. C.12(c) Estimated Auto-Correlation Function of Dry Density Data: Group 3 (N=169)

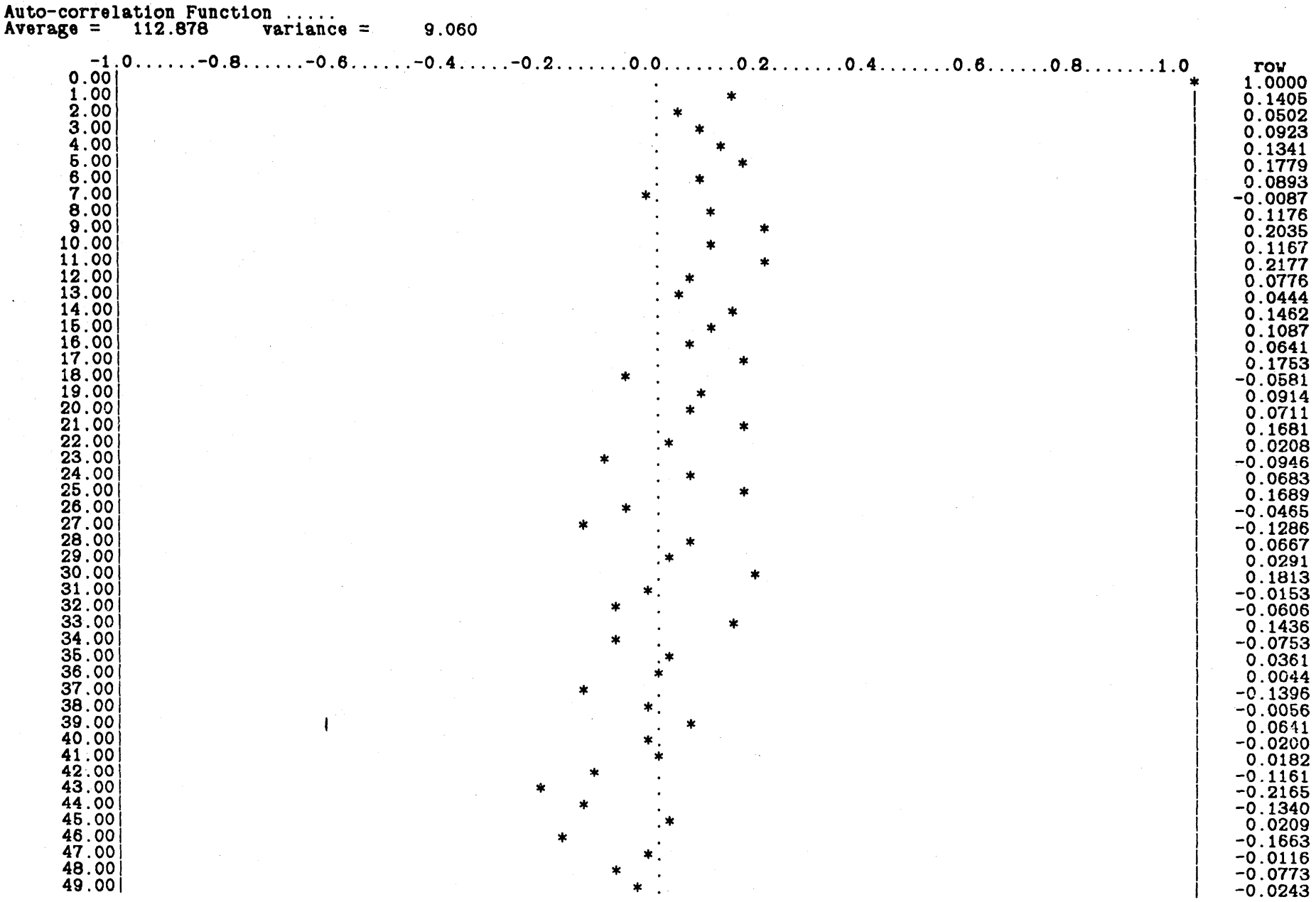

Fig. C.12(d) Estimated Auto-Correlation Function of Dry Density Data: Group 7 (N=167)

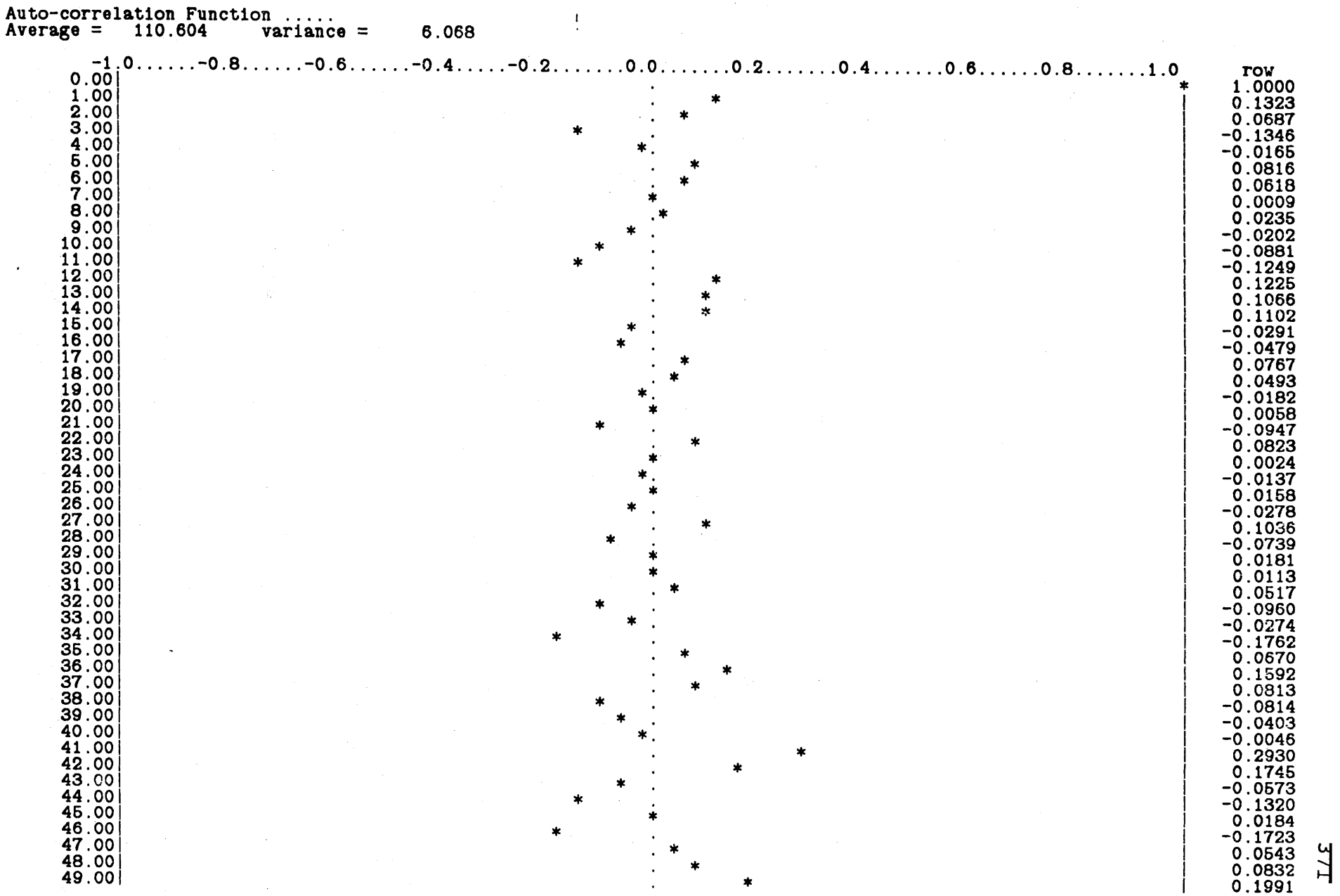

Fig. C.12(e) Estimated Auto-Correlation Function of Dry Density Data: Group 6 (N=122)

Zoning based on the combinations of Core material and Transition material

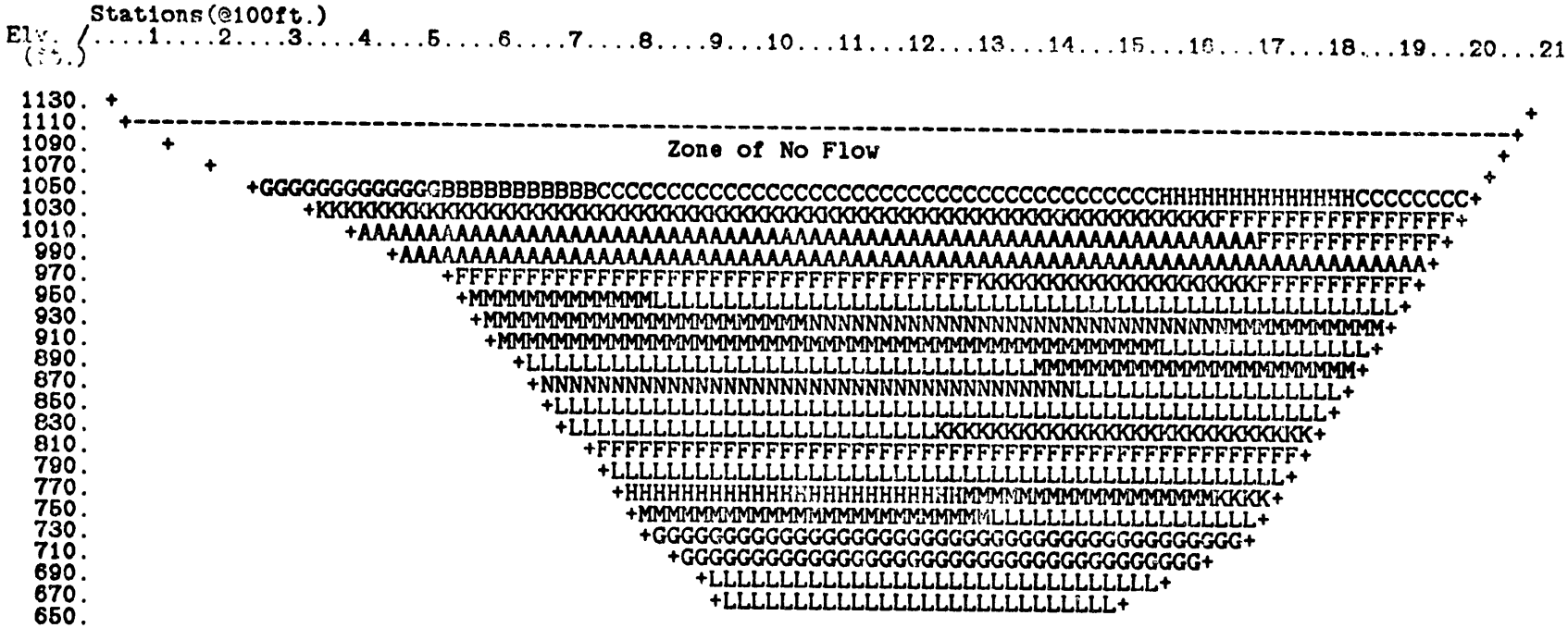

Fig. C.13 Zoning Based on the Combinations of Core and Transition Zone Materials

REFERENCES:

Aitchison, G.D. & Wood, C.C. (1965): "Some Interactions of Compaction, Permeability and Post-Construction Deflocculation Affecting the Probability of Piping Failure in Small Earth Dams", Proc. 6th ICSMFE, Vol. 2, pp. 442-446.

Arulanandan, K. & Perry, E.B. (1983): "Erosion in Relation to Filter Design Criteria in Earth Dams", Proc. ASCE, J. Geotechnical Eng., Vol. 107, No. 5.

Baecher, G., Pate, M.E. & de Neufville, R. (1980): "Dam Failure in Benefit/Cost Analysis", Proc. ASCE, Vol. 106, No. GT1, pp. 101-105.

Bartlett, M.S. and Besag, J.E. (1969): "Correlation Properties of Some Nearest-Neighbor Models," Bull. International Statistical Institute, Vol. 43, Book 2, pp. 191-3.

Bartlett, M.S. (1971): "Two-Dimensional Nearest-Neighbor Systems and Their Ecological Applications," in Statistical Ecology, Vol. 1, Spatial Patterns and Statistical Distributions, ed. Patil, G.P., Pielou, E.C., and Waters, W.E., The Pennsylvania State University Press.

Bartlett, M.S. (1971), "Physical Nearest-Neighbor Models and Non-Linear Time-Series", J. Appl. Prob. 8, 222-232.

Bartlett, M.S. (1975): The Statistical Analysis of Spatial Pattern, Chapman and Hall.

Bartlett, M.S. (1978): An Introduction to Stochastic Processes (third edition), Cambridge Univ. Press.

Bear, J. (1972): Dynamics of Fluids in Porous Media, American elservier.

Belyashevskii, N.N., et al (1972): "Behavior and Selection of the Composition of Graded Filters in Presence of Fluctuating Flow", Hydrotechnical Construction, No. 6, pp. 541-546.

Bertram, G.E. (1940), An Experimental Investigation of Protective Filters, Soil Mechanics Series No. 7, Graduate School of Engineering, Harvard Univ.

Besag, J.R. (1972): "Nearest-neighbor Systems and the Autologistic Model for Binary Data", J. Royal Statistic Soc. B34, pp. 75-83.

Besag, J.R. (1972): "Nearest-neighbor Systems and the Auto-logistic Model for Binary Data", J. Royal Statistic Soc. B34, pp. 75-83.

Besag, J. (1974): "Spatial Interaction and the Statistical Analysis of Lattice Systems", J. of Royal Statistical Soc. B36.

Boast, C.W. (1973): "Modeling the Movement of Chemicals in Soils with Water", Soil Science, Vol. 115, No. 3.

Cedergren, H.R. (1973): Seepage Control in Earth Dams, Ambankment Dam, Casagrande Volume (ed. by Hirschfed and Poulos), Wiley.

Charbenau, R.J. (1981): "Groundwater Contaminant Transport with Adsorption and Ion Exchange Chemistry: Method of Characteristics for the Case without Dispersion", Water Resources Research, Vol. 17, No. 3.

Cox, D.R. (1966): "Some Procedures Connected with the Logistic Qualitative Response Curve", Research Papers in Statistics: Essays in Honor of J. Neyman's 70th Birthday, pp. 55-71, Ed. by F.D. David, Wiley, London.

Cox, D.R. (1970): The Analysis of Binary Data, Chapman and Hall.

DeGraauw, A.F., Van Der Meulen, T. and M.R.V.D. DeBye (1984): "Granular Filters: Design Criteria", J. of Waterway, Port Coastal and Ocean Engineering (ASCE), Vol. 110, No. 1.

DeMello, V.F.B. (1975): "Some Lessons from Unsuspected, Real, and Fictitious Problems in Earth Dam Engineering in Brazil", Proc. 6th African Conf. Soil Mech. Fdn. Eng., Durham, Vol. 2, pp. 285-

DeMello, V.F.B. (1977): "Reflections on Design Decisions of Practical Significance to Embankment Dams," Geotechnique, Vol. 27, No. 3.

Dobson, A.J. (1983): An Introduction to Statistical Modeling, Chapman and Hall, London.

DuMouchel, W. & Waternaux, C. (1982): "Some New Dichotomous Regression Methods", Tech. Report No. NSF36, Statistics Center, M.I.T.

Fienberg, S.E. (1977): "The Analysis of Cross-Classified Categorical Data", The MIT Press, Cambridge, Massachusetts.

Goodman, R.E. & Sundaram, P.N. (1980): Permeability and Piping in Fractured Rocks, Proc. ASCE, Vol. 106, No. GT5.

Graauw, A.F., van der Meulen, T., & van der Dore de Bye, M.T., (1983): "Granular Filters: Design Criteria", Proc. ASCE, J. Waterways, Port, Coastal and Ocean Engineering, Vol. 110, No. 1.

Hendricks, D.W. (1978): "Sorption in Flow Through Porous Media", Proc. 3rd Symp. on Fundamentals of Transport Phenomena in Porous Media, IAHR, pp. 3840392.

Hjeldnes, E.I. & Lavania, B.V.K. (1980): "Cracking, Leakage, and Erosion of Earth Dam Materials, Proc. ASCE, Vol. 106, No. GT2.

Hoare, D.J. (1982): Synthetic Fabric as Soil Filters: A Review, Proc. ASCE, Vol. 108, No. GT10.

Honjo, Y. (1983): Reflections on Filter Criteria: A Probabilistic Approach, Masteral Thesis at M.I.T.

Horowitz, J.L. (1982): "Evaluation of Usefulness of Two Standard Goodness-of-fit Indicators for Comparing Non-Nested Random Utility Models", Transportation Research Record 874, National Research Council.

Hurley, H.W. & Newton, C.T. (1940): "An Investigation to Determine the Practical Application of Natural Bank Gravel as a Protective Filter", Masteral Thesis, M.I.T.

Hansen, R.B. (1983): "Dams and Public Safety", U.S. Department of the Interior, Bureau of Reclamation.

Karpoff, K.P. (1955), The Use of Laboratory Tests to Develop Design Criteria for Protective Filters, Proc. ASTM, Vol. 55, pp. 1183-1198.

Kassiff, G., Zaslavsky, D. & Zeitlen, J.G. (1965): Analysis of Filter Requirement for Compacted Clay, Proc. 6th ICSMFE, Vol. 2.

Kawakami & Esashi (1981): "On Drainage Filter for Earth Structure", Proc. 16th Annual Meeting, JSCE, (in Japanese).

Khan, I.H. (1983): "Failure of an Earth Dam: A Case Study", J. of Geotechnical Engineering (ASCE), Vol. 109, No. 2.

Kinderman, R. & Snell, J.L. (1980): "Markov Random Fields and Their Application", Contemporary Mathematics, Vol. 1, American Mathematical Society.

Kovacs, G. (1981): Seepage Hydraulics, Elsevier Scientific Publishing Company, Amsterdam, Oxford, New York.

Lambe, T.W. & Whitman, R.V. (1969): Soil Mechanics, John Wiley & Sons, Inc., New York.

Lapidus, L. & Amundson, N.R. (1952): "Mathematics of Adsorption in Beds: VI The Effect of Longitudinal Diffusion of Ion Exchanges and Chromatographic Colums", J. Physical Chemistry, Vol. 56, pp. 984-988.

Lawson, C.R. (1982): Filter Criteria for Geotextiles: Relevance and Use, Proc. ASCE, Vol. 108, No. GT10.

Leatherwood, F.N. & Peterson, D.F., Jr. (1954): "Hydraulic Head Loss at the Interface Between Uniform Sands of Different Sizes", Transactions, American Geophysical Union, Vol. 35, No. 4.

Lindstrom, F.T. & Boersma, L. (1970): "Theory of Chemical Transport with Simultaneous Sorption in a Water Saturated Porous Medium", Soil Science, Vol. 110, No. 1.

Lumley, J.L. & Panofsky, H.A. (1964): The Structure of Atmospheric Turbulence, Interscience Publishers.

Lund, A, "An Experimental Study of Graded Filters," Thesis presented to the University of London, at London, England in 1949, in fulfillment of the requirements for the degree of Master of Science.

McFadden, D. (1974): "Qualitative Response Models", A Chapter in Frontiers in Econometrics, ed. by P. Zarelmbka, Academic Press.

Mendez, M.P. (1981): "An Investigation into the Filtering Process in Various Types of Material", S.M. Thesis, University of London.

Mikuni, E. (1983): "Rockfill Dams - Leakage and Counter MEASURES", Tsuchi to Kiso, JSSMFE, Vol. 31, No. 4 (in Japanese).

Murali, V. & Aylmore, L.A.G. (1983): "Competitive Adsorption During Solute Transport in Soils: 1. Mathematical Models", Soil Science, Vol. 135, No. 3.

Papoulis, A. (1965): Probability Random Variables, and Stochastic Process, McGraw Hill, Inc., New York.

Ripley, P. (1981): Spatial Statistics, John Wiley & Sons.

Seed, H.B. and Duncan, J.M. (1981): "The Teton Dam Failure-A Retrospective Review," Proc. 10th ICSMFE, Vol. 4.

Sherard, J.L., Woodward, R.J., Gizienski, S.F. and Clevenger, W.A. (1963): Earth and Earth-Rock Dams--Engineering Problems of Design and Construction, John-Wiley and Sons, New York.

Sherard, J.L, Decker, R.S. & Ryker, N.L. (1972): "Piping in Earth Dams of Dispersive Clay", Proc. Specialty Conf. of ASCE, Perdue Univ., pp. 589-626.

Sherard, J.L. (1973): "Embankment Dam Cracking", in Embankment--Dam Engineering (Casagrande Volume) ed. R.C. Hirschfeld & S.J. Poulos.

Sherard, J.L. & Decker, R.S. (1976): Dispersive Clays, Related Piping, and Erosion in Geotechnical Projects, ASTM, special technical publication 623.

Sherard, J.L. (1979): "Sinkholes in Dams of Coarse, Broadly Graded Soils, 13tho ICLD, New Delhi.

Sherard, J.L., Dunnigan, L.P. & Talbot, J.R., (1984a): "Basic Properties of Sand and Gravel Filters", Proc. ASCE, J. Geotechnical Eng., Vol. 110, No. 6.

Sherard, J.L., Dunnigan, L.P. & Talbot, J.R. (1984b): "Filters for Silts and Clays", Proc. ASCE, J. Geotechnical Eng., Vol. 110, No. 6.

Silveria, A. (1965): An Analysis of the Problem of Washing Through a Protective Filter, 6th ICSMFE, Vol. 2.

Silveira, A., Peixoto, Jr., T.L. & Nogueira, J.B. (1975): On Void Size Distribution of Granular Materials, Proc. 5th Pan American Conf. SMFE.

Snedecor, G.W. & Cochran, W.G. (1980: "Statistical Methods (7th ed.)", The Iowa State University Press.

Soares, H.F. (1980): "Experiments on the Retention of Soils by Filters",A Thesis submitted to the University of London (Imperial College of Science and Technology), for the degree of Master of Philosophy in the Faculty of Engineering.

Southworth, M.J. (1978): An Experimental Evaluation of the Terzaghi Criterion for Protective Filters. A thesis submitted in partial fulfillment of the requirements for S.M. Degree, M.I.T.

Taylor, D.(1948): Fundamentals of Soil Mechanics, John Wiley & Sons, Inc., New York.

Takemura, G. & Yamamoto, H. (1961): "A Study on Filter", Graduation Thesis, Tohoku University, Japan (in Japanese).

Thanikachalam, V. & Sakthiradivel, R. (1974a): Grain Size Criteria for Protective Filters - An Enquiry Soils and Foundations, Vol. 14, No. 4.

Thanikachalam, V. & Sakthivadivel, K. (1974b): "Retentional Design Criteria for Protective Filters", Can. Geotech. J., Vol. 11, 309.

U.S. Corps of Engineers (1941): "Investigation of Filter Requirements for Underdrains", Tech. Memo. No. 183-1, U.S. Waterway Experiment Station, Vicksburg, Mississippi.

U.S. Corps of Engineers (1948): "Laboratory Investigations of Filters for Enid and Grenaala Dams", Tech. Memo, 3-150, U.S. Army Waterways Experimental Station, Vicksburg, Miss.

U.S. Corps of Engineerins (1953): "Filter Experiments and Design Criteria", U.S. Army Engineer Waterways Experimental Station, Tech. Memo. 3-360, Vicksburg, Miss.

Vanmarcke, E.H. & Honjo, Y. (1985): "Probabilistic Description of the Void Phase of Soil, with Reference to assessing the Risk of Internal Erosion", a paper submitted to the 4th International Conference on Structural Safety and Reliability, Kobe, Japan.

Vaughan, P.R., Lovenbury, H.T. & Horswill, P. (1975): "The Design, Construction and Performance of Cow Green Embankment Dam," Geotechnique, Vol. 25, No. 3.

Vaughan, P.R. & Soares, H.F. (1982): Design of Filters for Clay Cores of Dams, Proc. ASCE, Vol. 108, No. GT1.

Veneziano, D. (1983): Lecture Notes on "Reliability in Geotechnical Engineering", M.I.T.

Veneziano, D. & Liao, S. (1984): "Statistical Analysis of Liquefaction Data", 4th ASCE Speciality Conference on Probablistic Mechanics and Structural Reliability (ed. Wen, Y-K).

Wilson, S.D. & Marsal, R.J. (1979): Current Trends in Design and Construction of Embankment Dams, ASCE.

Witt, K.J. & Brauns, J. (1984): "The Influence of Parameter Variation on the Reliability of Filters", Proc. of the Internatinal Conf. on Safety of Dams (ed. J.L. Serafim), Cambra.

Wittman, L. (1979): "The Process of Soil Filtration - Its Physics and Approach in Engineering Practice", Proc. 7th Europian Conf. on SMFE, Vol. 1, pp. 303-310, Brighton, U.K.

Wittman, L. (1977): "Some Aspects of Transport Processes inPorous Media", Proc. 6th Australasian Hydraulics and Fluid Mechanics Conf., Adelaide.

Wittman, L (1978): "Phenomena and Parameters of Two-Component-Soil", Symp. on the Effects of Flow through Porous Media, IAHR, Greece.

Whittle, P. (1954): "On Stationary Process in the Plane," Biometrika, 41, pp. 434-449.

Yamaguchi, H. & Ohne, Y (1973): "Design and Construction of Fill Dams," Gihodo, Tokyo (in Japanese).

Zaslavsky, D. & Kassiff, G. (1965): "Theoretical Formulation of Piping Mechanism in Cohesive Soils", Geotechnique, Vol. 15, No. 3.